

University of Alberta

**Expression and Functional Significance of the Cystic Fibrosis
Transmembrane Conductance Regulator (CFTR) in human mast cells**

by

René Eugène Déry

A thesis submitted to the Faculty of Graduate Studies and Research
in partial fulfillment of the requirements for the degree of

Doctor of Philosophy in Experimental Medicine

Department of Medicine

©René Eugène Déry

Fall 2009

Edmonton, Alberta

Permission is hereby granted to the University of Alberta Libraries to reproduce single copies of this thesis and to lend or sell such copies for private, scholarly or scientific research purposes only. Where the thesis is converted to, or otherwise made available in digital form, the University of Alberta will advise potential users of the thesis of these terms.

The author reserves all other publication and other rights in association with the copyright in the thesis and, except as herein before provided, neither the thesis nor any substantial portion thereof may be printed or otherwise reproduced in any material form whatsoever without the author's prior written permission.

Examining Committee

Dr. A. Dean Befus, Medicine

Dr. Marek Duszyk, Physiology

Dr. James Young, Physiology

Dr. Neil Brown, Pulmonary Medicine

Dr. Bernard Thébault, Pediatrics

Dr. Soman Abraham, Pathology, Duke University

Dedication

I wish to dedicate this thesis to all the members of my family who stood by me during my arduous journey, and constantly instilled in me the belief that I would succeed.

Abstract

Mast cells (MC) are present in nearly all tissues in the body and participate in many physiological processes including allergy, tissue remodelling, fibrosis, angiogenesis, and autoimmunity. They can be activated by many stimuli, including allergic and innate immune stimulation. When activated, MC release mediators through which they can regulate inflammatory processes. Recently, we have discovered that rat and human MC express the Cystic Fibrosis Transmembrane Conductance Regulator (CFTR), the gene responsible for Cystic Fibrosis (CF). We showed that CFTR had functional activity in MC and its expression was differentially regulated by IFN γ . In this thesis, we compared CFTR expression between MC and epithelial cells (EC) by Western blot analysis and found that CFTR expression in MC is similar to that in EC, but there are some differences which suggest either glycosylation or post-transcriptional/translational differences between MC and EC. We also explored the role of CFTR in human MC secretion from various cellular compartments, in response to various stimuli. When we blocked CFTR using pharmacological inhibitors, there was an inhibition of cAMP-dependent Cl⁻ flux. Our data also shows that CFTR pharmacological inhibition had no effect on IgE/anti-IgE-mediated β -hexosaminidase or eicosanoid release from MC. When we stimulated MC with either IgE/anti-IgE or the adenosine receptor agonist NECA (3 μ M) for 24h in the presence of CFTR inhibitors, secretion of several mediators appeared to be dysregulated including IL-8, MIF, IL-13, IL-16, PAI-1 and CCL1. To add to these findings, we also used short hairpin RNA (shRNA) to reduce CFTR

expression in MC. CFTR deficient MC were unresponsive to NECA and showed reduced constitutive IL-6 secretion. Finally, we cultured MC from CF and non-CF donor peripheral blood progenitors and compared several phenotypic and functional aspects of the cells. We saw no difference in growth, protease content and surface marker expression between CF and non-CF MC, but stimulation of the cells with IgE/anti-IgE or *Pseudomonas aeruginosa* appeared to differentially induce cytokine synthesis and secretion from CF and non-CF MC. These findings suggest that MC function is dysregulated in CF and that CF MC may be involved in the pathophysiology of CF.

Preface

This thesis has been written in the traditional format following the style of the Journal of Experimental Medicine. Permission was granted for figure 1.1 as well as appendix 2.

The Journal of Histochemistry and Cytochemistry

Official Journal of the Histochemical Society
Kevin A. Roth, M.D., Ph.D.
Editor-in-Chief

Denis G. Baskin, Ph.D.
Executive Editor

Department of Biological Structure
HSB G-514 / Box 357420
University of Washington School of Medicine
Seattle, WA 98195-7420

Phone: (206) 616-5894 FAX: (206) 616-5842
johc@u.washington.edu
<http://www.jhc.org>

July 14, 2009

Rene Dery
University of Alberta
Dr. Dean Befus Lab
Edmonton, AB T6G 2S2 CANADA

Email: rene.dery@ualberta.ca

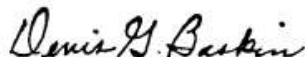
Dear Dr. Dery,

In response to your request dated 04/09/2009 permission is granted to reproduce, but not modify without prior consent, Figure 1 from the article "Ultrastructural Studies of Human Basophils and Mast Cells" published in the Journal of Histochemistry & Cytochemistry, Vol. 53, No. 9, pp. 1043-1070 (2005).

Note that you must cite full bibliographic reference in your published article. Credit for the cited material should appear as follows:

(Reproduced, with permission, from *author(s): article title*. Journal of Histochemistry & Cytochemistry *vol. no: page, year*)

Cordially,



Denis G. Baskin, Ph.D.
Executive Editor

Marianna Kulka
Research Officer
NRC-INH
550 University Avenue
Charlottetown, PEI
C1A 4P3
902-367-7550
Cell: 902-218-0372
marianna.kulka@nrc.ca

To Whom It May Concern:

This is to certify that René Déry has permission to use the following article as an appendix to his thesis:

Kulka, M., Déry, R.E., Nahrney D., Duszyk M., and Befus, A.D. 2005 Differential regulation of CFTR by interferon- γ in mast cells and epithelial cells. *Journal of Pharmacology and Experimental Therapeutics* 315(2): 563-570.

Sincerely,

A handwritten signature in black ink, appearing to read 'M. Kulka', with a long horizontal flourish extending to the right.

Marianna Kulka

Acknowledgements

This thesis is the culmination of the most difficult project I have ever accomplished in my life. My PhD project has been a difficult road peppered with technical speedbumps, but as I reach the final stages now, I realize that I have had the privilege of being a pioneer in the field of mast cell research. I have helped to set the stage for potentially groundbreaking discoveries in Cystic Fibrosis research.

For this opportunity, I would like to thank my supervisor Dr. Dean Befus. He has been a great mentor and role model, always encouraging objectivity, independent thought and critical analysis. Dean has helped me acquire the tools needed to become a great scientist and mentor. For allowing me to work in his lab and for his expert guidance along the way, I will forever be grateful. I also wish to thank all the members of the PRG past and present, many of whom have helped me in some way during my studies and some of whom have kept me sane with daily lunchtime poker. In particular, I want to thank Chris St-Laurent for his technical help and for alleviating my administrative workload so that I could focus on labwork during the last two years. I also want to thank Katherine Morris and Tae Chul Moon for their expert technical help and advice in many areas. Finally, I want to thank Lynelle Watt for her continued advice and administrative help.

On a personal note, I wish to thank my wife Carmen, for her unwavering support and encouragement. Carmen, you were always there for me when I

needed to vent. You are my inspiration and my life. I also want to thank my three kids Matthieu, Katelyn and Jillian who never really understood what I was working on, but encouraged me in their own special way. None of them ever complained when they did not get a summer vacation because their Dad was trying to finish his “homework”. I also want to thank my extended family who have always encouraged me and believed that I would get there.

Thank you all!

To raise new questions, new possibilities, to regard old problems from a new angle, requires creative imagination and marks real advance in science.

-Albert Einstein

Table of Contents

Chapter 1. General Introduction 1

A. Introduction to Mast cells 2

1. Mast cell biology..... 2

a) Localization and morphology 2

b. Heterogeneity 5

2. Mast cell activation 7

a) Calcium ionophores, compound 48/80 and neuropeptides 8

b) High affinity IgE receptor (FcεR1) 8

c) Pattern recognition receptors 11

d) Adenosine and adenosine receptors..... 12

3. Mast cell mediators 14

4. Mast cell secretory compartments 16

a) Granules 16

b) Small secretory vesicles..... 18

c) Lipid mediators 18

5. Mast cells in innate immunity and homeostasis 19

6. Mast cells in disease..... 20

B. Introduction to mast cell Cl⁻ channels 21

1. Overview of mast cell Cl⁻ conductance 21

a) ClC chloride channels..... 25

b) GABA receptors 26

c) Ca²⁺ activated Cl⁻ channels (CaCC)..... 26

C. Introduction to CFTR..... 27

1. CFTR structure and function 27

2. CFTR mutation classes and disease severity 30

a) Class I mutations..... 32

b) Class II mutations 32

c) Class III mutations 33

d) Class IV mutations..... 33

e) Class V mutations 34

3. Regulation of CFTR expression.....	34
a) Regulation of transcription	34
b) Regulation of translation	35
c) Post-translational modifications	36
4. CFTR protein interactions.....	37
5. Pharmacological inhibitors	40
6. CFTR in non-epithelial cells.....	43
a) Neutrophils.....	45
b) Muscle	46
c) Endothelium.....	46
d) Lymphocytes	46
e) Monocytes and macrophages.....	47
f) Neurons	48
g) Mast cells.....	48
D. Introduction to Cystic Fibrosis.....	49
1. Cystic Fibrosis and mast cells.....	52
E. Conceptual model, central hypothesis and aims.....	54
F. Overview of Rationale and Experimental Design	58
1. Aim 1: Characterization of CFTR expression in mast cells	58
2. Aim 2: Role of CFTR in human mast cell mediator secretion	59
3. Aim 3: Comparison of peripheral blood progenitor derived human cultured mast cells (PBMC) from Cystic Fibrosis and non-Cystic Fibrosis donors.....	60

Chapter 2. Materials and Methods.....63

A. Cell Culture	64
1. HMC-1	64
2. LAD2	65
3. Peripheral blood-derived mast cells (PBMC)	66
4. Calu-3.....	68
5. T84	69

B. Isolation of mouse bone marrow progenitors and rat peritoneal mast cells.....	70
1. Mouse bone marrow progenitors	70
2. Rat peritoneal mast cells	72
C. Characterization of CFTR expression by Western blot	73
1. Cell lysis and protein extractions	73
2. Sodium dodecyl sulfate-polyacrylamide gel electrophoresis (SDS-PAGE), Western blotting	73
D. Subcellular localization of CFTR in human and rat mast cells.....	76
1. Immunocytochemistry and confocal microscopy	76
2. Subcellular fractionation of rat peritoneal mast cells	79
E. Role of CFTR in human mast cell secretion	80
1. Pharmacological inhibition using CFTR inhibitors	80
2. Transfection of antisense and missense oligonucleotides (ASO) and (MSO).....	80
3. BLOCK-iT TM siRNA optimization	81
4. Transient transfection using small inhibitory RNA (siRNA)	82
5. Confocal microscopy of transfected HMC-1 (BLOCK-iT optimization).....	84
6. Measurement of puromycin resistance in cell lines	84
7. Stable transfection of CFTR short hairpin RNA (shRNA).....	86
F. Analysis of transfection efficiency and CFTR knockdown.....	87
1. Vector expression by flow cytometry	87
2. Cell lysis and mRNA extraction	88
3. Heparinase digestion	89
4. Primer efficiency calculations for quantitative PCR (qPCR)	90
5. Quantitative PCR (qPCR)	90

6. Non-quantitative reverse transcription-PCR (RT-PCR)	94
7. Nested RT-PCR	95
G. Effect of inhibition of CFTR on mast cell function	95
1. Measurement of Cl ⁻ Flux in cuvette assay	95
2. Increased throughput Cl ⁻ flux microplate assay	96
3. β -hexosaminidase release	98
4. Cytokine measurements	99
5. Eicosanoid production by LAD2 and PBMC	100
H. Comparison of peripheral blood-derived human cultured mast cells (PBMC) from non-Cystic Fibrosis and Cystic Fibrosis subjects.....	100
1. Tryptase chymase staining.....	100
2. Fc ϵ R1 and c-Kit expression	102
3. Cytokine array.....	102
I. Graphing and statistical analysis	104

Chapter 3. Results105

A. Cell proliferation	106
1. HMC-1 growth curves	106
2. LAD2 growth curves.....	108
3. Calu-3 growth curves	108
4. Peripheral blood-derived mast cells cultured from CD34 ⁺ progenitors	110
B. Characterization of Cystic Fibrosis and non-Cystic Fibrosis PBMC.....	112
1. CF but not non-CF PBMC express more MC _{TC} than MC _C	112
2. CF PBMC appear to express less surface c-Kit than non-CF PBMC.....	115

C. Mast cell mediator secretion	117
1. HMC-1 produce IL-8 in response to adenosine agonist NECA stimulation	117
2. LAD2 respond poorly to NECA, but strongly to Ca^{2+} ionophore A23187 and IgE/ α -IgE stimulation	118
D. Characterization of CFTR expression in mast cells.....	121
1. Mast cells express low levels of CFTR mRNA.....	121
2. CF-PBMC express intracellular but not plasma membrane CFTR	126
3. HMC-1 express higher levels of CFTR protein than LAD2.....	130
E. Comparison of epithelial cell and mast cell CFTR expression by Western blot analysis.....	135
1. Calu-3.....	135
2. LAD2	139
3. HMC-1	141
4. PMC	143
5. Rat peritoneal mast cells express both plasma membrane and intracellular CFTR, which is upregulated by $\text{IFN}\gamma$	146
6. CFTR is not detected in rat PMC granules by Western blotting:	146
F. Effect of pharmacological inhibition of CFTR on mast cell function	149
1. Pharmacological inhibitors downregulate c-AMP-dependent Cl^- flux in HMC-1	149
2. Pharmacological inhibitors differentially affect NECA-induced IL-8 and IL-6 secretion in HMC-1.....	151
3. Pharmacological inhibitors affect anti-IgE-induced but not NECA-induced degranulation in LAD2	153
4. Pharmacological inhibitors affect NECA and anti-IgE-induced cytokine release in LAD2	154

5. Pharmacological inhibitors do not affect anti-IgE-induced eicosanoid production in LAD2	157
G. Antisense oligonucleotide (ASO) knockdown of CFTR expression in MC..	158
1. CFTR knockout does not affect NECA-induced IL-6 secretion in mouse bone marrow cultured MC (BMMC).....	158
2. ASO downregulates Cl ⁻ flux in HMC-1.....	159
3. CFTR ASO non-specifically increases IL-6 and IL-8 secretion from HMC-1	162
H. Knockdown of CFTR expression in MC using siRNA	164
1. Optimization of siRNA transfection of MC by BLOCK-iT siRNA	164
2. Optimization of realtime PCR CFTR and β -actin primers	166
3. CFTR siRNA does not reduce CFTR protein expression in HMC-1	170
4. CFTR siRNA 794 does not affect IL-8 or IL-6 secretion from HMC-1	172
5. Confocal microscopy of BLOCK-iT transfected cells using short hairpin RNA (shRNA)	175
I. Stable knockdown of CFTR in HMC-1	178
1. Determination of HMC-1, LAD2 and Calu-3 puromycin susceptibility	178
2. Transfection of HMC-1 with lentiviral CFTR shRNA vector	179
3. CFTR shRNA but not scrambled control reduces CFTR mRNA expression in HMC-1	183
4. CFTR shRNA but not scrambled control reduces CFTR protein expression in HMC-1	183
5. CFTR shRNA reduces cAMP-dependent Cl ⁻ flux in HMC-1	192
6. CFTR shRNA ablates HMC-1 response to A _{2b} R agonist NECA	193

J. Comparison of Cystic Fibrosis and non-Cystic Fibrosis peripheral blood derived mast cells.....	196
1. CF PBMC may have dysregulated Cl ⁻ efflux in response to IgE/anti-IgE stimulation.....	196
2. β -hex secretion from CF PBMC in response to IgE/anti-IgE stimulation is not affected by absence of plasma membrane CFTR	198
3. PBMC from CF and non-CF donors exhibit differences in release of newly synthesized mediators in response to IgE/anti-IgE.....	199
4. PBMC from CF and non-CF donors exhibit differences in release of newly synthesized mediators in response to <i>Pseudomonas aeruginosa</i>	203
5. Absence of plasma membrane CFTR does not change LTC ₄ and PGD ₂ secretion in PBMC.....	204
6. Summary	206

Chapter 4. Discussion and future directions209

A. Characterization of CFTR expression in MC	212
1. CFTR mRNA expression in human mast cells.....	212
2. CFTR protein expression in human mast cells	213
3. Atypical CFTR bands	215
4. CFTR subcellular localization in rat peritoneal mast cells	220
B. Effect of pharmacological inhibition of CFTR on mast cell function.....	223
1. Cl ⁻ flux	225
2. β -hex secretion.....	226
3. IgE/anti-IgE-mediated cytokine secretion	229
4. NECA-mediated cytokine secretion	232
C. CFTR knockdown in mast cells	237
1. Antisense oligonucleotides (ASO).....	237

2. CFTR small inhibitory RNA (siRNA).....	238
3. CFTR short hairpin RNA (shRNA).....	239
D. Cystic Fibrosis vs non-Cystic Fibrosis peripheral blood derived mast cells .	243
E. Future directions.....	248
1. mRNA stability	248
2. WT-1	251
F. Conclusion	254
Endnotes	256
References	257
Appendix 1	292
Appendix 2	311

List of Tables

Chapter 1

1.1	Commonly used CFTR inhibitors.....	42
1.2	CFTR mRNA and protein expression in cells of non-epithelial origin...	44

Chapter 2

2.1	Small inhibitory RNA (siRNA) sequence.....	83
2.2	CFTR and β -actin reverse transcription and PCR primers.....	92

Chapter 3

3.1	Calu-3 Western blot conditions and band sizes.....	136
3.2	LAD2 Western blot conditions and band sizes.....	140
3.3	HMC-1 Western blot conditions and band sizes.....	142
3.4	PMC Western blot conditions and band sizes.....	144
3.5	Cytokine and chemokine release from Cystic Fibrosis and non-Cystic Fibrosis PBMC in response to IgE/anti-IgE stimulation.....	202
3.6	Cytokine and chemokine release from Cystic Fibrosis and non-Cystic Fibrosis PBMC in response to <i>P. aeruginosa</i>	205

List of Figures

Chapter 1

1.1	Ultrastructure of mast cells and basophils.....	3
1.2	Toluidine blue staining of human mast cells.....	4
1.3	Mechanisms of mast cell activation by FcεR1 aggregation.....	10
1.4	Adenosine synthesis and secretion pathways.....	13
1.5	Mast cell mediators.....	15
1.6	Mast cell secretory compartments.....	17
1.7	Transporters and chloride channels in mast cells and epithelial cells.....	22
1.8	Schematic representation of CFTR showing MA1-935 and 24-1 antibody binding sites.....	28
1.9	Schematic representation of ATP-driven channel function in CFTR.....	29
1.10	Schematic representation of CFTR mutation classes.....	31
1.11	Schematic representation of selected CFTR protein: protein interactions.....	38
1.12	Schematic representation of controversy behind etiology of CFTR.....	51
1.13	Conceptual model of mast cell involvement in the pathophysiology of Cystic Fibrosis.....	56

Chapter 2

2.1	Schematic representation of subcellular fractionation method.....	78
2.2	Diagram of CFTR and β -actin PCR primers and amplification products.....	93

Chapter 3

3.1	Seeding and growth curves for HMC-1.....	107
3.2	Seeding and growth curves for LAD2 and Calu-3.....	109
3.3	Comparison of Cystic fibrosis and non-Cystic Fibrosis CD34 ⁺ cells and growth curves over 8 wk in culture.....	111
3.4	Tryptase and chymase staining in Cystic Fibrosis and non-Cystic Fibrosis peripheral blood-derived mast cells.....	113
3.5	Comparison of tryptase and chymase positive cells in Cystic Fibrosis and non-Cystic Fibrosis peripheral blood-derived mast cells....	114
3.6	Comparison of stem cell factor receptor (c-Kit) and Fc ϵ R1 expression in Cystic Fibrosis and non-Cystic Fibrosis peripheral blood-derived mast cells.....	116
3.7	HMC-1 response to the adenosine receptor agonist NECA is potentiated by stem cell factor.....	119
3.8	LAD2 degranulation in response to Ca ²⁺ ionophore A23187 or IgE/anti-IgE stimulation.....	120

3.9	Comparison of reverse transcription using oligo dT primers vs CFTR and β -actin specific primers.....	123
3.10	CFTR and β -actin mRNA expression in Calu-3 LAD2 and HMC-1 cells.....	124
3.11	CFTR and β -actin mRNA expression in non-CF peripheral blood-derived mast cells.....	125
3.12	Western blot analysis of CFTR protein expression in peripheral blood-derived mast cells.....	127
3.13	Plasma membrane and intracellular expression of CFTR protein in Cystic Fibrosis vs. non-Cystic Fibrosis peripheral blood-derived mast cells protein assessed by flow cytometry.....	129
3.14	Plasma membrane and intracellular expression of CFTR protein in T84 epithelial cells and HMC-1 assessed by confocal microscopy.....	131
3.15	Comparison of CFTR protein expression in Calu-3 and LAD2 cells using intracellular staining in flow cytometry.....	132
3.16	Comparison of calculated molecular weights of CFTR in Calu-3, LAD2, HMC-1 and PMC.....	134
3.17	Western blot comparison of CFTR banding patterns on same gels in LAD2, Calu-3 and HMC-1.....	137
3.18	Western blot comparison of CFTR banding patterns from different gels in LAD2, Calu-3 and HMC-1.....	138
3.19	Western blot analysis of subcellular localization of CFTR in rat peritoneal mast cells.....	145

3.20	Flow cytometric analysis of the effect of IFN γ on CFTR plasma membrane and intracellular localization in rat peritoneal mast cells.....	147
3.21	Effect of CFTR inhibitors on chloride flux from HMC-1.....	150
3.22	Effect of CFTR inhibitors on IL-8 and IL-6 secretion from HMC-1.....	152
3.23	Effect of CFTR inhibitors on the adenosine receptor agonist NECA or anti-IgE-mediated degranulation and cytokine synthesis in LAD2 cells.....	155
3.24	Effect of CFTR knockout on IL-6 secretion in mouse bone marrow derived mast cells (BMMC) following adenosine agonist NECA stimulation.....	159
3.25	Effect of CFTR antisense (ASO) or missense (MSO) oligonucleotides on CFTR expression and chloride flux in HMC-1.....	161
3.26	Effect of CFTR antisense (ASO) or missense (MSO) oligonucleotides on IL-8 and IL-6 secretion in HMC-1.....	163
3.27	Optimization of siRNA transfection efficiency using BLOCK-iT siRNA and Lipofectamine.....	167
3.28	Optimization of siRNA transfection efficiency, realtime PCR CFTR and β -actin primer efficiency comparison and Calu-3 CFTR siRNA transfection.....	168
3.29	Optimization of siRNA transfection efficiency using FuGENE HD and BLOCK-iT siRNA.....	169
3.30	Flow cytometric analysis of effect of siRNA on CFTR protein expression in HMC-1.....	171

3.31	Effect of 48 h CFTR siRNA transfection on adenosine receptor agonist NECA-induced IL-8 and IL-6 release from HMC-1	173
3.32	Confocal imaging of BLOCK-iT siRNA in HMC-1 cells.....	174
3.33	Effect of puromycin on untransfected and CFTR shRNA transfected HMC-1 viability.....	176
3.34	Effect of puromycin on untransfected LAD2 and Calu-3 cells.....	177
3.35	Green fluorescence protein (GFP) expression in CFTR shRNA transfected HMC-1, LAD2 and Calu-3 cells 24 h after transfection.....	180
3.36	GFP expression in CFTR shRNA stably transfected HMC-1 cells.....	182
3.37	Realtime PCR analysis of CFTR mRNA expression in untransfected, scrambled or CFTR shRNA transfected HMC-1 cells.....	184
3.38	Western blot analysis of CFTR protein expression in untransfected, scrambled or CFTR shRNA transfected HMC-1 cells.....	185
3.39	Flow cytometric analysis of CFTR plasma membrane protein expression in untransfected, scrambled or CFTR shRNA transfected HMC-1 cells.....	187
3.40	Flow cytometric analysis of CFTR intracellular protein expression in untransfected, scrambled or CFTR shRNA transfected HMC-1 cells.....	189
3.41	Effect of CFTR shRNA on cAMP-dependent chloride flux in HMC-1 cells.....	191
3.42	Effect of CFTR shRNA on adenosine receptor agonist NECA-induced IL-8 and IL-6 secretion.....	194

3.43	Comparison of IgE/anti-IgE-mediated chloride flux and β -hexosaminidase release from Cystic Fibrosis and non-Cystic Fibrosis peripheral blood-derived mast cells.....	197
3.44	Protein array comparison of newly synthesized mediator production from Cystic Fibrosis and non-Cystic Fibrosis peripheral blood-derived mast cells.....	200
3.45	Comparison of LTC ₄ and PGD ₂ secretion from Cystic Fibrosis and non-Cystic Fibrosis peripheral blood-derived mast cells in response to 30 min IgE/anti-IgE stimulation.....	207

Chapter 4

4.1	Diagram of potential Proline-Glutamic acid-Serine-Threonine (PEST) sequences in CFTR protein.....	219
4.2	Proposed mechanism of action of CFTR inhibitors on IgE/anti-IgE mediated β -hex release in LAD2 cells.....	228
4.3	Proposed role of G-protein regulated kinase 2 (GRK2) and phosphatidylinositide-3 kinase (PI3K) interactions with CFTR on regulation of adenosine receptor expression in mast cells.....	230
4.4	Proposed mechanism of action of CFTR inhibitors on IgE/anti-IgE mediated cytokine release in LAD2 cells.....	233
4.5	Proposed mechanism of action of CFTR inhibitors on adenosine receptor agonist NECA-mediated cytokine release in HMC-1 cells.....	234
4.6	Proposed synthesis, trafficking and processing pathways of CFTR in mast cells and potential disruptions in these pathways following stable CFTR knockdown using shRNA.....	241
4.7	Proposed mechanism of IFN γ regulation of CFTR expression in epithelial cells and mast cells.....	249

4.8	Putative binding site for the MMP-9 repressor WT-1 in the first intron of the CFTR gene.....	252
4.9	Proposed mechanism of WT-1 regulation of CFTR expression through a nitric oxide dependent pathway.....	253

List of Abbreviations

A _{2a} R	Adenosine 2a receptor
A _{2b} R	Adenosine 2b receptor
ANOVA	Analysis of variance
AP-1	Activator protein-1 transcription factor
ARE	AU-rich element on messenger RNA
AREbp	AU-rich element binding protein
ASL	Airway surface liquid
ASO	Antisense oligonucleotide
ATF1	Activating transcription factor-1
β ₂ AR	Beta-2 adrenergic receptor
β-hex	Beta hexosaminidase enzyme
BMMC	Bone marrow derived mast cells
CaCC	Calcium activated chloride channel
Calu-3	Cancer lung-3 epithelial cell line
cAMP	Cyclic adenosine monophosphate
CBMC	Cord blood derived mast cells
CBP	cAMP response element binding protein
cDNA	Complementary DNA
CF	Cystic Fibrosis
CFTR	Cystic Fibrosis Transmembrane conductance Regulator

CFTR _{inh-172}	3-[(3-trifluoromethyl) phenyl]-5-[(4-carboxyphenyl)methylene]-2-thioxo-4-thiazolidinone
c-Kit	Stem cell factor receptor (CD117)
ClC	Voltage gated chloride channel family
CPA	Carboxypeptidase A
CTMC	Connective tissue mast cells
ΔF508	Deletion of phenylalanine at position 508
DAG	Diacylglycerol
DAPI	4',6-diamidino-2-phenylindole
DEPC	Diethyl pyrocarbonate
DIDS	4,4'-diisothiocyano-2,2'-stilbene disulphonic acid
DMSO	Dimethyl sulphoxide
DNA	Deoxyribonucleic acid
DOTAP	N-(1-(2,3-dioleoyloxy)propyl)-N,N,N-trimethyl ammonium methyl sulphate
DPC	diphenylamine-2-carboxylate
EBP50	Ezrin binding protein of 50 kilo daltons
EC	Epithelial cell
ER	Endoplasmic reticulum
FBS	Fetal bovine serum
FcεR1	High affinity receptor for IgE
FcγR1	High affinity receptor for IgG

FITC	Fluorescein isothiocyanate
GABA	Gamma-aminobutyric acid
GFP	Green fluorescent protein
GlyH-101	N-(2-naphthalenyl)-[(3,5-dibromo-2,4-dihydroxyphenyl) methylene]glycine hydrazide
GM-CSF	Granulocyte-macrophage colony stimulating factor
HBSS	Hanks' balanced salt solution
HCO ₃ ⁻	Bicarbonate
HEPES	4-(2-hydroxyethyl)-1-piperazineethanesulfonic acid
HMC-1	Human mast cell line-1
Hsp	Heat shock protein
HTB	HEPES-Tyrode's buffer
IBMX	Isobutyl methylxanthine
IFN _γ	Interferon-gamma
IgE	Immunoglobulin E
IκB	Inhibitor of NF-κB
IL	Interleukin
IMDM	Iscoe's Modified Dulbecco's Medium
IP3	Inositol triphosphate
IR	Infra Red
ITAM	Immunoreceptor tyrosine-based activation motif
JAK	Janus kinase

K _{Ca} ²⁺	Calcium activated potassium channel
kDa	Kilodalton
KSCN	K ⁺ isothiocyanate
LAD2	Laboratory of Allergic Disease mast cell line-2
LAT	Linker for Activation of T-cells
LPS	Lipopolysaccharide
LTA ₄	Leukotriene A ₄
LTC ₄	Leukotriene C ₄
MAPK	Mitogen-activated protein kinases
MC	Mast cells
MC _C	Mast cells positive for chymase only
MC _{CT}	Mast cells positive for chymase and tryptase
MC _T	Mast cells positive for tryptase only
MCP	Mast cell protease
MEM	Minimum essential medium
MIF	Macrophage migration inhibitory factor
MMC	Mucosal mast cell
MQAE	N-[ethoxycarbonylmethyl]-6-methoxy-quinolinium bromide
mRNA	Messenger RNA
MSO	Missense oligonucleotide
MW	Molecular weight

NBD	Nucleotide binding domain
NECA	5'-(N-Ethylcarboxamido)adenosine
NF- κ B	Nuclear factor kappa B transcription factor
NHERF	Na ⁺ /H ⁺ exchanger regulatory factor
NO	Nitric oxide
NOS	Nitric oxide synthase
NPPB	5-nitro-2(3-phenylpropyl-amino) benzoate
ORCC	Outwardly rectifying chloride channels
PAF	Platelet activating factor
PAI-1	Plasminogen activator inhibitor-1 (Serpine1)
PAMP	Pathogen-associated molecular pattern
PAO1	<i>Pseudomonas aeruginosa</i> strain O1
PBMC	Peripheral blood-derived mast cells
PBS	Phosphate buffered saline
PCR	Polymerase chain reaction
PDE	Phosphodiesterase
PDZ	Post synaptic density protein (PSD95), D rosophila disc large tumor suppressor (DlgA), and Z onula occludens-1 protein (zo-1)
PGD ₂	Prostaglandin D ₂
PGN	Peptidoglycan
PI3K	Phosphatidylinositide-3 kinase
PIP ₂	Phosphatidylinositol 4,5-bisphosphate

PKA	Protein kinase A
PKC	Protein kinase C
PLA ₂	Phospholipase A ₂
PMC	Peritoneal mast cells
Poly I:C	Poly inosinic: polycytidylic acid
PVDF	Polyvinylidene fluoride
RANTES	Regulated upon activation normal T-cell expressed and secreted
RBL-2H3	Rat basophilic leukemia cell line
RCMC	Rat cultured mast cell line
RIPA	Radio immunoprecipitation assay
RNA	Ribonucleic acid
RT	Reverse Transcription
SCF	Stem cell factor
SCR	Scrambled
SDS	Sodium dodecyl sulphate
shRNA	Short hairpin RNA
STAT	Signal transducer and activator of transcription
TESS	Transcription element search system
TLR	Toll-like receptor
TRPV4	Transient receptor potential V4 ion channel
VEGF	Vascular endothelial growth factor
VRAC	Volume regulated anion channel

Chapter 1. General Introduction

A. Introduction to Mast cells

1. Mast cell biology

a) Localization and morphology

Mast cells were discovered more than 100 years ago by Paul Ehrlich who named them *mastzellen* which means “well fed” or “fat” cells because of their heavily granulated appearance and staining by aniline dyes (Figure 1.1 A and 1.2) (1, 2). MC can contain up to 200 to 300 granules, which stain dark purple with toluidine blue, alcian blue or red with safranin red, depending on their phenotype (3-6). MC are widely distributed in the body, found in virtually every tissue and vascularized organ (7). In mice, MC originate from $CD34^+$, $c-kit^+$, $Fc\epsilon R1^+$ multipotent MC/basophil progenitors which in turn originate from upstream pluripotent progenitors in the bone marrow (7, 8). Mast cell/basophil progenitors migrate to the tissues and give rise to either MC or basophils under the regulation of the cytokine and growth factor microenvironment found in that tissue (Figure 2) (7, 8). In humans, interleukin (IL)-3, IL-6 and stem cell factor (SCF) are important maturation and differentiation, and are critical MC maturation factors (9). In humans, as in mice, MC progenitors migrate from the blood into peripheral tissues where they undergo differentiation and maturation (10-12). Mast cells aggregate around blood vessels and nerves, as well as epithelia in the airways and gastrointestinal tract, and are responsive to neuropeptides such as substance P, vasoactive intestinal peptide, nerve growth factor (NGF) and calcitonin gene related peptide (13, 14).

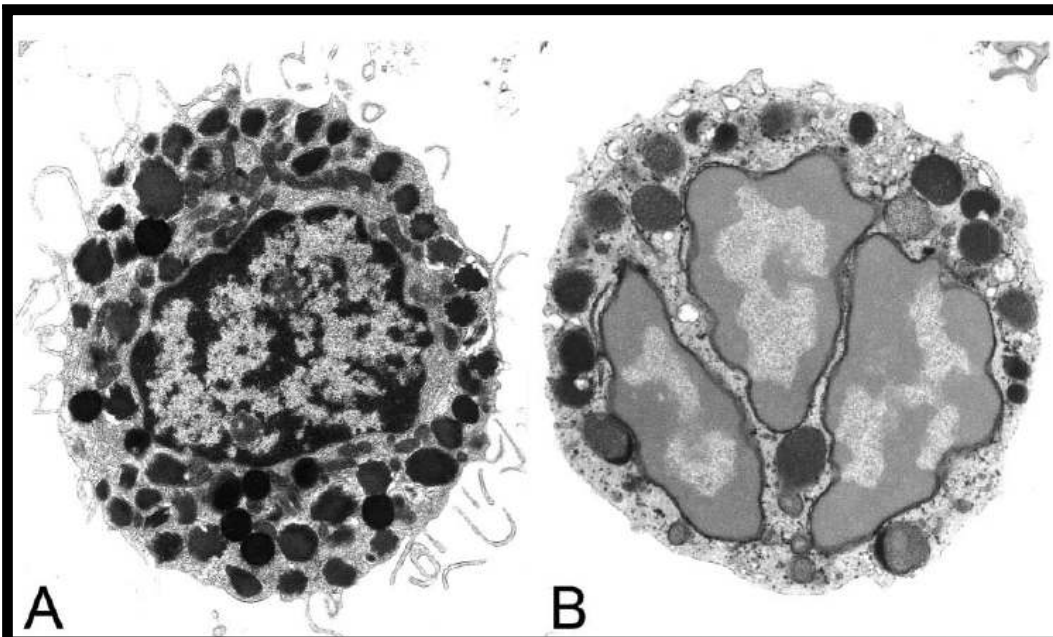


Figure 1.1 A) Ultrastructure of human mast cells (HMCs) and human basophils (HBs). (A) Human lung mast cells (HLMC) after isolation and culture for 36 hr show electron-dense secretory granules, a monolobed nucleus, and numerous narrow surface folds. (B) HB isolated from the peripheral blood has electron-dense secretory granules and a polylobed nucleus. (A) X 10,000; (B) X 17,000. Reproduced, with kind permission, from Dvorak, A.M. 2005. Ultrastructural studies of human basophils and mast cells. *J Histochem & Cytochem* 53 (9): 1043-1070.

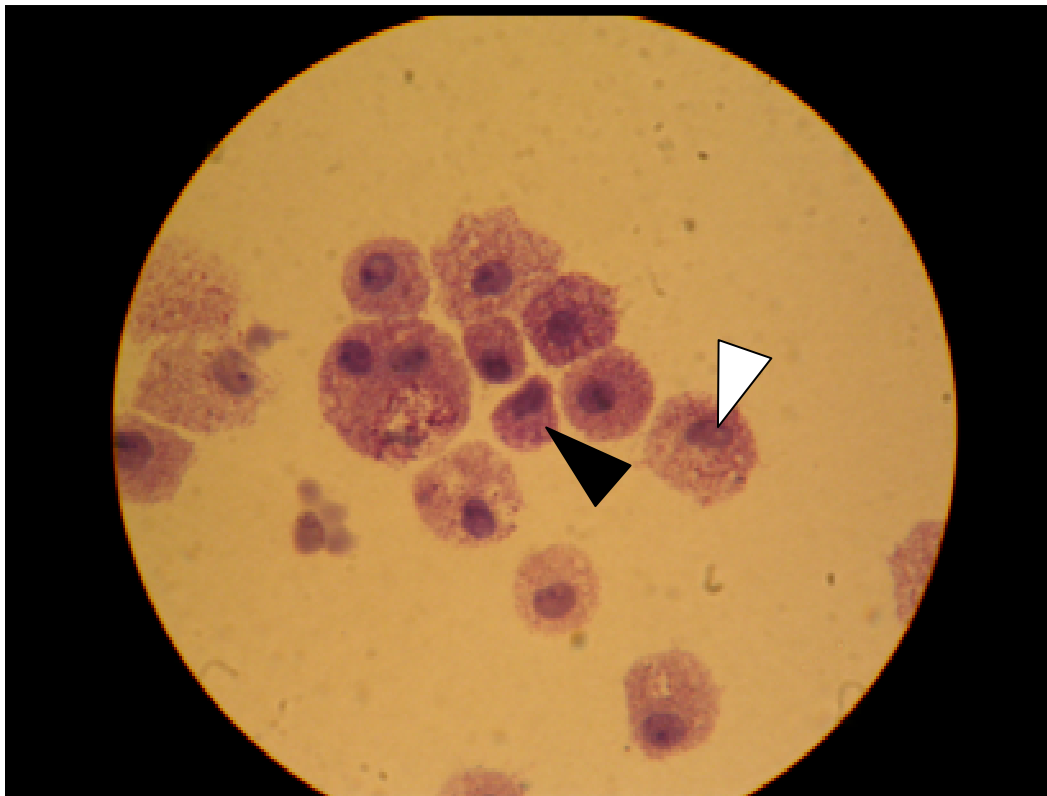


Figure 1.2 LAD2 mast cells stained with toluidine blue showing secretory granules (closed arrow) and monolobed nucleus (open arrow).

Although MC are most often thought of in the context of IgE-mediated allergic reactions, they are involved in normal physiological responses and numerous inflammatory responses involving activation by several IgE-independent pathways, ranging from complement components, FcγR1 aggregation, immunoglobulin light chains, neuropeptides and pattern recognition receptors (PRR) associated with innate immunity (13, 15-19). Recently, the focus has been on involvement of MC in innate immunity, and their ability to respond to pattern recognition receptors such as Toll-like receptors (TLR)-2 and -4 and other innate immune molecules such as the cellular stress-related molecule adenosine through its 2b receptor (A_{2b}R) (20, 21). These pathways are all likely to be highly relevant to MC function in the context of disease, as it is now well known that MC are key players in host defense and immunity (1).

b. Heterogeneity

MC are heterogeneous in their biochemical staining characteristics, protease content, mediator secretion and activation patterns depending on the tissue and microenvironment in which they reside (22). Two MC subsets have been described in rodents: 1) connective tissue (CTMC) and 2) mucosal MC (MMC) (1, 2). CTMC are found in skin and peritoneal cavity, whereas MMC are found in the lamina propria or epithelial layers of mucosal tissues, (1, 2, 22). Heterogeneous expression of granule proteases was first described in rat and mouse MC (22). CTMC are heavily laden with proteoglycan heparin and histamine containing granules which contain mast cell protease (MCP)-4, 5, 6 and

carboxypeptidase A (1, 23). In contrast to CTMC, MMC granules contain chondroitin sulphate rather than heparin, MCP-1 and 2 but no CPA (1, 2, 23). Also, MMC granules do not contain as much histamine as CTMC (1). Because of these biochemical differences, rodent MMC and CTMC can be recognized by their different staining patterns. CTMC stain with both alcian blue and safranin, but MMC do not stain with safranin due to the absence of heparin (5, 6).

MCP content has been well characterized in rodents and few differences exist. In mice, MCP-1, 2, 4, 5 and 9 are classified as chymases, whereas MCP-6, 7 and 11 are subtypes of tryptase (2, 24, 25). In rats, MCP-1, 2, 3, 4 and 5 are classified as chymases, whereas MCP-6 and 7 are classified as tryptases (22). Rat MCP-1, 2 and 3 are homologous to mouse MCP-5, and rat MCP-1 is the counterpart to mouse MCP-4, 1 and 5 respectively (23, 24). MCP-8 does not belong to the tryptase or chymase family, but was rather found to be more closely related to granzymes and cathepsins (26). Expression of MCP-8 was low in normal tissues and found in association with MCP-5 expressing MC (26). Another protease; the metalloexopeptidase carboxypeptidase A (CPA), is found in certain subsets of rodent MC (2, 23).

As in rodents, human MC populations are heterogeneous, but their phenotypic and functional differences are less well defined and less well understood (22). They are classified by most literature as being either tryptase positive (MC_T) or both tryptase and chymase positive (MC_{CT}) (1, 2). However, MC positive for only chymase (MC_C) also exist. Tryptase positive MC_T are found at mucosal sites and are thought to be similar to MMC, whereas double positive

MC_{CT} are similar to CTMC and are located in connective tissue of the skin and intestine (1, 2). MC_C have been associated with atherosclerotic lesions, and their numbers increase in those lesions (27). Recent evidence however, suggests that human enteric MC_T contain low levels of chymase as well as tryptase (22). Furthermore, it has been shown that human but not rodent MMC, contain low levels of heparin (22). This evidence suggests that in humans the classification of MC as belonging to the MMC or CTMC phenotype may be incorrect. Interestingly, it has been shown that MC transplanted from one anatomical site to another can change their phenotype (28). This suggests that the phenotype of MC does not rely on the type of tissue they are found in, but rather on the cytokine milieu which exists in that tissue at the time of their extraction development and removal from the tissue.

2. Mast cell activation

MC are present in nearly all tissues in the body and participate in many physiological processes including allergy, tissue remodelling, fibrosis, angiogenesis, and autoimmunity (29). They can be activated by a plethora of different pathways, and release numerous mediators, many of which will not be discussed here. This section is not meant to be an exhaustive review of MC activation, but rather to give the reader a sense of the secretory capacity of MC. Thus, only the pathways of mast cell activation most relevant to this thesis will be discussed.

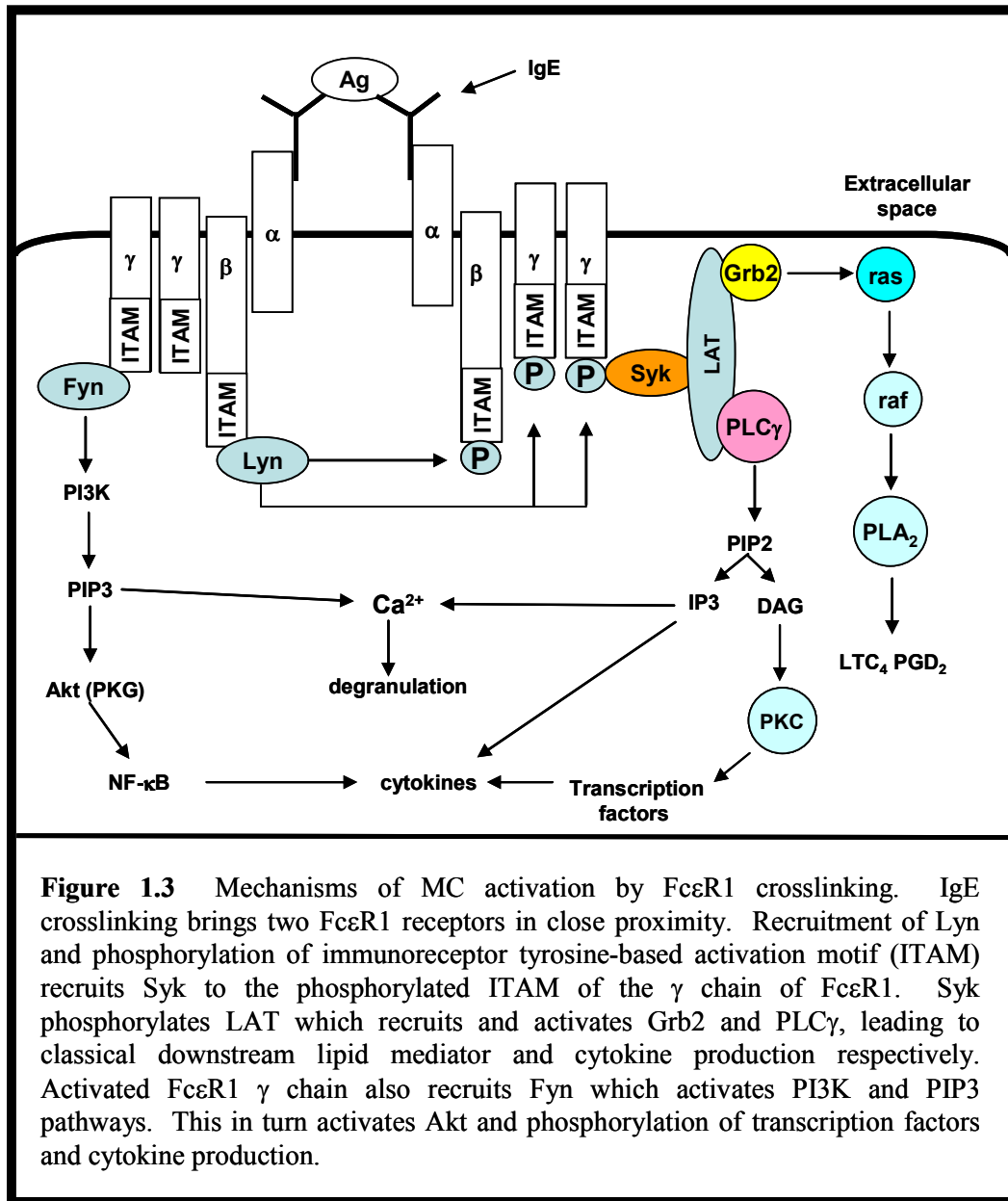
a) Calcium ionophores, compound 48/80 and neuropeptides

Mast cells can be activated to release their granules by compounds that induce Ca^{2+} entry into the cell. Some compounds such as the yeast antibiotic calcium ionophore A23187, form stable complexes with divalent cations and form pores in the plasma membrane, which allows Ca^{2+} to cross the cell membrane (30). Other compounds such as 48/80 or the wasp venom compound mastoparan can activate the cells by binding to G-protein coupled receptors (31, 32). Substance P is an undecapeptide belonging to the tachykinin family. It stimulates MC secretion through the neurokinin-1 (NK-1) receptor belonging to the G-protein coupled receptor family of receptors (13, 33). Substance P can also activate MC in a receptor-independent manner through peptidergic cationic charge activation (34). This mechanism is associated with neurogenic inflammation and is thought to be restricted to serosal MC (34). This agonist of MC is important in neuroimmunology, since MC are closely associated with nerves and their activation is mediated by neurons during neurogenic inflammation as seen in itching and some forms of allergic rhinitis (35).

b) High affinity IgE receptor (FcεR1)

FcεR1 is the high affinity IgE receptor. It is a heterotetrameric molecule composed of an α chain which binds IgE, a β chain along with two common γ chains which provide intracellular signalling via immunoreceptor tyrosine-based activation motifs (ITAM) (Figure 1.3) (10, 36). Expression of FcεR1 MC is

regulated by several factors including IL-4, IFN γ and IgE receptor occupancy (10, 37, 38). The binding of IgE to Fc ϵ R1 has a high affinity ($1 \times 10^{10} \text{ M}^{-1}$), and a slow rate of dissociation, allowing MC to remain sensitized for months or even years (10). Signalling mechanisms through Fc ϵ R1 are complex. When bound to the Fc ϵ R1, two IgE molecules can be cross-linked by a cognate antigen, which triggers mast cell activation (Figure 1.3) (10, 36). Upon cross-linking, the ITAM motif recruits the kinase Lyn, which phosphorylates the β and γ chains of Fc ϵ R1, which in turn bind the kinase Syk. Binding of Syk phosphorylates linker for T-cell activation (LAT) which recruits phospholipase C-gamma (PLC γ) (Figure 1.3). Activated PLC γ forms inositol triphosphate (IP3) and diacylglycerol (DAG) from phosphatidylinositol 4, 5-bisphosphate (PIP $_2$) (10, 36). IP3 causes Ca $^{2+}$ release from cellular stores through IP3 receptors on the endoplasmic reticulum, and induces degranulation. DAG activates protein kinase C (PKC) which phosphorylates transcription factors and leads to production of newly synthesized mediators such as cytokines (10, 36). Phosphorylation of LAT also recruits Grb2, and initiates the ras/raf signalling cascade leading to lipid mediator production (10, 36). Lyn also exerts a regulatory role in Fc ϵ R1 mediated activation, as Lyn deficient mice are hyperresponsive to Fc ϵ R1 crosslinking (11). The recruitment of the tyrosine kinase Fyn is important in MC, as this activates phosphatidylinositol triphosphate kinase (PI3K) leading to protein kinase G (Akt) phosphorylation and gene transcription through phosphorylation of inhibitor of NF-kB kinase (IKK) and inhibitor of NF-Kb (IkB), leading to activation of NF- κ B (10, 11).



c) Pattern recognition receptors

Mast cells are recognized as efficient sentinel cells that play a crucial role in homeostasis, as well as initiation and perpetuation of inflammation in response to pathogens (16, 39). The discovery of pattern recognition receptors (PRR) such as TLR, nucleotide oligomerization domain (NOD) and c-type lectin receptors has led to a better understanding of how immune cells respond to infection. TLR are a family of conserved PRR which are present on all immune cells in various combinations. There are currently 11 known TLR receptors in humans, 2 of which are formed by dimers of other TLR receptors. TLR bind to various pathogen associated molecular patterns (PAMP). For a complete review of these receptors and their ligands, the reader is referred to reference (18). Depending on their source and culture conditions, human MC differentially express different combinations of TLR (1, 16, 39-41). Most prominent in mast cell activation however, are TLR-2 and TLR-4, which recognize peptidoglycan (PGN) and lipopolysaccharide (LPS) respectively (16, 20). Mast cells can also be activated via TLR-3 by synthetic polyinosinic:polycytidylic acid (poly I:C) (42). Thus, MC are positioned in the body to respond to bacterial, viral, and fungal invasion, in the first line of defense against infections. NOD receptors and c-type lectins receptors are also PRR which play a role in the antimicrobial function of MC (43), but these receptors will not be discussed further.

d) Adenosine and adenosine receptors

Adenosine was first described in cardiac tissue by Drury and Szent-Gyorgyi in 1929, as “a potent inotropic agent and coronary vasodilator (44). The effects of adenosine can often appear paradoxical because they depend on its extracellular concentration, as well as co-expression of its four known receptors. There has recently been an explosion of literature focusing on the emergence of adenosine as an innate immune molecule, particularly in the context of inflammatory diseases (Figure 1.4) (44). Many of these studies suggest that adenosine is produced in elevated quantities by inflamed, damaged or stressed tissues (44). There is an emerging link in the literature between the innate immune system and potentiation of inflammatory diseases such as asthma, by adenosine activity on effector cells such as MC (45).

Under conditions of hypoxia or cellular stress, extracellular adenosine levels can rise by two orders of magnitude (44). This increase in adenosine levels during cellular stress results in activation of low affinity adenosine receptors, which alters cellular responses. There are four known G-protein coupled receptors for adenosine. Human MC express two of the four receptors, the high affinity A_{2a} receptor ($A_{2a}R$), and the low affinity A_{2b} receptor ($A_{2b}R$) (46). The $A_{2a}R$ has 100-fold higher affinity to adenosine than the other three receptors, and is thought to be the major homeostatic adenosine receptor in immune cells, because sub-micromolar levels of adenosine can stimulate $A_{2a}R$ but not the other receptors.

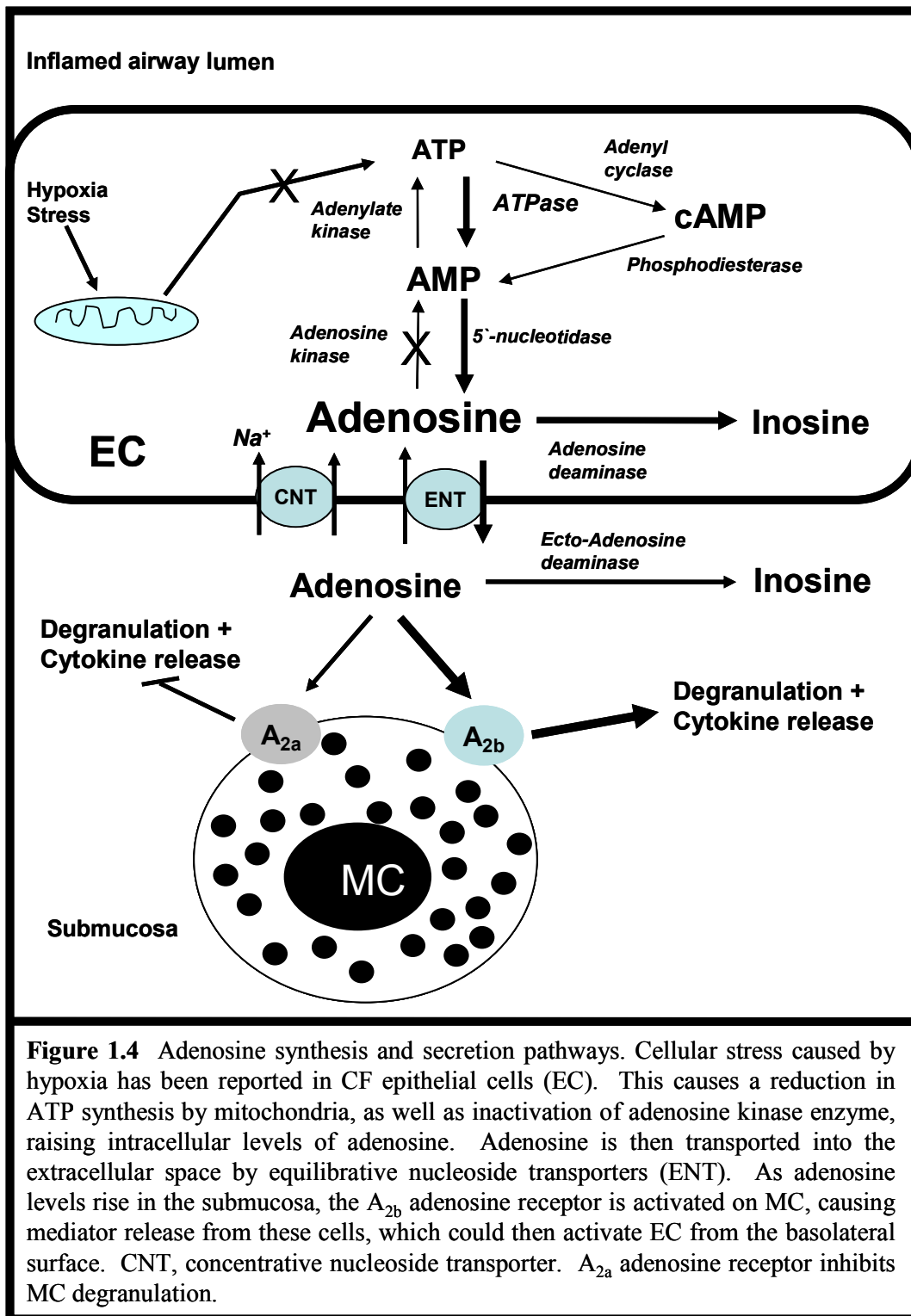
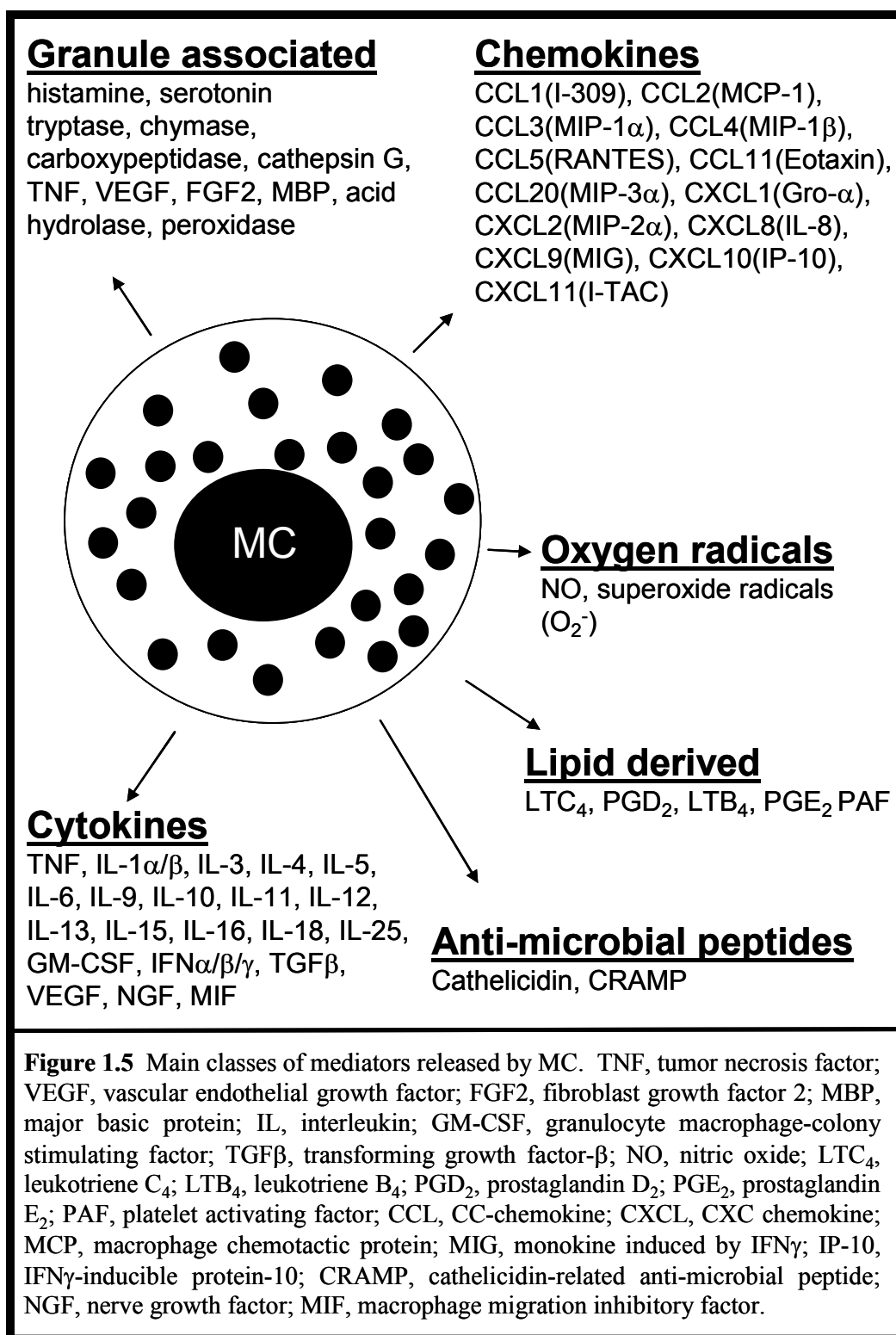


Figure 1.4 Adenosine synthesis and secretion pathways. Cellular stress caused by hypoxia has been reported in CF epithelial cells (EC). This causes a reduction in ATP synthesis by mitochondria, as well as inactivation of adenosine kinase enzyme, raising intracellular levels of adenosine. Adenosine is then transported into the extracellular space by equilibrative nucleoside transporters (ENT). As adenosine levels rise in the submucosa, the A_{2b} adenosine receptor is activated on MC, causing mediator release from these cells, which could then activate EC from the basolateral surface. CNT, concentrative nucleoside transporter. A_{2a} adenosine receptor inhibits MC degranulation.

The activation of A_{2a}R has inhibitory effects on many cell types, especially cells of the immune system (47, 48). The opposing effects of adenosine in different tissues results from co-expression of A_{2a}R with one or more of the remaining three receptor subtypes, which are differentially expressed depending on cell type, and species (47, 48). Under homeostatic conditions, constitutive adenosine levels downregulate MC activation by activating the high affinity A_{2a}R (46). However, under conditions of decreased metabolic fuel, or cellular stress, high extracellular concentrations of adenosine can stimulate the lower affinity A_{2b}R, which mediates activation of human MC (44, 49).

3. Mast cell mediators

MC are granular immune cells that are located at mucosal barriers and are involved in inflammation (50, 51). These cells play a key role in diseases such as asthma and allergies (52, 53). The granules of MC contain multiple inflammatory mediators such as histamine, heparin, and serine proteases. Once activated, MC can release these granules into the surrounding tissue (39, 40, 52, 54, 55). Activation of MC degranulation and can be induced by various stimuli, such as through A_{2b}R, FcεR1 and TLR-2 (21, 44, 56, 57) to name only a few. MC can also release a large number of newly formed pro-inflammatory mediators such as cytokines and lipid mediators, and modify their pattern of secretion based on the stimulus they receive (1, 17). Degranulation is associated with the early phase of inflammation, while release of some newly formed mediators is associated with late phase inflammation.



MC mediators are divided into four main classes: 1) granule associated preformed mediators, 2) de novo synthesized lipid derived mediators and 3) de novo synthesized cytokines/chemokines and growth factors and 4) oxygen radicals (Figure 1.5) (10, 40, 58). MC have the ability to differentially synthesize mediators based on their microenvironment, as well as the stimulus they receive, such as TLR agonists, FcεR1 or FcγR1 aggregation (1, 10, 11, 36, 59-61). This means that not all MC will produce all mediators listed in Figure 1.5 upon any given stimulus, but rather selectively release mediators to appropriately deal with a given situation in a given tissue. Because of this arsenal of potent biologically active mediators, MC have long been considered key players in the induction of allergy and protection against certain unwanted parasites (10, 62). MC can also release mediators either through selective release of individual granules (63), through piecemeal degranulation (61) or multivesicular compound exocytosis, in which multiple granules fuse together before being released from the cell (64).

4. Mast cell secretory compartments

a) Granules

Mediator release from MC occurs from various subcellular compartments and is regulated by different mechanisms (Figure 1.6). MC granules are lysosome-related organelles which are synthesized by incorporation of material from intermediate granules called progranules (Figure 1.6) (65). MC granules have an acidic pH, and store mediators such as histamine, β-hexosaminidase (β-hex), and proteases such as tryptase and chymase. Upon stimulation of the cell by

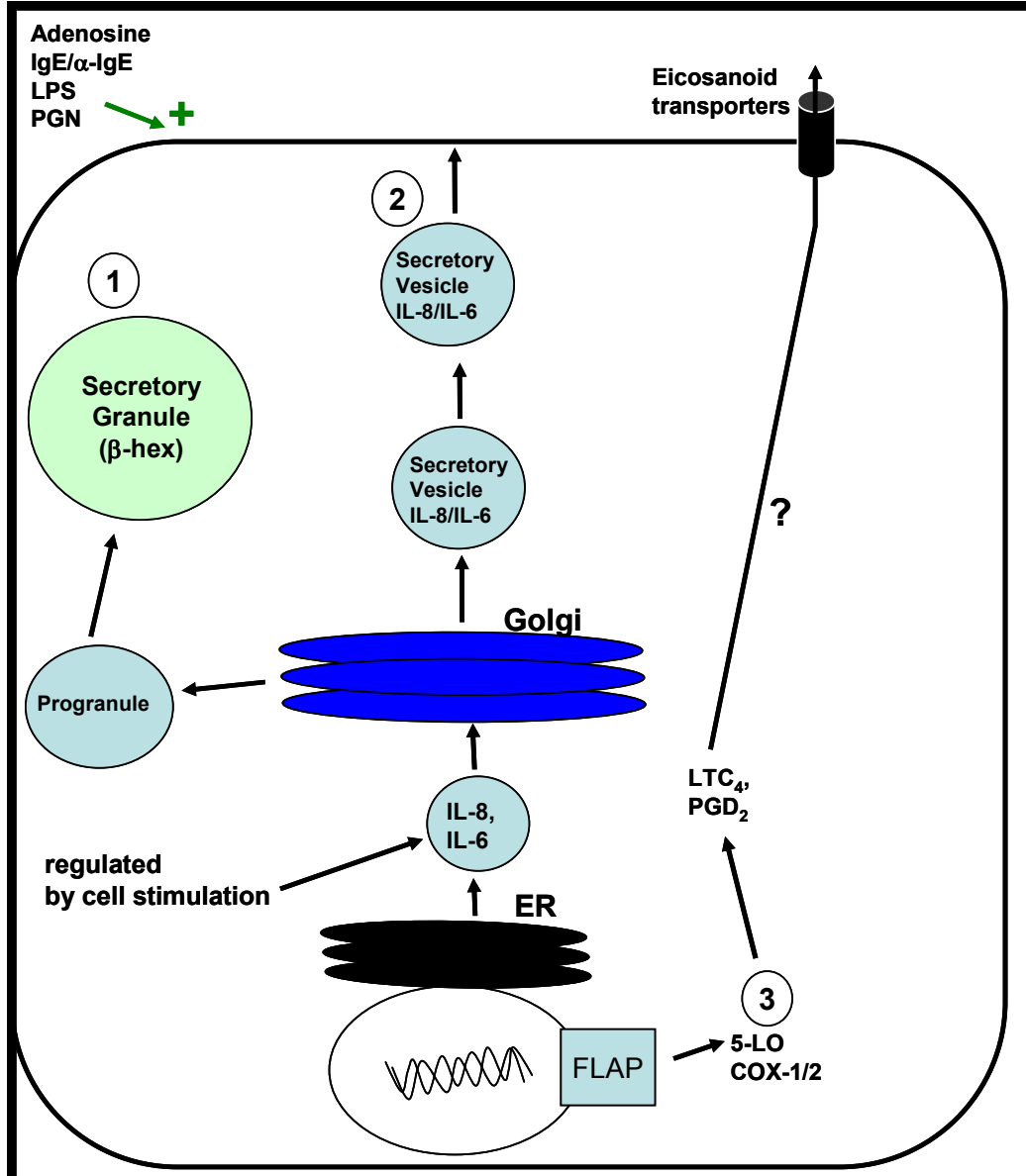


Figure 1.6 MC compartments and secretory mediators released from selected intracellular compartments. Three compartments were analyzed in this thesis. 1) Release of β -hexosaminidase (β -hex) from stored mediator compartment (secretory granules). 2) Cytokine release from newly synthesized mediator compartment which consists of small secretory vesicles whose trafficking and contents is regulated by cell stimulation. 3) Lipid mediator compartment. Lipid mediators leukotriene C₄ (LTC₄) and prostaglandin D₂ (PGD₂) are not secreted by secretory vesicles, but are transported to the outside of the cell by eicosanoid transporters which are not well described (66). 5-LO, 5-lipoxygenase; COX, cyclooxygenase. FLAP, 5-lipoxygenase activating protein.

mechanisms such as FcεR1 aggregation, a signalling cascade is initiated involving Ca^{2+} proteins of the synaptotagmin family, which initiates granule fusion with the plasma membrane and mediator release (65).

b) Small secretory vesicles

Another type of vesicle can form in MC called small secretory vesicles. The exact mechanism of formation of these vesicles has not been fully elucidated, but it is thought that proteins are specifically sorted to these vesicles in the Golgi, or that proteins not necessary in a specific vesicle are removed by budding off the secretory vesicles following release from the Golgi (65). Once sorted and packaged, these vesicles leave the Golgi and migrate to the plasma membrane where they fuse and release their content extracellularly. Some of these vesicles are not regulated by cell stimulation and carry constitutively synthesized and released cargo, whereas other small secretory vesicles are regulated by cell stimulation and only fuse to the plasma membrane upon stimulation of the cell, and carry inflammatory mediators such as CXCL8 (IL-8) and IL-6 (Figure 1.6).

c) Lipid mediators

Eicosanoids are not stored in granules or vesicles as are other mediators. Instead, following activation of the cells by external stimuli such as FcεR1 aggregation, phospholipase A₂ (PLA₂) translocates to the nuclear membrane and converts nuclear membrane phospholipids to arachidonic acid (figure 1.6) (66). Arachidonic acid then binds to 5-lipoxygenase activating protein (FLAP), which

is anchored to the nuclear membrane and supplies the lipids to 5-lipoxygenase (5-LO) for generation of LTA_4 and subsequently LTC_4 by a series of other enzymes. Prostaglandin D_2 (PGD_2) is synthesized in much the same way, but synthesis is mediated by the nuclear membrane anchored enzymes cyclooxygenase (COX)-1 and -2 (66). Once synthesized, LTC_4 and PGD_2 are released from the cells through an unidentified transporter (66).

5. Mast cells in innate immunity and homeostasis

It is becoming increasingly evident that MC have a sentinel role in the innate immune system, and their presence is critical in the recruitment of neutrophils and other immune cells in response to bacterial invasion (16, 39). Mast cells are multifunctional tissue dwelling cells critical in maintaining tissue integrity and function through the production of growth factors, angiogenic and neurogenic factors such as granulocyte macrophage-colony stimulating factor (GM-CSF), vascular endothelial growth factor (VEGF) and NGF respectively (1, 67, 68). They can promote homeostasis by participating in wound healing and tissue remodelling (69, 70). They are also strategically located at many anatomical sites of potential entry by pathogens, and serve in the first line of defense against invading pathogens (39, 67). When stimulated by pathogen associated molecular patterns (PAMP) from these organisms, MC become less responsive to $\text{Fc}\epsilon\text{R1}$ activation, and upregulate genes associated with innate immunity (71-74). MC and their production of neutrophil chemotactic factors such as tryptase, IL-8 and PAF are critical for the recruitment of neutrophils to the

site of bacterial infection (39, 75, 76). MC also have a key role in the recruitment of neutrophils in autoimmune diseases (77, 78). MC can differentially release cytokines depending on which stimulus activates the cell. For example, rat MC activated by LPS through TLR-4 secrete TNF without degranulating, while TLR-2 activation by PGN induces degranulation (79, 80). Furthermore, LPS induces secretion of TNF, IL-1, IL-6 and IL-13 from rat MC, whereas PGN induces secretion of IL-4, IL-6 and IL-13, but not IL-1 or TNF (81).

6. Mast cells in disease

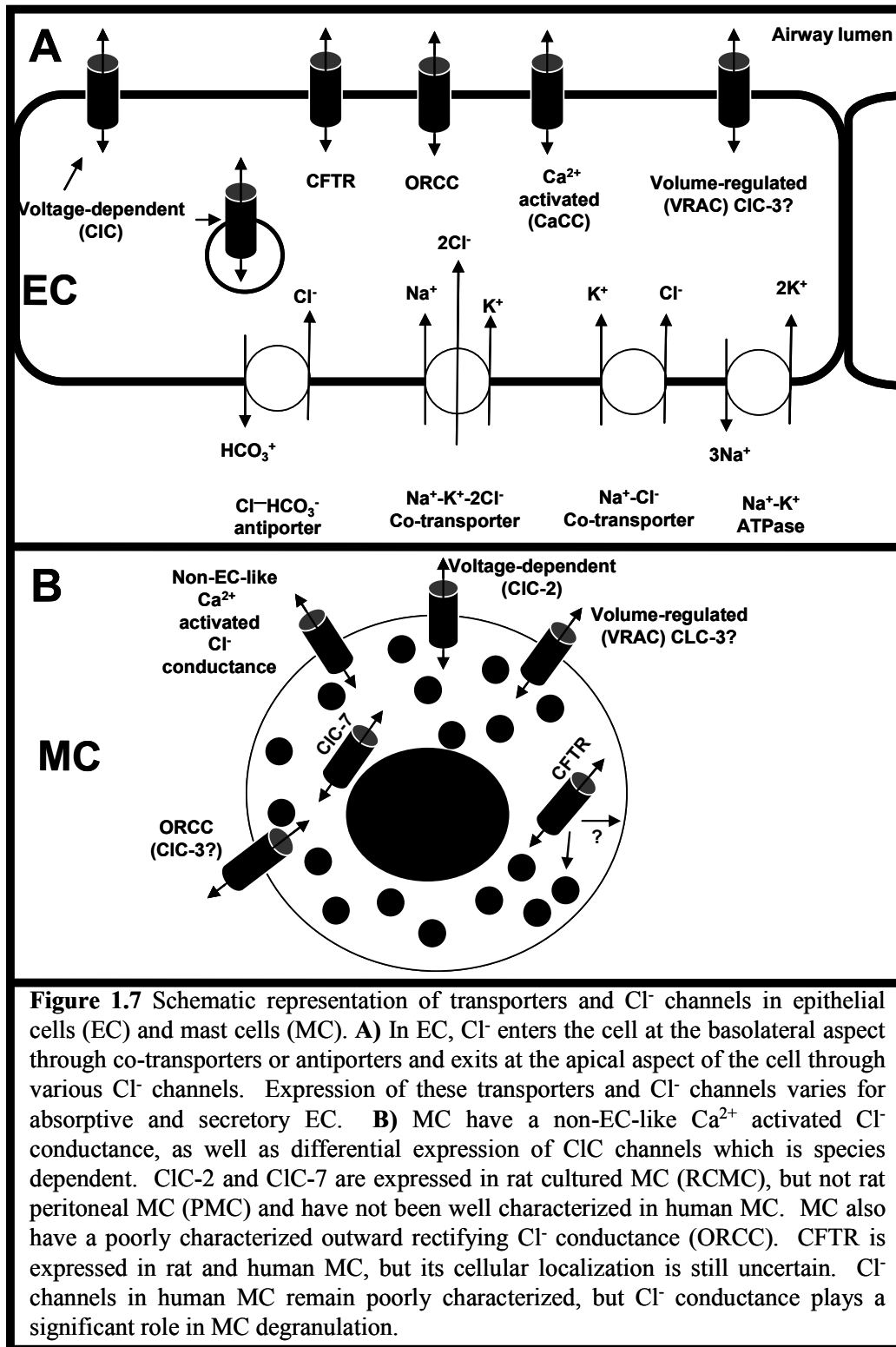
MC are implicated in many diseases including chronic bronchitis, atopic dermatitis, systemic mastocytosis, atherosclerosis, inflammatory bowel disease, cancer, allergies and asthma (82-87). MC have long been known to be key players in the initiation and propagation of both the early and late phase of the allergic response through production of histamine, cytokines and lipid mediators such as LTC₄ and PGD₂ (Figure 1.5)(29, 61). MC numbers are increased within airway smooth muscle of asthmatic patients, which is thought to facilitate airway hyperresponsiveness through localized mediator release or direct cell-cell contact (83). MC produce IL-4 and IL-5, classical TH2 cytokines that can induce B-cell class switching to IgE, and enhance eosinophil survival (88, 89). Furthermore, MC can also produce pro-inflammatory cytokines such as TNF, and IL-6, as well as neutrophil chemotactic factors tryptase, CXCL8 (IL-8) and platelet activating factor (PAF) (40, 75, 76, 89). MC have been shown to produce IL-13, which promotes airway hyperresponsiveness (75, 89).

Recently, adenosine was implicated as an important mediator in allergic asthma (45, 90). Elevated adenosine levels have been measured in exhaled breath condensates of asthmatic patients (91), and inhaled adenosine in these patients causes marked airway bronchoconstriction (45). It has been suggested that adenosine is a better diagnostic tool for asthma than methacholine, because non-asthmatics do not respond to inhaled adenosine (45). The bronchoconstriction to inhaled adenosine results from activation of MC in the airway mucosa (21). Adenosine causes histamine and spasmogenic leukotriene release from MC, which both act as potent bronchoconstrictors (48).

B. Introduction to mast cell Cl⁻ channels

1. Overview of mast cell Cl⁻ conductance

Chloride channels are the most abundant anion channels in mammals, since Cl⁻ is the most abundant extracellular anion (92). Cl⁻ channels play a significant functional role in many cell types, regulating such things as intracellular pH, cell cycle, cell volume, apoptosis, synaptic transmission and cell excitability (92). Many types of Cl⁻ channels have been described, including voltage dependent chloride channels (ClC) channels, protein kinase A (PKA)/nucleotide dependent cystic fibrosis transmembrane conductance regulator (CFTR), Ca²⁺ dependent Cl⁻ channels (CaCC), volume regulated Cl⁻ channels (VRAC), ligand gated Cl⁻ channels such as gamma amino butyric acid (GABA), and outwardly rectifying Cl⁻ channels (ORCC), which are defined only



functionally so far (Figure 1.7) (92, 93). Most of these channels have been described in epithelial cells (EC), but the expression of Cl^- channels in MC is not well characterized because of MC heterogeneity. To date, several different types of Cl^- channels have been described on various MC of rodent and human origin (14, 93-101).

MC degranulation is dependent upon ion flux, particularly Ca^{2+} influx; as such any ion currents (including Cl^-) that modulate the flow of Ca^{2+} into MC will directly affect its secretory activity (102). In MC, stimulation through $\text{Fc}\epsilon\text{R1}$ mechanisms induces significant Cl^- uptake by the cell regulating volume and excitability (96, 99). It has been shown that hyperpolarization of the plasma membrane is required for full MC excitability as negative membrane potentials drive Ca^{2+} entry into the cell (98). To maintain membrane hyperpolarization during activation, MC utilize Ca^{2+} -dependent K^+ efflux through large conductance $\text{K}_{\text{Ca}}^{2+}$ as well as Ca^{2+} -independent Cl^- influx through Cl^- channels to counteract the depolarizing effect of Ca^{2+} influx into the cytoplasm (14, 96, 97, 100, 101, 103). Several substances have inhibitory effects on several inflammatory cells including MC (104, 105). One such compound is sodium cromoglycate, which is derived from toothpickweed (*Ammi visnaga*) (104). This compound has long been used as a MC stabilizer which inhibits MC Cl^- channels preventing hyperpolarization and degranulation (104-106).

While Ca^{2+} -independent outwardly rectifying Cl^- channels are only functionally defined, they have been shown to exist in cells of non-epithelial origin (92). In 1989, a report was published describing a Ca^{2+} -independent and

cAMP-dependent Cl^- conductance in rat PMC (14). This Cl^- conductance took tens of seconds to develop, was sensitive to 4,4'-diisothiocyano-2,2'-stilbene disulphonic acid (DIDS) in a patch clamping assay, and responded to the non-hydrolyzable guanine triphosphate- γ -S (GTP- γ -S), suggesting that a G-protein was involved in the development of this conductance. This report also showed that activation of the Cl^- conductance made the cell more responsive to stimulus through hyperpolarization mechanisms (14). Our previous work on rat peritoneal MC (PMC), as well as our observations of CFTR expression in rat PMC (Appendix 2), suggest that this 1989 report was measuring a CFTR current in MC, and that CFTR regulates secretion of preformed inflammatory mediators from MC granules (107).

At rest, MC are electrically silent, but activation of Cl^- channels during cellular activation acts to clamp the membrane potential at around -40 mV, maintaining the driving force for Ca^{2+} entry into the cell (96, 98). Blocking Cl^- conductance by DIDS or 5-nitro-2(3-phenylpropyl-amino) benzoate (NPPB) prior to activation of the cell by antigen downregulated degranulation of MC (96, 100). Recently, we showed that pharmacological inhibition of CFTR using diphenylamine-2-carboxylate (DPC) in PMC inhibits IgE-induced secretion of β -hex (107). MC CFTR was sensitive to cAMP stimulation and inhibition by DPC and glibenclamide, typical features of CFTR (108). As CFTR inhibitors had no effect on β -hex release if cells were stimulated with the Ca^{2+} ionophore A23187 or compound 48/80, this suggests that CFTR-mediated Cl^- conductance plays a role in antigen-mediated degranulation of MC, but not mediator secretion induced

by all secretagogues (108). The above evidence suggests that mutant CFTR could cause long term changes in signalling in MC, which could contribute to the excessive inflammatory response seen in CF patients. From this information it is reasonable to associate CFTR with MC secretion, and potentially implicate MC in CF pathology (see below).

a) ClC chloride channels

There are nine different genes that encode for ClC channels (92). These channels are widely expressed in many cell types (109). They are voltage-gated chloride channels and most are expressed intracellularly with the exception of ClC-1, 2 and 3 which are found on the plasma membrane (92, 109). Depolarization activates the fast gating ClC-1, whereas hyperpolarization triggers a slow gating, inwardly rectifying ClC-2 (92). The kinetics and pharmacology of all ClC channel family members, and their physiological role is still incompletely understood, and their gating mechanisms and structures are complex (92). It is thought that many ClC act as antiporters and regulate organellar pH by exchanging Cl^- for H^+ (109). ClC-1 is only expressed on skeletal muscle, whereas ClC-2 is thought to be ubiquitous (92). ClC-4 has been shown to be co-localized with CFTR in enterocytes (110). ClC-5 and 7 have been shown to regulate ionic composition of intracellular compartments, whereas ClC-3 is important in the regulation of cell volume (96, 101). The activity of ClC-3 is enhanced by cell swelling, but inhibited by PKC activation (92). Some of the ClC channels such as ClC-3, 4 and 5 show strong outward rectification, and may be the elusive ORCC

channels described in MC (92, 111). In our lab, we previously tested for the presence of mRNA for ClC-1 to 7 as well as protein expression of ClC-2, 3 and 7 in rat PMC and rat cultured MC (RCMC). We showed that RCMC expressed mRNA for ClC-2, -3, -4, -5 and -7, and protein expression for ClC-2, and -7, whereas rat PMC expressed mRNA for ClC-7 but did not express protein for any of the ClC tested (111).

b) GABA receptors

The GABA_A receptor is a protein complex composed of heteromeric units forming a Cl⁻ channel (112). It is abundant in the brain. Recently, MC have been found to express mRNA for the α -1, 3, 4, 5, β -1, 2, 3, and γ -1, 2, 3 subunits of the GABA_A receptor (113). The only subunit that was detected by Western blot was α -1 and GABA treatment of MC inhibited IgE-dependent degranulation (113). However, it is unknown whether these subunits form a functional GABA Cl⁻ channel on MC.

c) Ca²⁺ activated Cl⁻ channels (CaCC)

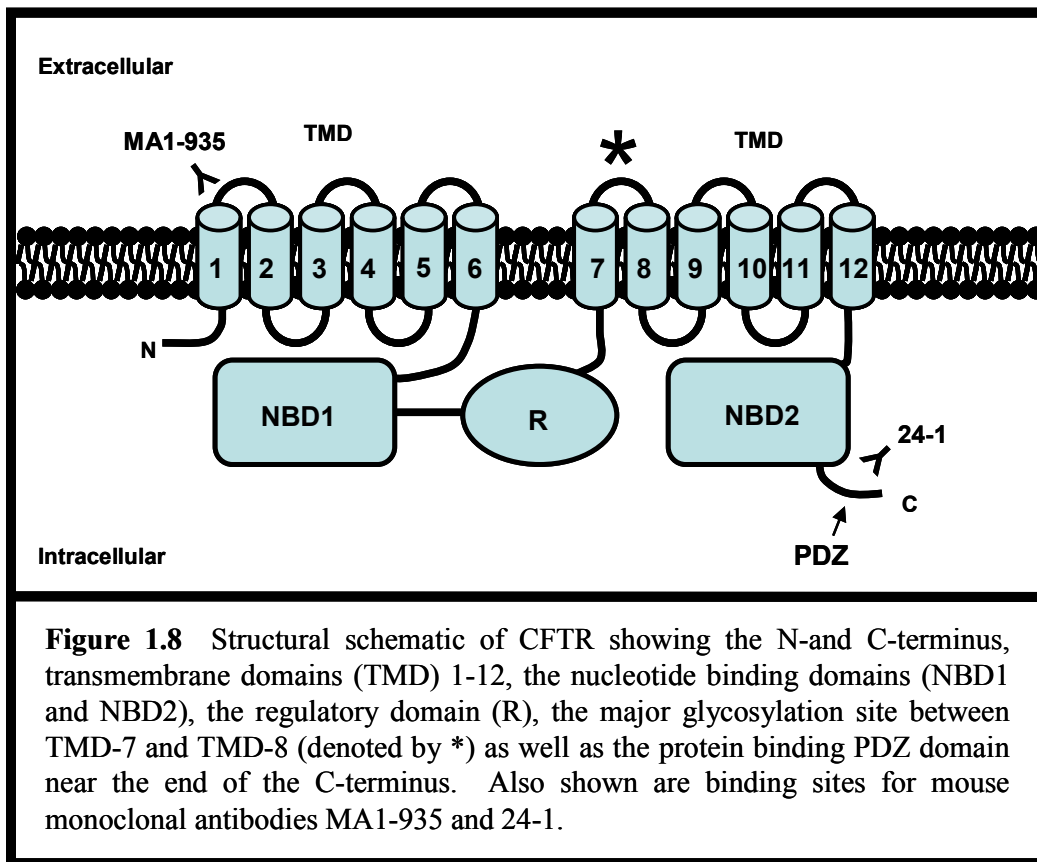
Many excitable and non-excitable cells express CaCC (92). These channels are small conductance, outwardly rectifying channels that alter the polarization of the plasma membrane in response to Ca²⁺, and are often coupled to the activity of voltage gated Cl⁻ channels (92). The molecular characteristics of these channels is not resolved (92). MC display Ca²⁺ activated Cl⁻ conductances that are not characteristic of EC or neuronal Ca²⁺ activated Cl⁻ conductances, and

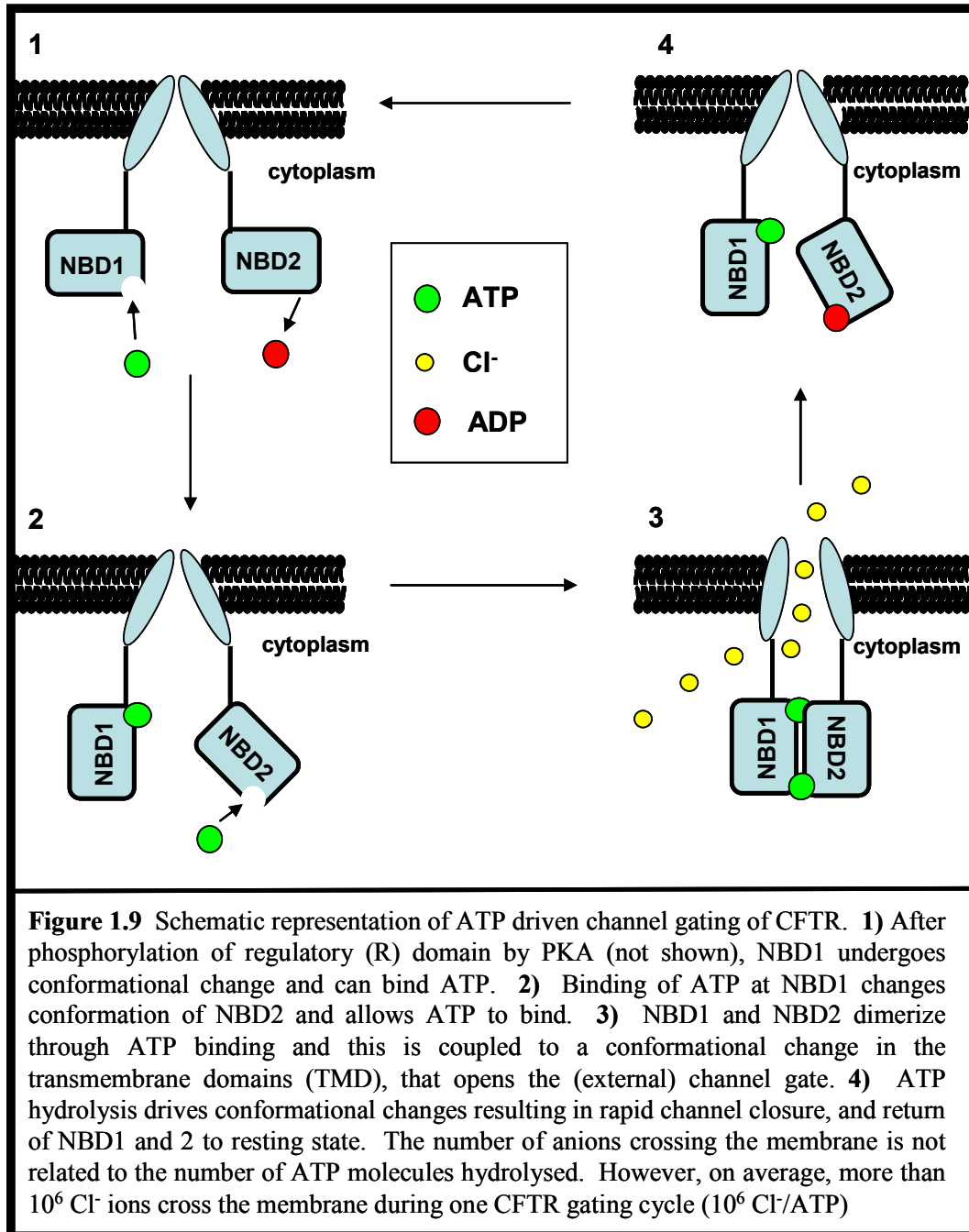
thus likely occur through an as yet unidentified Cl^- channel (96, 97, 101). Several studies have identified outwardly rectifying Cl^- conductances in MC, which are activated by immunological stimulation of the cells (93, 95, 97). Another study screened human MC from various sources for Ca^{2+} activated Cl^- , but did not find expression of Ca^{2+} activated Cl^- channels seen in EC (101).

C. Introduction to CFTR

1. CFTR structure and function

CFTR, also known as ABCC7, is a member of the ATP binding cassette (ABC) family of transporters, which are membrane-spanning proteins that couple ATP hydrolysis to the transport of molecules (Fig 1.8) (92, 114, 115). This protein possesses two membrane-spanning domains (MSD), each containing six alpha helices linked by a PKA/PKC sensitive intracellular regulatory (R) domain, which is unique to this member of the ABC family (92). To couple ATP hydrolysis to molecular transport, CFTR has two cytoplasmic nucleotide binding domains (NBD) (116). CFTR is thought to open by PKA phosphorylation of the regulatory domain, which causes ATP binding to NBD1. Binding of ATP on NBD1 causes a conformational shift in NBD2, which allows binding of ATP to NBD2. The two NBDs then bind to each other and this opens the channel, allowing Cl^- to flow through (Fig 1.9) (92, 117).





Hydrolysis of ATP by CFTR causes another conformational change, which results in rapid pore closure and inactivation of the channel (7, 115). Thus, the rate of binding of ATP at NBD1 controls the frequency of channel activity, whereas the rate of hydrolysis at NBD2 controls the duration of channel activity (7). It has been shown that regulating CFTR activity by PKA and PKC phosphorylation modifies a number of different cellular processes (118-124). Thus, functions of CFTR not obviously associated with ion channelopathy are becoming increasingly well recognized, but there is much controversy about these “regulator” functions and how CFTR acts to regulate cell function intracellularly.

2. CFTR mutation classes and disease severity

There are now over 1600 reported mutations in CFTR. These mutations can be divided into five classes based on the defect resulting from the mutation (Figure 1.10) (125). There is a useful website on CFTR mutations (<http://www.genet.sickkids.on.ca/cftr/>) that gives a comprehensive list of the mutations, their location on the gene, along with the most common mutations around the world and their ethnic prevalence. There is also a wealth of useful links for CFTR research. Much research has focused on abnormal synthesis, processing, recycling and degradation of mutant CFTR in various cellular compartments, but there are also mutations that affect CFTR activation and transport of anions.

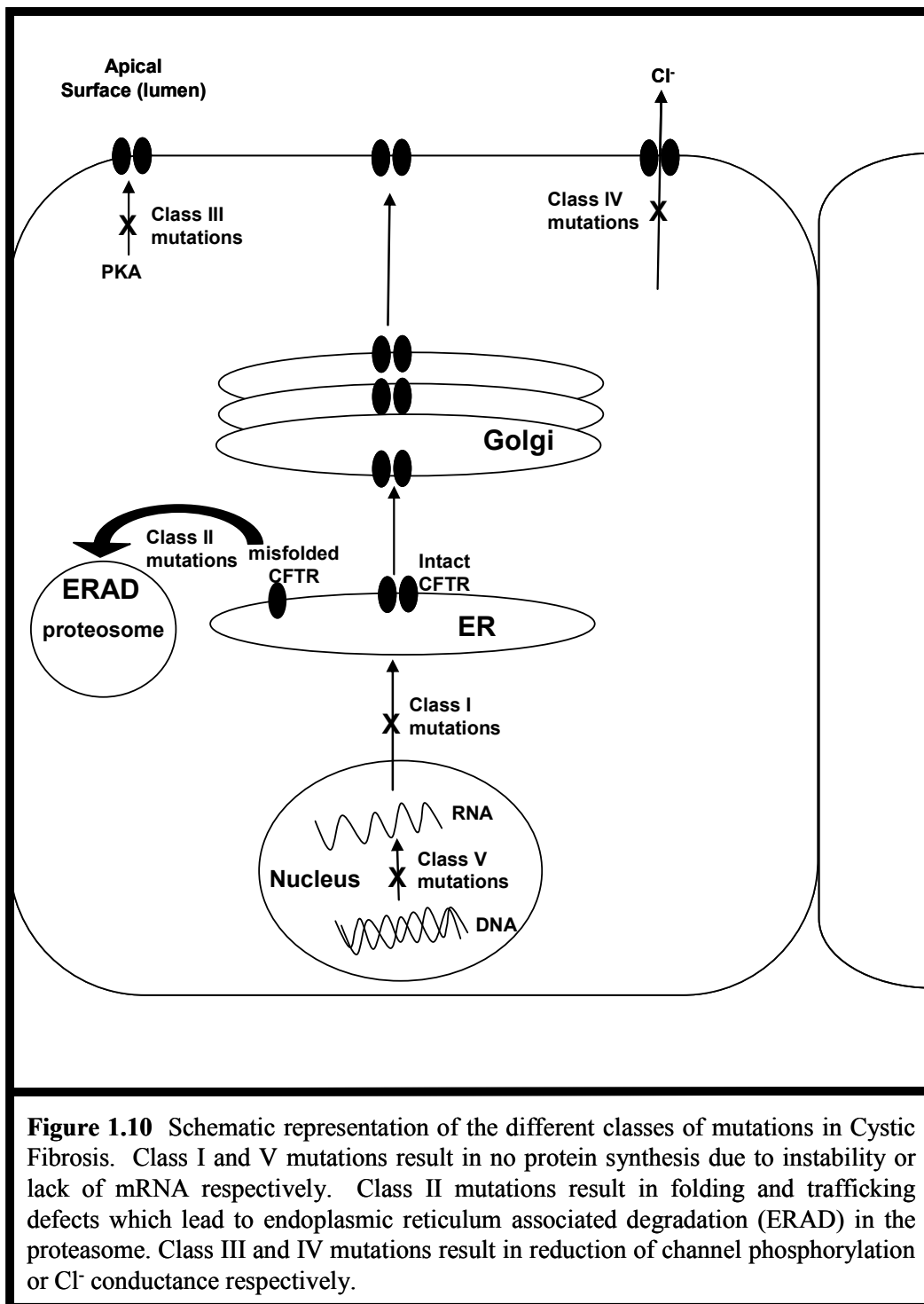


Figure 1.10 Schematic representation of the different classes of mutations in Cystic Fibrosis. Class I and V mutations result in no protein synthesis due to instability or lack of mRNA respectively. Class II mutations result in folding and trafficking defects which lead to endoplasmic reticulum associated degradation (ERAD) in the proteasome. Class III and IV mutations result in reduction of channel phosphorylation or Cl⁻ conductance respectively.

a) Class I mutations

Class I mutations of CFTR result in the absence of the protein in the cell (125). mRNA transcripts are present in the class I mutation, but the mRNA is unstable and not translated into protein. Reading frame shifts insert premature stop codons in the mRNA, resulting in translational arrest (125). There are several point mutations that result in this translational arrest, but the most common example is the G542X mutation, which is the most prevalent CFTR mutation in people of Spanish descent (<http://www.genet.sickkids.on.ca/cftr/>). Class I mutations result in severe clinical manifestations, including early onset pancreatic insufficiency and progressive lung disease (125). Interestingly, aminoglycoside antibiotics such as Geneticin (G418) and neomycin can cause read through of the stop codon, and partially rescue CFTR translation (125-127).

b) Class II mutations

Class II mutations result in alterations of the three dimensional structure of CFTR. These mutations result from changes or deletions of amino acids, which change the way that the protein folds or interacts with endoplasmic reticulum (ER) chaperones (92, 125). Class II mutated CFTR completes translation in the ER, but is retained or inefficiently trafficked to the Golgi, which triggers the unfolded protein response and ER-associated degradation (ERAD) of the protein (125, 128-130). The most common class II mutation is the delta F508 ($\Delta F508$), which is a deletion of the phenylalanine at position 508. This deletion prevents the first NBD from folding, resulting in 99% of the protein being targeted for

ERAD (129, 130). Class II mutations are associated with severe lung pathology, and have been overcome by chemical chaperones, or by lowering the temperature at which cells were incubated (131) (132). However, because of the low temperature or the high concentrations of these molecular chaperones required to rescue CFTR expression *in vitro*, these therapies remain impractical in patients (125).

c) Class III mutations

Class III CFTR mutations disrupt activation and regulation of plasma membrane expressed CFTR (125). For example, G551D CFTR localizes to the plasma membrane, but exhibits deficient ATP binding and Cl⁻ conductance in response to cAMP (125, 133, 134). Many class III mutations are associated with pancreatic insufficiency, and severe phenotype (125). Other class III mutations can also result in decreased R domain phosphorylation, or ATP hydrolysis (125). Molecules which can activate CFTR channel function such as genistein or therapies that restore these functions may alleviate the symptoms associated with class III mutations (125, 135).

d) Class IV mutations

Class IV mutations have normal synthesis, folding and trafficking to the plasma membrane, but display reduced Cl⁻ conductance due to defects of channel gating. These mutations occur in regions of the molecule that form the ion pore (125). An example of this class of mutation is R347P, which affects the attraction

of Cl⁻ into the pore and reduces Cl⁻ flow through the channel (125). Other mutations such as R117H result in reduction of channel open time (125). These mutations are associated with mild pancreatic insufficiency (125). Type III phosphodiesterase (PDE) inhibitors such as Milrinone which are specific for PDE3, or adenosine nucleotides combined with IBMX, have been shown to induce Cl⁻ currents in class IV mutants such as R117H and A455E, suggesting that agents that prolong cAMP elevation in cells may be beneficial for treating class IV mutations by encouraging CFTR activation (125, 136).

e) Class V mutations

Class V mutations result from changes in the CFTR promoter, introns that regulate mRNA splicing, or amino acid substitutions that reduce the amount of normal CFTR protein expression (125). Most of the mutations in this class are alternatively spliced mRNA transcripts such as 3849 + 10kbC→T which creates a partially active splice site in intron 19, inserting an 84 bp segment containing a stop codon between exon 19 and exon 20 (125, 137). Therapeutic strategies for this type of mutation have included agents such as mitomycin C which elevate the production of CFTR mRNA (125, 138).

3. Regulation of CFTR expression

a) Regulation of transcription

The precise mechanisms of the regulation of CFTR expression are slowly being elucidated. Regulation of CFTR expression is highly complex and begins

at the chromosomal level (139). CFTR shows a tightly regulated pattern of temporal and cell-type specific expression, which likely involves regulation by epigenetic mechanisms (139, 140). The CFTR promoter has a cAMP response element (CRE) and several glucocorticoid response elements (GRE) (139). The promoter also has binding sites for several transcription factors, including the cAMP CCAAT-enhancer binding protein (C/EBP), as well as NF-kB, Sp1, hGCN5, ATF-1 and CBP (139). Hormones have also been shown to affect CFTR expression in female rodents, with maximal expression during the pro-oestrus phase (141). Studies have also reported multiple transcriptional start sites in the promoter, depending on cell type and fetal vs adult CFTR gene (139, 142). CFTR introns 1, 2, 3, 10, 16, 17a, 18, 20 and 21 all have DNase hypersensitive (DHS) sites. Only the DHS site in intron 1 was present in all cell lines tested in (139, 143, 144). Intronic regulation of gene expression is not uncommon, and has been reported for heat shock protein-47 (hsp47), collagen-binding heat shock protein, flk-1, angiotensin II, protein C, troponin 1 and acetylcholinesterase (143). Thus, there may be transcription factor binding sites in these introns that may be active or inactive depending on cell type or epigenetic regulation.

b) Regulation of translation

Another important layer of regulation for CFTR expression is mRNA stability. This regulation has also been shown to be stimulus and cell type dependent (145). The regulation of CFTR mRNA stability is dependent on AU rich element (ARE) binding proteins (AREbp) such as HuR1 or tristetraprolin

(TTP), which are activated by MAP kinases (MAPK) and act as mRNA stabilizers or destabilizers (145, 146). Many AREbp-mRNA interactions are induced by cytokine signalling. In Calu-3 EC, IL-1 β has been shown to destabilize CFTR mRNA in a p42/44 MAPK-dependent fashion, whereas in HT-29 EC, TNF was shown to destabilize CFTR mRNA in a p38MAPK-dependent fashion (145). Thus, CFTR expression may be tightly regulated by cytokine signals such as IL-1 β , which has been shown to be downregulated in bronchoalveolar lavage fluid (BALF) in CF (147).

c) Post-translational modifications

In EC, fully glycosylated mature CFTR is 1480 amino acid residues with a molecular weight (MW) of 168.14 kilodaltons (kDa) predicted by computer modelling (Protparam: ExPASy online tools). The mature protein is N-glycosylated and matures from a non-glycosylated nascent protein in the endoplasmic reticulum (ER) (band A), becoming core glycosylated in the ER (band B), and fully glycosylated (band C) by further N-glycosylation in the Golgi apparatus (148, 149). During synthesis, the nascent CFTR protein enters the endoplasmic reticulum through the ribosome-translocon complex (band A) and is co-translationally N-glycosylated with high mannose residues for recognition by chaperone proteins of the folding machinery (band B) (149, 150). CFTR is then shuttled to the Golgi where it is further glycosylated to its mature state (band C). The experimentally reported MW of the three forms of CFTR varies widely in the literature, ranging from 127-130 kDa for band A, , 130-150 kDa for band B and

160-200 kDa for band C (148, 149, 151-160). Thus from the immature to the mature form of CFTR, there is a reported molecular weight range of 127-200 kDa.

4. CFTR protein interactions

The regulation for CFTR expression involves trafficking to the plasma membrane from the ER and Golgi. This regulation occurs through protein-protein interactions between CFTR and its chaperones. It has recently been shown in EC that CFTR can bind to many proteins and that these binding partners act in concert with CFTR to regulate cell function. Binding partners for CFTR include ion channels, transporters, kinases, phosphatases, receptors, trafficking proteins and cytoskeletal elements (Figure 1.11) (161). CFTR can bind to proteins either at its N-terminal or C-terminal ends, depending on the proteins. Syntaxin 1A and SNAP-23 have been shown to interact with CFTR and downregulate its function (162, 163). Whereas the N-terminal end of CFTR tends to associate with these SNAP receptor (SNARE) proteins, the C-terminal end can associate with many trafficking and cytoskeletal proteins via its post synaptic density protein (PSD95), *Drosophila* disc large tumor suppressor (DlgA), and zonula occludens-1 protein (zo-1) (PDZ) binding domain. PDZ proteins mediate homotypic and heterotypic binding of proteins carrying the PDZ binding domain (Figure 1.11) (161).

Five PDZ proteins have been reported to bind to CFTR: Na⁺/H⁺ exchange regulatory factor (NHERF)1, 2, NHERF-3 (E3KARP/CAP70), CFTR associated ligand (CAL) and NHERF-4 (IKEPP) (161). CAL and NHERF-3 are trafficking proteins with opposing effects on CFTR expression (161). NHERF proteins anchor CFTR to the cytoskeleton and to the β_2 adrenergic (β_2 AR) and A_{2b}R (164-166). Loss of these PDZ interactions results in dysregulation of CFTR trafficking (167). The β_2 AR and the A_{2b}R are expressed by human MC (49, 168), but it remains unknown whether they associate with CFTR as has been shown in EC (169). Others have reported that CFTR can bind directly to clathrin-forming protein complexes (AP-2), and to AMP kinase (AMPK) as well as to PKA through ezrin binding (161, 170, 171). AP-2 seems to regulate CFTR endocytosis, whereas AMPK binding inhibits CFTR function, and ezrin sequesters PKA near CFTR for activation (161).

Through its PDZ domain, CFTR seems to be a negative regulator of the transcription factor NF- κ B in EC, as it has been shown that CFTR deficient EC have constitutively high levels of active NF- κ B and hypophosphorylated I κ B- β resulting in increased IL-8 production (172, 173). Interestingly, a recent study has linked CFTR to NF- κ B signalling and production of RANTES via an ezrin-dependent pathway (174). This study showed that CFTR insertion into the plasma membrane and intact C-terminus of CFTR and ezrin binding protein of 50 kDa (EBP50) are required for proper immune signalling via NF- κ B and AP-1 (174). Furthermore, the authors suggest that EBP50 may act as a scaffolding protein linking CFTR to NF- κ B binding and RANTES expression. Similar

pathways may be dysregulated in CF, resulting in NF- κ B-dependent inappropriate production of cytokines such as IL-8 and IL-10 (175, 176). Interestingly, it has also been shown that cAMP can activate certain signaling pathways in a PKA independent manner, such as guanine nucleotide exchange factors (GEF)-like proteins that can cross talk with MAPK kinase pathways and activate NF- κ B, leading to excess mediator secretion (177). Thus, it is possible that lack of CFTR leads to loss of PKA sequestration, and inappropriate activation of NF- κ B signalling pathways.

5. Pharmacological inhibitors

The most widely used CFTR blockers such as 5-nitro-2(3-phenylpropyl-amino)benzoate (NPPB) and diphenylamine-2-carboxylate (DPC) are open channel blocking anions, which are attracted to the large inner vestibule of the intracellular CFTR pore by positively charged residues such as Lys95 (Table 1.1) (178-180). NPPB and DPC are voltage and pH dependent arylaminobenzoate blockers of CFTR (178, 180, 181 #1254) capable of crossing the plasma membrane by non-ionic diffusion to access their binding site in the inner vestibule of the CFTR pore (179, 182). It has been shown that upon addition of the drugs to cells, 50-95% of the drug makes it through the plasma membrane (179, 180). The use of these inhibitors to block CFTR is controversial because some studies report good specificity (182, 183), while others report non-specific effects such as inhibition of cAMP and COX at doses between 300-1000 μ M (179, 184-186). Glibenclamide, another open channel blocker, inhibits CFTR by complex allosteric interactions with the NBD and inhibition of phosphorylation by PKA or

PKC, preventing the pore from opening (180, 187). Despite the many known CFTR inhibitors, issues of specificity and potency have remained an intractable problem (188), until the recent discovery of several new, more specific CFTR inhibitors such as N-(2-naphthalenyl)-[(3,5-dibromo-2,4-dihydroxyphenyl)methylene]glycine hydrazide (GlyH-101) (189) and 3-[(3-trifluoromethyl)phenyl]-5-[(4-carboxyphenyl)methylene]-2-thioxo-4-thiazolidinone (CFTR_{inh-172}) (182, 187-193) (Table 1.1). CFTR_{inh-172} is a thiazolidinone drug highly specific for CFTR, but its main drawback is its limited solubility in water (about 5 μ M), slow rapidity of action, and probable effect on Na⁺ transport (187-189). For these reasons, the search continued for better CFTR inhibitors, and recently GlyH-101, was discovered (187, 189). Unlike all other known CFTR inhibitors, GlyH-101 blocks CFTR by occlusion of the pore on the extracellular side of the membrane (187, 189). GlyH-101 overcomes the solubility problems of CFTR_{inh-172}, (1 mM in water) (187, 189), and has a novel mechanism of action, and no reported non-specific effects, which makes it the best blocker of CFTR available (189). Disulfonic stilbenes such as DIDS are structurally related to glibenclamide (183) and block CFTR only from the cytoplasmic side of the membrane, with no affinity for the extracellular pore (183). DIDS is unable to cross the plasma membrane by diffusion and has profound inhibitory effects on Cl⁻ conductance from other Cl⁻ channels such as the K⁺/Cl⁻ co-transporter (179, 180).

Table 1.1 Commonly used CFTR inhibitors and their characteristics. NPPB, 5-nitro-2(3-phenylpropyl-amino)benzoate; DPC, diphenylamine-2-carboxylate; CFTRinh-172, 3-[(3-trifluoromethyl) phenyl]-5-[(4-carboxyphenyl)methylene]-2-thioxo-4-thiazolidinone; GlyH-101, N-(2-naphthalenyl)-[(3,5-dibromo-2,4-dihydroxyphenyl) methylene]glycine hydrazide; DIDS, (4,4'-diisothiocyano-2,2'-stilbene disulphonic acid).

Inhibitor	IC₅₀	Commonly used Doses	Binding site	Specific activities	Possible non-specific activities
NPPB	40 μ M	50 μ M	Pore inner vestibule	Open channel blocker	cAMP inhibition, Eicosanoid inhibition $\text{Na}^+/\text{K}^+/\text{2Cl}^-$ transporter inhibition
DPC	26 μ M	10-1000 μ M	Pore inner vestibule	Open channel blocker	cAMP inhibition, Eicosanoid inhibition $\text{Na}^+/\text{K}^+/\text{2Cl}^-$ transporter inhibition
CFTR _{inh} -172	300 nM	5-20 μ M	Pore inner vestibule	Open channel blocker	Decreased Na^+ conductance
GlyH-101	5 μ M	10-50 μ M	Outer pore	Open channel blocker	None reported
DIDS (patch clamp only)	30 μ M	1.6-300 μ M	Pore inner vestibule	Non-selective Cl^- conductance inhibitor	General decrease in Cl^- conductance and may affect cytosolic Ca^{2+} levels

6. CFTR in non-epithelial cells

CFTR has long been considered to be exclusively expressed in EC, but evidence is emerging that many other cell types express CFTR (Table 1.2). In some non-EC cell types, abundance of CFTR mRNA transcripts is 200 to 400 fold lower than in EC (194, 195). In many cell types, the Cl^- transport function of CFTR contributes to the regulation of cellular processes, for example, in capacitation of mouse spermatozoa or membrane depolarization and growth rate of fibroblasts (194, 196, 197). The protein binding capacity of CFTR also likely plays a significant role in cell signalling in many cell types, and the fact that the cause of the chronic inflammation in CF remains controversial strengthens this hypothesis. Furthermore, there is evidence that inflammation in lungs of CF patients can occur at an early age, even in the absence of infection, suggesting that cell types other than EC play a role in the pathophysiology of CF (198-200). Our recent work on MC and CFTR (107, 201), combined with that of others discussed below, suggests several regulatory roles for CFTR in cells of non-EC origin. Indeed, the polyfunctionality of CFTR has been the subject of considerable discussion, both in EC and in non-EC.

Table 1.2 CFTR expression in cells of non-EC origin. Low expression levels is denoted by the symbol \pm

Cell type	mRNA expression	Protein expression
Monocytes	+	+
Macrophages	+	+
T-Lymphocytes	\pm	\pm
B-Lymphocytes	+	+
Neutrophils	+	+
Cardiac myocytes	\pm	\pm
Hypothalamic neurons	+	+
Spermatozoa	\pm	+
Endothelial cells	+	+
Smooth muscle cells	+	+
Mast cells	\pm	\pm

a) Neutrophils

CFTR has been detected in neutrophils, and it has been shown that human neutrophils taken from lungs of CF patients display a dysfunctional phenotype (202, 203). Neutrophils taken from CF patient lungs undergo conventional activation, but were found to mobilize CD63⁺ elastase rich granules, and lose surface expression of CD16 and CD14, which are key receptors in phagocytosis (203). Furthermore, these cells express CD80, MHC class II, and the PGD₂ receptor chemoattractant receptor-homologous molecule expressed on TH2 cells (CRTH2) (DP-2), which were all normally associated with other cell lineages (203). CF neutrophils are inefficient at phagocytosing zymosan particles or killing *Pseudomonas aeruginosa*, when compared to non-CF controls (202, 204, 205). In mice with severe combined immune deficiency (SCID) given human fetal lung grafts, neutrophils infiltrated airways of CF grafts to a greater extent than non CF grafts, suggesting that CF mutations predispose to neutrophilic inflammation (206). Transgenic Δ F508 CF mice have a depressed anti-microbial response, as evidenced by reduced cellular uptake and clearance of *P. aeruginosa* and increased bacterial burdens (207). Mice with a G551D mutation in CFTR showed enhanced neutrophil accumulation in the lungs and their macrophages were hypersensitive to LPS exposure (208). These findings could partially explain the chronicity of inflammation in CF lungs.

b) Muscle

CFTR has been reported in cardiac myocytes, and appears to mediate β_2 agonist and cAMP-dependent Cl^- flux (209-212). CFTR expression in myocytes was detected in ventricular sub, mid and endocardium, but was not detected in the atrium (211, 212). Furthermore, protein levels of CFTR in these cells seems to be extremely low, such that nested PCR was required to detect mRNA transcripts (211, 212). Some researchers have reported CFTR expression in smooth muscle cells, and that the role of CFTR in these cells seems to be regulation of optimal Ca^{2+} release from sarcoplasmic reticulum and endothelium-independent vasorelaxation and bronchodilation (213-215).

c) Endothelium

CFTR was detected in endothelial cells of the cornea and lung (216, 217). In corneal endothelium, CFTR is responsible for maintaining corneal hydration and transparency, whereas in lung endothelium, CFTR seems to play an important role in regulation of the ceramide: sphingosine-1 phosphate ratio, which is linked to stress-induced apoptosis upon exposure to cellular stressors such as hydrogen peroxide (216). The authors of this study suggest that CFTR regulates lung vascular homeostasis by providing death signals to redundant cells (216).

d) Lymphocytes

There are a number of reports on CFTR expression in lymphocytes (194, 195, 199, 218-221). In these cells, CFTR seems to play a role in cAMP

dependent Cl^- currents (195, 199, 220, 221), as well as in secretion from these cells (218-220). It was also shown that B-cells deficient in CFTR had reduced immunoglobulin light chain secretion (218). Also, T-cells deficient in CFTR secreted lower levels of IL-10 and $\text{IFN}\gamma$ than normal T-cells in response to phorbol myristate acetate (PMA) or concanavalin A (ConA) stimulation (219, 220). One study showed that CFTR antisense oligonucleotide (ASO) treatment eliminated the cell-cycle-dependent Cl^- permeability, inducing a CF phenotype on the cells. However, the authors were unable to detect CFTR protein by Western blot or immunoprecipitation, and estimated that CFTR expression was 1000 fold lower in lymphocytes than in T84 EC (195).

e) Monocytes and macrophages

CFTR expression has also been detected in monocytes and macrophages (194, 222-226). The role of CFTR in these cells has been reported to be in regulation of acidification of intracellular organelles such as the endosomes and lysosomes. This hyperacidification interferes with proper regulation of endocytic compartment recycling of receptors such as the transferrin receptor (227). However, the direct involvement of CFTR in macrophage organelle hyperacidification has recently come under some criticism, and is no longer thought to be correct (228, 229). A more accepted model for the role of CFTR in hyperacidification is the indirect downregulation of nitric oxide cGMP signalling cascade (230, 231).

f) Neurons

CFTR expression was detected in hypothalamic neurons and heart ganglion cells, and seems to be involved in cAMP dependent Cl^- flux and the regulation of gonadotropin-releasing hormone (GnRH) secretion in the brain (232). The effects of normal CFTR on GnRH secretion have not been evaluated in the context of mutant CFTR, although it is interesting that delayed sexual maturation occurs in CF (232). This may result from a GnRH secretion defect which is linked to defects in CFTR signalling through its binding partner(s) in neurons.

Many of the above studies suggest that a CFTR plays a central role in the regulation of secretion of various mediators. These reports and Bradbury summarized the literature on compromised exocytosis and endocytosis associated with mutant CFTR (233). Thus, a common model of CFTR function associated with several types of secretory cells, not just EC is evident. If this is true, then MC are excellent models for study as professional secretory cells, and may contribute significantly to the pathology of CF if their secretion is dysregulated in this disease.

g) Mast cells

We have recently reported that CFTR is expressed in MC (107, 201). Using pharmacological inhibitors, we have shown that inhibition of CFTR downregulates rat PMC degranulation, and that CFTR is differentially regulated

by IFN γ in human MC and EC. CFTR expression in MC and its functional significance will be discussed in greater detail in a subsequent section.

D. Introduction to Cystic Fibrosis

Cystic fibrosis (CF) is the most common monogenic hereditary disease of people of European descent, with a frequency of 1:3200 in caucasians (234). It is caused by mutations in the Cystic Fibrosis Transmembrane Conductance Regulator (CFTR), a protein widely expressed in polarized epithelial cells (EC) (235). In CF, function of EC in many organs is affected, but the lung pathophysiology is the major source of morbidity and mortality in CF patients. In lung EC, absence of CFTR results in deregulation of other ion channels and intracellular signalling, leading to hyperabsorption of Na⁺ and H₂O, as well as abnormal cytokine secretion (198, 200, 206, 236, 237). CFTR deficient EC are unable to properly regulate ion flux and absorptive processes, and the periciliary fluid or airway surface liquid (ASL) is abnormal (235, 238). As a result, Na⁺ hyperabsorption from the ASL, leads to osmotic H₂O hyperabsorption and ASL volume reduction. To compensate for this loss of ASL volume, the overlying mucous releases water into the ASL, thus becoming denser and severely impairing mucocilliary clearance rate (235). Since mucocilliary clearance rate exerts no regulatory control over goblet cell activity, mucus production is not decreased, which creates mucous plugs that obstruct the airways (235). Loss of mucocilliary clearance among other factors, leads to colonization of the lungs with *Staphylococcus aureus* and *Hemophilus influenza* soon after birth, followed by opportunistic and chronic colonization with *P. aeruginosa* (239, 240). In

response to this, a chronic but ineffective neutrophilia develops, leading to perpetual inflammation of the airways. This chronic inflammation is in part due to the EC, but likely involves cells of the immune system.

Inflammation of the lungs is a hallmark of CF, but there is much debate as to whether colonization by bacteria occurs before the onset of inflammation, or if CFTR deficiency leads to an imbalance in homeostasis, which triggers inflammatory events in the CF lung (Figure 1.12) (206, 237, 241-244). ASL from EC derived from CF patients is less efficient at microbial killing than ASL from healthy patients, an effect which is not dependent on salt concentrations or mediated by direct effects on leukocyte function (238). Tracheobronchial EC lines or primary cells from CF patients can produce more inflammatory cytokines than those of normal patients (198, 200, 245, 246). Furthermore, it has recently been shown that CF tracheal glands are unable to mount a normal antimicrobial response to *P. aeruginosa* (247). Neutrophils infiltrate human fetal CF airway grafts in the absence of infection in a time dependent fashion (206).

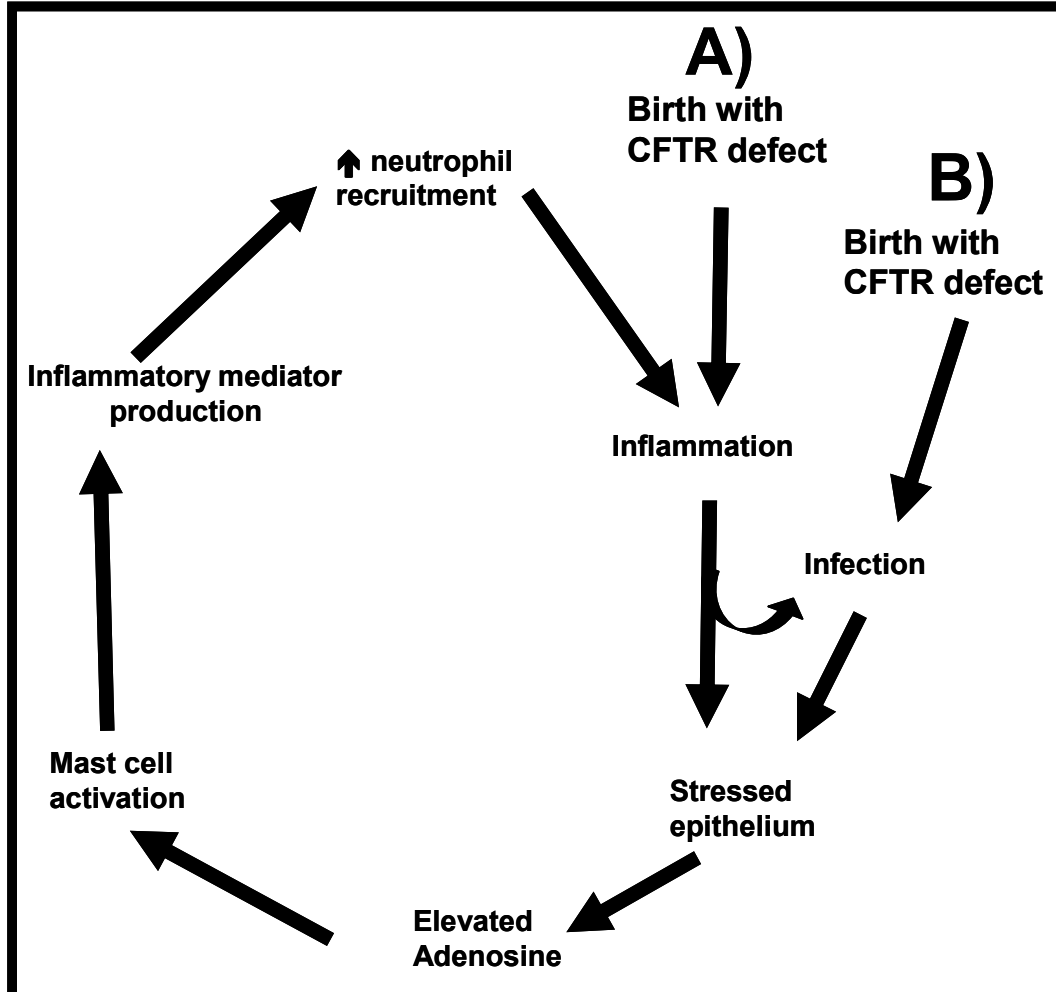


Figure 1.12 Schematic of the controversy behind the onset of Cystic Fibrosis (CF) pathophysiology. **A)** Birth of person with CF mutation results in an intrinsic defect in immune regulation which triggers inappropriate inflammation. This leads into the vicious cycle of cellular stress, immune activation and inflammatory mediator release that recruits other inflammatory cells and generates perpetual inflammation. Colonization by bacteria is a secondary event in this model, and results from reduced mucociliary clearance and thickened mucous. **B)** Birth of a person with CF, followed by infection with bacteria due to poor mucociliary clearance and thick mucous. Infection triggers immune activation and inflammation in the airways, and cannot be removed because of neutrophil defects in phagocytosis and bacterial killing. MC are hypothesized to participate in both models.

Conversely, other studies showed that primary cultured tracheobronchial EC or primary EC from CF patients do not produce more inflammatory cytokines than those of normal patients, unless they are first primed with TNF or TLR-2 agonists (173, 248). Perhaps the most compelling evidence that inflammation occurs before infection however, comes from the fact that many CF patients who receive lung transplants still suffer from chronic *P. aeruginosa* infections which continue to be the primary cause of death in these patients (249, 250). It is tempting to speculate that immune cells repopulating the lung from bone marrow or other sites may be functionally abnormal because of lack of CFTR, and contribute to re-establishing the chronic lung inflammation even after transplantation, a process that may centrally involve MC. All of this evidence argues that CFTR deficiency in EC alone is not sufficient to induce the chronic inflammation observed in CF. Support for this hypothesis comes from the fact that CFTR is not only expressed on EC, but mRNA has been detected in many other cell types, and recently in MC as well (107, 201).

1. Cystic Fibrosis and mast cells

Little is known about the role that MC play in CF. MC are classically known to be involved in the pathology of allergic diseases by their activation through FcεR1. Interestingly, our group discovered that rat PMC, as well as human MC express CFTR, and that CFTR seems to play a functional role in stored mediator release from these cells (107, 201). Our recent work on MC and

CFTR combined with work from others on other types of secretory immune cells such as B-lymphocytes, and T-lymphocytes, suggests that CFTR plays a regulatory role in mediator secretion in cells of non-epithelial origin (218, 219). If this is true, then MC are an excellent candidate to study this, since they are professional secretory cells. MC possess the armamentarium of mediators, and are strategically located in tissues to initiate strong inflammatory responses, and communicate with cells of the adaptive and innate branches of the immune system (251). Recently, focus has been on the involvement of MC in innate immunity and their ability to respond to pattern recognition receptors such as TLR-2 and -4, and other innate immune molecules such as adenosine (16, 49, 252).

Adenosine is produced in large amounts in stressed cells, because of reduced ATP synthesis, increased ATP hydrolysis and simultaneous inhibition of adenosine kinase enzymes (Figure 1.3) (253). Elevated adenosine is shunted to the extracellular space via equilibrating nucleoside transporters (ENT) (254). Absorptive EC in the lung possess ENTs only on their basolateral membrane, and under stress release substantial amounts of adenosine into the lamina propria, which can activate MC through the A_{2b}R (48, 255). Thus in CF, MC may be activated by the stressed epithelial production of molecules such as adenosine and in turn, mediators from MC could contribute to the inflammatory state of CF (49). More evidence for MC involvement in the pathology of CF comes from studies showing that MC are present in increased numbers in *cfr^{tm1UNC}* CFTR^{-/-} mouse intestines, human fetal CF lungs, adult CF patient nasal polyps, as well as in fibrosing colonopathy tissue from young children with CF (256-260).

Interestingly, in nasal polyps of CF patients, a high proportion of MC were found to have degranulated (256). Furthermore, when *cfr^{tm1UNC}* CFTR null mice were compared to wild type controls, expression of 61 genes was more than two-fold increased in the gut of the CFTR null mice. Several MC associated genes such as MCP-1 and -2, as well as CPA were among those genes upregulated (259). Recent evidence that EC and MC may communicate during lung homeostasis comes from a study showing that human alveolar EC express membrane bound, and soluble SCF (261). It has been shown that soluble SCF, which is essential for MC growth and differentiation is released from human alveolar EC, influencing MC phenotype (261). Human MC can suppress secretory leukocyte protease inhibitor (SLPI) production by EC, which is an elastase, cathepsin G, trypsin, chymotrypsin, chymase and tryptase inhibitor found to be deficient in CF (262, 263). MC secrete tryptase, and increased tryptase levels in asthmatic lungs have been linked to adenosine stimulation (264). Furthermore, it has been reported that tryptase is elevated in CF and can activate EC when applied to the basolateral membrane, by cleaving and activating the protease activated receptor-2 (PAR-2) (263, 265). Thus, bidirectional MC-EC interactions are important in the lung, and are likely dysregulated in CF.

E. Conceptual model, central hypothesis and aims

The fact that CF is not nearer to being cured than it was 20 years ago, makes it easy to speculate that we have been looking at the “small picture”, as far as the pathophysiology is concerned. There is plenty of evidence in the literature

suggesting that cells other than EC are also involved in chronic inflammation and gastrointestinal pathology observed in CF. Taken together, the evidence suggests that MC deficient in CFTR will be functionally different than normal MC. There is strong evidence that the interaction between MC and EC is somehow dysregulated in CF and that MC may play a significant role in either the initiation and/or the perpetuation of inflammation. Since MC are abundant in the lungs, and have been shown to increase in numbers and activation state in CF tissue, the elucidation of the role of CFTR in MC is an important endeavour.

Our conceptual model is that in a CF lung, there is an EC-mediated dysregulation of the submucosal microenvironment. This dysregulation involves cytokines and/or innate immune molecules such as adenosine, which could activate MC to release their armamentarium of mediators. We also conceptualize that because CFTR is expressed in MC, mediator release from MC is dysregulated in CF because of the microenvironmental differences and/or CFTR deficiency in MC (figure 1.13). Based on previous experiments (Appendix 2), we have evidence that CFTR expression pattern is different in MC than EC. Thus, our global hypothesis is that dysregulation of inflammatory mediator secretion from MC contributes to the chronic inflammation observed in CF, an effect which is mediated through Cl^- anion transport and/or interaction with its protein binding partners. We also postulate that CFTR expression is an important component of the regulation of MC response to various agonists, but will exert regulatory control over MC secretion in an agonist- and compartment-specific manner

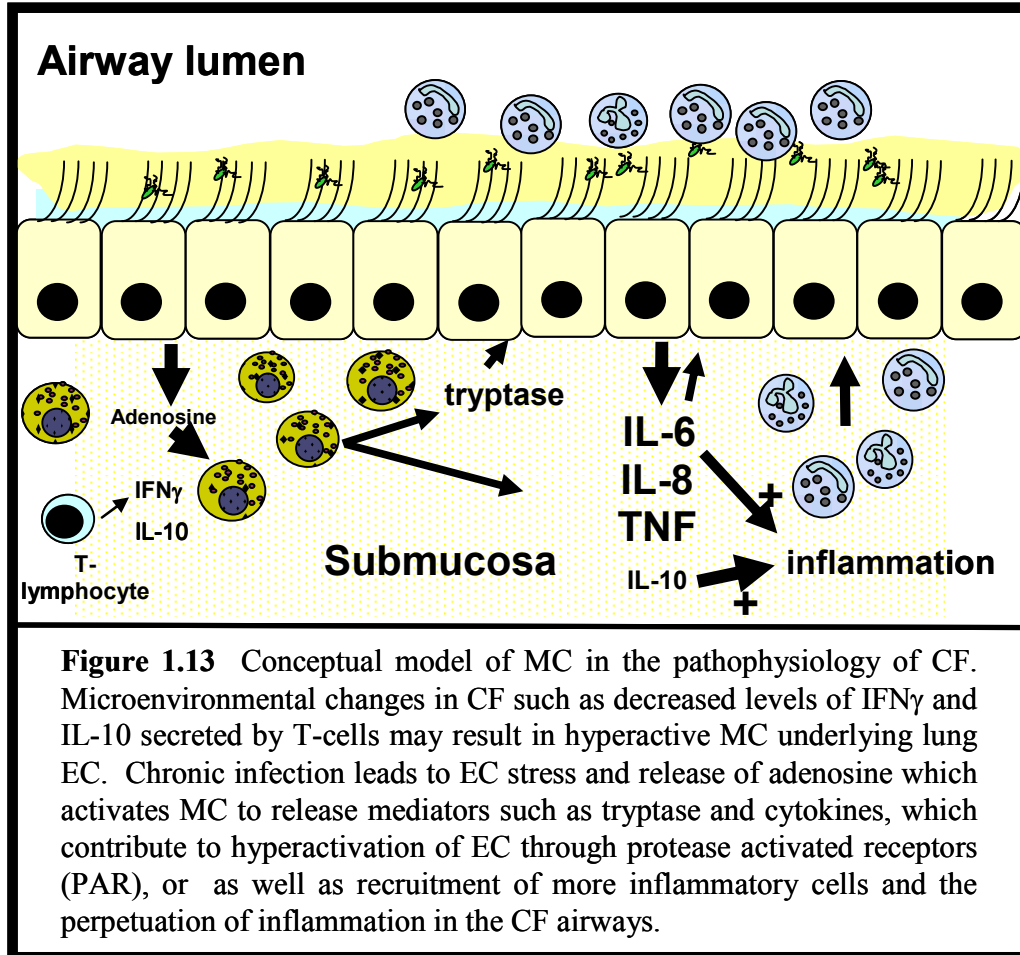


Figure 1.13 Conceptual model of MC in the pathophysiology of CF. Microenvironmental changes in CF such as decreased levels of IFN γ and IL-10 secreted by T-cells may result in hyperactive MC underlying lung EC. Chronic infection leads to EC stress and release of adenosine which activates MC to release mediators such as tryptase and cytokines, which contribute to hyperactivation of EC through protease activated receptors (PAR), or as well as recruitment of more inflammatory cells and the perpetuation of inflammation in the CF airways.

(Figure 1.6). To test components of this global hypothesis, this thesis has three specific aims. 1) To characterize the expression and subcellular localization of CFTR in human and rat MC in comparison to EC. 2) To investigate the functions of CFTR in selected secretory pathways (IgE/anti-IgE, adenosine, innate immune activation) in human MC lines. 3) Compare growth, morphology, surface markers, and secretory function of primary cultures of human peripheral blood-derived MC (PBMC) from $\Delta F508$ CF and non-CF subjects.

Understanding these differences will enhance our knowledge of the regulation and functions of CFTR and its role in various secretory cells and in the pathogenesis of CF. Therefore, we will test the above hypotheses using several different approaches in three different types of human MC 1) human mast cell line-1 (HMC-1), 2) Laboratory of Allergic Diseases-2 (LAD2), and peripheral blood-derived MC (PBMC) from non-CF and $\Delta F508$ CF subjects. Initially, we want to characterize the expression and subcellular localization of CFTR in MC in comparison to EC. We have preliminary evidence (Appendix 2), that PMC express CFTR on their granules, and we want to determine if this is true for human MC and validate it using other methodologies. Using these cell types, we will also examine the role of CFTR in Cl^- flux and mediator secretion originating from different cellular compartments (basal, stored, *de novo* synthesized and lipid synthesis pathways). We will also assess release of mediators from these compartments following activation of MC with different stimuli.

F. Overview of Rationale and Experimental Design

1. Aim 1: Characterization of CFTR expression in mast cells

It has been reported that glycosylation of proteins is differentially regulated in different cell types (149). In EC, immature (band B) CFTR is thought to be expressed only in the ER, whereas the mature (band C) CFTR is expressed in compartments distal to the Golgi such as the plasma membrane or recycling endosome (266). Other studies have shown that in polarized EC, most of the CFTR signal is located in the apical plasma membrane with little or no basolateral membrane and perinuclear staining (267, 268). Interestingly, these same studies showed that in non-polarized cells HeLa and 3T3 cells, CFTR staining was mostly intracellular, which was markedly different than in EC. Our confocal microscopy images (Appendix 2), suggest that rat PMC immunostained with anti CFTR antibodies exhibit patterns of staining consistent with MC granules, but these observations have yet to be confirmed. The above evidence shows that CFTR glycosylation and localization can be cell-type dependent. Therefore, we wish to further characterize the expression and localization of CFTR in PMC by subcellular fractionation and Western blot, to determine if it is similar to that reported in EC. Furthermore, we wish to examine expression and subcellular localization of CFTR in human MC. This characterization will help to clarify the role this protein plays in the processes surrounding inflammatory mediator release.

Using Calu-3 EC as a positive control for CFTR expression, we will characterize the expression of CFTR by Western blot in PMC, HMC-1, LAD2 and primary cultured human MC from peripheral blood CD34⁺ progenitors (PBMC). We will examine intracellular localization of CFTR in human MC using confocal laser scanning microscopy in LAD2 cells. We will also investigate the subcellular localization of CFTR in PMC by subcellular fractionation and Western blot, using a method previously described by Swieter et al. (Figure 2.1) (269). Once CFTR has been characterized and localization in MC has been established, further research into this protein's role in MC activation and mediator secretion can be pursued.

2. Aim 2: Role of CFTR in human mast cell mediator secretion

Since Cl⁻ plays an important role in MC secretion, we hypothesize that pharmacological inhibition of CFTR will affect mediator secretion in human MC. Furthermore, we hypothesize that absence of CFTR seen in Δ F508 CF patients will also affect secretion in human MC, as CFTR has been shown to participate in many protein-protein interactions in EC, which also undoubtedly occurs in MC. Furthermore, we hypothesize that CFTR regulation of MC secretion is not all-encompassing, but rather stimulus-dependent and compartment-specific within the cell. Thus, deficiency of CFTR function would differentially affect release of mediators originating from distinct cellular compartments such as secretory granules, small secretory vesicles, or lipid mediator synthesis. The stimuli we chose to use were IgE/anti-IgE, as well as the adenosine agonist 5'-(N-

Ethylcarboxamido)adenosine (NECA), which binds to the A_{2a}R and A_{2b}R, and has been linked to MC degranulation and asthmatic responses. Adenosine likely plays a role in the pathophysiology of CF as the lungs are under the constant stress of bacterial infection (83, 270).

To test our hypotheses that Cl⁻ regulation by CFTR is important in MC secretion, we pharmacologically inhibited CFTR in MC using the inhibitors NPPB, CFTR_{inh}-172, and GlyH-101 (Table 1.1) in two human MC lines HMC-1, and LAD2. We used DIDS as a control because it blocks many Cl⁻ channels, but not CFTR when administered extracellularly (183). Since some of these inhibitors have been reported to have non-specific effects (Table 1.1), we also attempted to knock down CFTR using RNA interference (RNAi) technology. Following pharmacological inhibition or knockdown of CFTR in HMC-1 and LAD2 cells, we stimulated the cells with either NECA, or IgE/anti-IgE and assessed the effect of the various stimuli on Cl⁻ flux and release of β -hex from granule stores. Furthermore, we assessed the effect of CFTR inhibition on an array of cytokines and chemokines including IL-8, and IL-6, which originate from small secretory vesicles, and have been reported to be elevated in CF (147, 271). Lastly, we also assessed lipid mediator secretion from LAD2 MC.

3. Aim 3: Comparison of peripheral blood progenitor derived human cultured mast cells (PBMC) from Cystic Fibrosis and non-Cystic Fibrosis donors

MC are difficult cells to study because they are tissue resident cells and are not present in the blood or body fluids (11, 272, 273). Therefore, until

recently, they had to be isolated from tissues such as human foreskin and lung and the experiments performed on these cells were restricted by size of biopsy and number of cells contained within this tissue (274, 275). Compounding this difficulty was the lack of highly differentiated human MC lines. The most widely used cell line to study MC was HMC-1. These cells were derived from a patient with mast cell leukaemia, and have a constitutive phosphorylation mutation in their SCF receptor c-Kit that renders them growth factor independent (276, 277). As a result, these cells replicate quickly, doubling every 3 days in 10% serum, and do not mature and develop granules typical of MC. As a consequence, HMC-1 are not heavily granulated and do not express FcεR1, so they do not respond to FcεR1 aggregation (276). In 2003, a new MC line was developed by Drs. Arnold Kirshenbaum and Dean Metcalfe at the National Institutes of Health (NIH) (277). These cells were derived from a bone marrow biopsy of a mastocytosis patient. This cell line was named LAD2 (Laboratory of Allergic Disease-2), and was characterized as a MC. LAD2 cells are SCF dependent and grow much more slowly than HMC-1, exhibiting features of mature MC such as granule formation, and release of granule stores, cytokines and lipid mediators in response to FcεR1 aggregation. Furthermore, these cells stain with toluidine blue, a hallmark feature of MC (Figure 1.2). About 98% of the cells are positive for tryptase and 37% are positive for both tryptase and chymase (277).

Recently, advances have been made in the availability of human MC. The current gold standard for studying MC *in vitro* is the use of human cultured MC. Until recently, the main source of cultured MC was from CD34⁺ progenitors in

fetal cord blood called cord blood derived MC (CBMC). These CD34⁺ cells differentiated into MC in culture in the presence of SCF and IL-6 for ≥ 8 weeks. CBMC respond to Fc ϵ R1 aggregation, and display the hallmark staining characteristics of MC, but may not necessarily reflect their tissue counterparts, and their phenotype and/or responsiveness may reflect different culture conditions used (278, 279). More recently, MC cultured from adult peripheral blood CD34⁺ progenitors, called peripheral blood derived MC (PBMC), have been widely accepted as a good source of MC (279). These cells have been widely used in recent years, and are becoming as widely accepted as CBMC to study human MC. As we gained access to CD34⁺ PBMC progenitors from CF patients through collaboration with Dr. Neil Brown, the Director of the CF clinic at the University of Alberta Hospital, we conclude this thesis by examining expression and functional role of CFTR in PBMC. We compared the expression and role of CFTR in PBMC from Δ F508 CF patients to PBMC from non-CF subjects. We examined percentage of CD34⁺ progenitors in the blood, c-Kit and Fc ϵ R1 surface expression, CFTR expression, Cl⁻ flux, β -hex release, cytokine and lipid mediator secretion in response to Fc ϵ R1 aggregation and innate immune stimulation by *P. aeruginosa*. This study has yielded valuable clues as to the role of MC in the pathophysiology of CF.

Chapter 2. Materials and Methods

A. Cell Culture

1. HMC-1

The human MC line HMC-1 are a mast cell like cell line that was developed at the Mayo clinic by Dr. J.H. Butterfield) (276). These cells are stem cell factor independent and are undergo rapid cell division. They do not express the high affinity IgE receptor and do not become heavily granulated. HMC-1 are a useful tool to study mediator secretion in response to agonists other than IgE/anti-IgE. Cells were cultured in 75 cm² flasks (BD Falcon, Mississauga ON) in Iscove's complete media (IMDM) containing 2 mM L-glutamine (Invitrogen, Mississauga ON), and supplemented with 10% heat-inactivated FBS and 100 U/ml penicillin and 100 µg/ml streptomycin (Invitrogen). Supplemented IMDM is referred to as complete IMDM. Cultures were seeded at 1×10^5 cells/ml and maintained at 37°C and 5% CO₂ by passaging every 3 d. Passages were done by removing cells, counting and reseeding at the desired cell density in new 75 cm² flasks. Fresh media was added to 10 ml final volume. Cells were maintained for 50 passages and then fresh cultures were started. For cryopreservation of HMC-1, cells from a 75 cm² flask were spun at 120 x g and media was removed. Cells were resuspended in 0.5 ml heat inactivated FBS and 0.5ml heat inactivated FBS containing 20% dimethyl sulfoxide (DMSO) (Sigma Aldrich, Mississauga ON) was added. Cells were slowly frozen by adding vials to a room temperature "Mr. Frosty" cryopreservation container (Fisher Scientific, Mississauga ON), then placing at -20°C overnight, followed by -80 °C overnight. Cells were then placed in liquid N₂. When thawing cells, frozen vials were thawed at 37°C and cells

were added to 50 ml cold complete IMDM and spun at 120 x g for 5 min. Cells were resuspended in 10 ml cold complete IMDM and placed in incubator at 37°C in 5% CO₂. Cells were then passaged as described above. All cells were incubated in a humidified atmosphere of 5% CO₂ at 37°C and testing for Mycoplasma was conducted monthly using the MycoAlert Mycoplasma detection kit (Lonza, Rockland, ME).

2. LAD2

The LAD-2 mast cell line was recently developed by Dr. Arnold Kirshenbaum and Dr. Dean Metcalfe (Laboratory of Allergic Disease, NIH) and was cultured as previously described (277). LAD2 cells are stem cell factor dependent and have a slower growth rate than HMC-1. They contain more granulates than HMC-1 and unlike the latter, they express the high affinity IgE receptor FcεR1. LAD2 cells were grown in 75 cm² flasks (BD Falcon) in StemPro-34 serum free media (SFM) (Invitrogen) supplemented with supplied growth supplement, as well as 2 mM L-glutamine (Invitrogen), 100 U/ml penicillin, 100 µg/ml streptomycin (Invitrogen), and 100 ng/ml stem cell factor (Peprotech, Rocky Hill, NJ). This supplemented media is referred to as complete Stempro-34. Cells were incubated in a humidified atmosphere of 5% CO₂ at 37°C. Cells were hemidepleted weekly by removing half of the old media and replenishing media to 10 ml with fresh complete Stempro-34. When cell density reached 0.5 x 10⁶/ml, cells were split by resuspending the cells and pipetting half the volume of the flask into a new flask. Volume was then replenished to 10 ml

in both flasks with complete Stempro-34. Cell density was never allowed to exceed $0.5 \times 10^6/\text{ml}$. Cells were kept in culture until FcεR1 no longer caused β -hex release, at which time cells were discarded and fresh cells were thawed (average of 50 passages). For cryopreservation of cells, up to 1×10^7 cells were pooled and resuspended in 1.5 ml Pzerve cryopreservative (Celox Laboratories, St-Paul MN) and 100 ng/ml recombinant SCF was added. Cells were slowly frozen by placing vials in a room temperature “Mr. Frosty” cryopreservation container, then placing at -20°C overnight, followed by placing at -70°C overnight, then in liquid N_2 . When thawing, cells were removed from liquid N_2 , thawed and placed in a 25 cm^2 flask on a rocking platform at room temperature for 6 h to equilibrate. Following equilibration, 1.5 ml complete Stempro-34 was added and cells placed in a 37°C , 5% CO_2 incubator overnight. On the following day, 3 ml complete Stempro-34 was added, and cells were allowed to proliferate for 1 wk, at which point regular hemidepletion was implemented as described above. LAD2 cells were maintained in a humidified atmosphere of 5% CO_2 at 37°C , and Mycoplasma was conducted monthly using MycoAlert Mycoplasma detection kit.

3. Peripheral blood-derived mast cells (PBMC)

Ethical approval for Peripheral blood $\text{CD}34^+$ cultures was obtained from the University of Alberta Health Research Ethics Board. Non-CF donor volunteers were recruited from members of the laboratory. CF donors were over 18 y of age with a confirmed $\Delta\text{F}508$ genotype CF by molecular diagnosis.

Donors were excluded if they had active infection, were within 30 d of either i.v. antibiotics, surgery, elective surgery or had a hemoglobin count less than 100 at their last visit to the clinic. The donors were screened by Dr. Neil Brown, and informed consent was given. Fifty ml of blood was drawn from the donors in 10 ml Vacutainer Na⁺-heparin (NH) collection tubes (BD Biosciences) by standard phlebotomy techniques. Blood from non-CF donors was obtained by the Pulmonary Research Group phlebotomist, whereas blood from CF donors was obtained at the University of Alberta Hospital. To purify CD34⁺ progenitors, cells density gradients were prepared by overlaying 6 ml of whole blood onto 6 ml of Histopaque 1077 (Sigma Aldrich) and tubes were spun at 450 x g for 30 min at room temperature. Buffy coat was removed from the tube by aspiration with a transfer pipette and washed 2 x by centrifugation in 50 ml sterile phosphate buffered saline (PBS) (1.62 mM NaH₂PO₄, 8.33 mM Na₂HPO₄, 154 mM NaCl, pH 7.2). Cells were resuspended in 20 ml sterile PBS containing 1mM EDTA and 2% FBS (PBS/EDTA/FBS), counted in trypan blue and resuspended in PBS/EDTA/FBS at 2 x 10⁸ cells/ml. Cells were subjected to magnetic separation using the EasySep CD34⁺ positive selection cell separation kit (StemCell Technologies, Vancouver, BC), according to manufacturer's protocol. This kit reports CD34⁺ cell average purity of 96%. Magnetically purified cells were then resuspended in 1 ml Stempro-34. CD34⁺ cells were counted, and transferred to 25 cm² flasks at a density of 50 000 cells/ml in Stempro-34. Human recombinant SCF (Peprotech) as well as human recombinant IL-6 (Peprotech) were added at 100 ng/ml, and human recombinant IL-3 (Peprotech) was added at 30 ng/ml.

Cells were incubated for 1 wk at 37°C at which time cells were maintained in Stempro-34 containing SCF and IL-6 (100 ng/ml), but not IL-3 by hemidepletion every 4 d. Cell density was maintained at 50 000 cell/ml and cells were transferred to 75cm² flasks when volume of media exceeded 5 ml. Cells were also transferred to new flasks when adherent cells were detected, and at wk 4, 90% of the media was replaced with fresh media containing 100 ng/ml SCF and IL-6. PBMC cultures were maintained in a humidified atmosphere of 5% CO₂ at 37°C, but were not subjected to Mycoplasma testing to minimize manipulation of the cultures.

4. Calu-3

Calu-3 cells were cultured in 75 cm² flasks (BD Falcon) in Minimum Essential Medium (MEM) (Invitrogen) supplemented with 10% heat inactivated FBS, 2 mM L-glutamine, 100 U/ml penicillin, 100 µg/ml streptomycin, 100 nM non-essential amino acids (NEAA) (100x stock), 20 mM Na⁺ Pyruvate (Invitrogen), 15 mM HEPES and 20 mM NaHCO₃⁻ (Sigma Aldrich). This supplemented media is referred to as complete MEM. Calu-3 media was replaced twice weekly, and cells were sub-cultured at 80% confluence. Sub-culturing of Calu-3 cells was done by one rinse with 2.5 ml 0.05% (1X) trypsin-EDTA solution (Invitrogen) followed by a 20 min incubation with 2.5 ml 0.5% trypsin-EDTA solution. Cells were then diluted with 7.5 ml complete MEM to inactivate the trypsin, spun at 120 x g for 5 min, and resuspended in 10 ml complete MEM. Three ml of cell suspension was then added to new 75 cm² flasks containing 7 ml

fresh complete MEM (BD Falcon). All cells were incubated in a humidified atmosphere of 5% CO₂ at 37°C, and Mycoplasma testing was conducted monthly using MycoAlert Mycoplasma detection kit. Cells were frozen and thawed as described for HMC-1.

5. T84

Human intestinal EC (T84) were obtained as a generous gift from Dr. Karen Madsen in the Department of Medicine, University of Alberta. Cells were cultured in 75 cm² flasks (BD Falcon) in Ham's/F12 (Invitrogen) supplemented with 2.5 mM L-glutamine, 100 U/ml penicillin, 100 µg/ml streptomycin (Invitrogen) and 10% heat inactivated FBS (Invitrogen). Media was replaced twice weekly, and cells were sub-cultured at 80% confluence. Sub-culturing of T84 cells was done as described for Calu-3 cells above, but complete Ham's/F12 was used instead of MEM. All cells were incubated in a humidified atmosphere of 5% CO₂ at 37°C, and Mycoplasma testing was conducted monthly using MycoAlert Mycoplasma detection kit. Cells were frozen and thawed as described for HMC-1.

a) HMC-1, LAD2 and Calu-3 proliferation

To assess proliferation of cells in culture, HMC-1, LAD2 and Calu-3 cells were seeded at various densities in appropriate culture media on d 0. For HMC-1, growth in both 5% and 10% heat inactivated FBS was assessed. To count HMC-1 and LAD2 cells, flasks were gently resuspended, and 1 ml of cell supernatant was

taken from the flask. Cells were counted by trypan blue exclusion to determine cell number and viability, and cell suspension was then returned to the flask to maintain volume. HMC-1 were counted daily, whereas LAD2 were counted only at 7 d and 14 d. Having an adherent phenotype, Calu-3, are impossible to count without trypsinization, so we estimated % confluence daily rather than counting the cells. Proliferation of T84 cells was not assessed, and cells were used when they appeared to be approximately 70-80% confluent.

b) PBMC proliferation

To determine whether non-CF and CF PBMC exhibit similar growth characteristics, cells were counted weekly starting at wk 2. Briefly, cells were gently resuspended in their culture flasks, and 1 ml was removed, being careful to maintain sterile conditions. From this aliquot, cells were taken and counted in trypan blue. After counting, remaining cells were returned to their respective culture flasks and this procedure was repeated each wk until the cells were harvested for experiments at wk 8.

B. Isolation of mouse bone marrow progenitors and rat peritoneal mast cells

1. Mouse bone marrow progenitors

Wild type and B6.129S6-Cfr^{tm1Kth} male mice, a generous gift from Dr. Marek Duszyk at the University of Alberta, were housed in a specific pathogen-free environment at the Health Sciences Lab Animal Services (HSLAS) facilities,

in accordance with the Canadian Council on Animal Care (CCAC) guidelines and Health Sciences Animal Policy and Welfare Committee, University of Alberta. Animals were kept on a Peptamen (Nestlé Nutrition, Minnetonka, MN) liquid diet to prevent intestinal obstruction in the *Cftr*^{-/-} animals. Animals were weaned at 21 d and genotyped by ear clip genomic DNA analysis in Dr. Duszyk's lab by Dr. Rebecca Lam as previously described (280). Following DNA analysis, mice were sacrificed by CO₂ asphyxiation followed by cervical dislocation. Mice were placed ventral side up and small midline incision was made in the belly to allow access to the hip joint (femur-pelvis interface). Both legs were removed at the hip joint and fur was removed by pulling skin over the foot. Foot and skin were removed from the legs and legs placed in 25 ml RPMI on ice. In a sterile hood, marrow was isolated from the femurs by cutting 3 mm in from the ends of the bone and flushing out the marrow with 2 x 2.5 ml RPMI using a 5 ml syringe with a 30 gauge needle. Bone marrow was pipetted repeatedly to disperse cells, and centrifuged at 150 x g for 10 min at 4°C. Pellets were resuspended with 20 ml warm fresh RPMI supplemented with 2 mM L-glutamine, 100 U/ml penicillin, 100 µg/ml streptomycin (Invitrogen) and 10% heat inactivated FBS. Cells were cultured as previously described (281). Briefly, cells were placed in a 75 cm² flask and murine recombinant IL-3 and SCF were added at 10ng/ml each. Bone marrow cultures were given fresh media every 3 d following centrifugation and counting of cells. Cells were resuspended in fresh 37°C RPMI at a concentration of 1 x 10⁶/ml in new 75 cm² flasks. Fresh IL-3 and SCF were added at 10 ng/ml

each time. After 3 wk in culture, 98% of cells are bone marrow-derived MC (BMMC) as described previously (281).

2. Rat peritoneal mast cells

Male Sprague-Dawley rats between 350-400 g (Charles River, St. Constant, QC) were sacrificed via CO₂ inhalation followed by cervical dislocation. After removal of hair and skin, peritoneal cavities were injected with 20 ml of sterile, ice-cold HEPES-Tyrodé's buffer (HTB) (chemicals from Sigma Aldrich) (136 mM NaCl, 5.5 mM glucose, 2.6 mM KCl, 1 mM CaCl₂·2H₂O, 1% bovine serum albumin (BSA), 12 mM (4-(2-hydroxyethyl)-1-piperazineethanesulfonic acid) (HEPES), 0.52 mM NaH₂PO₄·H₂O, pH 7.2) and massaged gently for 1 min. The fluid in the peritoneal cavity was then extracted through an incision and centrifuged and 120 x g for 3 min. Cells from three rats were resuspended in a total of 5 ml ice cold HTB and layered over 30%/80% Percoll gradients prepared with complete RPMI and isotonic Percoll. Isotonic Percoll was prepared by adding 4.7 ml 10X Hanks' Balanced Salt Solution (HBSS) (Invitrogen), 0.5 ml 1 M HEPES and 3 drops 1N HCl (Fisher Scientific) to 50 ml of stock Percoll solution (GE Healthcare, Baie d'Urfe, QC). Cells were centrifuged at 300 x g for 20 minutes and pelleted PMC were collected after removal of Percoll being careful not to disturb the pellet. Purified PMC were then washed in ice-cold PBS three times and counted for cell number and viability by trypan blue exclusion method.

C. Characterization of CFTR expression by Western blot

1. Cell lysis and protein extractions

Whole cell pellets were washed 2x in PBS, then lysed by repeated pipetting in ice-cold lysis Radio Immuno Precipitation Assay (RIPA) buffer (25 mM Tris-HCl, 150 mM NaCl, 1% Triton X-100, 1% Na deoxycholate, 0.1% Sodium dodecyl sulphate (SDS)) (Sigma Aldrich), with 1X Protease Arrest cocktail (G-Biosciences, Maryland Heights, MO) and incubated at 4°C with agitation for 45 min. Cell lysates were centrifuged at 12 000 x g for 20 min to remove cell debris. Supernatants were collected and bicinchoninic acid (BCA) test (Pierce Biotechnology, Nepean, ON) was performed to measure protein concentration. One volume of 2X protein loading buffer (125 mM Tris-HCl (pH 6.8), 10% glycerol, 4% SDS, 1.8% β -mercapto ethanol (BME), 0.006% bromophenol blue) (Sigma Aldrich), was added. Samples were either boiled for 3 minutes or left unboiled depending on experiment performed, and loaded on polyacrylamide gels.

2. Sodium dodecyl sulfate-polyacrylamide gel electrophoresis (SDS-PAGE), Western blotting

Western blotting was performed using either the photographic film method, or with Odyssey infra-red (IR) imager (Li-Cor Biosciences, Lincoln NE).

Samples were run on 7.5%-10% polyacrylamide gels in Tris-glycine running buffer (24.9 mM Tris-base, 191.9 mM glycine, 3.47 mM SDS) at 100 V for 90-120 minutes using Mini-Protean 3 dual cell system (Bio-Rad Laboratories, Mississauga ON). Polyvinylidene Fluoride (PVDF) or nitrocellulose membranes (Millipore, Billerica MA) and gels were equilibrated in transfer buffer (25 mM Tris-base, 190 mM glycine, 0.05% SDS, 20% Methanol, pH 8.0) (Sigma Aldrich) for 5 min. Proteins were transferred onto nitrocellulose membrane via either semidry transfer at 15 V for 80 min, or overnight wet transfer at 0.1 amp constant current. Transfer conditions were not method dependent, but rather optimization dependent. Some blots were stained for 5 min with Ponceau S (0.1% Ponceau S, 5% acetic acid) to assess protein loading. Ponceau S stains protein bands bright red, and can be removed by washing with water, having no effect on subsequent blotting.

For film method, membranes were blocked for 1-2 h at room temperature in blotto consisting of TBS-Tween (20 mM Tris-base, 136 mM NaCl, with 0.1% Tween 20) (Sigma Aldrich), containing 5% fat free milk (Bio-Rad Laboratories). For Odyssey IR method, proprietary blocking buffer (Li-Cor Biosciences) diluted 1:1 in PBS was used and blocking was for 1 h at room temperature. Primary antibodies were diluted in respective blocking buffer (see Tables 3.1 to 3.4 for dilutions) and incubated with the membrane overnight at 4°C on a rocker platform. Primary antibodies used were the MA1-935 mouse monoclonal anti-human CFTR (Affinity BioReagents, Golden CO) or the 24-1 mouse monoclonal anti-human CFTR (R&D Systems, Burlington ON). MA1-935 binds to an

epitope in the first extracellular loop of CFTR, whereas 24-1 binds to the cytoplasmic tail of CFTR (Figures 1.8 and 4.1). Isotype control antibodies for MA1-935 were mouse IgM (Serotec) and isotype control antibodies for 24-1 were mouse IgG_{2a} (R&D Systems). For traditional Western blot method, secondary antibodies for MA1-935/isotype and 24-1/isotype were goat anti-mouse IgM conjugated to horseradish peroxidase (HRP) (AbD Serotec, Raleigh, NC) and goat anti-rabbit IgG (rat adsorbed), conjugated to HRP (AbD Serotec) respectively. For Odyssey method, secondary antibodies to MA1-935/isotype or 24-1/isotype were either goat anti-mouse IgM conjugated to Alexa680 or goat anti-mouse IgG conjugated to 680nm or 800nm IRDye (Li-Cor Biosciences). Membranes were washed 3 x 15 min in TBS-Tween and incubated for 1 h at room temperature with secondary antibodies diluted in appropriate blocking buffer (see tables 3.1 to 3.4 for dilutions). Membranes were rinsed and then washed 5 x 15 min in TBS-Tween. For film method, blots were incubated for 5 min in either SuperSignal West Femto or SuperSignal West Pico ECL (Pierce), exposed to Kodak BioMax MR film (Kodak, Toronto, ON), and developed on a SRX-101A developer (Konica, Mississauga ON). For Odyssey, blots were scanned with Odyssey IR imager immediately following final washing step. Blots were never stripped and reprobed when using the Odyssey method.

To strip the blots for the film method, membranes were incubated at 50°C for 45 min in 50 ml stripping buffer (61.9 mM Tris-base, 69.4 mM SDS, pH 6.7) with 350µl β-mercaptoethanol (BME). Membranes were then rinsed with TBS-Tween twice and washed 2 x 10 min in TBS-Tween. Reprobing of membranes

was performed as described above beginning with a new blocking step. For film method, developed films were scanned as 8-bit grayscale images with 1200 dpi resolution. After resizing images to 600 dpi with Photoshop 4.0 (Adobe, Toronto, ON), scanned images were digitized using Un-Scan-it gel (Silk Scientific, Orem UT). Background was subtracted by lane upper and lower pixel intensity interpolation method. Gels were digitized using linear density calculation in standard drawing mode. Relative MW were calculated using the proportional to log MW comparison method, by entering known MW of Precision plus unstained or High Range MW standards (Bio-Rad Laboratories). Interpolated MW were rounded to the nearest kDa. For the Odyssey method, gels were background corrected using the Odyssey software v. 1.2 by linearization of the signal between the highest and lowest signal on the gel. Band MW were calculated by comparison to known MW standards as above, and rounded to the nearest kDa.

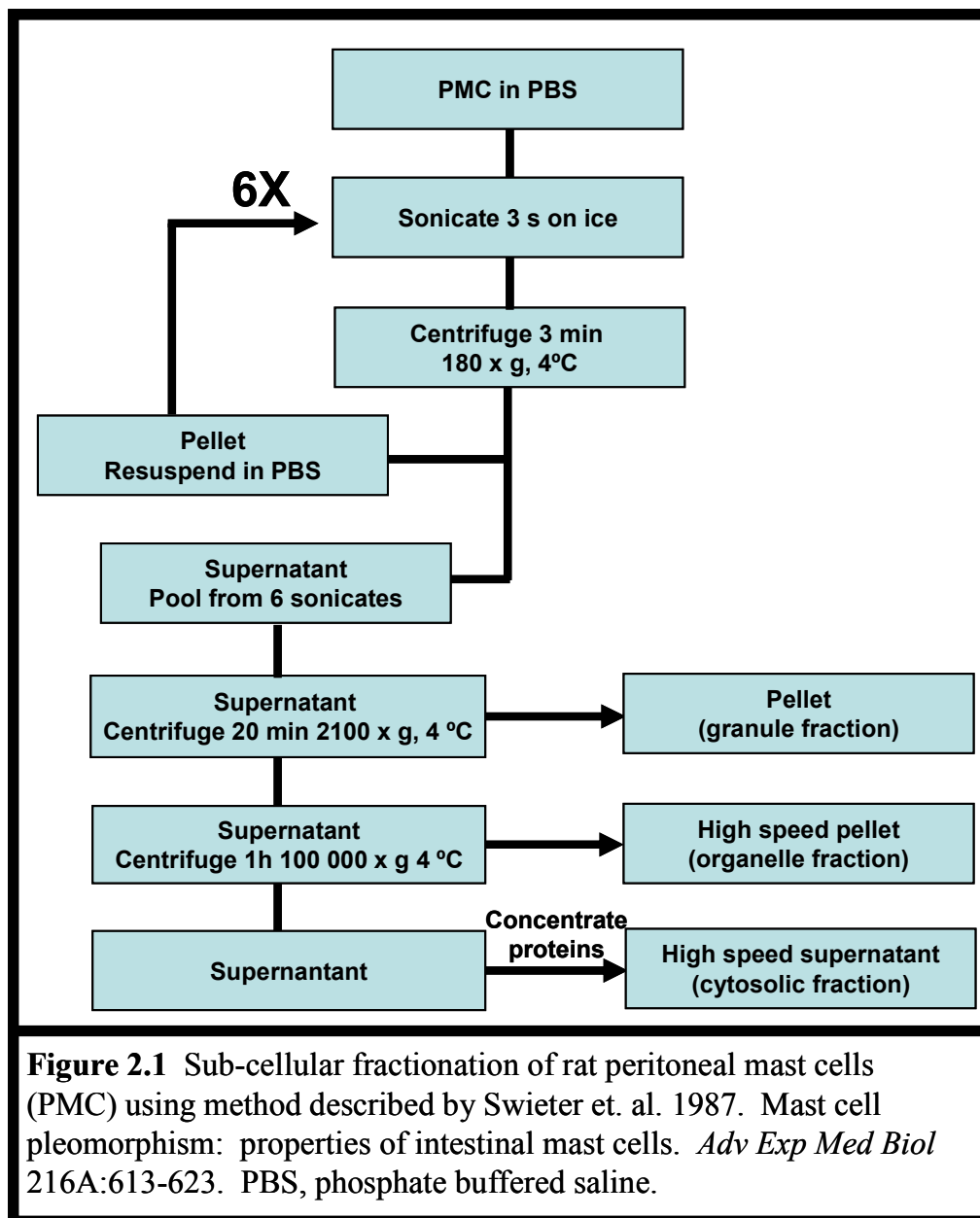
D. Subcellular localization of CFTR in human and rat mast cells

1. Immunocytochemistry and confocal microscopy

Cytospins were made on a Shandon cytospin 2 cytocentrifuge (Fisher Scientific). Briefly, cytospin clips were assembled using superfrost plus microscope slides (Fisher Scientific) as per manufacturer's instructions. Cells were resuspended at 2×10^5 /ml in growth media and 100 μ l cell suspension was added to cytospin funnel pre-loaded with 100 μ l phosphate buffered saline PBS containing 20% heat inactivated FBS. Cells were spun at 200 rpm (4 x g) for 5

min, slides removed from clips and allowed to air dry overnight. Cells were used in experiments or wrapped back to back in aluminum foil and stored at -20°C until needed.

Cytospins were used for confocal microscopy. Cell spot on cytospin was circled with hydrophobic PAP pen (Research Products International Corporation, Mount Prospect IL) and allowed to air dry. In a humid chamber consisting of a petri dish, cells were fixed with 75%/25% acetone/ethanol for 20 min, then washed 3 x for 5 min in PBS. Blocking and permeabilization was performed by incubating cells with PBS containing 3% BSA + 10% goat serum for 2 h at room temperature. Cells were washed 3 x 5 min in PBS and primary antibody MA1-935 or 24-1 (1:50) was added in PBS containing 3% BSA + 10% goat serum, and incubated 2 h 4°C. Isotype controls were the same as described in section C.2. Cells were washed in 3 x in PBS and secondary antibody goat anti-mouse IgM conjugated to Alexa:680 (Invitrogen) (1:50) or goat anti-mouse IgG conjugated to Alexa:488 (Invitrogen) (1:50) was added in PBS containing 3% BSA and 10% goat serum for 1 h at room temperature. Cells were washed 1 x in PBS then 2 x in H₂O to remove salts. Slides were mounted immediately with 20 µl Fluormount G (Southern Biotech, Birmingham AL), dried overnight and analyzed by confocal microscopy on an FV-1000 confocal microscope (Olympus, Markham, ON). Settings on the microscope were set so that weak baseline fluorescence was visible on isotype control slides, and then were left untouched for analysis of all other slides. Settings varied from experiment to experiment, but were always relative to isotype control slide.



2. Subcellular fractionation of rat peritoneal mast cells

Subcellular fractionation was performed as previously described (269) (Figure 2.1). Briefly; purified PMCs were suspended on ice in protein free PBS with 1X protease arrest (G-Biosciences), and sonicated for 3 s using a 60 Sonic Dismembrator probe sonicator (Fisher Scientific) on an intensity setting of 2. Cell suspensions were then centrifuged at 180 x g for 3 min and the supernatants collected. Pellets were resuspended in PBS with Protease arrest, and the sonication, centrifugation, collection steps repeated 5 times. Supernatants were pooled and centrifuged at 2100 x g for 20 min. Pellets from this spin were collected and resuspended in ice-cold RIPA buffer containing 1X protease arrest. The pellet from this spin is referred to as the granule fraction (Figure 2.1). The supernatant was spun at 1×10^5 x g for 60 min on an XL-90 ultracentrifuge (Beckman Coulter, Mississauga ON), using a Ti90 fixed angle rotor (Beckman Coulter). The pellet from this high speed spin was resuspended in ice-cold RIPA buffer with 1X protease arrest and is referred to as the high speed pellet. This fraction is thought to contain cellular components that were too light to pellet at 2100 x g, such as small vesicles, plasma membrane, endoplasmic reticulum (ER) and Golgi membrane components. Supernatant from the high speed spin was collected and proteins were concentrated using Ultrafree MC 10 000 NMWL filter unit (Millipore) spin columns. This fraction contains mostly cytosolic components and proteins that did not have sufficient density to pellet at 100 000 x g.

E. Role of CFTR in human mast cell secretion

1. Pharmacological inhibition using CFTR inhibitors

To inhibit CFTR in MC, pharmacological inhibitors were preincubated with MC for 15 min in Cl⁻ flux experiments, or for 30 min in other experiments. Without washing out inhibitors, cells were used in Cl⁻ flux assay or were stimulated with NECA or anti-IgE. For all experiments using CFTR inhibitors, these were present throughout the experiments and did not have any significant effect on cell viability unless doses reached 100 μ M (not shown).

2. Transfection of antisense and missense oligonucleotides (ASO) and (MSO)

Antisense Oligonucleotide technology was used to knock down CFTR as previously described (282). Briefly, a pair of adjoining 18-mers 5'-CAGAGGCGACCTCTGCAT-3' (ASO-1) and 5'-GACAACGCTGGCCTTTTC-3' (ASO-2) complementary to nucleotides 1-18 and 19-36 of CFTR mRNA, along with control missense oligomers 5'-CAGCGGCGACCGATGCAG-3' (MSO-1) and 5'-GACAACTCTGGACGTTTA-3' (MSO-2) were synthesized by the Institute for Biomolecular Design (University of Alberta). Phosphorothioated nucleotides were used to prevent rapid intracellular degradation by nucleases. For transfection into cells, 6 μ l of 20 μ M oligo 1 (ASO-1 or MSO-1) and 6 μ l of 20 μ M oligo-2 (ASO-2 or MSO-2), were combined and then added to 24 μ l

liposomal transfection reagent DOTAP (N-(1-(2,3-dioleoyloxy)propyl)-N,N,N-trimethyl-ammoniummethyl sulphate), (Roche Diagnostics, Indianapolis, IN). Mixture was incubated for 15 min at room temperature, and then added to 1×10^6 cells in 1 ml serum-free IMDM. After 2 h incubation at 37°C, 10% heat inactivated FBS was added to the cells, and cells were incubated for 12 h at 37 °C. After 12 h incubation, the cells were washed, and the above treatment was repeated in serum-free medium to replenish the oligos. After a further 2 h incubation at 37 °C, 10% heat inactivated FBS was added to the cells. After a total of 24 h incubation in the presence of FBS, the cells were washed and used in experiments.

3. BLOCK-iT™ siRNA optimization

Using BLOCK-iT™ siRNA (Invitrogen), which is a fluorescein isothiocyanate (FITC) labeled non-specific siRNA, HMC-1 cells were transfected using different doses of siRNA and either RNAifect (Qiagen, Mississauga ON), Lipofectamine (Invitrogen) or FuGene HD (Roche), to determine the best dose of siRNA and transfection reagent to use. Briefly, HMC-1 cells were seeded at 500 000/ml in 400 µl antibiotic-free complete IMDM in Corning 12-well plates (Fisher Scientific), and placed in incubator until ready to be transfected. Lipofectamine, RNAifect or FuGene HD and BLOCK-iT™ were diluted separately in Opti-MEM (Invitrogen) in 50 µl volumes at different doses and incubated for 5 min at room temperature. Diluted siRNA was then added to diluted transfection reagent, and allowed to form nucleic acid:lipid complexes for

30 min in the dark at room temperature. Following this incubation, siRNA:transfection reagent complexes (100 μ l) were added dropwise to the cells, plates were rocked gently back and forth to mix and incubated at 37°C, 5% CO₂ for 24 h. The fluorescent viability dye To-Pro-3 (Invitrogen) was then added to the cells at 1/1000 dilution of stock. Cells were washed 2x in flow buffer (PBS containing 0.1% BSA and 0.1% NaN₃) and fixed in 1% paraformaldehyde (PFA). Cells were analyzed by flow cytometry on a FACSCalibur instrument (Beckton Dickinson, Mississauga ON) using 488 (FL-1) and 633 (FL-4) lasers. The ratio of transfection reagent and siRNA giving the highest fluorescent signal by flow cytometry is used in subsequent experiments.

4. Transient transfection using small inhibitory RNA (siRNA)

Following optimization of lipid:siRNA ratio to use in MC transfections, we purchased several siRNA oligos (Table 2.1). Lipofectamine transfection reagent was used to transfect these siRNA into the cells. For CFTR knockdown experiments, siRNA (40 nM) in 50 μ l Opti-Mem (Invitrogen) was incubated with 1 μ l Lipofectamine in 42 μ l Opti-MEM for 30 min at room temperature to allow formation of complexes. Complexes were added dropwise to 1×10^6 cells in 900 μ l serum-free medium, and incubated for 3 h at 37°C. Following incubation, 10% heat inactivated FBS was added to the cells. Cells were incubated for 24-72 h to allow knockdown of CFTR mRNA and, in turn, reduce protein levels.

Table 2.1 (CFTR and missense siRNA sequences)

siRNA	Source	Sequence (5' to 3')
CFTR siRNA	Ambion	GUG UCA UCU GAA UGU AGC CUC
Non-silencing control #1 siRNA	Ambion	proprietary
Stealth siRNA 503	Invitrogen	GCA UAG GCU UAU GCC UUC UCU UUA U
Stealth siRNA 794	Invitrogen	CGU CUG CCU UCU GUG GAC UUG GUU U
Stealth siRNA 2068	Invitrogen	GGA UGU GAU UCU UUC GAC CAA UUU A
Non-silencing siRNA	Invitrogen	GGU AGC AUA CUC AGC AAG AAA CCA A

This incubation time should be sufficient to reduce CFTR protein expression, as CFTR mRNA half life has been estimated at 10-12 h (283, 284). Cells were then used in experiments.

5. Confocal microscopy of transfected HMC-1 (BLOCK-iT optimization)

Cytospins of transfected HMC-1 were used for confocal microscopy. The cell spot on the cytospin was circled with hydrophobic PAP pen and allowed to air dry. In a humid chamber, cells were fixed with 3% PFA for 20 min, then washed 3x for 5 min in PBS. Blocking and permeabilization was performed by incubating cells with PBS containing 3% goat serum and 0.1% Triton X-100 and 10 µg/ml 4',6-diamidino-2-phenylindole (DAPI) (Invitrogen). Cells were washed 3 x 5 min in PBS then 2 x in water to remove salts. Slides were mounted immediately with 20 µl Fluormount G (Southern Biotech), and dried overnight. Fluorescence was analyzed by confocal microscopy on an FV-1000 confocal microscope (Olympus) using ultraviolet laser and the 488 nm laser for DAPI and FITC respectively.

6. Measurement of puromycin resistance in cell lines

Puromycin is an aminonucleoside antibiotic produced by *Streptomyces alboniger*. It has an inhibitory effect on growth of many organisms including bacteria, protozoa, parasitic worms, algae, plants as well as mammalian cells

(285). Puromycin has homology to phenylalanine, and can bind to tRNA and be transferred to nascent polypeptide chains on the ribosomes by its amino group (285). However, the carboxy group of puromycin contains an amide group rather than an ester group, such that it does not allow further amino acids to bind, and this terminates translation (285). Thus, the main mechanism of action of puromycin is inhibition of protein synthesis, which kills the cells by translational arrest. The effects of puromycin can be counteracted by addition of the puromycin N-acetyl-transferase (PAC) enzyme, also found in *S. alboniger*. PAC inactivates puromycin by acetylating the amino group such that it can no longer bind to nascent polypeptide chains (286).

HMC-1, LAD2 and Calu-3 resistance to puromycin was assessed at the recommended dosage range supplied by the company (InvivoGen, San Diego, CA), but was found to kill HMC-1 and LAD2 at the lowest recommended dosage of 1000 ng/ml. Therefore, we performed puromycin killing assays on HMC-1, LAD2 and Calu-3 to determine the optimal dose to use in transfection. Briefly, untransfected cells were seeded at 100 000 cells/ml and puromycin was added at various doses to determine toxicity threshold for each cell line. For HMC-1 and LAD2 cells, cells were counted daily by removal of 1 ml cell suspension and counting cells in trypan blue to determine viability. Fresh media containing the same concentration of puromycin was added to the flask each time. For Calu-3 cells, confluence was estimated daily rather than trypan blue exclusion.

7. Stable transfection of CFTR short hairpin RNA (shRNA)

To stably knock down CFTR expression in HMC-1 and LAD2 cells, we purchased GIPZ lentiviral vectors encoding either CFTR shRNA (V2LHS 233316) or non-silencing scrambled (SCR) control short hairpin RNA (shRNA) (Open Biosystems, Huntsville AL). Vectors were cloned according to manufacturer's protocol and purified using the Qiaprep spin miniprep kit (Qiagen). For transfections, 1×10^6 cells were seeded in 1.8 ml or either complete IMDM without FBS for HMC-1, or complete Stempro-34 for LAD2. DNA (4 μ g) was diluted in 100 μ l Opti-mem (Invitrogen), and 16 μ l FuGENE HD (Roche) was diluted in 100 μ l Opti-MEM. DNA was added to FuGENE HD and incubated at room temperature for 30 min to allow complexes to form. DNA:lipid complexes were added to cells in a dropwise fashion, and allowed to incubate for 3 h. Following 3 h incubation, 3 ml complete media with 10% FBS was added to Calu-3 and HMC-1 but not LAD2 cells, where 3 ml complete Stempro-34 was added. Cells were incubated for 48 h following transfection, and then puromycin was added to kill untransfected cells and establish stably transfected cell lines. For HMC-1, initial dose of puromycin was 200 ng/ml, doubled each wk until the maintenance dose of 8000 ng/ml was reached. Cells were then grown in the presence of 8000 ng/ml puromycin to kill all untransfected cells. In the case of LAD2 and Calu-3 cells, initial dose of puromycin was 200 ng/ml, and 2000 ng/ml respectively. Final doses of puromycin for LAD2 and Calu-3 will be discussed in chapter 3.

F. Analysis of transfection efficiency and CFTR knockdown

1. Vector expression by flow cytometry

To assess the presence of CFTR or SCR shRNA as well as CFTR expression in HMC-1 cells, flow cytometry for green fluorescent protein (GFP) and CFTR using Alexa-647-conjugated anti-mouse IgG and IgM antibodies was performed. Signals were acquired on a FACSCalibur instrument (BD Biosciences), using the 488 and 633 lasers respectively. To prepare cells for flow cytometry, 100 000 cells/ treatment were fixed for 5 min in 5% formalin then washed and flow buffer containing 5% milk was added. Blocking was done overnight at 4°C. For intracellular staining (24-1 antibody), blocking buffer also contained 0.1% saponin (Sigma Aldrich) to permeabilize the cells. Primary antibodies were added to the cells at a 1/1000 dilution (MA1-935 and IgM isotype) in blocking buffer, or at 5 µg/ml (24-1 and IgG_{2a} isotype) in 100 µl blocking buffer containing 0.1% saponin. Primary antibody was incubated overnight at 4°C. Cells were then washed 1x by adding 1ml flow buffer and spinning at 120 x g for 5 min at room temperature, and resuspending in 100 µl blocking buffer. Secondary antibodies (goat anti-mouse IgM:Alexa-647 or goat anti-mouse IgG_{2a}:Alexa-647) were added at 1/100 dilution in blocking buffer and incubated in the dark for 1 h at room temperature. Cells were washed 2x as described above and resuspended in 400 µl flow buffer. Cells were kept cold and in the dark until same day analysis.

2. Cell lysis and mRNA extraction

RNA extraction was performed by solution D method as previously described (287). Briefly, up to 5×10^6 cells were washed 1x in PBS, then lysed by repeated pipetting in 200 μ l solution D containing 7.2 μ l/ml BME in 1.5 ml eppendorf tubes and incubated on ice for 45 min. To the lysate was added 24 μ l 2M sodium acetate ($C_2H_3NaO_2$), 240 μ l water saturated phenol and 48 μ l 49:1 chloroform:isoamyl alcohol, and mixture vortexed for 10 s. Lysates were incubated 30 min on ice then spun at 12000 x g for 30 min at 4°C. Upper aqueous phase containing RNA was removed and transferred to a fresh 1.5 ml eppendorf tube, being careful not to disturb white interphase containing DNA. Two volumes of ice cold absolute ethanol was added to tubes and incubated at -20 °C overnight. RNA was pelleted at 12 000 x g for 30 min at 4 °C then resuspended in 100 μ l solution D containing 7.2 μ l/ml BME. RNA was precipitated by adding 2 volumes of absolute ethanol and incubating at -20 °C for 1 h. RNA was pelleted at 12 000 x g for 30 min at 4 °C, then resuspended in 75 μ l diethylpyrocarbonate (DEPC) treated water. RNA was precipitated once more by adding, 7 μ l 2M $C_2H_3NaO_2$, followed by 165 μ l absolute ethanol and incubating at -20 °C for 1 h. RNA was pelleted at 12 000 x g for 30 min at 4 °C, then washed by overlaying with 200 μ l 70% ethanol and spinning at 12 000 x g for 10 min. Supernatant was discarded and RNA samples were air-dried for 10-20 min under vacuum until no liquid was visible, being careful not to overdry. RNA was resuspended in 20 μ l DEPC-treated water and heated at 60°C for 10 min to fully solubilize. RNA was quantitated by measuring absorbance at 260 nm and 280 nm on DU-640

spectrophotometer (Beckman Coulter). RNA was then treated with Turbo DNase (Ambion, Austin, TX) following manufacturer's instructions to remove any contaminating genomic DNA. Inactivation of DNase was performed by adding 0.75 μ l 500 mM EDTA containing 40 U/ml RNaseOUT (Invitrogen) and heating at 75°C for 10 min then cooling on ice, and either proceeding directly to reverse transcription, or freezing at -80°C until use. Quality of RNA was assessed by OD_{260/280} ratio ≥ 1.5 and when enough RNA was extracted, 1 μ g was run on 1% agarose gels to determine quality and integrity of RNA before analysis by PCR (not shown).

3. Heparinase digestion

It has been reported that in rodent MC RNA preparations, heparin is co-purified with RNA because of its highly negative charge, and that this proteoglycan inhibits reverse transcriptase and Taq polymerase enzymes (288, 289). This has been speculated to occur in human MC as well, as it has been found that degranulation of human cord blood MC inhibited gene amplification when compared to unstimulated MC (290). Thus, to improve the efficiency of our PCR reactions, we treated certain samples with heparinase I (Sigma Aldrich), as previously described to digest and remove the heparin contaminants in the RNA preparation (288). Briefly, 1 μ g RNA was digested with 5 U of heparinase I in a reaction mixture (5 mM Tris-HCl pH 7.5, 1 mM CaCl₂, 50 U RNAsin (Invitrogen)) for 2 h at room temperature. Following digestion, RNA was used in RT-PCR reaction

4. Primer efficiency calculations for quantitative PCR (qPCR)

Following reverse transcription of 100 ng RNA extracted as described above, two-fold dilutions (100 ng to 6.3 ng of cDNA assuming 100% RT efficiency) were prepared in 5 µl, and 2.5 µl of each dilution was used as starting template in a PCR reaction as described below, using 200 nM actin or CFTR primers (Table 2.2). Following PCR reaction on a Rotorgene (Corbett Research, Montreal QC), threshold cycle (C_T) for each dilution was determined using the RotorGene analysis software. For each primer pair (actin or CFTR), primer efficiencies were determined by plotting the C_T value of each cDNA dilution against the log concentration of cDNA in each dilution. The slope of the resulting regression line was used in the following formula:

Equation 1) Primer efficiency (E) = $-1 + 10^{(-1/\text{slope})}$

5. Quantitative PCR (qPCR)

Relative quantitation of transcripts was performed using a two-step realtime qPCR kit (Invitrogen) on a RotorGene realtime PCR machine (Corbett Research). Following kit instructions, extracted RNA described above was used as starting template for reverse transcription in 20 µl reaction volume, by incubating with 10 µl 2x RT reaction mix, 2 µl RT enzyme mix, variable µl RNA (100 ng), variable µl DEPC H₂O to 20 µl. Reverse transcription mixture was incubated at 25°C for 10 min, followed by 42°C for 50 min for reverse transcription. RT reaction was terminated by incubating at 85°C for 5 min, and

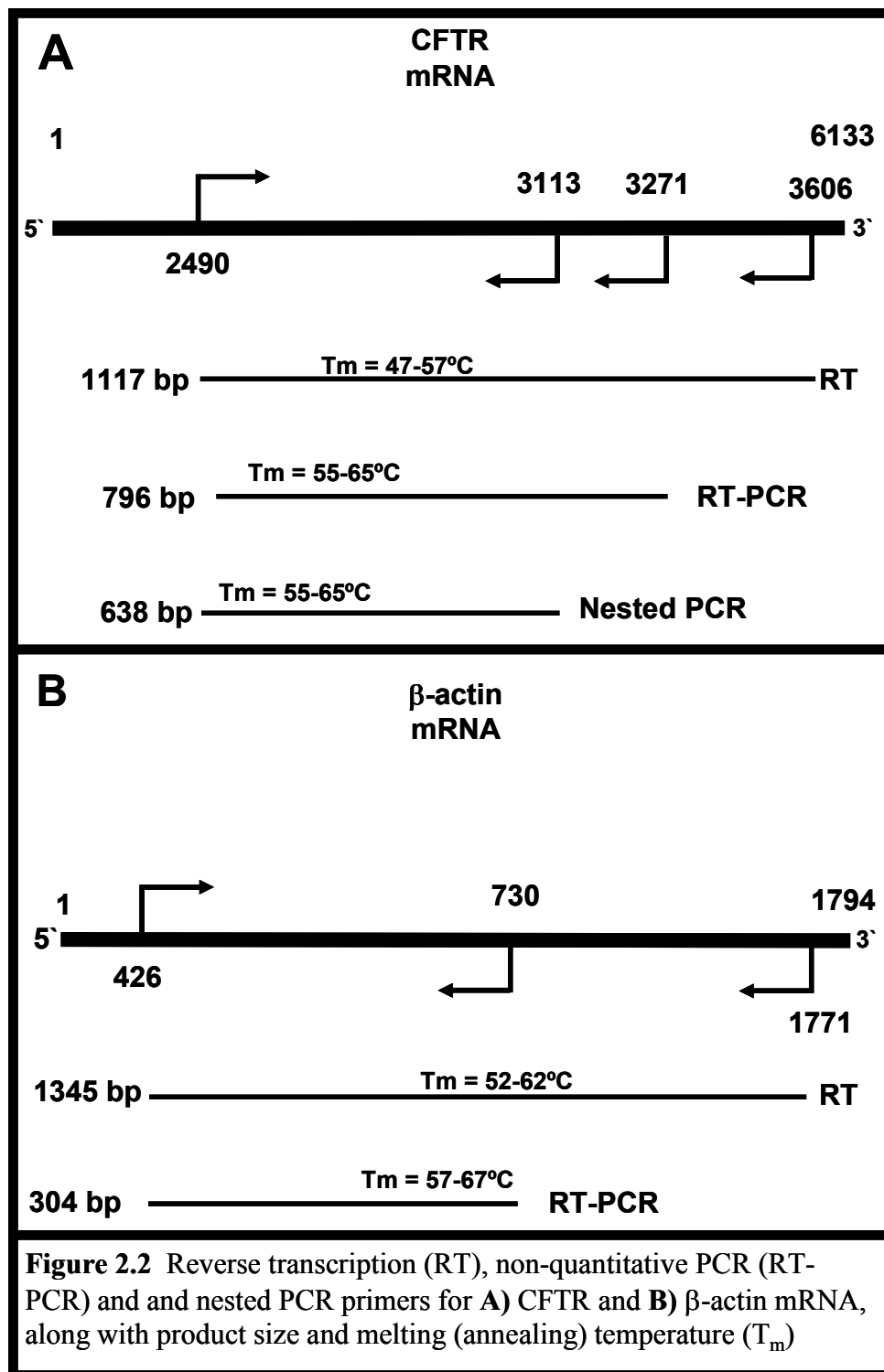
finally, template RNA was removed by incubation with 2 U *E. coli* RNase H (Invitrogen) at 37°C for 20 min. Following this reaction, 2.5 µl cDNA was added to 12.5 µl Platinum Quantitative PCR Supermix-UDG, 0.5 µl light upon extension (LUX) labeled primer (10 µM) (Table 2.2), 0.5 µl unlabeled primer (10 µM) (Table 2.2), and variable µl ultrapure water (Sigma Aldrich) to 25 µl total volume. Samples were placed on Rotorgene and qPCR was performed as instructed in the two-step realtime PCR kit (Invitrogen) by one cycle of 50° for 2 min, one cycle of 95°C for 2 min followed by 45 cycles of 95°C for 15 s, 60°C for 30 s. After final cycle, melt curve analysis was done by increasing temperature in 1°C increments from 50°C to 99°C and acquiring signal at every step. Calculation of fold change in mRNA expression were performed as follows:

$$\text{Equation 2)} \quad \text{mRNA ratio} = \frac{(E_{\text{target}})^{\Delta CT_{\text{target (control - treated)}}}}{(E_{\text{reference}})^{\Delta CT_{\text{reference (control - treated)}}}}$$

Where E is primer efficiency (equation 1), and ΔCT is the change in threshold cycle. mRNA ratio refers to fold change in mRNA transcripts of a target gene in a particular treatment measured against change in the same target gene in a control sample. This method of relative quantification of mRNA is based on the Pfaffl quantitation method and is considered to be more quantitative than the $\Delta\Delta CT$ method which does not take primer efficiency of target and reference genes into account (291).

Table 2.2 reverse transcription and PCR primers

Primer		Source	Sequence (5' to 3')	Product Size (bp)
β-actin	reverse transcription primer	Integrated DNA technologies	TGG TCT CAA GTC AGT GT	>1117
CFTR	reverse transcription primer	Integrated DNA technologies	TCG CAT CAA GCT ATC	>1345
CFTR sense (292)		Integrated DNA technologies	GAC AAC AGC ATC CAC ACG AA	796
CFTR (292)	antisense	Integrated DNA technologies	AAT TGG ACT CCT GCC TTC AG	796
CFTR sense (nested)		Integrated DNA technologies	TGG AGA GCA TAC CAG CAG TG	638
CFTR antisense (nested)		Integrated DNA technologies	CTC CTG CCT TCA GAT TCC AG	638
CFTR sense (realtime PCR)		Invitrogen	GGC ATA CTG CTG GGA AGA AGC AA	100
CFTR antisense (realtime PCR)		Invitrogen	ACA TAG GCT GCC TTC CGA GTC	100
β-actin sense		Integrated DNA technologies	AGA TGA CCC AGA TCA TGT TTG	326
β-actin antisense		Integrated DNA technologies	ACG TAG CAC AGC TTC TCC TTA	326
β-actin sense (realtime PCR)		Invitrogen D-LUX	Not given	100
β-actin antisense (realtime PCR)		Invitrogen D-LUX	Not given	100



6. Non-quantitative reverse transcription-PCR (RT-PCR)

Following RNA extraction and DNase digestion as described above, 1 µg RNA was reverse transcribed by adding either 1 µl oligo dT (Invitrogen) or 10 pM each actin and CFTR specific RT primers (Figure 2.2 and Table 2.2), and sterile water (Sigma Aldrich) to a final volume of 11 µl in 200 µl PCR tubes (Axygen, Union City CA). RNA was heated to 70°C for 10 min and cooled to 4 °C prior to addition of 9 µl RT master mix (Invitrogen) (1 µl Moloney-murine leukemia virus (M-MLV) reverse transcriptase, 4 µl 5x first strand buffer, 2 µl 0.1 M dithiothreitol (DTT), 1 µl 10 mM dNTP and 1 µl Sterile H₂O) x number of samples. RT reaction was carried out on Bio-Rad iCycler at 37 °C for 1 h, followed by 70°C for 10 min and 4°C indefinite cooling step. Following RT, PCR was performed by adding 2-4 µl of cDNA template to 18 µl master mix (2 µl 10x PCR buffer, 0.4 µl 10 mM dNTP, 0.3 µl 5' primer, 0.3 µl 3' primer, 0.4 µl MgCl₂, 0.2 µl Platinum Taq, 16.4 µl H₂O). All PCR reagents were from Invitrogen and PCR cycling was performed on Bio-Rad iCycler as follows for both actin and CFTR primers (292) (Figure 2.2 and Table 2.2) (1 cycle of 94 °C 5 min, 30 – 45 cycles of 94 °C 1 min, 63 °C 1 min, 72 °C 3 min, 1 cycle of 72 °C 5 min, and indefinite 4 °C cooling). Following PCR, 1/10 volume of 10X loading buffer (30% glycerol, 0.025% Xylene cyanol, 0.025% bromophenol blue) was added and 10 µl PCR product was resolved on 1% agarose gels in Tris acetate EDTA (TAE buffer) (40 mM Tris-base, 1.1ml glacial acetic acid, 1 mM EDTA), using 1 Kb track-it DNA ladder (Invitrogen) as a size marker.

7. Nested RT-PCR

In some experiments, nested PCR was performed when bands were not detected in the first PCR amplification. Briefly, 1 μ l of original PCR product was added to 19 μ l of master mix (2 μ l 10x PCR buffer, 0.4 μ l 10 mM dNTP, 0.3 μ l 5' primer, 0.3 μ l 3' primer, 0.4 μ l $MgCl_2$, 0.2 μ l Platinum Taq, 17.4 μ l H_2O). PCR was performed on a Bio-Rad iCycler using same cycling parameters described in previous section but only allowing the reaction to perform 30 cycles of amplification. CFTR nested primers are described in Table 2.2.

G. Effect of inhibition of CFTR on mast cell function

1.Measurement of Cl^- Flux in cuvette assay

To determine whether ASO treatment affected Cl^- flux, 1×10^6 cells/ml were resuspended in 1 ml HTB. Cells were incubated for 30 min at 37 °C with 10 mM N-(ethoxycarbonylmethyl)-6-methoxyquinolinium bromide (MQAE) (Molecular Probes, Eugene OR), which is quenched by Cl^- anions. The cells were then washed twice and resuspended in 50 μ l HTB. To produce a driving force for Cl^- efflux, the cells were added to 1 ml of a Cl^- free solution, in which 140 mM NaCl of HTB was replaced by equimolar Na-gluconate. To compare the effects of ASO with those of 5-nitro-2-(3-phenylpropylamino) benzoic acid (NPPB, Sigma; 50 μ M), a Cl^- channel blocker commonly used to inhibit CFTR, experiments were

performed in the presence of this drug. When Cl^- leaves the cell, it dissociates from MQAE and fluorescence increases. ASO to CFTR but not MSO should inhibit this readout. MQAE fluorescence was excited at 350 nm and the emission was measured at 450 nm with a PTI spectrofluorimeter (Photon Technology Int., London, Ontario), using Felix software (version 1.42). All experiments were performed at 37 °C. Cl^- flux was calculated as the initial rate of change of MQAE fluorescence after addition of cells to the low- Cl^- solution. The increase in MQAE fluorescence was linear for at least 1-2 min before reaching a plateau. The slope of this linear portion is proportional to Cl^- efflux. For quantitative analysis, the data collected in the first 60 s were fitted using linear regression, and the slope was used as a measure of Cl^- efflux. To compensate for variations in absolute Cl^- flux between different cell preparations, each value in an individual data set was expressed relative to the mean control value for that set, and then the relative change in Cl^- flux was calculated from all sets.

2. Increased throughput Cl^- flux microplate assay

To increase throughput of Cl^- flux assay, we used the Cl^- sensitive fluorescent dye MQAE (Molecular Probes) based on a 96 well plate assay as previously described (293). Briefly, to determine whether CFTR regulates Cl^- flux in human MC, 1×10^6 cells were seeded in 1 ml of culture media. Cells were then incubated with 10 mM MQAE for 1 h at 37°C. Cells were washed twice in HTB and resuspended in 1 ml HTB containing appropriate drugs (Table 1.1). Cells were aliquoted into 1.5 ml eppendorf tubes (2.5×10^5 in 200 μl volume),

and untransfected cells were pre-incubated in HTB with the inhibitors NPPB (50 μ M) (Sigma Aldrich) or CFTR_{inh-172} (100 nM) (Calbiochem, Gibbstown NJ) 15 min prior to addition cAMP elevating agent forskolin (FSK) (50 μ M) (Sigma Aldrich) and phosphodiesterase inhibitor isobutyl methylxanthine (IBMX) (50 μ M) (Sigma Aldrich) for 5 min in HTB to activate cAMP-dependent CFTR Cl⁻ flux. To produce a driving force for Cl⁻ efflux, the cells were centrifuged at 120 x g for 30 s and resuspended in 10 μ l HTB containing inhibitors and/or FSK/IBMX. Cell suspensions were then added to 200 μ l of Cl⁻ free buffer in which 140 mM NaCl of HTB was replaced by equimolar NaNO₃. This was done in the presence of inhibitors and/or FSK/IBMX, in flat bottom, 96 well black plates with clear bottoms (Fisher Scientific). MQAE fluorescence was excited at 360 nm and the emission was measured at 460 nm on an FLX-800i fluorescence plate reader with temperature control capability (Fisher Scientific), reading from the bottom of the wells at sensitivity 60. Fluorescence was measured every 10 s for 5 min, followed by addition of 0.2% Triton X-100 for maximum fluorescence and then 150 mM potassium thiocyanate (KSCN) (Sigma Aldrich) to quench MQAE signal and get background fluorescence. Following background correction, initial fluorescence (F_0) was adjusted to zero for all treatments, then Cl⁻ flux was calculated as $F_t - F_0$, where F_t is the fluorescence at a given time point and F_0 is fluorescence at time 0 (293). For quantitative analysis, the data were fitted using linear regression, and the slope was used as a measure of Cl⁻ efflux with slopes of all inhibitor treatments being compared to the slope of the positive controls during the first 60 s of the assay.

3. β -hexosaminidase release

As HMC-1 do not contain many granules, and do not express the high affinity IgE receptor (276), release of a stored mediator, β -hex, was measured from LAD2 MC. Briefly, cells were washed in HTB and resuspended at 1×10^6 cells/ml in complete Stempro 34. Cells were then sensitized overnight in $1 \mu\text{g/ml}$ IgE (Calbiochem). For assay, cells were washed twice in HTB and aliquoted in 1.5 ml eppendorf tubes at 2×10^5 cells in $200 \mu\text{l}$ volume. Cells were then incubated with CFTR inhibitors (15 min), and activated with $2 \mu\text{g/ml}$ rabbit anti human IgE (Dako, Mississauga ON) for 30 min at 37°C . The Ca^{2+} ionophore A23187 (200 nM) was used as a positive control for β -hex release. After 30 min, supernatants were collected, and pellets were lysed in 0.2% Triton X-100, vortexed for 10 s on highest setting, and lysate spun at $120 \times g$ for 1 min. From each supernatant and lysate, $25 \mu\text{l}$ was diluted with $25 \mu\text{l}$ HTB in triplicate and incubated with $50 \mu\text{l}$ of β -hex substrate (4-methylumbelliferyl N-acetyl- β -D-glucosaminide) (Sigma Aldrich) in flat bottom, 96 well black plates with clear bottoms (Fisher Scientific) for 1 h at 37°C . Reaction was stopped using $100 \mu\text{l}$ 0.2M Tris-base, and fluorescence was excited at 360 nm and the emission was measured at 460 nm on a FLX-800i fluorescence plate reader (Fisher Scientific), reading from the bottom of the wells at sensitivity 30. To assess β -hex release, triplicate fluorescence values for pellets and supernatants were averaged, blank

readings (buffer + substrate) were averaged and subtracted from all readings and the following formula was used:

$$\text{Equation 3)} \quad \% \text{ release} = \frac{\text{Supernatant}}{(\text{Supernatant} + \text{Pellet})} \times 100$$

4. Cytokine measurements

Release of IL-8, IL-6 and TNF was measured with BD OptEIA human cytokine set kits (BD Pharmingen, San Diego CA). Untreated, NPPB or GlyH-101 treated HMC-1 cells (1×10^6 /ml in culture medium) were incubated with or without NECA (3 μ M) for 24 h in complete growth medium. Cytokine release from LAD2 was also assessed following CFTR inhibition and either NECA (3 μ M) or IgE (1 μ g/ml)/anti-IgE (2 μ g/ml) stimulation for 24 h. After incubations, cells were spun at 120 x g for 30 s, and supernatants were frozen at -80°C until analysis. The addition of inhibitors or NECA had no effect on cell viability in either cell types as established by trypan blue vital staining (not shown). To screen for cytokine changes resulting from CFTR inhibition, LAD2 cells were treated with CFTR inhibitors and activated with anti-IgE (2 μ g/ml) as described above. Cell free supernatants were then assayed using the human cytokine array kit panel A (R&D Systems). Membranes were developed by incubating membranes with ECL Western blot detection reagent (GE Healthcare) for 5 min, followed by exposure to Kodak Biomax MR film (Kodak) for 5 min. Films were then developed on SRX-101A developer (Konica). All membranes were developed on the same piece of film and the image was scanned as 16-bit 1200

dpi grayscale and saved as a Tif image using an Epson Perfection 4490 photo scanner (Epson, Toronto ON). Films were digitized using the Odyssey software version 1.2, and integrated pixel density was calculated by the computer for each spot on the membrane.

5. Eicosanoid production by LAD2 and PBMC

MC were sensitized with 1 $\mu\text{g/ml}$ human IgE (Calbiochem) overnight at 37°C, 5% CO₂. Cells were washed 2 x in HTB, and resuspended at 1 x 10⁶/ml in complete StemPro-34 medium supplemented with IL-6 (100 ng/ml) for PBMC only. LAD2 cells were preincubated with CFTR inhibitors for 15 min and then activated with 2 $\mu\text{g/ml}$ rabbit anti-human IgE (Dako) for 30 min at 37°C. PBMC were not treated with CFTR inhibitors, but were stimulated with 2 $\mu\text{g/ml}$ rabbit anti-human IgE for 30 min at 37 °C. The reactions were stopped by centrifugation at 150 x g for 5 min at 4 °C. The supernatants were retained at -80 °C for assay of PGD₂ and LTC₄ using PGD₂-MOX EIA kit or LTC₄ EIA kit (Cayman Chemical, Ann Arbor, MI) according to the manufacturer's instructions.

H. Comparison of peripheral blood-derived human cultured mast cells (PBMC) from non-Cystic Fibrosis and Cystic Fibrosis subjects.

1. Tryptase chymase staining

After 8 wk in culture, PBMC were stained for tryptase and chymase expression using the following protocol. Briefly, cytopins were prepared as

described above and allowed to air dry overnight. Cell spots on cytopins were then circled with PAP pen and pre fixed in 100% methanol containing 0.6% H₂O₂ for 30 min at room temperature to inhibit endogenous peroxidase. Cells were then rinsed with H₂O and stored at 4 °C for up to 1 wk. To stain the cells, 50 µl of biotin-conjugated isotype control antibody clone 107.3 (BD Biosciences) or biotin-conjugated anti-chymase clone B7/B (Millipore) at 3 µg/ml were diluted with Dako antibody diluent with background reducing components (Dako). Slides were incubated overnight in a humid chamber. Slides were rinsed with 75 µl H₂O then washed 3 x 5 min in 75 µl TBS containing 0.05% Tween 20, then 1 x in 75 µl H₂O. H₂O was removed and 2 drops of ready to use streptavidin-HRP (Vector Laboratories, Burlingame CA) were added to the cells for 1 h at room temperature in a humid chamber. Slides were washed as described above and 100 µl NovaRED substrate was used to develop chymase color (Vector Laboratories). Reaction was stopped by immersing slides in H₂O for 5 min. Chymase stained slides were then incubated with 50 µl anti-tryptase antibody clone G3/AP (Chemicon) at 1.5 µg/ml diluted with antibody diluent with background reducing agent (Dako). Slides were washed as described above, and tryptase color was developed by adding 2 drops of prepared substrate from the Vector Blue Alkaline Phosphatase kit (Vector Laboratories). Cells were incubated with substrate for 10-20 min in a dark humid chamber and reaction was stopped by adding assay buffer (100 mM Tris-HCl pH 8.2) then rinsing slides in H₂O for 5 min. Permanent mounting of slides was done by adding 30 µl of Cytoseal™ (Fisher

Scientific) and placing a 1.8 x 1.8 mm coverslip (Fisher Scientific) onto mounting medium. Slides were allowed to dry overnight before visualizing by microscopy.

2. FcεR1 and c-Kit expression

Cells were resuspended at 1×10^6 /ml in flow buffer containing 5% milk (Bio-Rad Laboratories) and 10% human AB serum (Sigma Aldrich) and incubated for 30 min at 4°C. Cells were washed 2 x in flow buffer and then aliquoted into Falcon 2054 flow cytometry tubes (BD Biosciences) at 100 µl/tube. FITC conjugated FcεR1 and isotype antibodies (EBioscience, San Diego CA) were added to tubes. Phosphatidylethanolamine (PE) conjugated isotype and c-Kit antibodies (BD Biosciences) were added to separate tubes. Cells were mixed and incubated at 4°C for 1 h. Cells were washed 2 x 5 min in flow buffer and resuspended in 400 µl flow buffer. FcεR1 and c-Kit expression was analyzed on FACScan flow cytometer (BD Biosciences), using FL-1 and FL-2 channels for FITC and PE respectively.

3. Cytokine array

We assessed synthesis and secretion of *de novo* synthesized mediators from non-CF and CF PBMC to determine if the two cell genotypes differentially expressed cytokines and chemokines. Our initial strategy was to screen for cytokine and chemokine secretion using the Proteome Profiler™ cytokine array panel A (R&D Systems, Minneapolis, MN). Briefly, cells were hemidepleted as

described previously and incubated with IgE (1 $\mu\text{g/ml}$) overnight at $1 \times 10^6/\text{ml}$. Cells were then washed and resuspended in the same volume of Stempro-34 containing 100 ng/ml SCF and 100 ng/ml IL-6 to maintain health of the cells. Cells were plated in 24-well plates at $1 \times 10^6/\text{ml}$ in 1000 μl volume. Cells were treated with sham or anti-IgE (2 $\mu\text{g/ml}$) for 48 h. After stimulation, cells were harvested and supernatant was added to protein array membranes and blotted for as per manufacturer's instructions. Membranes were then incubated with ECL reagent (GE Healthcare) for 5 min, and exposed to Hyperfilm (GE Healthcare) for 5 min, then developed on a SRX-101A developer (Konica).

To confirm and extend the data obtained with the protein array, PBMC supernatants were sent to for Searchlight multiplex analysis of cytokines and chemokines (Aushon Biosystems, Billerica, MA). To prepare samples, cells were hemidepleted and incubated with IgE (1 $\mu\text{g/ml}$) overnight at $1 \times 10^6/\text{ml}$. Cells were then washed and resuspended in the same volume of Stempro-34 containing 100 ng/ml SCF and 100 ng/ml IL-6, added to maintain health of the cells. Cells were then aliquoted into 48 well plates at $1 \times 10^6/\text{ml}$ in 200 μl volume. Cells were treated with anti-IgE (2 $\mu\text{g/ml}$). After 48 h, cell-free supernatants were harvested and stored at -80°C . Cells were resuspended in 200 μl fresh Stempro 34 and lysed by 3 cycles of 30 s freezing in liquid N_2 , followed by 120 s thawing in an FS30H sonicator bath (Fisher Scientific). Lysate was spun at $10\,000 \times g$ for 5 min to remove cell debris, and supernatant was frozen at -80°C . Samples were sent to Aushon for analysis in batches of 20 samples (2 separate non-CF PBMC) and 37 samples (3 separate experiments each of non-CF PBMC and CF PBMC).

In all experiments, one well of cells were stimulated with *P. aeruginosa* strain PAO1 rather than anti-IgE as *P. aeruginosa* has been reported to induce cytokine and chemokine secretion from human MC (294-296). PAO1 strain of *P. aeruginosa*, was a generous gift from Dr. Randy Irvin, Medical Microbiology and Immunology, University of Alberta. Bacteria were fixed by 0.1% formalin and killed with (100 µg/ml) gentamycin for 2 h before adding to PBMC because live bacteria induce apoptosis in human MC (297). Killed bacteria were added to MC at a multiplicity of infection (MOI) ratio of 25 bacteria:MC cell (25:1). In these experiments, PBMC were incubated for 24 h as described previously (294-296). Harvesting of samples was conducted in the same way as with anti-IgE stimulation. For both IgE/anti-IgE and PAO1 treatments, total cytokine content was calculated (supernatant + lysate), and % secretion was calculated as above (equation 3).

I. Graphing and statistical analysis

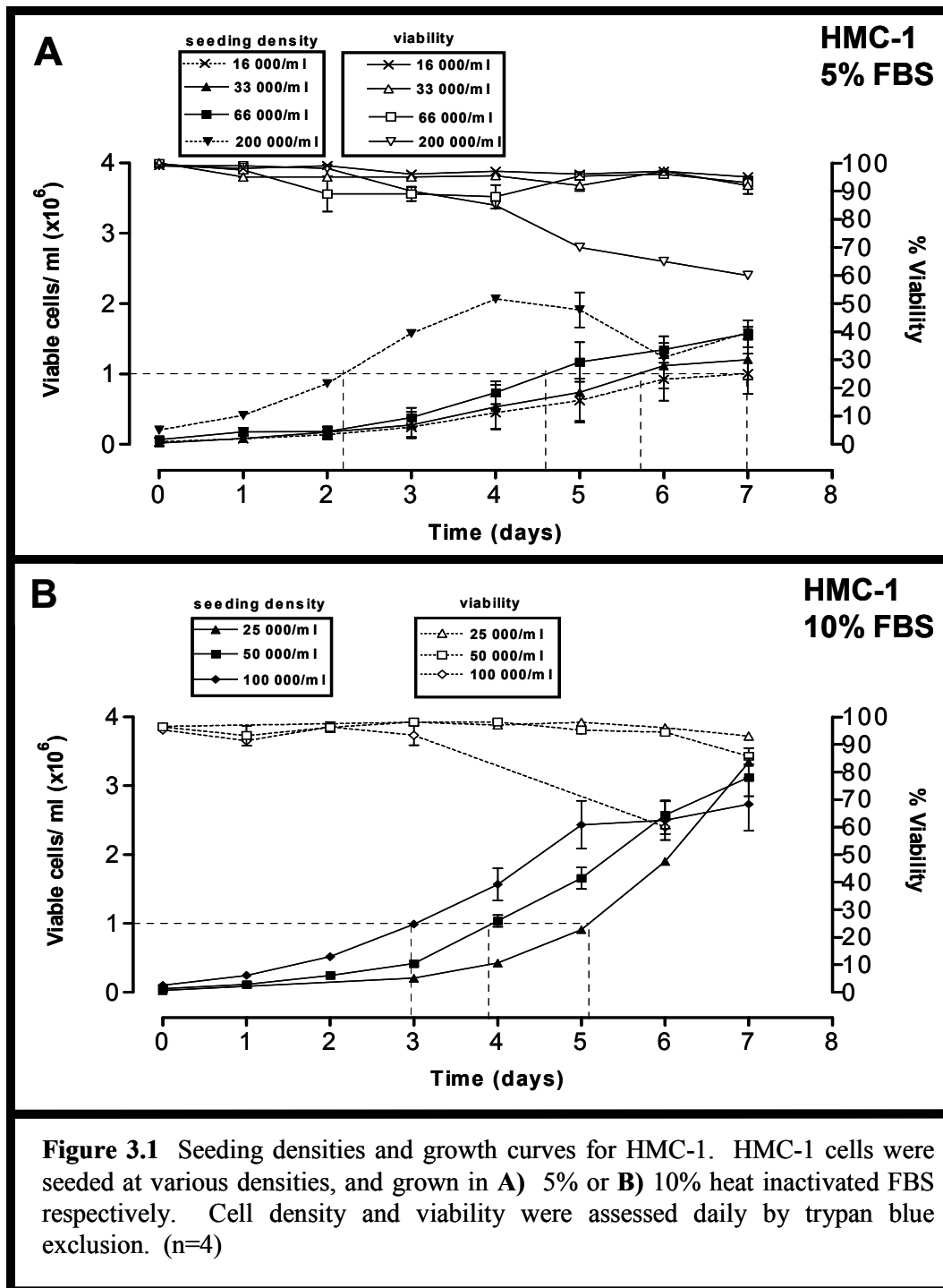
The InStat program (GraphPad Software, La Jolla CA) was used for statistical analysis. All data are shown as mean values \pm SEM. In all experiments, Tukey's test comparing different treatments was performed following determination of significance by one way ANOVA analysis. If data was not found to be significant by ANOVA, Tukey's test was not performed by the software. A p-value < 0.05 was considered statistically significant and represented by an asterix (*).

Chapter 3. Results

A. Cell proliferation

1. HMC-1 growth curves

HMC-1 have been extensively used to study MC. The conditions of HMC-1 culture are either reported as passage schedule (3-4 d) or maintaining cells at a certain density (between 3×10^5 and 1×10^6 cells/ml), or are ambiguous (49, 298-300). Studies reporting passage schedule often do not give seeding densities, whereas studies reporting seeding densities do not give passage schedule. Thus, we standardized seeding densities and passage times in our laboratory and compared the growth characteristics of our HMC-1 with those in other studies. HMC-1 proliferation experiments used 5% or 10% heat inactivated FBS at various seeding densities (Figure 3.1). When HMC-1 cells were seeded at 16 000, 33 000, 66 000 and 200 000 cells/ml in medium containing 5% FBS, they reached 1×10^6 cells/ml within 7, 6, 4.5 and 2 d respectively (Figure 3.1 A). When HMC-1 were seeded at 25 000, 50 000 or 100 000 cells/ml in media containing 10% FBS, they reached 1×10^6 cells/ml within 5, 4 and 3 d respectively (Figure 3.1 B). Cells were not seeded at 200 000 cells/ml in 10% FBS as they would reach 1×10^6 cells/ml within 24h. When 200 000 cells/ml were seeded in 5% FBS, 1×10^6 cells/ml was reached within 2 d, which required passaging every 2-3 d as viability began to drop at 4 d (Figure 3.1 A). Seeding of cells at 100 000/ml in media containing 10% FBS resulted in proliferation of the cells so that the passage rate of 3-4 d and maximum cell density of 1×10^6 cells/ml reported previously could be achieved (49, 298).

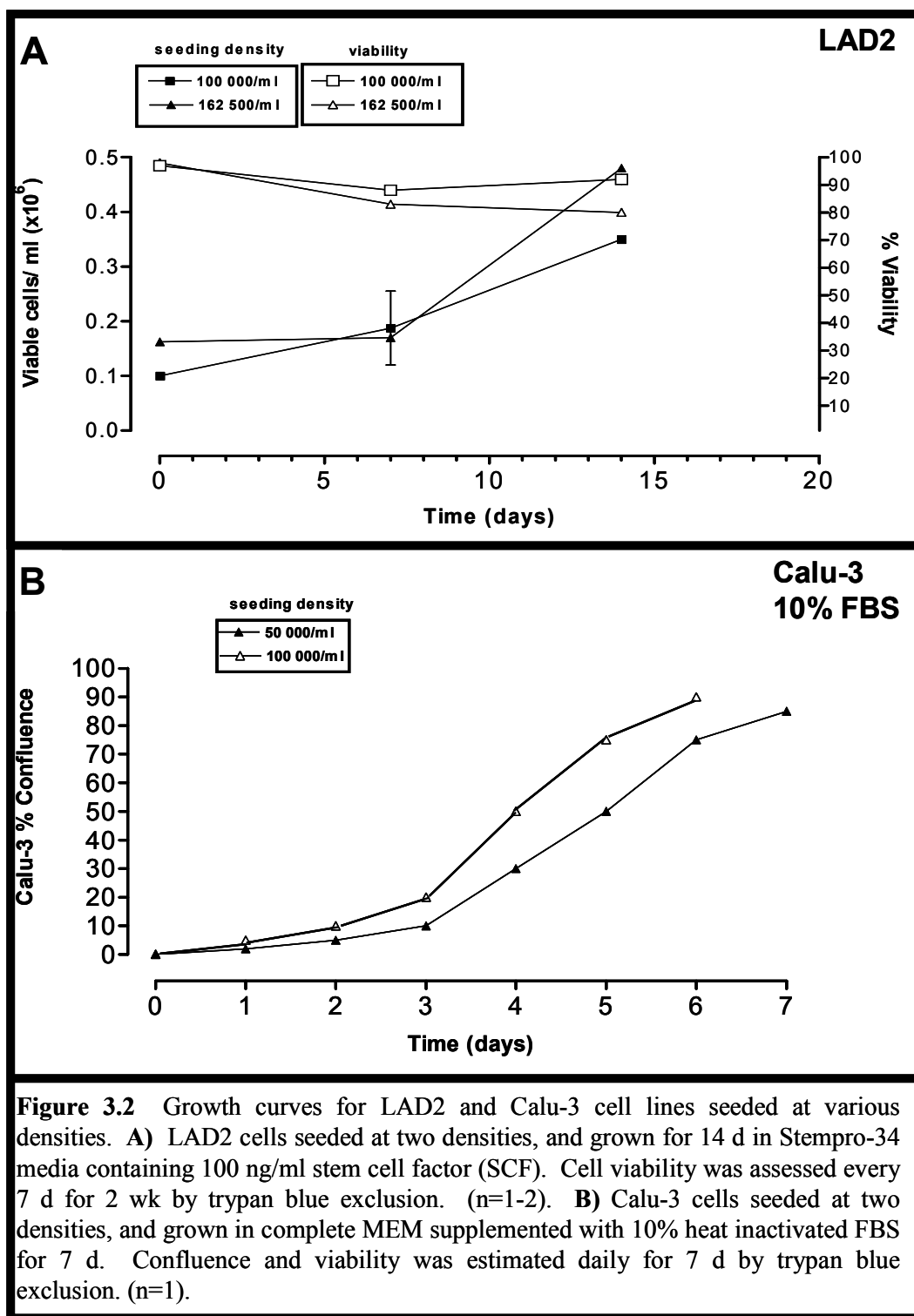


2. LAD2 growth curves

For LAD2 cells, the recommended maximal cell density was previously established as being 0.5×10^6 , and LAD2 cells have been reported to double every 10 d (277, 301). We performed growth experiments to confirm this in our hands. Cells seeded at either 1×10^5 or 1.625×10^5 /ml in 10 ml complete Stempro-34 were counted every wk to determine growth of the cells (Figure 3.2 A). The proliferation slope for 1.625×10^5 cells/ml and 1×10^5 cells/ml were similar between 0 d and 7 d, but was steeper for 1.625×10^5 cells/ml than for 1×10^5 cells/ml from 7 d to 14 d indicating more rapid proliferation with increased cell density (Figure 3.2A). With initial seeding density of 1.625×10^5 cells/ml, cell density at 14 d was near the recommended maximal cell density of 0.5×10^6 /ml, whereas using 1×10^5 cells/ml the cell concentration still below the recommended maximal cell density. Thus, to keep cell density below the recommended maximal cell density and prevent LAD2 overgrowth, we decided to use 1×10^5 cell/ml as an initial seeding concentration for maintaining the cells in culture. Furthermore, cells were never allowed to exceed 14 d in the same flasks without reseeding new flasks or using cells for experiments.

3. Calu-3 growth curves

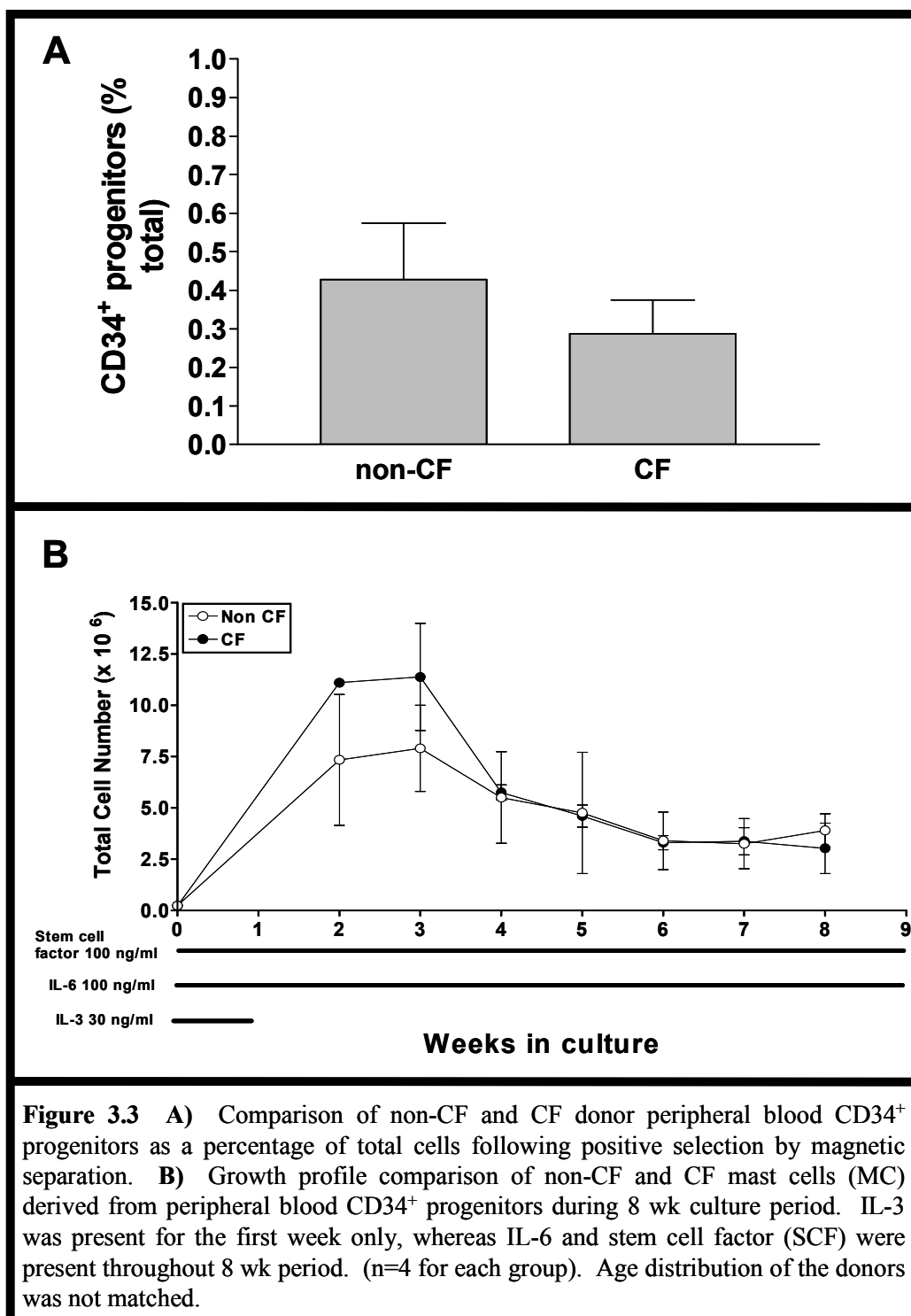
Confluence in Calu-3 was determined as the absence of cell-free areas on the bottom of the flasks. Calu-3 cells were seeded at either 50 000 or 100 000 cells/ml and confluence was estimated daily for 7 d (Figure 3.2 B).



Confluence did not increase significantly until 3 d, at which point cell growth became exponential, and flasks reached 70-80% confluence after 7 d. 100% confluence was never observed, as the cells began to die and detach from the flask if they were not split at 7 d (not shown).

4. Peripheral blood-derived mast cells cultured from CD34⁺ progenitors

We also determined proliferation characteristics of CF and non-CF PBMC (Figure 3.3). We isolated CD34⁺ progenitors from peripheral blood by density separation and magnetic positive selection as described in chapter 2. After purification, the recovery of CD34⁺ cells was $0.42\% \pm 0.15\%$ and $0.29 \pm 0.09\%$ of the starting number of cells in non-CF and CF donors respectively (Figure 3.3 A). This difference was not statistically significant. Purity of the cells after magnetic separation was not assessed as flow cytometric analysis would require the entire sample and there would be no cells left to culture. Cells were placed in culture as described in chapter 2, and cell growth was tracked weekly starting at wk 2 to determine if any differences exist in growth characteristics of PBMC from CF and non-CF progenitors. As can be seen in Figure 3.3 B, there is an exponential growth of cell numbers within the first 2 wk in culture, which appeared to reach its maximum at 2-3 wk and thereafter declined until about wk 6 when a constant cell number was reached. We followed the growth of four CF and four non-CF cultures and found no statistically significant differences in growth profile and cell numbers during 8 wk culture period (Figure 3.3 B).



Also, PBMC from CF and non-CF donors did not appear different visually during the 8 wk period.

B. Characterization of Cystic Fibrosis and non-Cystic Fibrosis PBMC

1. CF but not non-CF PBMC express more MC_{TC} than MC_C

To determine if MC cultured from CF and non-CF patient peripheral blood progenitors are phenotypically and biochemically similar, we examined tryptase and chymase expression in PBMC. Figure 3.4A shows a representative field of PBMC from non-CF subjects, whereas Figure 3.4B shows a representative field of PBMC from $\Delta F508$ CF patients. Cells are stained for tryptase (blue), chymase (red) or tryptase/chymase (red and blue). Double positive cells stain with both blue and red and are more difficult to identify than single positive cells. These representative images suggest that non-CF PBMC have more intensely stained chymase positive cells (red) than non-CF PBMC, but if there are other differences, they are not obvious. When counted by three people separately in a blinded fashion, non-CF PBMC are $20 \pm 3\%$ tryptase only positive, $44 \pm 6\%$ chymase only positive and $37 \pm 5\%$ tryptase/chymase double positive (Figure 3.5). In non-CF PBMC, there were significantly more chymase only positive cells than tryptase only positive cells, but the difference between tryptase/chymase positive cells and either subtype of single positive cells was not significant (Figure 3.5).

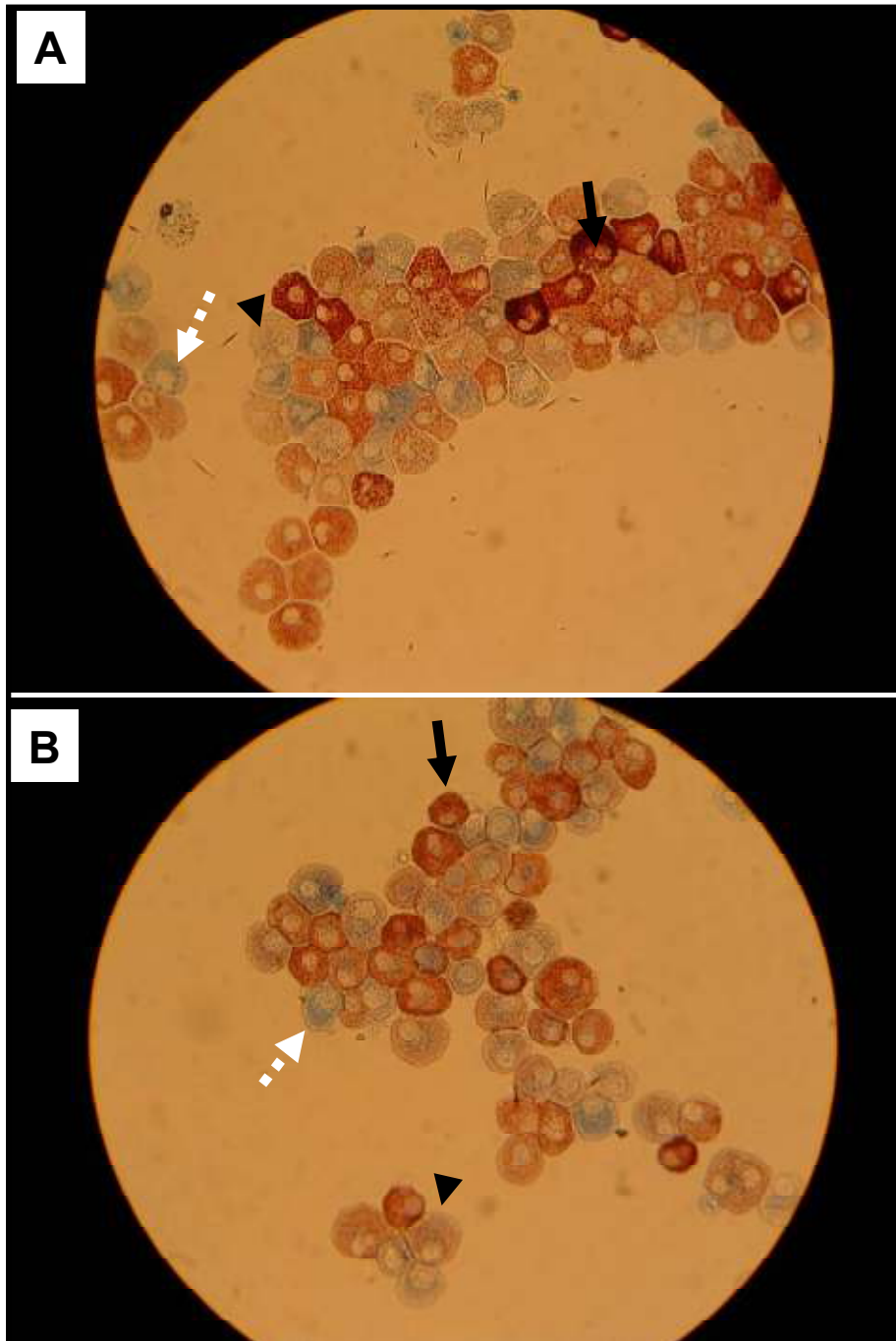
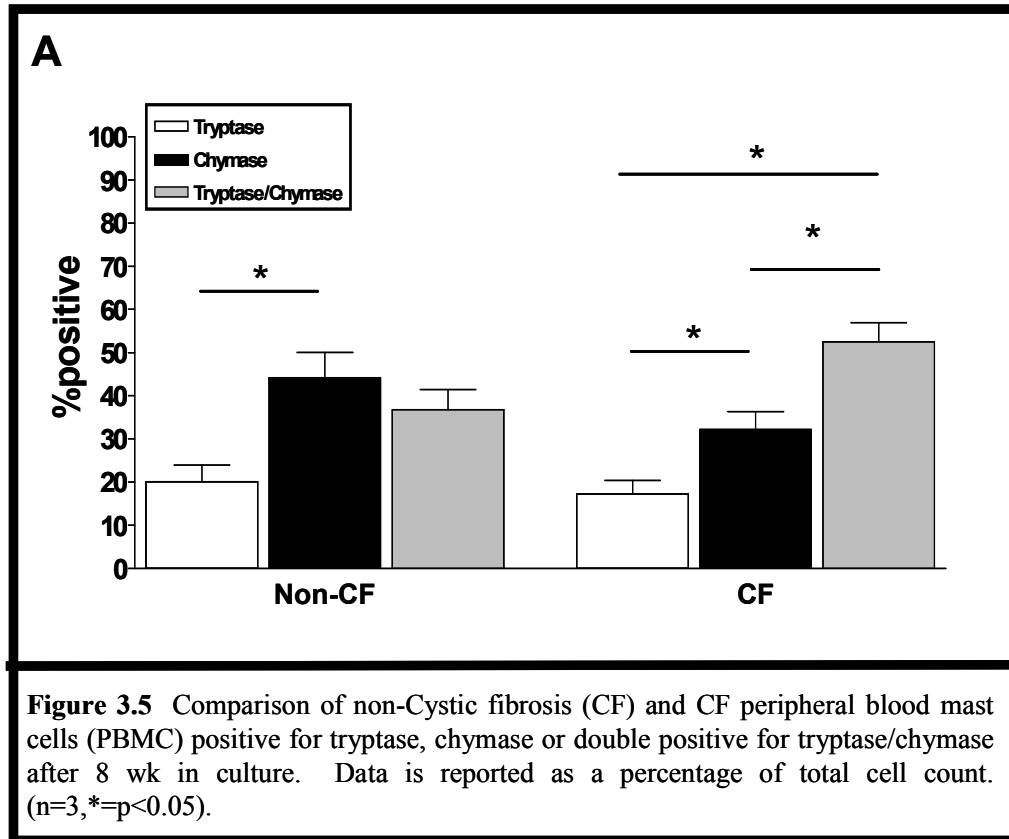


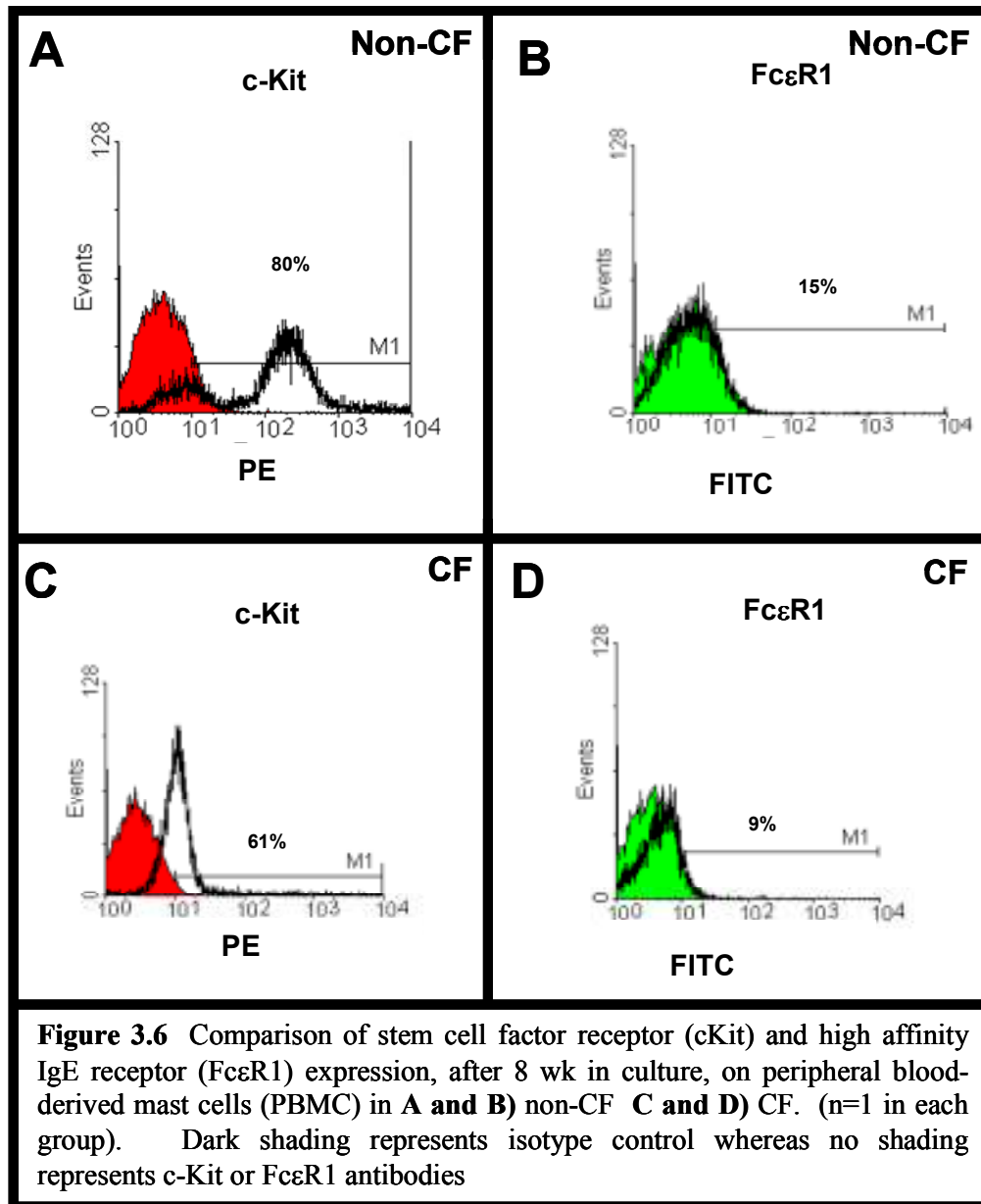
Figure 3.4 Comparison of tryptase (blue) (dashed arrow), chymase (red) (black arrow) and tryptase/chymase (red/blue) (black arrowhead) staining in peripheral blood derived mast cells (PBMC) after 8 wk in culture. PBMC derived from **A)** Non-Cystic fibrosis (CF) CD34⁺ peripheral blood progenitors and **B)** CF CD34⁺ peripheral blood progenitors. Data is representative of 4 blindly counted slides counted in each group.



In CF PBMC, $17 \pm 3\%$ were tryptase only positive, $32 \pm 4\%$ chymase only positive and $53 \pm 4\%$ tryptase/chymase positive (Figure 3.5). In CF PBMC, there were significantly more chymase positive cells than tryptase positive cells, as well as significantly more tryptase/chymase positive cells than chymase only or tryptase only positive cells (Figure 3.5). The difference between tryptase/chymase and chymase positive cells was also significant in CF, but not in non-CF PBMC (Figure 3.5). Our data also suggests that there is no difference in tryptase only positive cells between CF and non-CF PBMC, but that there is a trend towards a greater proportion of tryptase/chymase double positive cells in CF PBMC. This difference suggests that CF PBMC are more polarized towards the connective tissue MC phenotype than non-CF MC. This may prove to be statistically significant, given the opportunity to test a larger sample size.

2. CF PBMC appear to express less surface c-Kit than non-CF PBMC

After 8 wk in culture, we compared the expression of both SCF receptor (c-Kit) and FcεR1 on the plasma membrane of non-CF and CF PBMC (Figure 3.6). From the 4 CF donors studied, we used the cells as efficiently as possible for all experiments, and as a result, we only had enough cells remaining to perform one experiment, which we paired with one experiment of non-CF cells for comparison. In this experiment, 80% of non-CF PBMC were positive for c-Kit, whereas 61% of CF PBMC were positive for c-Kit (Figure 3.6 A and C).



In non-CF PBMC, there were two subpopulations of PBMC (c-Kit^{lo} and c-Kit^{hi}). In CF PBMC, only one c-Kit subpopulation was present and appeared to be c-Kit^{mid}. This data suggests that a difference in c-Kit expression exists between the two cell types which could be linked to uptake of SCF as c-Kit is a desensitizing and non-recycling receptor (302). FcεR1 was similar between the two PBMC genotypes with 15% of the non-CF cells and 9% of the non-CF PBMC expressing FcεR1 (Figure 3.6 B and D). Basal expression of FcεR1 is known to be low in MC and is significantly upregulated by IgE sensitization or IL-4 treatment (89, 303). Because of limited availability of CF PBMC, we were not able to compare IgE or IL-4 mediated upregulation of FcεR1 in non-CF and CF PBMC. Although it remains to be tested, the difference in c-Kit expression in CF vs non-CF PBMC, may explain the differences in protease content as it has been shown that the presence or absence of SCF can regulate MC phenotype (CTMC vs MMC) (304, 305).

C. Mast cell mediator secretion

1. HMC-1 produce IL-8 in response to adenosine agonist NECA stimulation

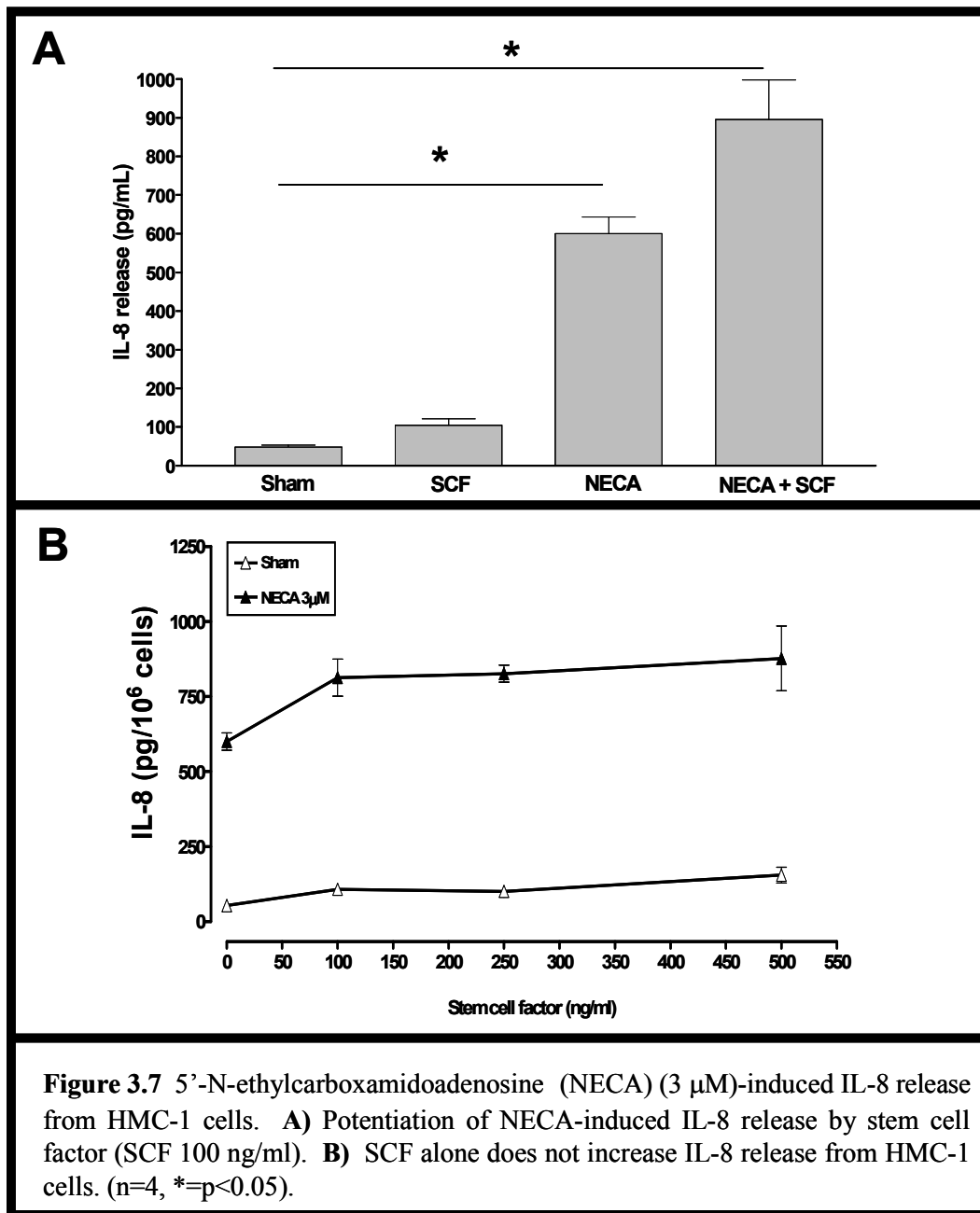
As a physiological stimulus of MC, we chose NECA (3 μM) which was previously shown to induce significant IL-8 release from HMC-1 cells (49). This study also showed that addition of recombinant SCF to the cells concurrently with NECA potentiated the release of IL-8 (49). We confirmed these findings, and showed that basal IL-8 secretion of 47 ± 6 pg/10⁶ cells non-significantly increased

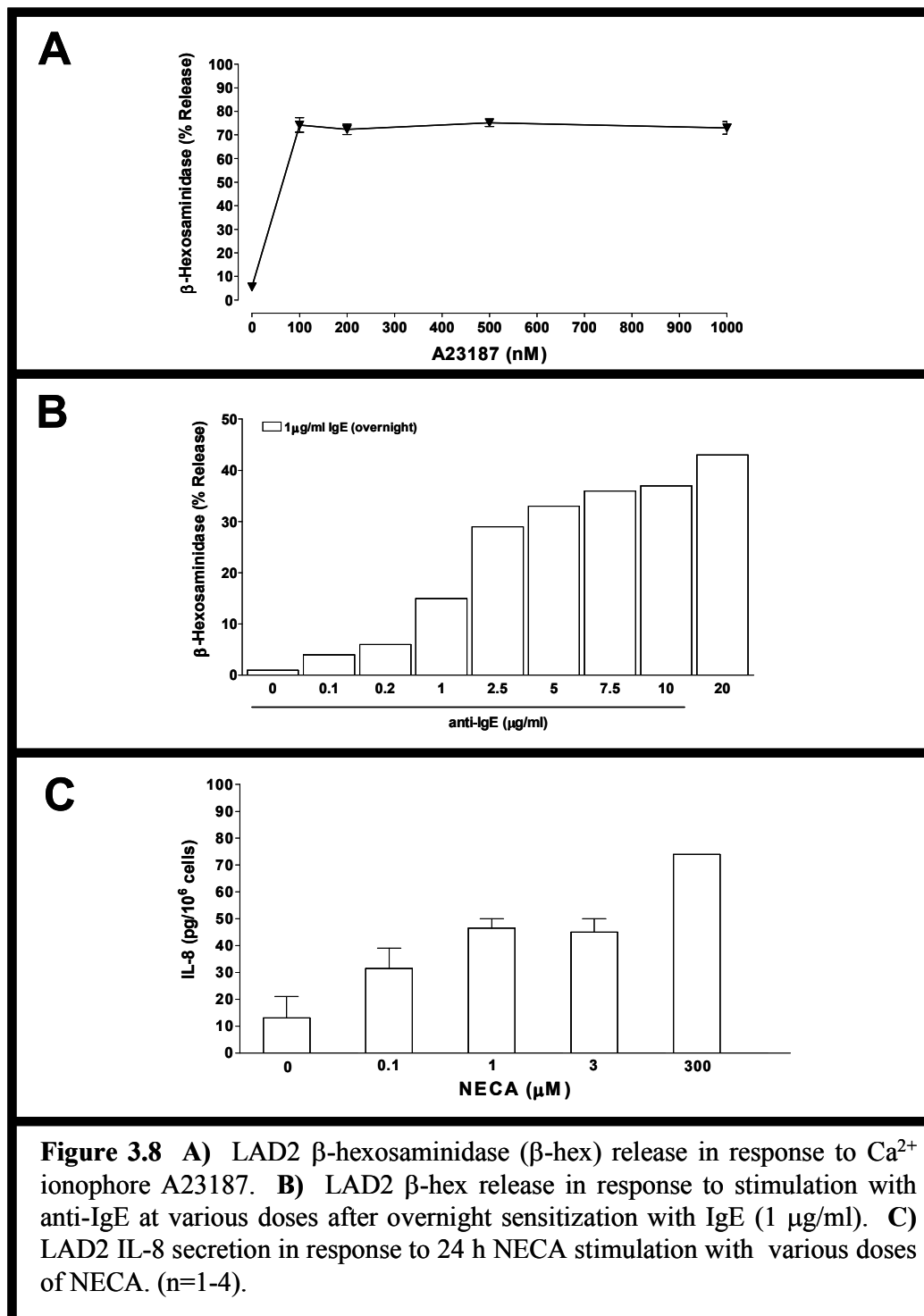
to 100 ± 17 pg/ 10^6 cells after addition of SCF alone, but significantly increased to 600 ± 43 and 894 ± 103 pg/ 10^6 cells after 8 h stimulation with NECA or with NECA and SCF respectively (Figure 3.7 A). We also confirmed that increased doses of SCF did not increase potentiation of IL-8 release from HMC-1 over that seen with 100 ng/ml SCF, as previously reported (Figure 3.7 B) (49).

2. LAD2 respond poorly to NECA, but strongly to Ca^{2+} ionophore A23187 and IgE/ α -IgE stimulation

We assessed the response of LAD2 cells to stimulation with various doses of A23187, IgE/anti-IgE and NECA (Figure 3.8). LAD2 cells spontaneously released $6 \pm 4\%$ β -hex when sham treated (Figure 3.8 A and B). Treatment with 100 nM A23187 caused $74 \pm 3\%$ β -hex release from LAD2 cells, and doses of 200 nM to 1000 nM A23187 did not increase β -hex release. Thus, in subsequent experiments, we used 200 nM A23187 to stimulate LAD2 cells and ensure maximal release of β -hex as a positive control.

We also assessed release of β -hex from LAD2 cells in response to Fc ϵ R1 aggregation. Maximal β -hex release of 42% was reached by stimulating the cells with 20 μ g/ml anti-IgE (Figure 3.8 B). We wanted to use a submaximal dose of anti-IgE to stimulate the cells so that any potential differences induced by CFTR inhibition would not be masked by over stimulation of the cells. Thus, we chose to use 2 μ g/ml in subsequent experiments because it gave similar results





as 2.5 $\mu\text{g/ml}$ (20-25% release) as shown in subsequent figures, and required less antibody. As NECA did not induce β -hex release from LAD2 cells, we assessed the capacity of NECA to induce IL-8 secretion from LAD2 as previously demonstrated in HMC-1 cells (49). We showed that LAD2 cells release 40 pg/ml IL-8 when stimulated with 3 μM NECA (Figure 3.8 C). One hundred fold more NECA only increased IL-8 production to 80 pg/ml (Figure 3.8 C). Thus, we used 3 μM NECA in subsequent experiments, the same dose used in HMC-1 stimulation (Figure 3.7).

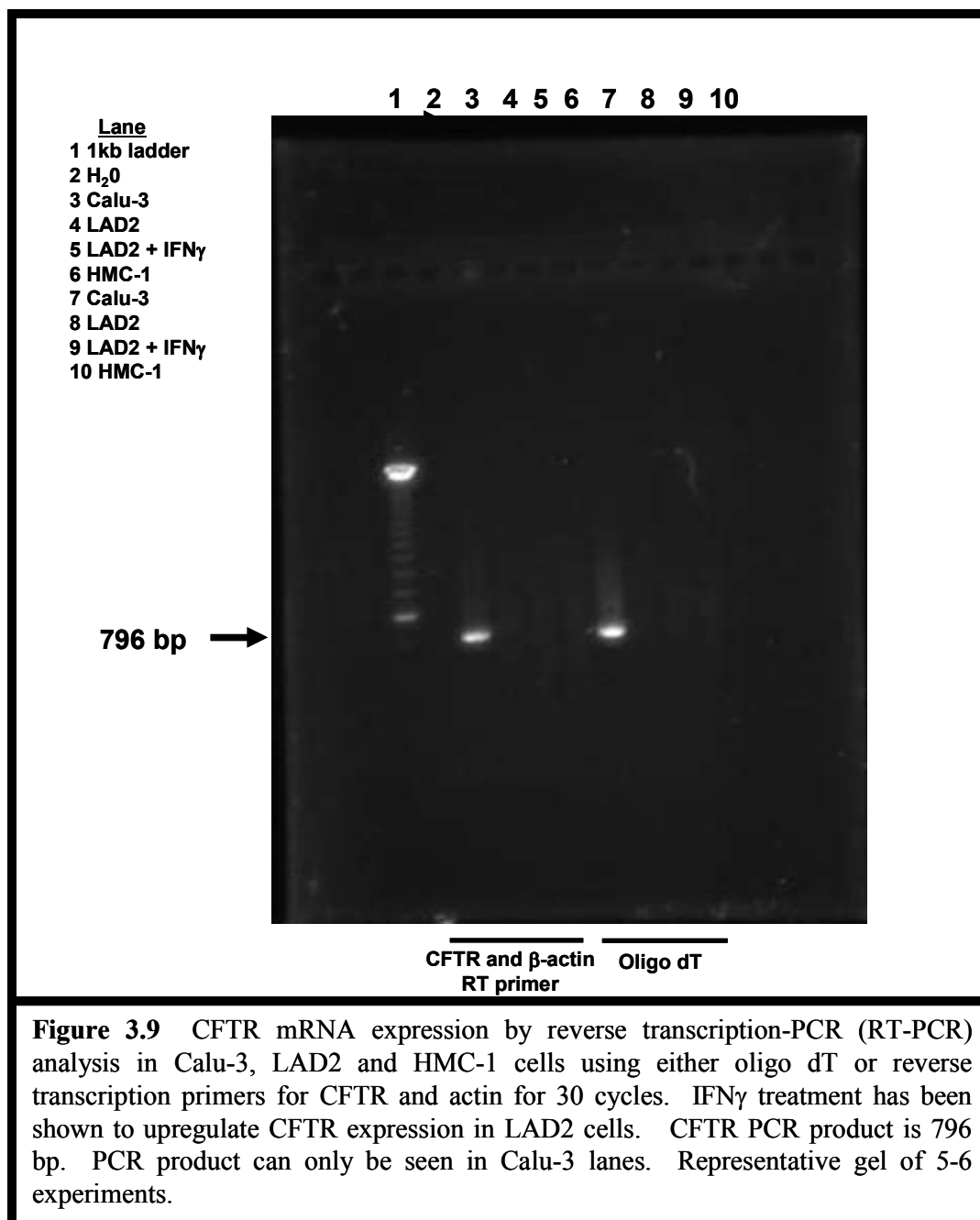
D. Characterization of CFTR expression in mast cells

1. Mast cells express low levels of CFTR mRNA

Preliminary experiments to optimize PCR conditions showed that the best conditions to detect CFTR with the primers designed (Table 2.1) were with a melting temperature (T_m) of 63°C and a MgCl_2 concentration of 0.5 mM (not shown). Under these conditions, we saw the strongest amplification with the lowest background (smearing) and non-specific amplification (multiple bands) after 30 cycles (not shown). Thus, we used these conditions for subsequent RT-PCR.

Using both oligo dT and specific RT primers for CFTR and β -actin (Figure 2.2 and Table 2.2), we ran RT-PCR on HMC-1, LAD2, and Calu-3. After 30 cycles of amplification, we saw CFTR transcripts in Calu-3 lanes, but not

HMC-1 or LAD2 lanes, even in the presence of IFN γ which upregulates CFTR in MC (Appendix 2) (Figure 3.9). Using the same cDNA, we ran another PCR using 45 cycles of amplification testing for both β -actin and CFTR to ensure that the cDNA was of good quality in all treatments (Figure 3.10). We show that reverse transcription was successful in Calu-3, LAD2 and HMC-1 by the presence of actin bands at 304 bp after 45 cycles of amplification (Figure 3.10). CFTR transcripts also appeared in all treatments in this PCR reaction, but Calu-3 expressed a strong signal, whereas in LAD2, LAD2 treated with IFN γ and HMC-1 cells a very faint band appeared at the same product size as in Calu-3 cells (Figure 3.10). In our previous work, we showed CFTR mRNA expression in rat MC by regular RT-PCR and in human MC by qPCR (107, 201). In these experiments, we showed by regular RT-PCR that human MC CFTR express mRNA but that these transcripts are not abundant. To determine if PBMC express CFTR mRNA, we also performed PCR on non-CF PBMC following mRNA extraction. After 30 cycles of amplification, we saw the appearance of β -actin transcripts at 304 bp in both PBMC and Calu-3 (Figure 3.11 A). The actin signal was weaker in PBMC, and there seemed to be no difference in signal intensity with or without heparinase treatment. Calu-3 and T84 cDNA were positive for CFTR transcripts at 796 bp, but no CFTR transcripts were detectable in PBMC (Figure 3.11 A).



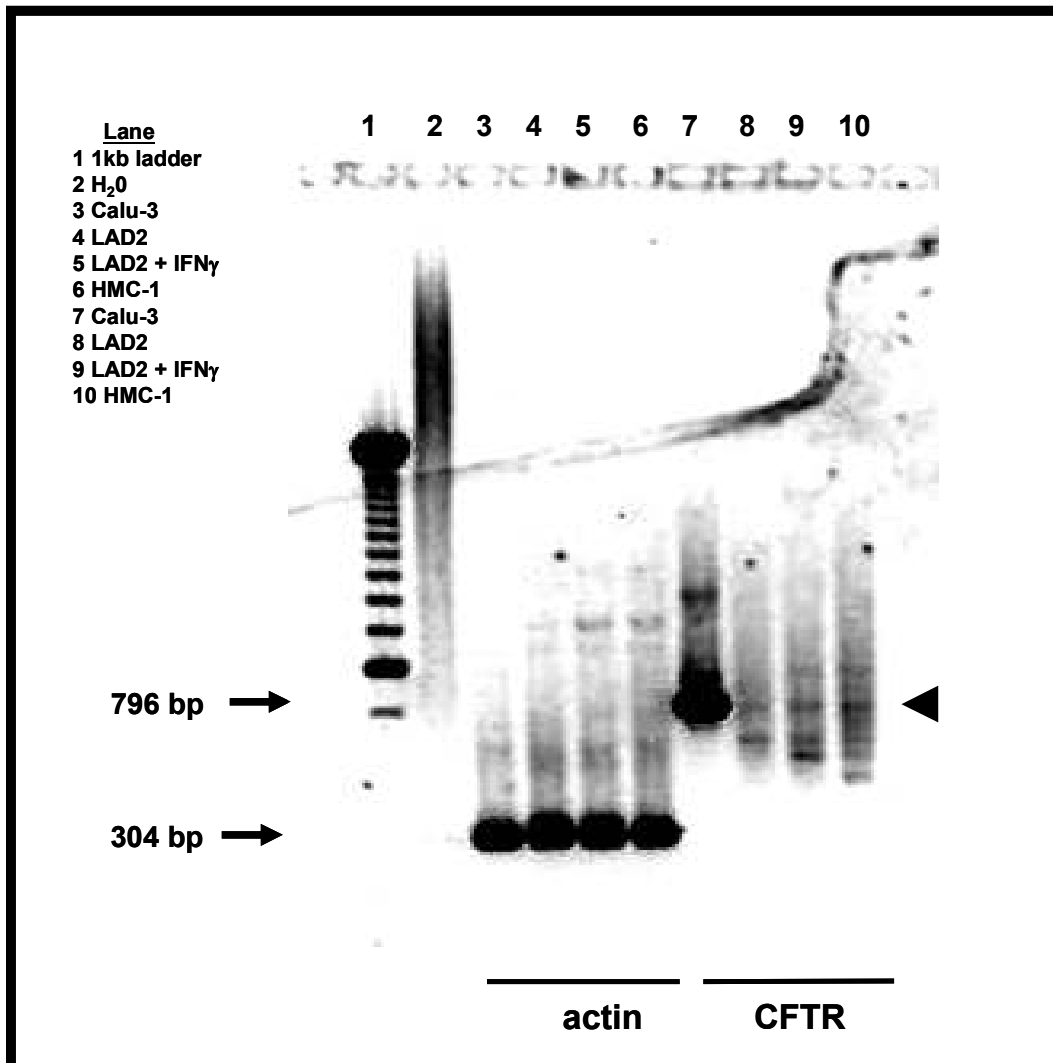
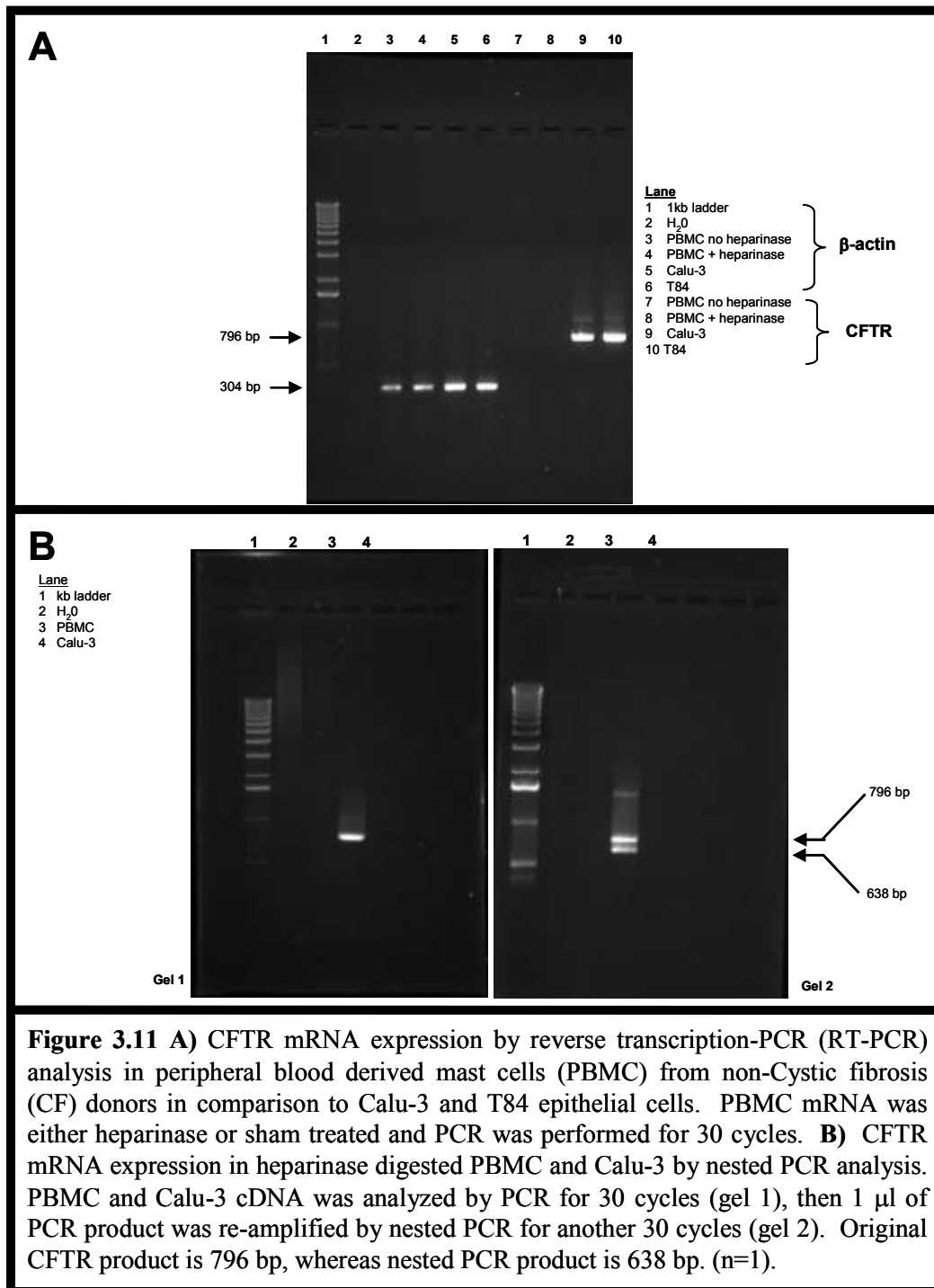


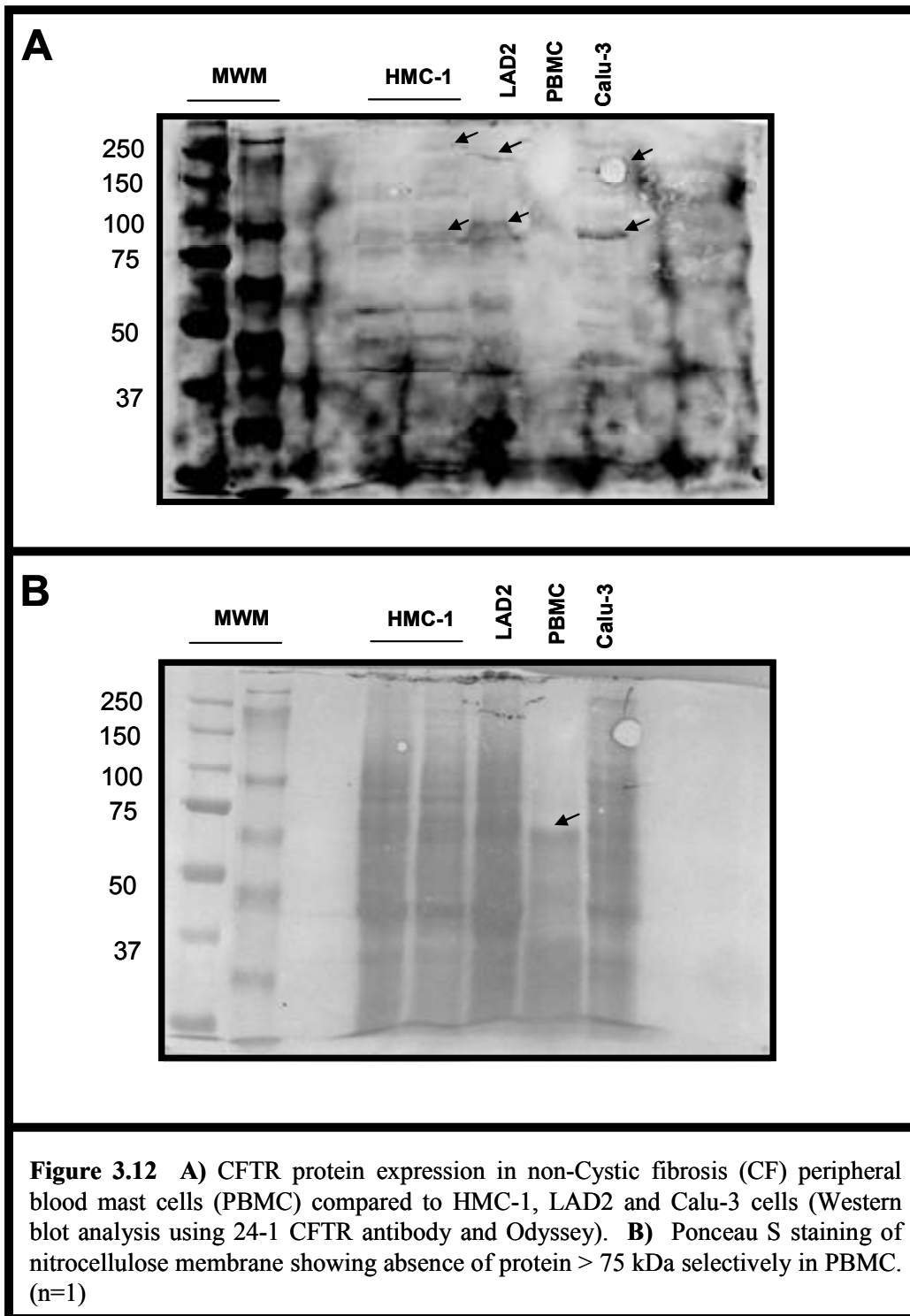
Figure 3.10 CFTR mRNA expression by reverse transcription-PCR (RT-PCR) analysis in Calu-3, LAD2 and HMC-1 cells using β -actin (304 bp) or CFTR (796 bp) primers for 45 cycles. CFTR mRNA is present as a weak band in LAD2, LAD2 + IFN γ and HMC-1 cells (arrowhead), but expression is low compared to Calu-3 CFTR mRNA (lane 7). Image was inverted and contrast adjusted to improve resolution of weak bands in lanes 8, 9 and 10 (n=1). High cycle number resulted in appearance of multiple bands which may or may not be CFTR.



In an attempt to boost the signal, we performed nested PCR reaction using only heparinase digested PBMC and Calu-3 cDNA. After 30 cycles of amplification in the initial PCR reaction, we only saw the appearance of CFTR transcripts in the Calu-3 sample (Figure 3.11 B gel 1). After 30 cycles of reamplification of the product by nested PCR, CFTR transcripts were still undetectable in PBMC, but were detectable in Calu-3, with the appearance of the original 796 bp product, as well as the expected 638 bp nested PCR product and an unexpected band near the 2000 bp marker (Figure 3.11 B gel 2). Thus, PBMC did not express transcripts for CFTR detectable by RT-PCR in these experiments. The absence of mRNA transcripts in PBMC does not preclude expression of protein and could be due to several factors including cyclical transcription and message stability. We have previously detected CFTR mRNA (201, 306).

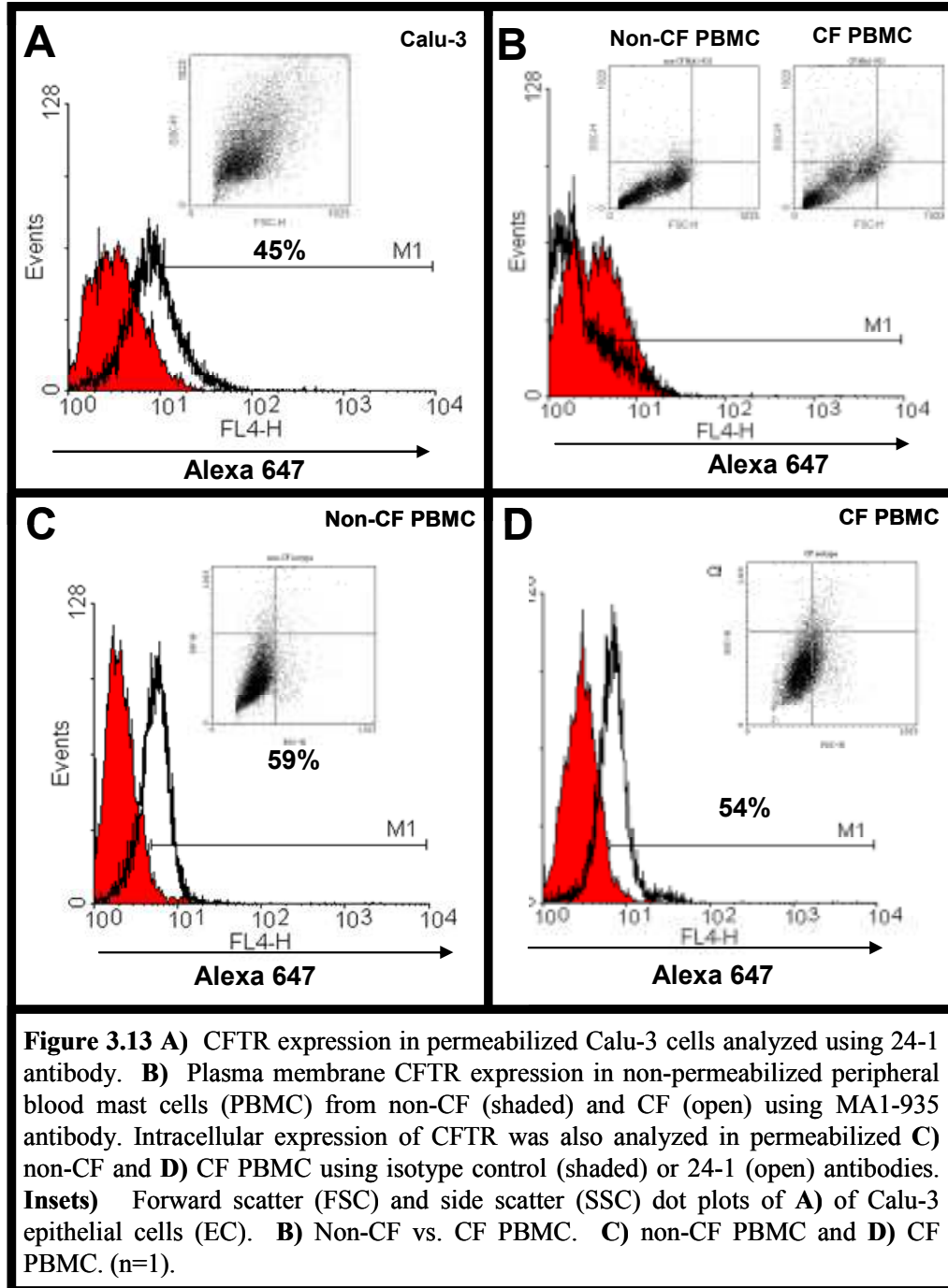
2. CF-PBMC express intracellular but not plasma membrane CFTR

The absence of mRNA transcripts in a cell does not always correlate with absence of protein expression, as protein turnover combined with epigenetic regulation of transcription, mRNA stability and other factors regulate the number of mRNA transcripts and proteins within cells. Therefore, with a limited number of PBMC, we attempted to detect CFTR protein expression in PBMC by Western blot analysis. Figure 3.12 shows results of this Western blot analysis with mouse monoclonal anti-human CFTR antibody 24-1 using Odyssey



IR on Calu-3, two separate HMC-1 lysates, LAD2 and PBMC. Calu-3 express a weak band 169 kDa, as well as a band at 100 kDa. One HMC-1 lysate did not express high MW bands, whereas the other lysate expressed a band at approximately 201 kDa. Smaller bands in both HMC-1 lanes were detected at 98 and 60 kDa. In LAD2 cells, we detected a band at 185 kDa, and two smaller bands at 100 and 59 kDa. In PBMC however, we did not detect any bands by Western blot. To determine why PBMC showed no signal for CFTR, membranes were stained with Ponceau S prior to blotting. The Ponceau S stained membrane shows that no proteins above 75 kDa transferred onto the membrane in PBMC sample, whereas good transfer occurred in Calu-3, HMC-1 and LAD2 samples (Figure 3.12 B). While this experiment gave poor resolution of CFTR in Calu-3, HMC-1 and LAD2 cells, our interpolations are that the lack of detectable transfer of proteins above 75 kDa in PBMC is a result of abundance of MCP in the PBMC lysate. It is well known that MCP are the most abundant proteins in fully differentiated MC (23, 307). As PBMC are the most mature MC phenotype we have studied, it is likely that they contain significantly more proteases than HMC-1 or even LAD2, resulting in undetectable amounts of CFTR being loaded into the gels in proportion to total protein contained in a defined quantity of cell lysate.

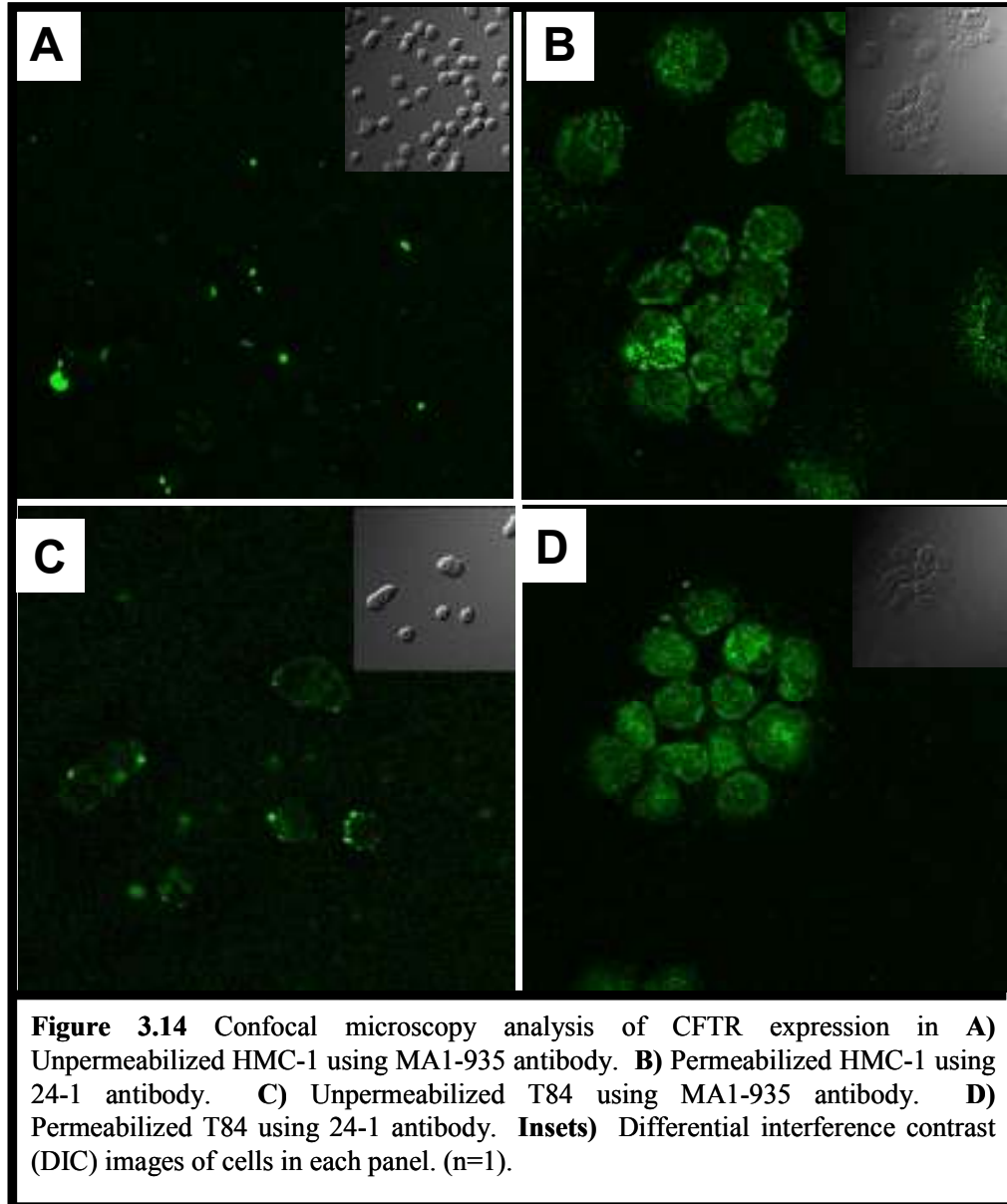
Because of the difficulty in obtaining large numbers of PBMC for Western blot, we used flow cytometry to characterize CFTR protein expression in PBMC. Using Calu-3 EC as positive control for CFTR expression, we assessed CFTR expression in permeabilized CF and non-CF PBMC (Figure 3.13). At least 45% of permeabilized Calu-3 cells were positive for CFTR when stained with 24-1

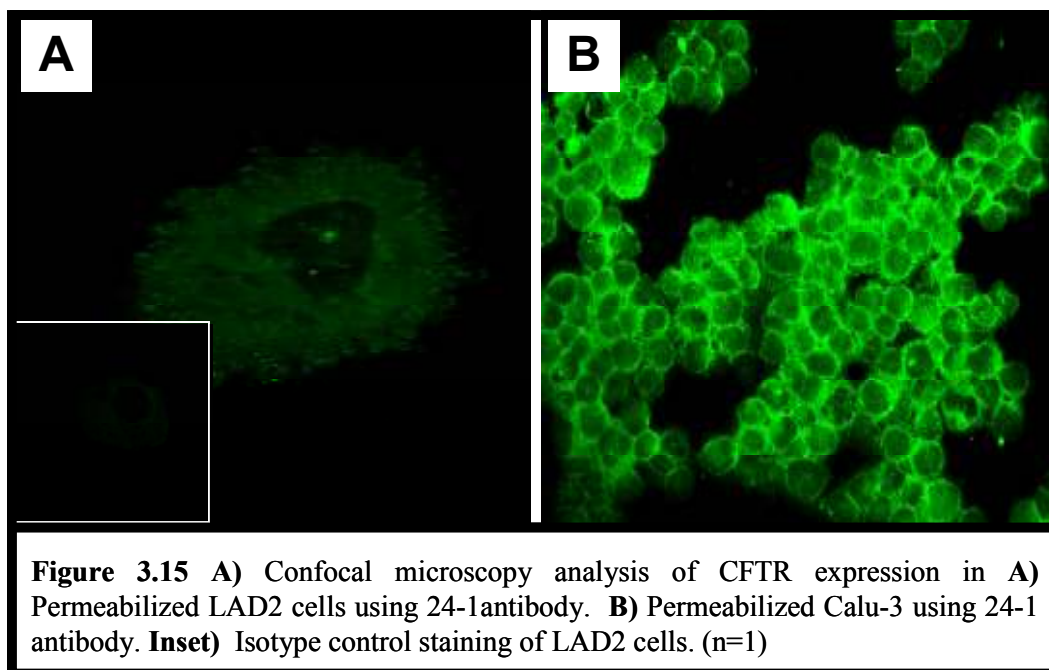


(Figure 3.13 A). When non-CF and CF PBMC were stained with 24-1, 59% and 54% of the cells were positive for CFTR respectively (Figure 3.13 C and D). This is not surprising given that our CF donors are all of the $\Delta F508$ genotype; a class II mutation resulting in loss of surface expression, but not of protein synthesis (125). When we stained unpermeabilized PBMC with MA1-935, the antibody recognizing the first extracellular loop of CFTR in unpermeabilized PBMC, we found that non-CF PBMC were positive for CFTR, whereas the CFTR signal did not appear in CF PBMC (Figure 3.13 B). This data shows that PBMC derived from CF peripheral blood progenitors express CFTR intracellularly (Figure 3.13 D), but that CFTR does not get to the plasma membrane (Figure 3.13 B). This figure also shows that non-CF have less FSC compared to CF PBMC. This indicates that non-CF PBMC are smaller than CF PBMC, which could implicate CFTR in volume regulation of the cells. This will be discussed further in chapter 4.

3. HMC-1 express higher levels of CFTR protein than LAD2

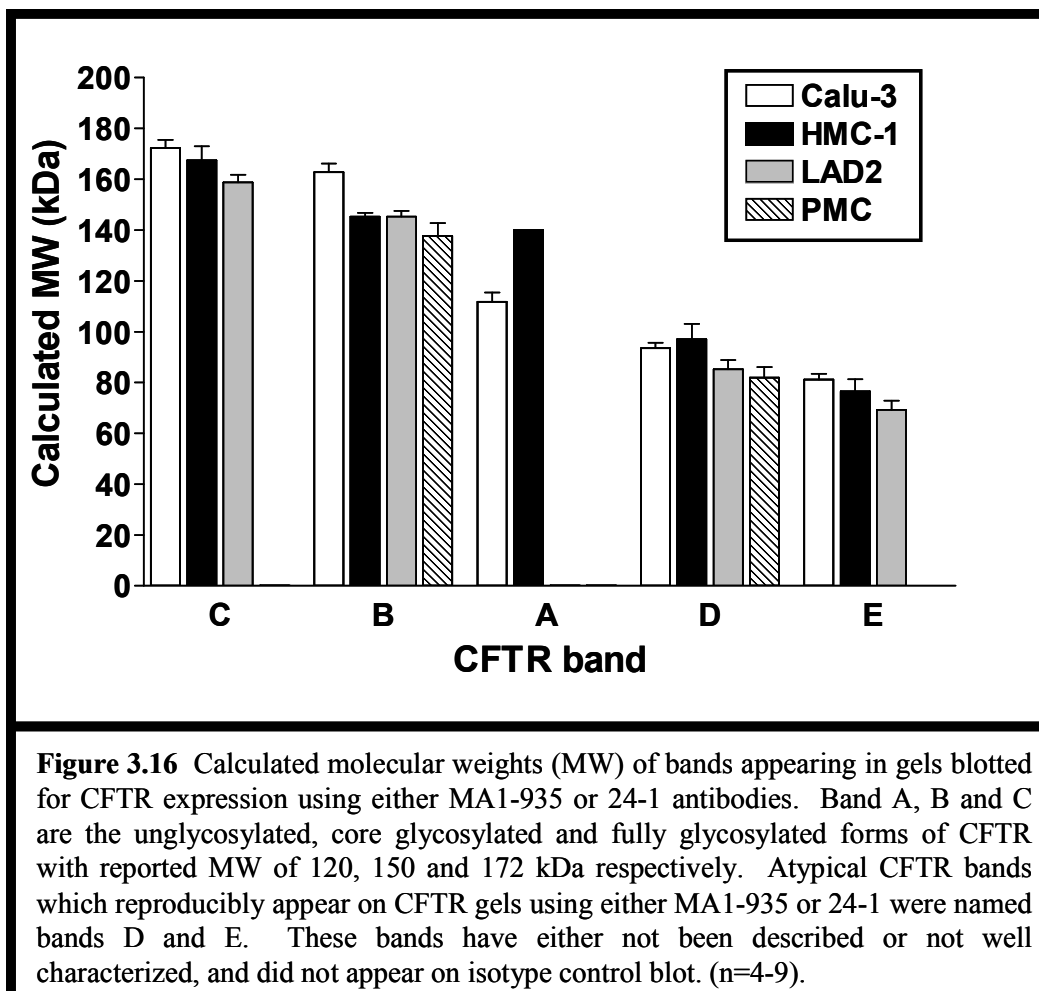
We compared extracellular and intracellular CFTR expression in HMC-1, T84, LAD2 and Calu-3 by confocal microscopy. Isotype controls mouse IgM and mouse IgG_{2a} did not result in significant staining in any of the cells tested, using the same settings on the microscope as for MA1-935 and 24-1. Microscope settings varied between experiments and antibodies, but were never different than those used for isotype controls within experiments as described in chapter 2. Unpermeabilized HMC-1 cells showed sparse and weak punctuate staining with





the extracellular loop CFTR antibody MA1-935 (Figure 3.14 A). This staining pattern is similar to that observed in unpermeabilized T84 cells, and is consistent with membrane expression of CFTR (Figure 3.14 C). When HMC-1 were permeabilized with saponin and stained with the CFTR antibody 24-1, CFTR signal was more abundant and diffuse throughout the cells with some punctate intracellular localization (Figure 3.14 B). Again, this staining pattern was consistent with that observed in permeabilized T84 cells, suggesting intracellular localization of CFTR in MC.

Staining of unpermeabilized LAD2 by MA1-935 did not result in a CFTR signal above background (not shown), but permeabilization and staining of LAD2 cells with 24-1 gave faint and diffuse intracellular staining (Figure 3.15 A). Staining of permeabilized Calu-3 cells with 24-1 antibody resulted in intense intracellular signal with weak signal in the nuclear region of the cells (Figure 3.15 B). This data shows that LAD2 express intracellular CFTR. This data also suggests that either LAD2 do not express CFTR at the plasma membrane, or that CFTR is different in LAD2 cells such that fixation and preparation protocols removed the MA1-935 epitope(s) on LAD2 cells.



E. Comparison of epithelial cell and mast cell CFTR expression by Western blot analysis

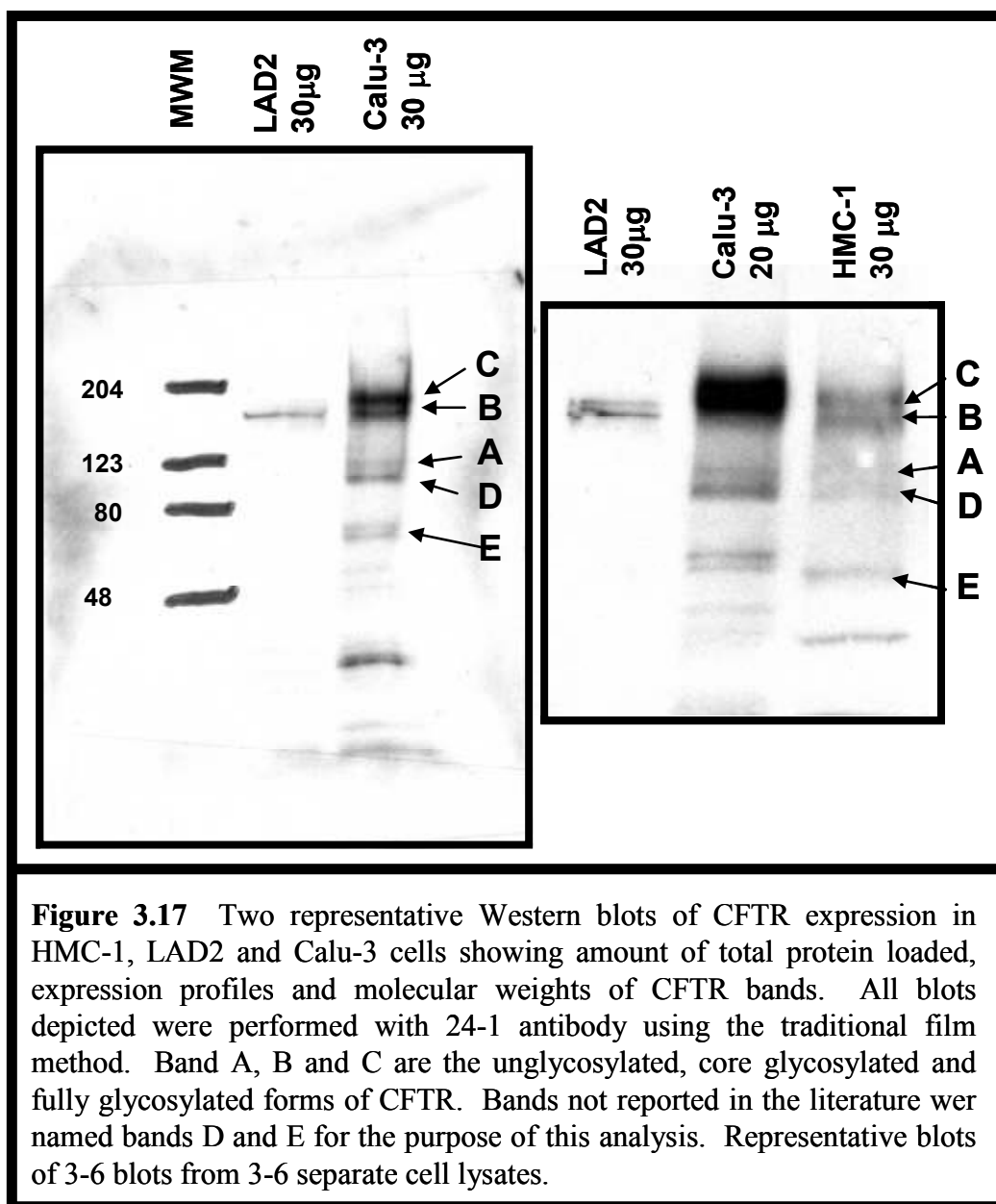
1. Calu-3

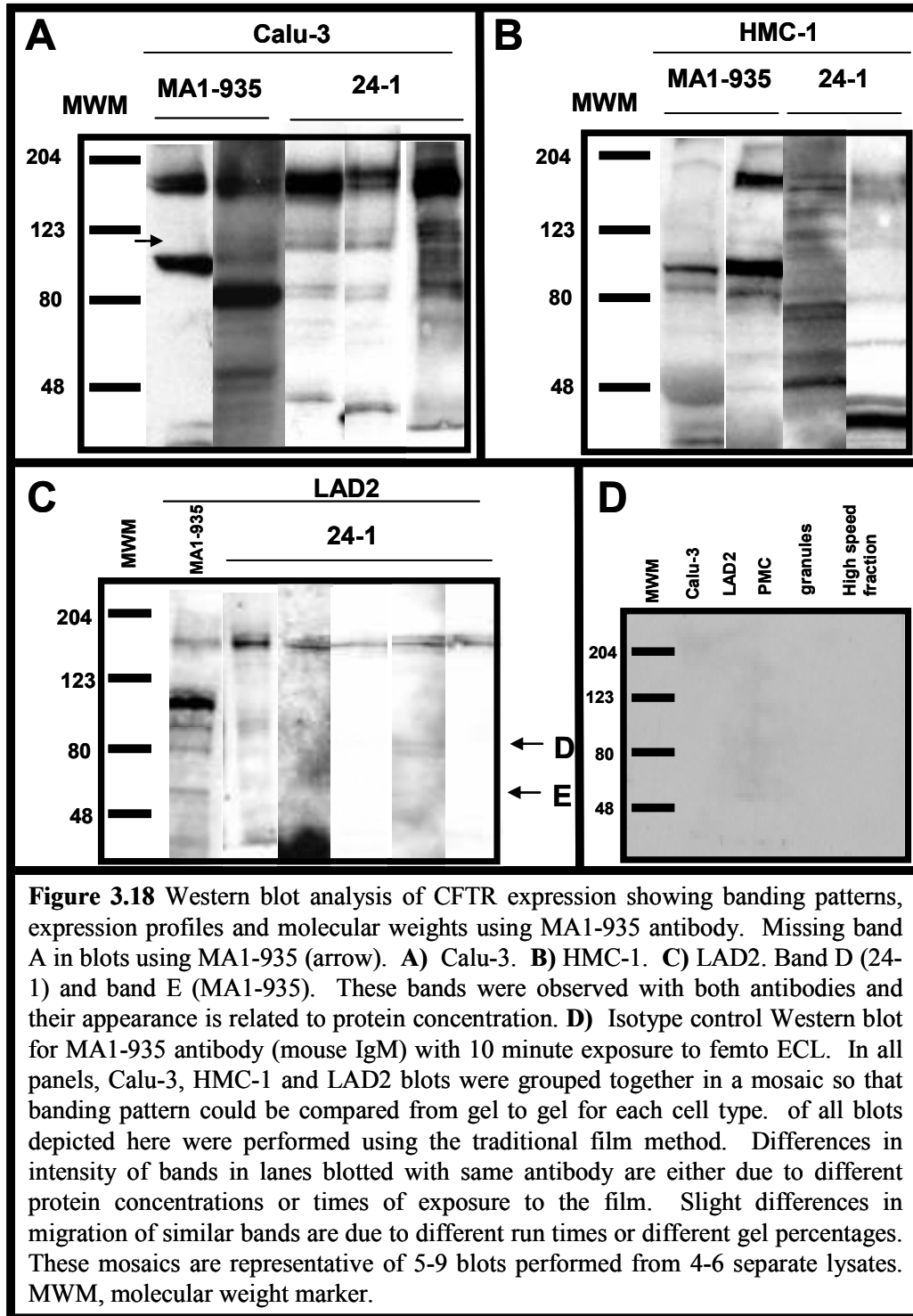
Because of the differences we observed between HMC-1 and LAD2 cells by confocal microscopy, we wanted to characterize CFTR expression in HMC-1 and LAD2 cells by Western blot to determine if their pattern of expression is similar to Calu-3 EC. Western blot using MA1-935 or 24-1 isotype control antibodies did not result in the appearance of any bands (not shown). Western blot on Calu-3 lysate using CFTR antibodies MA1-935 or 24-1 yielded results similar to those reported previously (chapter 1). Western blots of Calu-3 lysate showed a doublet appearing at the reported MW of bands B and C (Figure 3.17 and 3.18). The upper band of the doublet had a calculated average MW of 172 ± 3 kDa, and the lower band had a calculated average MW of 162 ± 3 kDa (Figure 3.16). There was an average of 10 kDa separation between the two bands. The higher band was observed in 6 of 9 separate gels (once by MA1-935 and 5 times by 24-1) and the lower band in 6 of 9 separate gels (once by MA1-935 and 5 times by 24-1) (Table 3.1). Calu-3 band A had an average MW of 111 ± 4 kDa (Figure 3.16, 3.17 and 3.18) and was observed in 3 of 9 separate gels (3 times with 24-1), but was not observed when MA1-935 was used (Figure 3.18) (Table 3.1). Calu-3 also reproducibly expressed other prominent bands, one of which fell within the reported MW range of band A, the other two of which were atypical CFTR bands that we named bands D and E for the purposes of this analysis (Figure 3.16 to

Table 3.1 Calu-3: Western blot conditions and results

Blot	Conditions	Band C	Band B	Band A	Band D	Band E
1	1° Antibody: MA1-935, 1/1000 2° Antibody: GAM-IgM-HRP 1/5000 ECL: Femto			117	98	89
2	1° Antibody: MA1-935, 1/1000 2° Antibody: GAM-IgM-HRP 1/5000 ECL: Femto				89	76
3	1° Antibody: MA1-935, 1/1000 2° Antibody: GAM-IgM-HRP 1/5000 ECL: Femto	175	173			88
4	1° Antibody: 24-1, 1/1000 2° Antibody: GAM-IgG-HRP 1/5000 ECL: Pico	162	159	114	91	85
5	1° Antibody: 24-1, 1/1000 2° Antibody: GAM-IgG-HRP 1/5000 ECL: Pico					
6	1° Antibody: 24-1, 1/1000 2° Antibody: GAM-IgG-HRP 1/5000 ECL: Pico	184	169	115		76
7	1° Antibody: 24-1, 1/1000 2° Antibody: GAM-IgG-HRP 1/5000 ECL: Pico	167	152	101	80	
8	1° Antibody: 24-1, 1/1000 2° Antibody: GAM-IgG-HRP 1/5000 ECL: Pico	176	168		96	
9	1° Antibody: 24-1, 1/1000 2° Antibody: GAM-IgG-HRP 1/5000 ECL: Pico	170	155			74
Average mass		172 ± 3	162 ± 3	111 ± 4	94 ± 2	81 ± 2

1°, primary antibody; 2°, secondary antibody; GAM, goat anti-mouse; HRP, horseradish peroxidase; ECL, enhanced chemiluminescence reagent (pico or femto kit, Pierce);





3.18). These bands appear with more variability than bands A, B and C. The significance of this is unknown, but could represent some form of post-translational processing such as cleavage or deglycosylation. Band D had a calculated average molecular mass of 94 ± 2 kDa (Figure 3.16), and was observed in 5 of 9 separate gels (2 times by MA1-935 and 3 times by 24-1) (Figure 3.17) (Table 3.1). Band E in Calu-3 had a calculated average MW of 81 ± 4 kDa (Figure 3.16), and was observed in 6 of 9 separate gels (3 times with MA1-935 and 3 times with 24-1) (Table 3.1).

2. LAD2

Detection of CFTR in LAD2 cells required the loading of 30 to 50 μ g total protein in comparison with Calu-3 and HMC-1 which only routinely required the loading of 20-30 μ g of lysate. This suggests that CFTR is either less abundant in LAD2 cells than in Calu-3 or HMC-1, or as we saw in PMBC, there is abundant low MW protease content in LAD2 cells that reduces the amount of CFTR loaded as a proportion of total protein (Figure 3.13). When we analyzed CFTR expression in LAD2 cells, we detected either a single band or a faint doublet near the reported MW of band B (Figure 3.17 and 3.18 C). The single band in LAD2 appeared to migrate to the reported MW of band B with a calculated average MW of 154 ± 4 kDa (Figure 3.16). This single band appeared in 5 of 9 separate gels, (2 times by MA1-935 and 3 times by 24-1) (Table 3.2). In 4 separate gels (1 time by MA1-935 and 3 times by 24-1) (Table 3.2), a doublet appeared rather than a single band. The upper band of this doublet had a calculated average MW of 159 ± 4 kDa, whereas the lower band had a calculated average MW of 145 ± 2 kDa

Table 3.2 LAD2: Western blot conditions and results

Blot	Conditions	Band C	Band B	Band D	Band E
1	1° Antibody: MA1-935, 1/1000 2° Antibody: GAM-IgM-HRP 1/5000 ECL: Femto	169	142		
2	1° Antibody: MA1-935, 1/1000 2° Antibody: GAM-IgM-HRP 1/5000 ECL: Femto		142	89	76
3	1° Antibody: MA1-935, 1/1000 2° Antibody: GAM-IgM-HRP 1/5000 ECL: Femto	163		85	67
4	1° Antibody: 24-1, 1/1000 2° Antibody: GAM-IgG-HRP 1/5000 ECL: Pico	162	152		
5	1° Antibody: 24-1, 1/1000 2° Antibody: GAM-IgG-HRP 1/5000 ECL: Pico	151	145		
6	1° Antibody: 24-1, 1/1000 2° Antibody: GAM-IgG-HRP 1/5000 ECL: Pico	166			
7	1° Antibody: 24-1, 1/1000 2° Antibody: GAM-IgG-HRP 1/5000 ECL: Pico	144		75	60
8	1° Antibody: 24-1, 1/1000 2° Antibody: GAM-IgG-HRP 1/5000 ECL: Pico	162		92	74
9	1° Antibody: 24-1, 1/1000 2° Antibody: GAM-IgG-HRP 1/5000 ECL: Pico	153	143		
Average mass		159 ± 3	145 ± 2	85 ± 4	69 ± 4

1°, primary antibody; 2°, secondary antibody; GAM, goat anti-mouse; HRP, horseradish peroxidase; ECL, enhanced chemiluminescence reagent (pico or femto kit, Pierce);

(Figure 3.16 and 3.17). Furthermore, we show that when run on the same gels as Calu-3, the high band in the LAD2 doublet migrates to within 5 kDa of the low band of the Calu-3 doublet (Figure 3.17). This suggests that glycosylation of CFTR in LAD2 may not be complete, or may have a different pattern than in EC. In addition to the doublet at high MW, LAD2 cells also expressed bands D and E. Band D had a calculated average MW of 85 ± 4 kDa and appeared in 4 of 9 separate gels (2 times with MA1-935 and 3 times with 24-1) (Table 3.2). Band E had a calculated average MW of 69 ± 4 kDa, and appeared in 4 of 9 separate gels (2 times with MA1-935 and 2 times with 24-1). These bands were observed in some, but not all of the gels, and seemed to appear with loading of more cell lysate than for Calu-3 cells (40-50 μ g vs. 20-30 μ g) of total protein in each lane (Figure 3.16).

3. HMC-1

In HMC-1, we consistently observed a high MW doublet near the reported MW of CFTR. The upper band of this doublet had a calculated average MW of 167 ± 6 kDa, while the lower band of the doublet had a calculated average MW of 145 ± 2 kDa (Figure 3.16 and 3.17). The upper band of the doublet was observed 5 times from 5 gels (2 times with MA1-935 and 3 times with 24-1) (Table 3.3) and these two bands corresponded well with the reported MW of bands C and band B in EC (Figure 3.16). HMC-1 also expressed, in 1 of 5 separate gels (with 24-1), a band at 140 kDa which falls between the reported size of bands A and B. In that same gel, the doublet band was at 174 and 161 kDa, indicating the band at

Table 3.3 HMC-1: Western blot conditions and results

Blot	Conditions	Band C	Band B	Band A	Band D	Band E
1	1° Antibody: MA1-935, 1/1000 2° Antibody: GAM-IgM-HRP 1/5000 ECL: Femto	171			97	88
2	1° Antibody: MA1-935, 1/1000 2° Antibody: GAM-IgM-HRP 1/5000 ECL: Femto	175	147		86	75
3	1° Antibody: 24-1, 1/1000 2° Antibody: GAM-IgG-HRP 1/5000 ECL: Pico	174	161	140	120	77
4	1° Antibody: 24-1, 1/1000 2° Antibody: GAM-IgG-HRP 1/5000 ECL: Pico	172	147		88	83
5	1° Antibody: 24-1, 1/1000 2° Antibody: GAM-IgG-HRP 1/5000 ECL: Pico	145	142		94	60
Average	167 ± 6	167 ± 6	145 ± 2	140 ± 0	97 ± 6	77 ± 5

mass

1°, primary antibody; 2°, secondary antibody; GAM, goat anti-mouse; HRP, horseradish peroxidase; ECL, enhanced chemiluminescence reagent (pico or femto kit, Pierce);

140 kDa may in fact be band A (Figure 3.18 B). HMC-1 also reproducibly expressed bands D and E in 5 of 5 separate gels (2 times by MA1-935 and 3 times by 24-1). Bands D and E reproducibly appeared on the same gels, and had calculated average MW of 97 ± 6 kDa and 77 ± 5 kDa respectively (Figure 3.16). In a few gels a band as low as 43 kDa appeared, which could represent degradation products of CFTR, whereas bands D and E could represent alternative splice variants of CFTR.

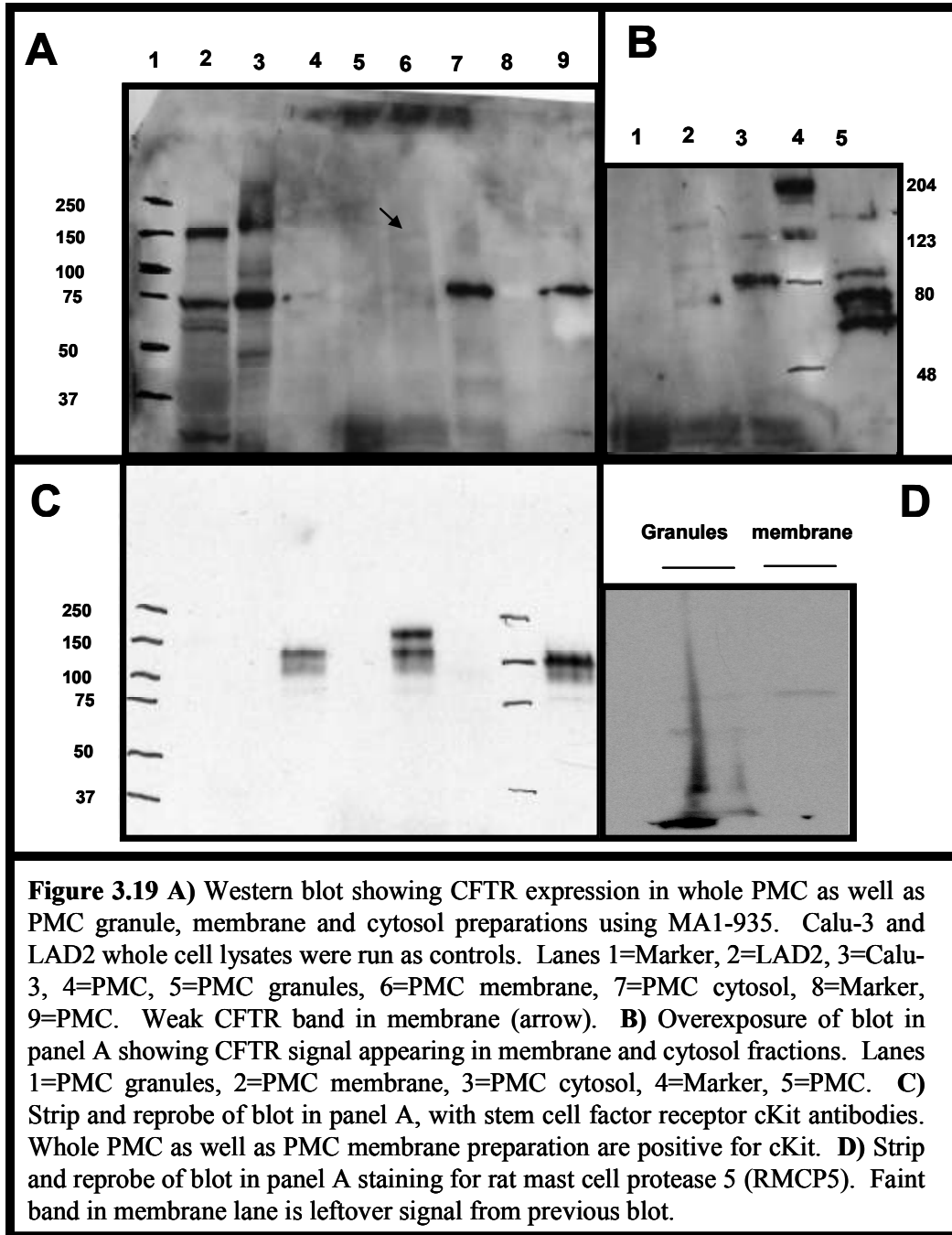
4. PMC

When probed for CFTR, PMC only exhibited a band at 80 kDa, and no signal was observed at the reported size ranges of band A, B and C, unless films were exposed for longer times (Figure 3.19 B versus A). With longer exposure, LAD2 and Calu-3 lanes were overexposed (not shown), and PMC expressed a single band near the reported MW of band B with an average molecular mass of 137 ± 5 kDa (Figure 3.16 and 3.19 B). This band was very faint, and was observed once with MA1-935 and twice with 24-1 (Table 3.4). Whole cell PMC lysate also expressed a band at 82 ± 4 kDa when probed with MA1-935 and with 24-1 (Figure 3.16 and 3.19 B). When membranes were overexposed we also detected similar fragments of CFTR as we observed in Calu-3, HMC-1 and LAD2 cells. This suggests that CFTR expression in PMC is less abundant than LAD2 MC.

Table 3.4 PMC: Western blot conditions and results

Blot	Conditions	Band C	Band B	Band A	Band D	Band E
6	1° Antibody: 24-1, 1/1000 2° Antibody: GAM- IgG-HRP 1/5000 ECL: Pico		130			77
9	1° Antibody: 24-1, 1/1000 2° Antibody: GAM- IgG-HRP 1/5000 ECL: Pico					92
10	1° Antibody: 24-1, 1/1000 2° Antibody: GAM- IgG-HRP 1/5000 ECL: Pico		136			74
11	1° Antibody: MA1- 935, 1/1000 2° Antibody: GAM- IgM-HRP 1/5000 ECL: Femto		147			85
Average mass			137 ± 5			82 ± 4

1°, primary antibody; 2°, secondary antibody; GAM, goat anti-mouse; HRP, horseradish peroxidase; ECL, enhanced chemiluminescence reagent (pico or femto kit, Pierce)

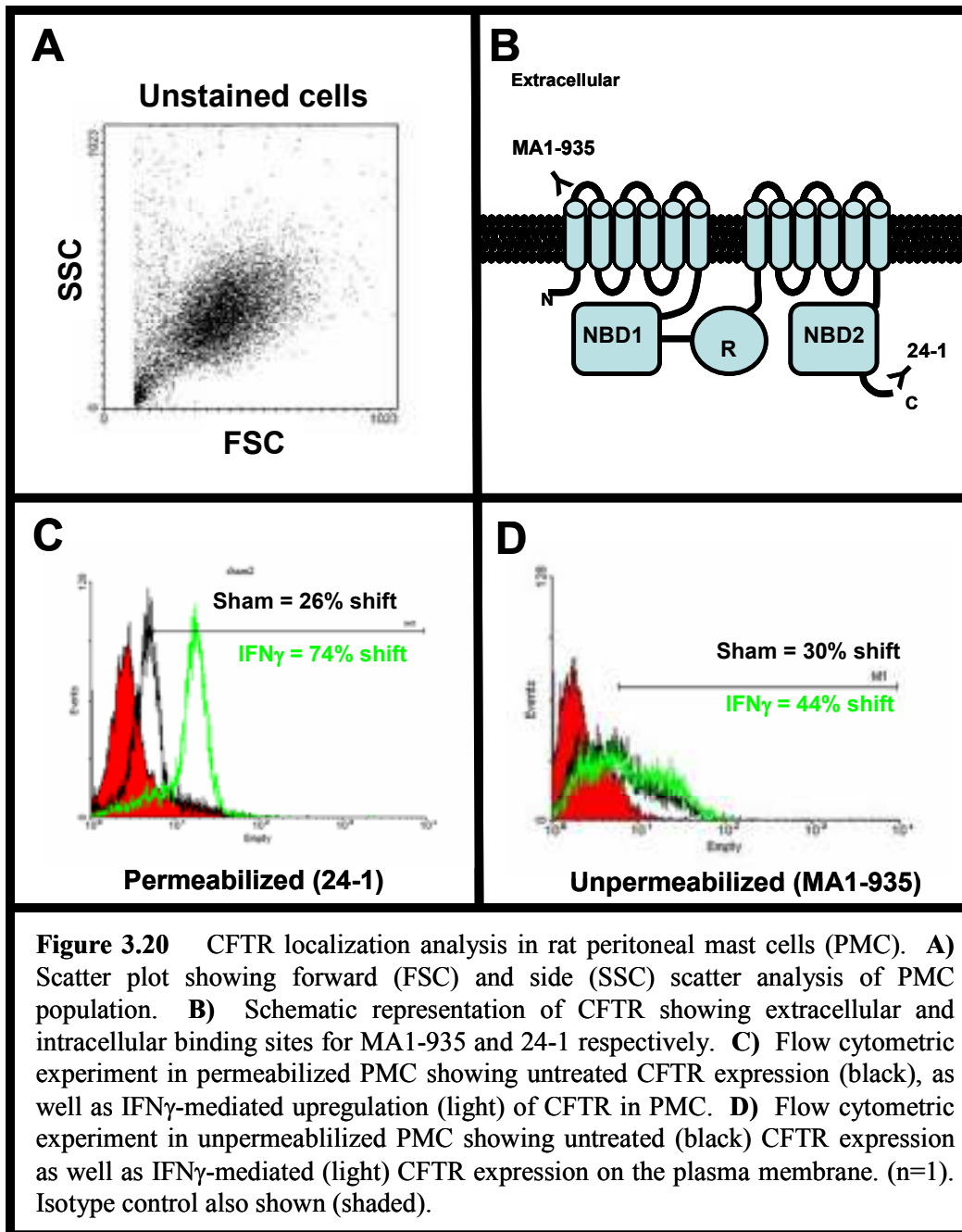


5. Rat peritoneal mast cells express both plasma membrane and intracellular CFTR, which is upregulated by IFN γ

Detection of CFTR expression in PMC is difficult, and our previous results did not demonstrate plasma membrane staining in PMC, as the fixation and permeabilization method used compromised the integrity of the cells (Appendix 2). Thus, we used flow cytometry with MA1-935 and 24-1 to differentiate between surface and intracellular staining of CFTR in PMC (Figure 3.20). Using both MA1-935 and 24-1 which recognize extracellular and intracellular epitopes respectively (Figure 3.20 B), we stained unpermeabilized and permeabilized cells to determine if CFTR is localized to the plasma membrane and/or intracellularly in PMC. Our flow cytometry data shows that PMC express intracellular as well as plasma membrane CFTR, as both staining with MA1-935 in unpermeabilized cells and 24-1 in permeabilized cells gave a signal for CFTR (Figure 3.20 C and D). We also showed that IFN γ upregulation of CFTR signal previously shown in Appendix 2, resulted in increase in CFTR expression both intracellularly and on the plasma membrane (Figure 3.20 C and D).

6. CFTR is not detected in rat PMC granules by Western blotting:

To pursue our preliminary data that MC express CFTR on their granules (Appendix 2), as well as our data suggesting that PMC express both plasma membrane and intracellular CFTR, we performed subcellular fractionation of PMC as previously described, and performed Western blot analysis for CFTR on



the various fractions (Figure 3.19). Using rat MC protease-5 (MCP-5) antibodies as a marker of rat MC granule protein, we confirmed that our granule preparations contained granule-associated proteins (Figure 3.19 D). However, we were not able to detect CFTR in PMC granule fractions in our experiments using Western blot analysis even if blots were overexposed (Figure 3.19 B). PMC membrane and cytosol fractions were characterized by staining with membrane associated SCF receptor c-Kit (Figure 3.19 C). The whole PMC as well as membrane fractions, but not granule or cytosol fractions exhibited doublet bands at calculated MW of 165 and 136 kDa, which is near the reported sizes of mature and immature c-Kit protein at 145 and 125 kDa respectively (308, 309) (Figure 3.19 C). The pellet of the PMC high speed fraction represents cellular membrane, components which include plasma membrane, and intracellular membranes, but exclude membrane from intact secretory granules. The pellet of the PMC high speed fraction expressed bands at calculated MW of 149, 99 and 76 kDa when probed with MA1-935 (Figure 3.19 B lane 2). The supernatant of the PMC high speed fraction (Figure 3.19 B lane 3), which represents cytosolic components expressed bands at calculated MW of 127 and 83 kDa when probed with MA1-935. This data shows that PMC express CFTR on cellular membranes, but not on granule membranes. Figure 3.19B (lane 5) also suggests that PMC express similar CFTR fragments as Calu-3, HMC-1 and LAD2 cells.

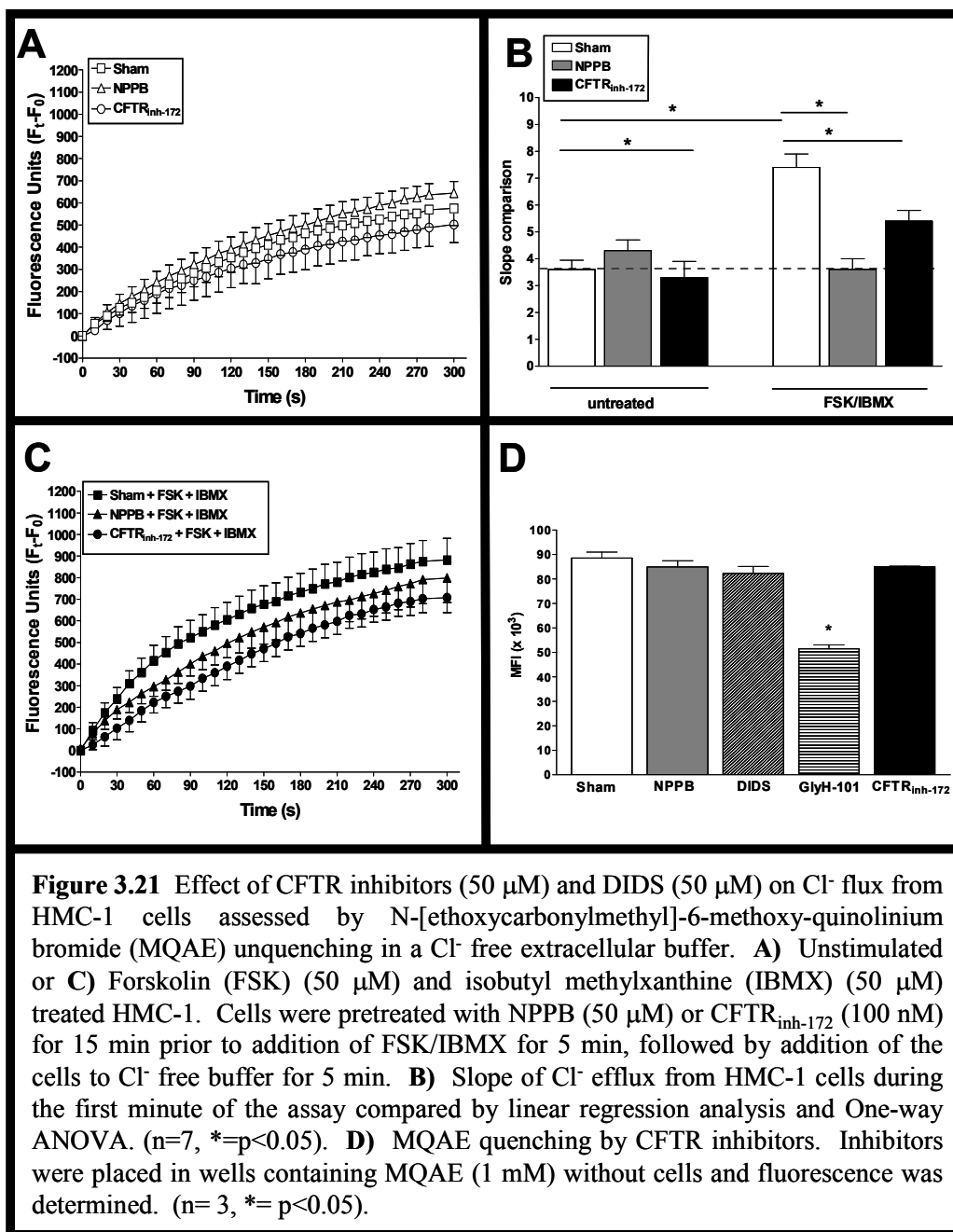
Thus, we established that MC express CFTR, although levels of expression appear to be cell type dependent. Moreover, we consistently detected unexpected bands in both MC and Calu-3. We postulate that bands D and E may

be alternative splice variants of CFTR and that smaller bands appearing at lower than 50 kDa in CFTR Western blots may be degradation products of CFTR. This hypothesis will be addressed in chapter 4.

F. Effect of pharmacological inhibition of CFTR on mast cell function

1. Pharmacological inhibitors downregulate c-AMP-dependent Cl⁻ flux in HMC-1

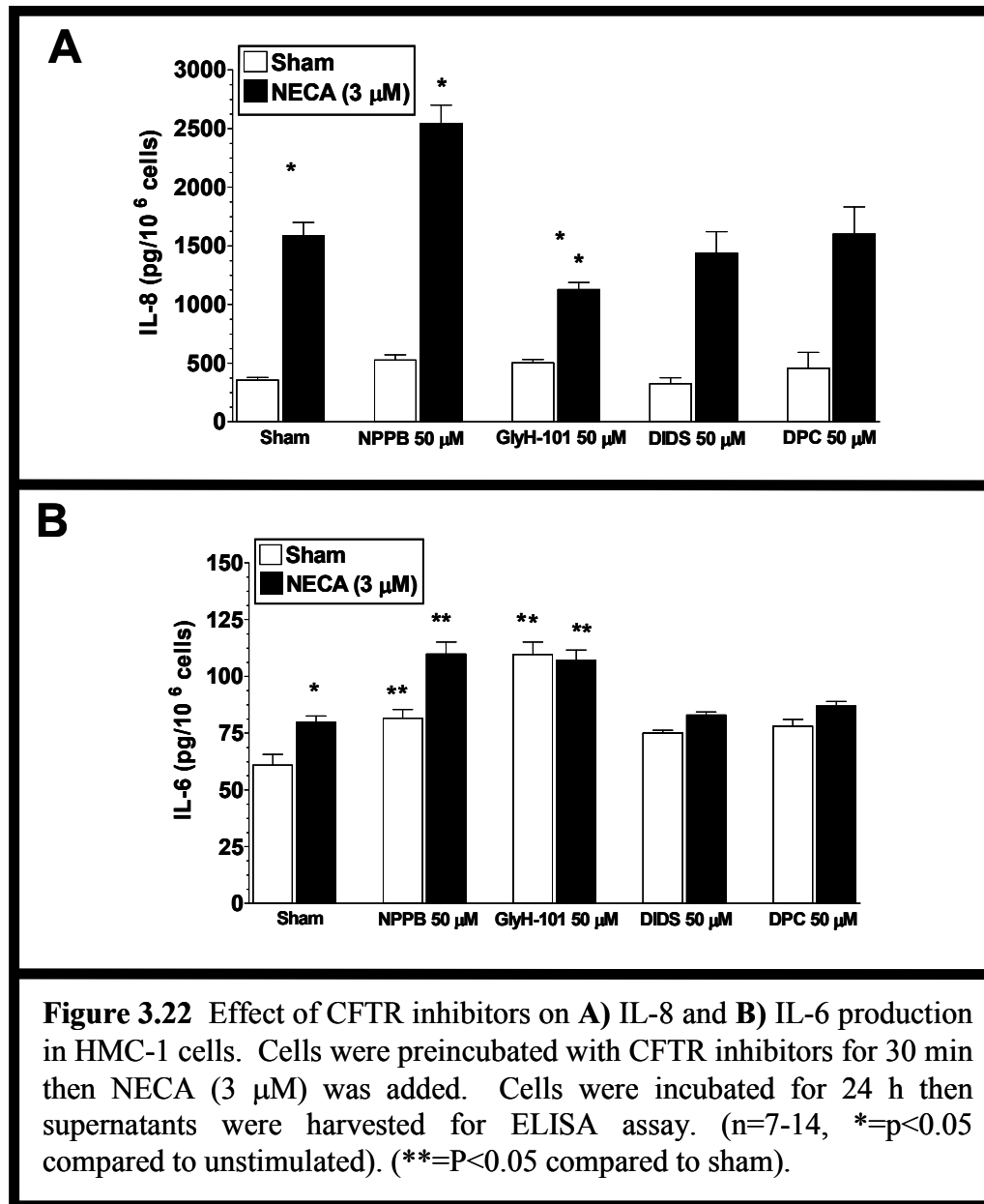
The effect of CFTR on the regulation of MC Cl⁻ flux induced by an intra- to extracellular Cl⁻ gradient was studied in HMC-1 cells using an MQAE assay which measures intracellular Cl⁻ levels. To activate CFTR we used the cAMP elevating agent forskolin (FSK) (50 μ M) and the non-specific phosphodiesterase inhibitor isobutyl methylxanthine (IBMX) (50 μ M) at doses previously reported in order to prevent degradation of cAMP and prolong the activity of CFTR (Figure 3.21) (310, 311). Under basal conditions, HMC-1 cells did not respond to NPPB (50 μ M) or CFTR_{inh-172} (100 nM) (Figure 3.21 A and B). GlyH-101 (50 μ M) decreased basal Cl⁻ flux in unstimulated HMC-1 cells by $70 \pm 10\%$ which was a puzzling result as cAMP activation of CFTR was not present (not shown). The reported specificity of GlyH-101 for CFTR suggests that application of this drug to the cells should have no effect on Cl⁻ flux unless cAMP is present. Therefore, upon further investigation of this phenomenon, we showed that decrease in fluorescence by GlyH-101 is a result of direct quenching of MQAE by



GlyH-101, which did not occur with the other inhibitors (Fig 3.21 D). As a result, we stopped using GlyH-101 in our MQAE experiments. Elevation of cAMP with FSK/IMBX in HMC-1 resulted in a $54 \pm 7\%$ increase of in the slope of Cl^- flux during the first minute compared to sham treated cells (Figure 3.21 B and C). The increase in Cl^- flux was significantly inhibited by NPPB (50 μM) and CFTR_{inh-172} (100 nM) by ($29 \pm 7\%$ and $52 \pm 11\%$ respectively), as assessed by slope comparisons (Figure 3.21 B). Neither NPPB nor CFTR_{inh-172} at the doses used were toxic as assessed by trypan blue dye exclusion (data not shown). This data shows that CFTR is involved in cAMP-mediated Cl^- flux in human MC.

2. Pharmacological inhibitors differentially affect NECA-induced IL-8 and IL-6 secretion in HMC-1

Next, we wanted to assess the role of pharmacological inhibition of CFTR on production of newly synthesized cytokines in response to the adenosine receptor agonist NECA. We chose to measure release of IL-8 and IL-6 by HMC-1 cells, since these mediators are produced by HMC-1 and have been shown to be elevated in CF (Figure 3.22) (49, 147). HMC-1 cells spontaneously release IL-8 (355 ± 24 pg/ml) and IL-6 (60 ± 5 pg/ 10^6 cells) after 24 h in culture (Figure 3.22 A and B). Stimulation with NECA for 24 h significantly increased secretion of IL-8 and IL-6 from HMC-1 (1588 ± 112 pg/ 10^6 cells and 79 ± 3 pg/ 10^6 cells respectively $p < 0.05$) (Figure 3.22 A and B). In the absence of stimulation, treatment with NPPB had no effect on IL-8 secretion, but significantly increased IL-6 secretion compared to sham treated HMC-1 cells (82 ± 5 pg/ 10^6 vs 60 ± 5



pg/10⁶ cells respectively) (Figure 3.22 B). NPPB significantly increased NECA-induced secretion of both IL-8 and IL-6 from HMC-1 (2545 ± 156 pg/10⁶ cell and 109 ± 6 pg/10⁶ cells respectively) (Fig 3.22 A and B). When unstimulated cells were treated with GlyH-101, IL-8 secretion was not affected, but GlyH-101 significantly increased IL-6 secretion from unstimulated cells compared to sham treatment (110 ± 5 pg/10⁶ vs 60 ± 5 pg/10⁶ cells respectively). NECA stimulation of GlyH-101 treated cells resulted in a significant downregulation of IL-8 secretion compared to control treatment (1130 ± 58 pg/10⁶ vs 1588 ± 112 pg/10⁶ cells) (Figure 3.22 A). Neither DIDS nor DPC had any significant effects on IL-8 or IL-6 release from HMC-1 cells when compared to sham treatment (Figure 3.22 A and B). These data suggest that CFTR has a role in cytokine secretion from MC, with different effects on IL-8 and IL-6 secretion, presumably downstream of transcription factor activation.

3. Pharmacological inhibitors affect anti-IgE-induced but not NECA-induced degranulation in LAD2

To determine whether pharmacological inhibition of CFTR affected release of stored mediators from MC, we measured β -hex secretion in LAD2 cells 30 min following anti-IgE stimulation. LAD2 spontaneously released 2 ± 0.2 % β -hex after 30 min of sham stimulation. In the absence of anti-IgE stimulation, none of the inhibitors significantly changed this spontaneous release (Figure 3.23 A). NECA stimulation did not induce β -hex release from LAD2 in any of the conditions tested (Figure 3.23 A). Stimulation of LAD2 with Ca²⁺ ionophore

A23187 or anti-IgE increased β -hex release to $72 \pm 2 \%$ and $23 \pm 1 \%$ respectively (Fig 3.23 A). Pre-treatment of cells with DIDS ($50 \mu\text{M}$) or NPPB ($50 \mu\text{M}$) significantly inhibited anti-IgE-mediated β -hex release by $57 \pm 0.5\%$ and $29 \pm 3\%$ respectively (Figure 3.23 A). Neither GlyH-101 ($50 \mu\text{M}$) nor DPC ($50 \mu\text{M}$) inhibited β -hex release from LAD2 upon anti-IgE stimulation (Figure 3.23 A). Neither A23187 or CFTR inhibitors had any toxic effects on cell viability as established by trypan blue vital staining (not shown). This data suggests that CFTR-mediated Cl^- flux is not involved in release of stored mediators from LAD2 MC. Thus, inhibition of β -hex release by NPPB and DIDS is likely through a non-CFTR-mediated event.

4. Pharmacological inhibitors affect NECA and anti-IgE-induced cytokine release in LAD2

To investigate whether CFTR influences release of newly synthesized inflammatory cytokines shown to be upregulated in CF, we measured the effects of various pharmacological inhibitors of CFTR on secretion of IL-8, IL-6 and TNF from LAD2 in response to the adenosine agonist NECA, or IgE/anti-IgE stimulation (Figure 3.23 B). Neither IL-6 nor TNF could be detected in LAD2 following NECA or IgE/anti-IgE stimulation (data not shown). The effect of CFTR on NECA or IgE/anti-IgE-induced IL-8 secretion in LAD2 was assessed using NPPB, GlyH-101 and DPC. LAD2 spontaneously released $13 \pm 3 \text{ pg}/10^6$ cells of IL-8 and anti-IgE treatment increased secretion to $77 \pm 11 \text{ pg}/10^6$ cells.

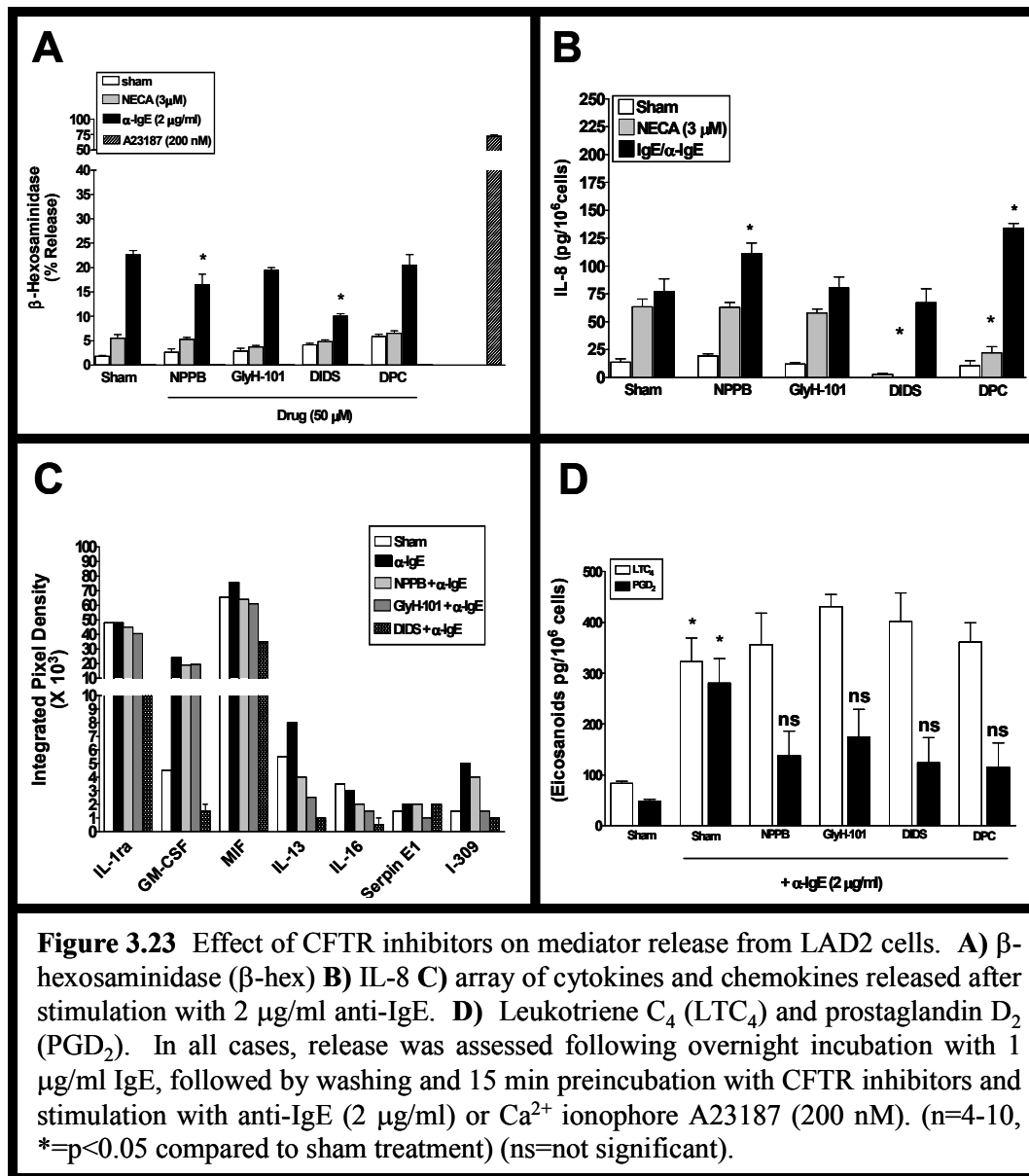


Figure 3.23 Effect of CFTR inhibitors on mediator release from LAD2 cells. **A)** β -hexosaminidase (β -hex) **B)** IL-8 **C)** array of cytokines and chemokines released after stimulation with 2 μ g/ml anti-IgE. **D)** Leukotriene C₄ (LTC₄) and prostaglandin D₂ (PGD₂). In all cases, release was assessed following overnight incubation with 1 μ g/ml IgE, followed by washing and 15 min preincubation with CFTR inhibitors and stimulation with anti-IgE (2 μ g/ml) or Ca²⁺ ionophore A23187 (200 nM). (n=4-10, * p <0.05 compared to sham treatment) (ns=not significant).

Pretreatment of LAD2 cells with NPPB or DPC significantly potentiated IL-8 release to 111 ± 9 pg/ 10^6 and 134 ± 4 pg/ 10^6 cells respectively (Figure 3.23 B). However, GlyH-101 or DIDS did not affect IL-8 secretion from these cells in response to anti-IgE (Figure 3.23 B). In contrast, neither NPPB nor GlyH-101 had any effect on NECA-induced IL-8 release of 63 ± 7 pg/ 10^6 cells, but pretreatment with DIDS or DPC significantly reduced NECA-induced IL-8 secretion in LAD2 cells (Figure 3.23 B). This suggests that CFTR mediated Cl^- flux is not involved in LAD2 IL-8 secretion.

Because we could not detect IL-6 or TNF secretion from LAD2 cells in response to IgE/anti-IgE, we performed a protein array to screen for other cytokines synthesized by LAD2 cells in response to anti-IgE stimulation (Figure 3.23 C). Cytokines were considered to be secreted from LAD2 cells when a discernable spot appeared on the film following exposure to the membrane for 5 min. Change in cytokine expression was quantitated by densitometric comparison of integrated pixel density between treatments. For cytokines with integrated pixel density above 1×10^4 , inhibition was assessed as a decrease in signal by at least 1×10^4 pixels compared to sham treatment. For cytokines with integrated pixel density under 1×10^4 , inhibition was assessed as decrease in signal by at least 1×10^3 pixels in inhibitor treatment + anti-IgE, compared to sham treatment + anti-IgE. (Figure 3.23 C). Using this approach, we showed that LAD2 cells secrete IL-1 receptor antagonist (IL-1ra), granulocyte-macrophage colony stimulating factor (GM-CSF), macrophage migration inhibitory factor (MIF), IL-13, IL-16, tissue plasminogen activator-inhibitor-1 (PAI-1 or SerpinE1) and I-309

(CCL1) in response to anti-IgE (Figure 3.23 C). NPPB treatment had no effect on anti-IgE stimulated IL-1ra, GM-CSF or PAI-1 secretion, but appeared to downregulate anti-IgE mediated MIF, IL-13, IL-16 and CCL1 secretion (Figure 3.23 C). GlyH-101 treatment gave similar results, as NPPB. DIDS treatment downregulated anti-IgE mediated secretion of all of the above cytokines except PAI-1 (Figure 3.23 C). Interestingly, IL-8 was not detected on the array, suggesting that the detection limit of the array, for this cytokine at least, is somewhere in the range of 150 pg/ml (see Figure 3.23 B). This data also suggests that CFTR is involved in secretion of the other newly synthesized mediators MIF, IL-13, IL-16, SerpinE1 and I-309.

5. Pharmacological inhibitors do not affect anti-IgE-induced eicosanoid production in LAD2

In sham-treated LAD2 cells, LTC₄ production was 83 ± 4 pg/10⁶ cells (Figure 3.23 D). When cells were stimulated with anti-IgE for 30 min, LTC₄ production significantly increased to 322 ± 47 pg/10⁶ (Figure 3.23 D). None of the inhibitors at the doses tested had any significant effects on LTC₄ production in LAD2 cells. Unstimulated LAD2 cells also produced 48 ± 4 pg/10⁶ PGD₂ (Figure 3.23 D). Following anti-IgE stimulation, PGD₂ production significantly increased to 281 ± 48 pg/10⁶ cells (Figure 3.23 D). Although NPPB, GlyH-101, DIDS and DPC all showed a trend towards decreased PGD₂ production in MC, this decrease was not statistically significant for any of the inhibitors (n=5-8) (Figure 3.23 D).

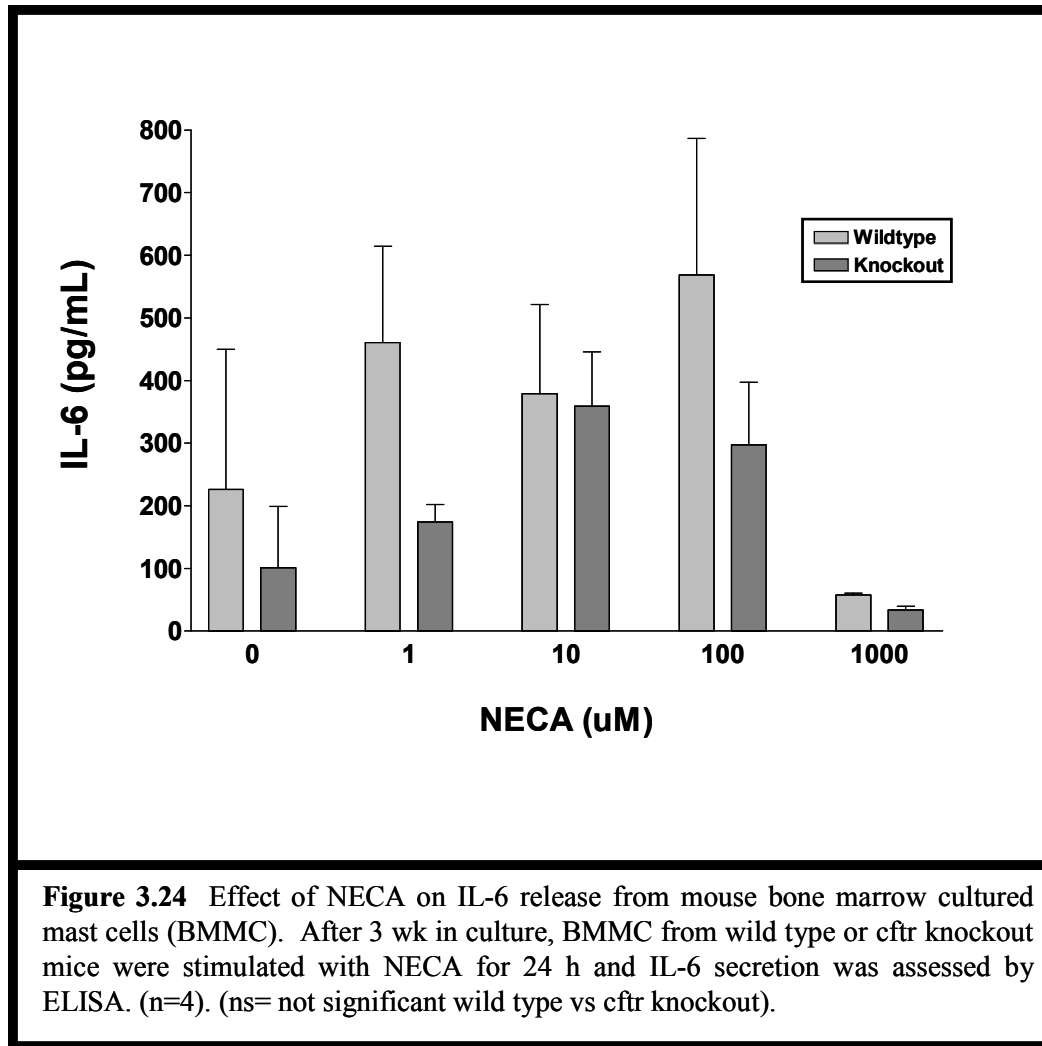
Our results suggest that some Cl⁻ flux occurs through CFTR in MC, but that this Cl⁻ flux is not involved in MC degranulation. However, CFTR function seems to be involved in secretion of IL-8 and other cytokines, as there was a

downregulation of several cytokines in HMC-1 and LAD2 following inhibition of CFTR using GlyH-101, the more specific CFTR inhibitor. The opposing effects of NPPB, DPC and GlyH-101 in certain assays may be due to non-specific activity of NPPB or DPC (Table 1.1). These effects of CFTR may be associated with localization to lipid rafts (312).

G. Antisense oligonucleotide (ASO) knockdown of CFTR expression in MC

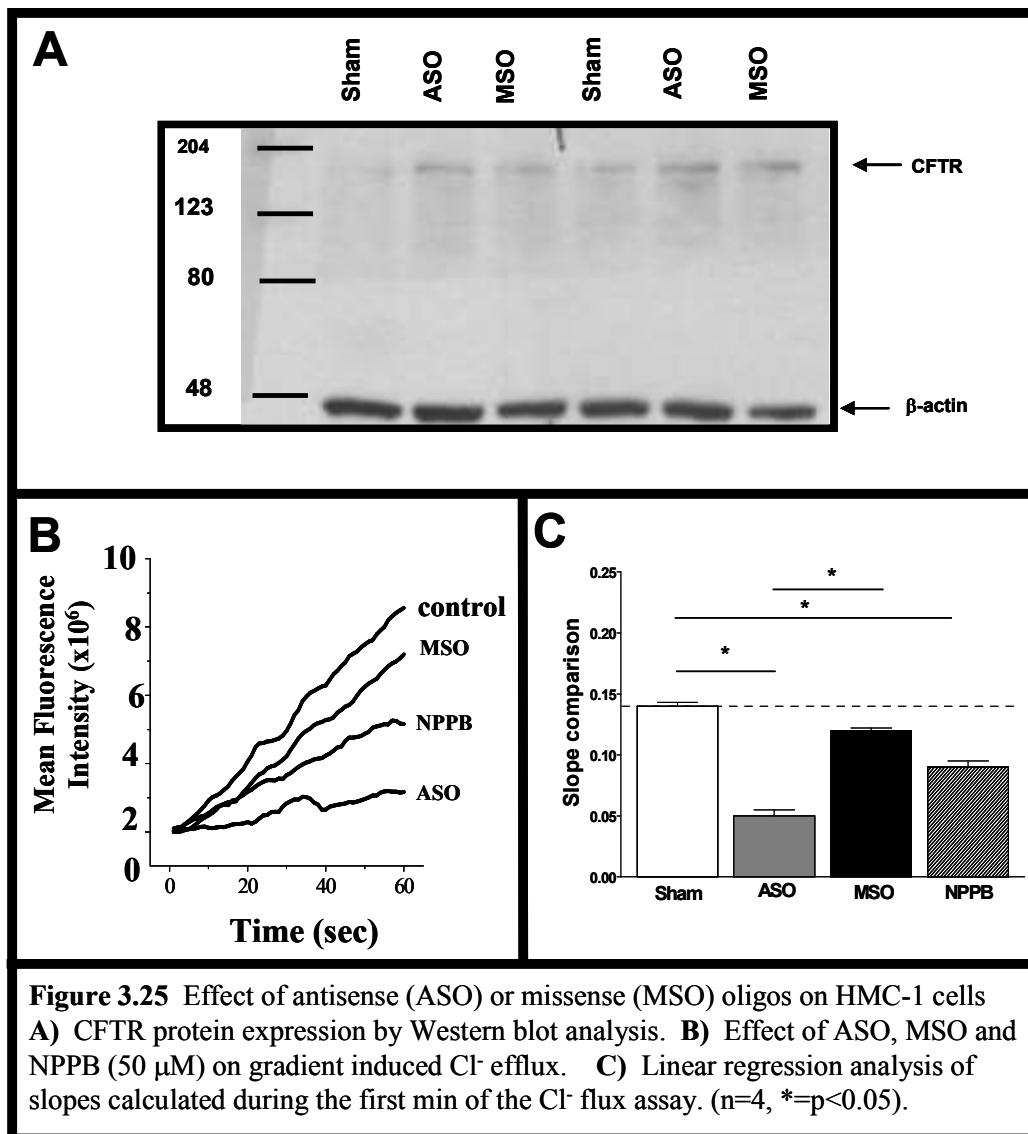
1. CFTR knockout does not affect NECA-induced IL-6 secretion in mouse bone marrow cultured MC (BMMC)

Because of the potential for known or unknown non-specific effects of CFTR pharmacological inhibitors, we wanted to further test our hypothesis that CFTR is involved in MC function by removing it from MC. Our initial approach was to use bone marrow cultured (BMMC) from wild type and CFTR knockout mice as described in chapter 2. Mature BMMC were stimulated with various doses of the adenosine receptor agonist NECA (Figure 3.24). After 24 h stimulation, we measured the amount of IL-6 secreted by the cells. Sham-treated BMMC from wild type and CFTR knockout mice spontaneously released 226 ± 223 pg/ml and 100 ± 98 pg/ml respectively (Figure 3.24). When stimulated with NECA at various doses, there was no significant difference (even at 1 μ M) in IL-6 secretion by wild type or CFTR knockout BMMC as determined by one way ANOVA (Figure 3.24). This data suggests that CFTR is not involved in IL-6 release from mouse BMMC in response to NECA.



2. ASO downregulates Cl⁻ flux in HMC-1

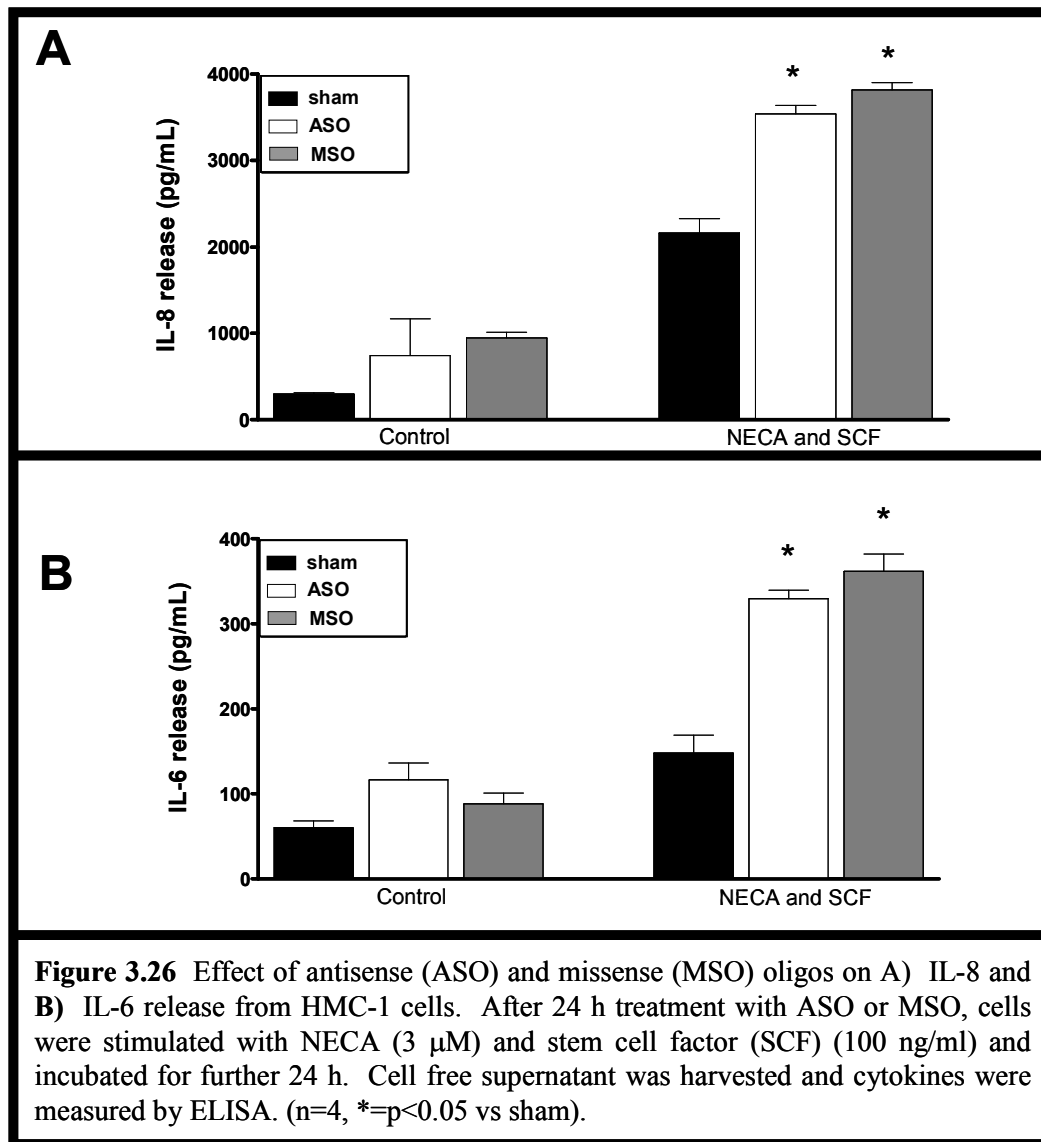
As CFTR knockout mice do not suffer from lung pathology as CF patients do and mouse and human MC exhibit many species differences, CFTR may be involved in human but not mouse MC cytokine secretion, function and CF pathophysiology. To test this, we knocked down CFTR in human MC HMC-1 using antisense oligonucleotide technology as described in chapter 2 (Figure 3.25). This work was initiated by Dr. Andreas Schwingshackl, a Post Doctoral fellow in our laboratory. After 24 h transfection of HMC-1 cells with sham, ASO or MSO, Dr. Scwhingshackl showed that CFTR expression was decreased in ASO treated cells, but not in sham or MSO transfected cells. Using these transfected cells in the MQAE Cl⁻ flux assay and both a β -hex and IL-6 release assay using the Ca²⁺ ionophore A23187, Dr. Schwingshackl showed that ASO but not MSO treatment downregulated Cl⁻ flux, β -hex release and IL-6 secretion for HMC-1 cells (unpublished data). However, this work did not use a physiological stimulus nor did it study a MC type more representative of mature MC. Thus I used NECA as a stimulus instead of A23187 (49). When I transfected HMC with ASO I could not confirm the decrease in protein expression on HMC-1 cells shown by Dr. Schwingshackl (Figure 3.25 A). However, I did reproduce Dr. Schwingshackl's data on Cl⁻ flux in ASO transfected HMC-1 (Figure 3.25 B). Our data showed that sham and MSO transfected HMC-1 had similar slopes during the first minute (0.14 ± 0.003 and 0.12 ± 0.002 respectively), indicating that MSO treatment had no effect on MC Cl⁻ flux (Figure 3.25 B and C).



The slope of ASO and NPPB (50 mM)-treated cells were 0.05 ± 0.005 and 0.09 ± 0.01 respectively, indicating that these two treatments significantly downregulated Cl^- efflux from HMC-1 compared to sham or MSO treatments (Figure 3.25 B and C).

3. CFTR ASO non-specifically increases IL-6 and IL-8 secretion from HMC-1

Having determined that NECA is a good physiological stimulus to induce IL-8 secretion from HMC-1 cells, we used it to stimulate HMC-1 cells transfected with ASO and MSO. Spontaneous release of IL-8 from sham stimulated, untransfected, ASO or MSO transfected HMC-1 was 299 ± 14 , 749 ± 423 , and 945 ± 67 pg/ 10^6 cells respectively (Figure 3.26 A). Upon 24 h stimulation with NECA (3 μM) and SCF (100 ng/ml), HMC-1 secretion of IL-8 increased to $2160 \pm$ pg/ 10^6 cells in untransfected cells (Figure 3.26 A). In ASO treated cells, NECA/SCF stimulated IL-8 secretion was significantly increased to 3540 ± 96 pg/ 10^6 cells. However, a significant increase in IL-8 secretion also occurred in MSO treated cells (3815 ± 85 pg/ 10^6 cells) (Figure 3.26 A). The same phenomena occurred when we examined IL-6 release from ASO and MSO treated HMC-1 (Figure 3.26 B). Spontaneous release of IL-6 from HMC-1 after 24 h was 60 ± 8 pg/ 10^6 cells (Figure 3.26 B). When cells were stimulated with NECA for 24 h, IL-6 secretion significantly increased to 148 ± 21 pg/ 10^6 cells.



ASO and MSO treatment did not significantly affect spontaneous IL-6 secretion. When ASO treated cells were stimulated with NECA, IL-6 secretion was significantly increased to 329 ± 10 pg/ 10^6 cells compared to sham treated NECA stimulated cells. Similarly, MSO treatment significantly increased IL-6 secretion to 362 ± 21 pg/ 10^6 cells. These data indicate that the ASO and MSO are non-specifically activating the cells, and that the effects we observed are not due to CFTR inhibition. Thus, we were forced to find an alternate way to reduce CFTR expression in MC, which lead us to the use of RNA interference (RNAi) by small inhibitory RNA (siRNA).

Although we appeared to be successful at knocking down CFTR using ASO technology when we measured Cl^- flux, we had difficulty in validating CFTR expression by Western blot. Although ASO seemed to downregulate Cl^- flux in MC, we cannot be sure that it did so in a CFTR-specific fashion as both ASO and MSO induced strong potentiation of IL-8 secretion from HMC-1 as a result of NECA stimulation.

H. Knockdown of CFTR expression in MC using siRNA

1. Optimization of siRNA transfection of MC by BLOCK-iT siRNA

Given that ASO and MSO non-specifically activated cytokine secretion from HMC-1, we moved to siRNA technology, a state-of-the-art method of knocking down proteins. When we began looking for alternate strategies to ASO technology, siRNA was gaining popularity. However, at the time, only two

papers on MC transfection had been published, including one study on electroporation and one study on lipofectamine transfection of rat basophilic leukemia-2H3 cells (RBL-2H3), a mucosal-like MC line (313, 314). We avoided electroporation as it is hard on the cells and MC may be particularly susceptible to activation, degranulation and death using this technique. We transfected cells with Lipofectamine and other transfection reagents such as RNAifect and FuGene HD. The Lipofectamine study on RBL-2H3 cells incubated the cells for 48 h with siRNA, but lacked detail about the transfection conditions. Thus, we optimized transfection of HMC-1 with BLOCK-iT FITC labeled siRNA complexed with increasing doses of Lipofectamine (Figure 3.27). Flow cytometric analysis showed that transfection of HMC-1 with 40 nM BLOCK-iT siRNA without Lipofectamine resulted in a 1% transfection rate (Figure 3.27 A). Transfection of cells with various ratios of siRNA:Lipofectamine increased the transfection rate to a maximum of 70% using 80 nM BLOCK-iT and 1 μ l Lipofectamine (Figure 3.27 C). Transfection of HMC-1 using 160 nM:1.5 μ l BLOCK-iT:Lipofectamine reduced transfection rate to 58% (Figure 3.27 D).

We also assessed RNAifect transfection efficiency in HMC-1 by flow cytometry using various BLOCK-iT:RNAifect ratios (Figure 3.28 A). We showed that RNAifect was not an effective transfection reagent for HMC-1 as the highest FITC signal achieved was $15 \pm 5\%$ using 7.7 μ l Block-iT and 18 μ l RNAifect as directed by manufacturer's instructions (Figure 3.28 A). However, when Lipofectamine was used instead of RNAifect, cells were 70% positive for FITC using 80 nM siRNA and 1 μ l Lipofectamine per transfection reaction

(Figure 3.28 B). Several flow cytometry experiments showed that 40 nM siRNA and 1 μ l Lipofectamine gave similar results ($63 \pm 7\%$) (Figure 3.28 B), and we used 40:1 ratio of siRNA:transfection reagent in subsequent transfection experiments in an attempt to minimize non-specific effects and cell activation.

2. Optimization of realtime PCR CFTR and β -actin primers

Using Calu-3 cells as positive control for knockdown, we transfected the cells using 40 nM siRNA complexed with 1 μ l Lipofectamine. After 48 h incubation with siRNA, we extracted RNA from the cells for realtime PCR analysis. We used some of the sham treated Calu-3 cDNA for determination of primer efficiencies to use in the Pfaffl realtime PCR calculations (chapter 2) (291). Based on the slope of the ΔC_T at different concentrations of cDNA, the efficiency of our β -actin primers was 1.97, whereas the efficiency of our CFTR primers was 1.14 (Figure 3.28 C). Primer efficiency of 2 represents 100% efficiency, thus our β -actin primers are 95% efficient, whereas our CFTR primers are 60% efficient. Due to this difference in efficiency, we did not perform multiplex PCR, but analyzed transcripts for β -actin and CFTR in separate tubes containing the same template material. In Calu-3, two separate experiments demonstrated that siRNA 503 and 794 transfected with Lipofectamine showed no reduction of CFTR mRNA levels (Figure 3.28 D). Since we saw no downregulation of message in Calu-3, and our intention was to transfect MC, we

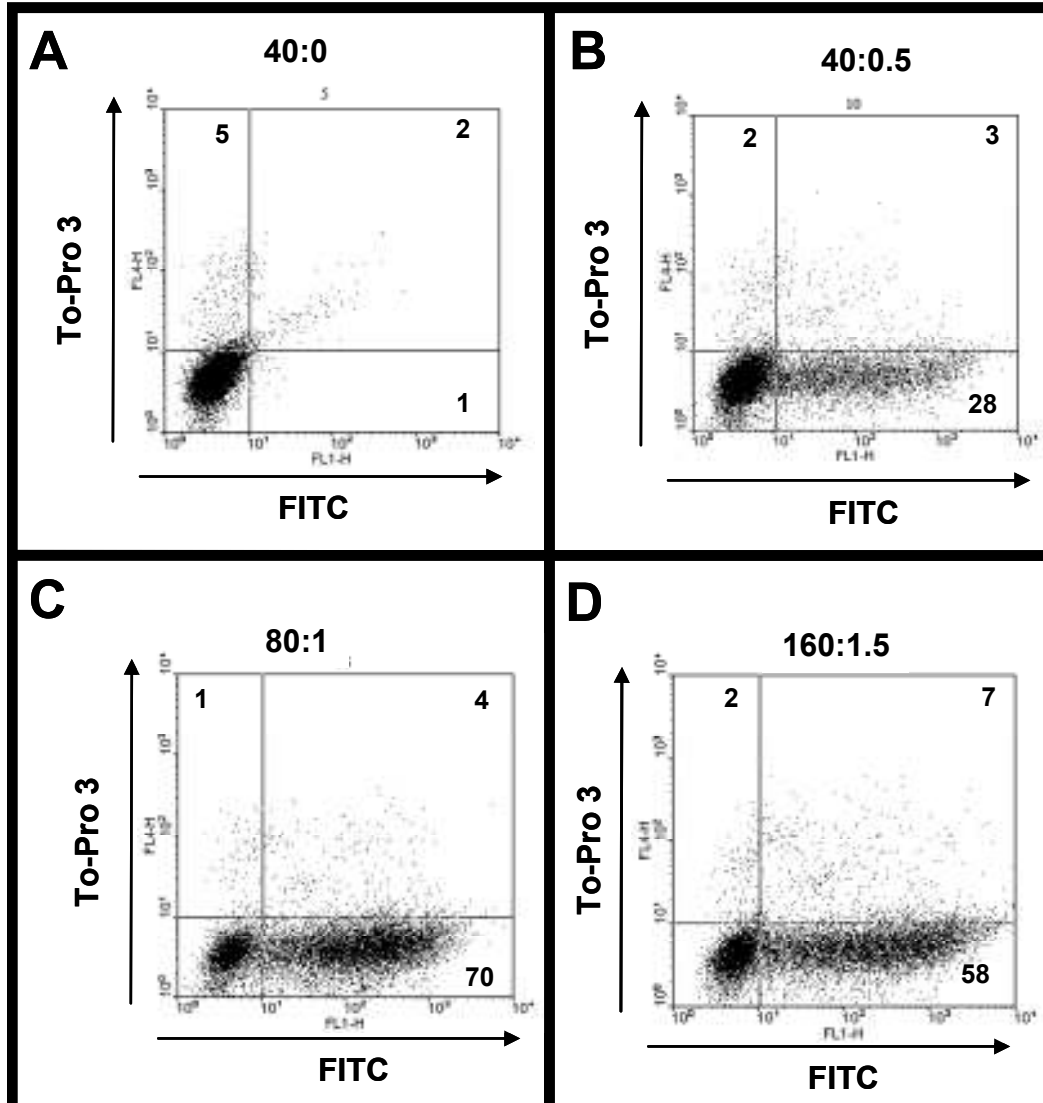


Figure 3.27 Optimization of transfection efficiency in HMC-1 using various ratios of nucleic acid:lipid (nM BLOCK-iT siRNA:μl lipofectamine). Cells were transfected for 24 h at 37°C and flow cytometric analysis was performed using FL-1 (FITC) and FL-4 (To-Pro3) channels. FITC measured BLOCK-iT fluorescence whereas To-Pro3 is a non-permeable nucleic acid stain that detects dead cells with compromised membrane integrity. Numbers in each quadrant represent % positive cells in that quadrant. (n=2).

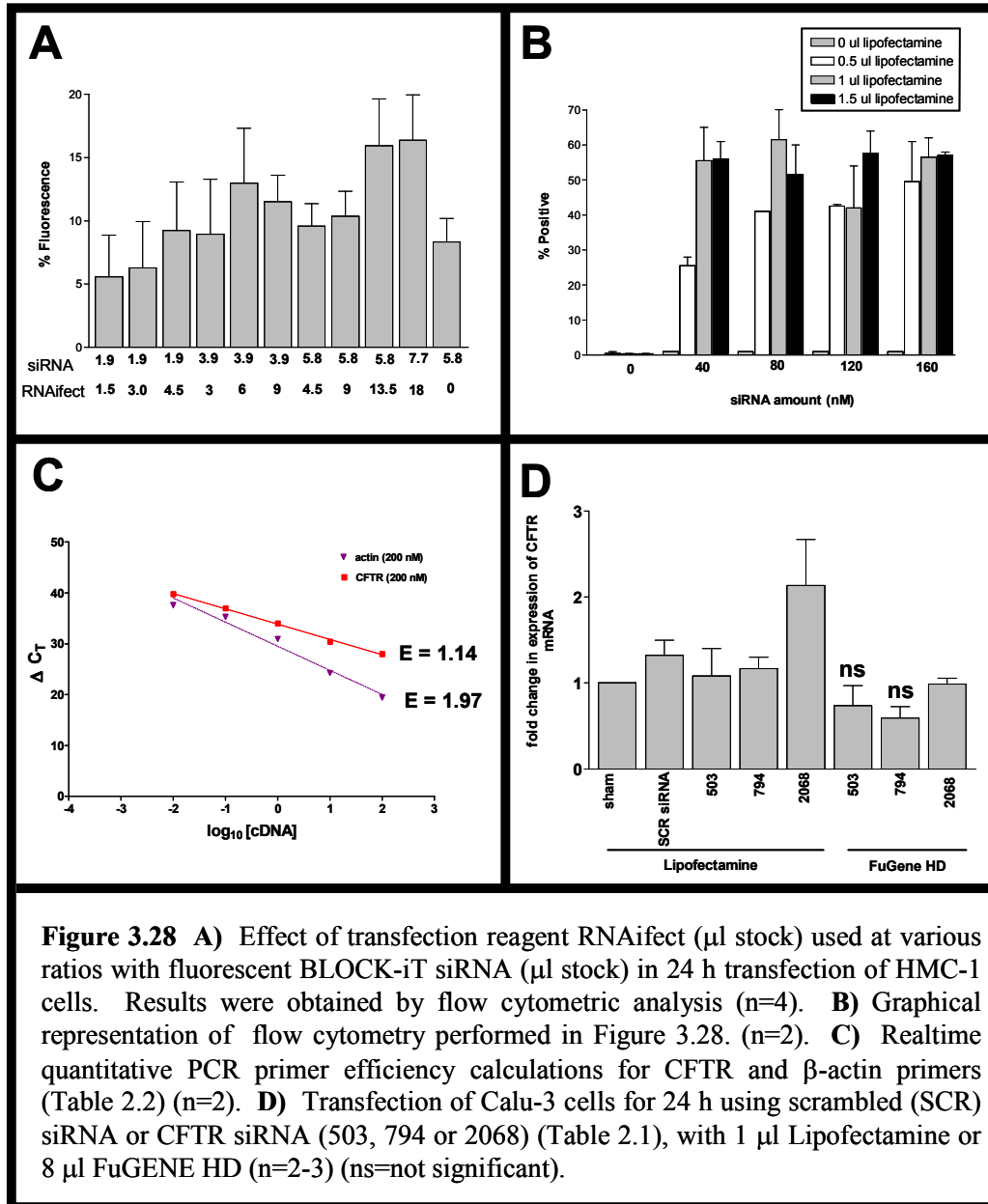
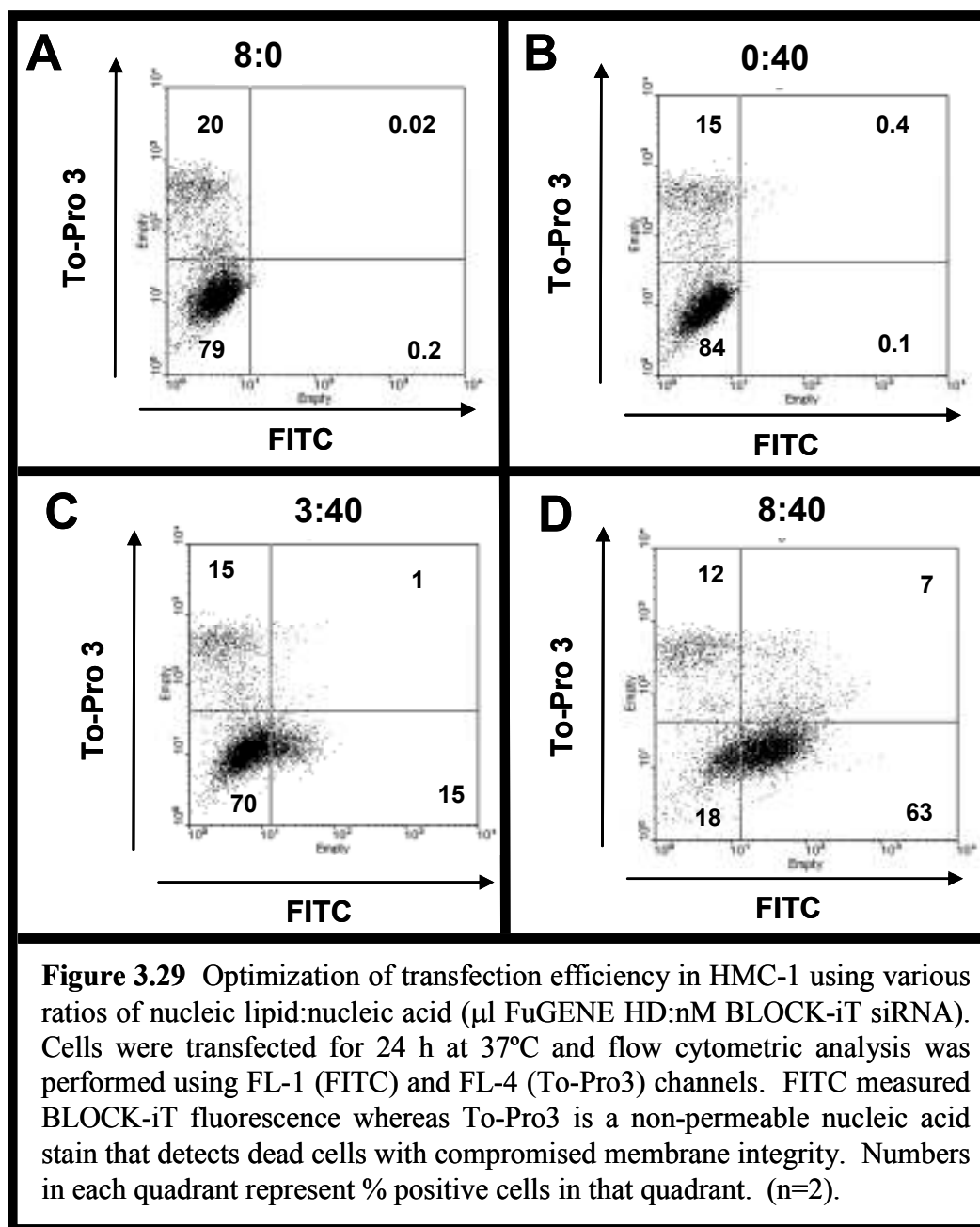


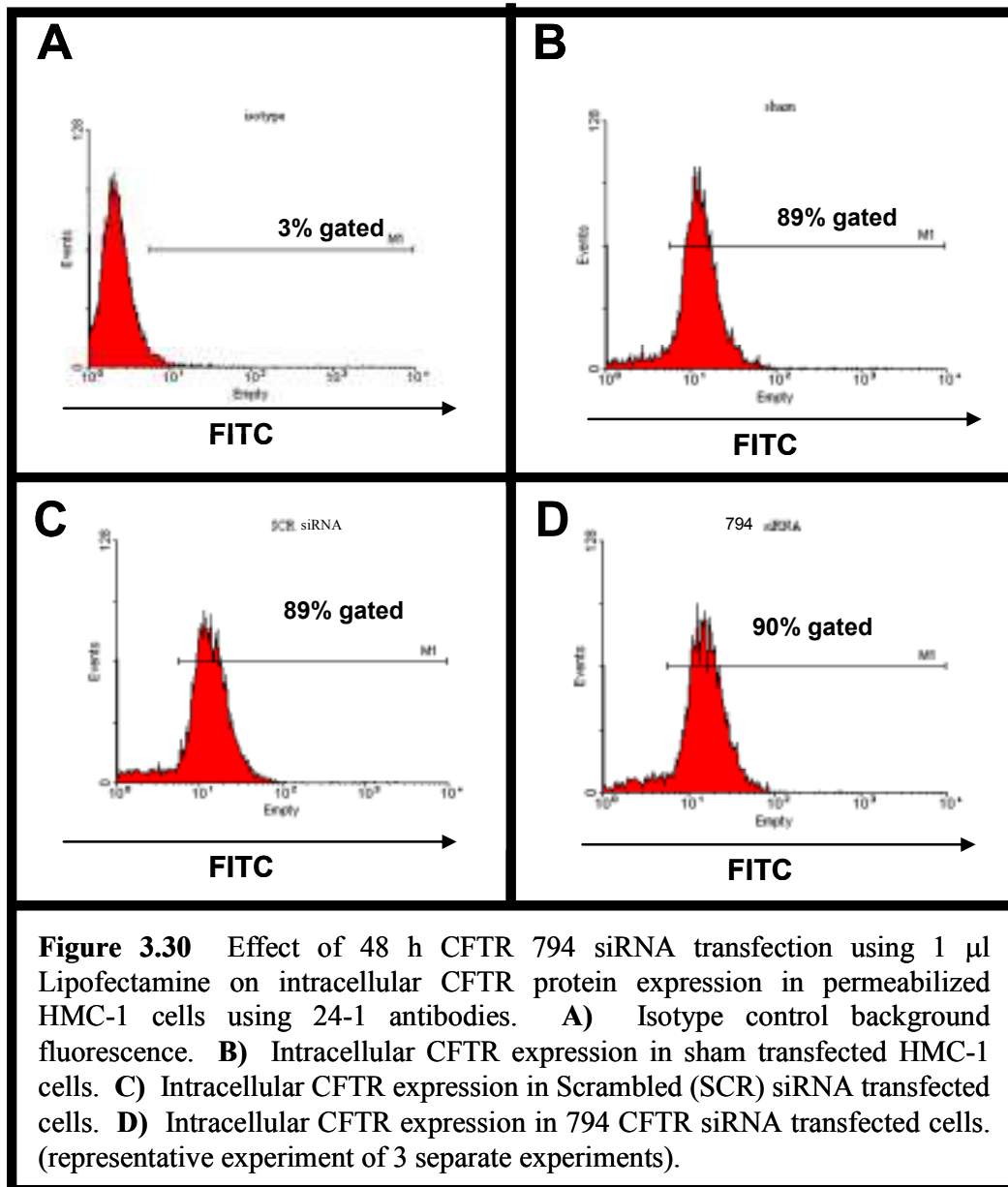
Figure 3.28 **A)** Effect of transfection reagent RNAiAfect (μ l stock) used at various ratios with fluorescent BLOCK-iT siRNA (μ l stock) in 24 h transfection of HMC-1 cells. Results were obtained by flow cytometric analysis (n=4). **B)** Graphical representation of flow cytometry performed in Figure 3.28. (n=2). **C)** Realtime quantitative PCR primer efficiency calculations for CFTR and β -actin primers (Table 2.2) (n=2). **D)** Transfection of Calu-3 cells for 24 h using scrambled (SCR) siRNA or CFTR siRNA (503, 794 or 2068) (Table 2.1), with 1 μ l Lipofectamine or 8 μ l FuGENE HD (n=2-3) (ns=not significant).



purchased FuGene HD transfection reagent, which according to the manufacturer, is better at transfecting non-adherent cells than Lipofectamine. We performed flow cytometry experiments using several FuGene HD:BLOCK-iT ratios as we did for Lipofectamine and RNAifect (Figure 3.29). We showed that without FuGene or siRNA, 0.2 and 0.1% of HMC-1 cells were positive for FITC signal (Figure 3.29 A and B). When 3 μ l FuGene HD is used to transfect 40nM siRNA, 15% of the cells were positive for FITC, whereas when 8 μ l FuGene is used to transfect 40 nM siRNA, 63% of the cells were positive for FITC (Figure 3.29 C and D). Transfection of cells with more than 8 μ l FuGene HD (9 and 10 μ l) with 40 nM siRNA decreased percentage of FITC positive cells (data not shown).

3.CFTR siRNA does not reduce CFTR protein expression in HMC-1

Transfection of Calu-3 cells with 503 and 794 complexed to FuGene HD rather than Lipofectamine resulted in downregulation of CFTR mRNA levels by $26 \pm 23\%$ and $40 \pm 11\%$ respectively (Figure 3.28 D). Protein analysis was not performed as Calu-3 overexpress CFTR and we did not expect to find a reduction in protein expression with an mRNA reduction of less than 50%. Thus we proceeded directly to transfection of HMC-1 cells using siRNA 794 with the optimized transfection conditions for FuGene HD (Figure 3.29). To determine if 794 siRNA downregulated CFTR protein expression in HMC-1 after 48 h, we performed flow cytometry using the 24-1 IgG_{2a} antibody on permeabilized HMC-1 cells (Figure 3.30).

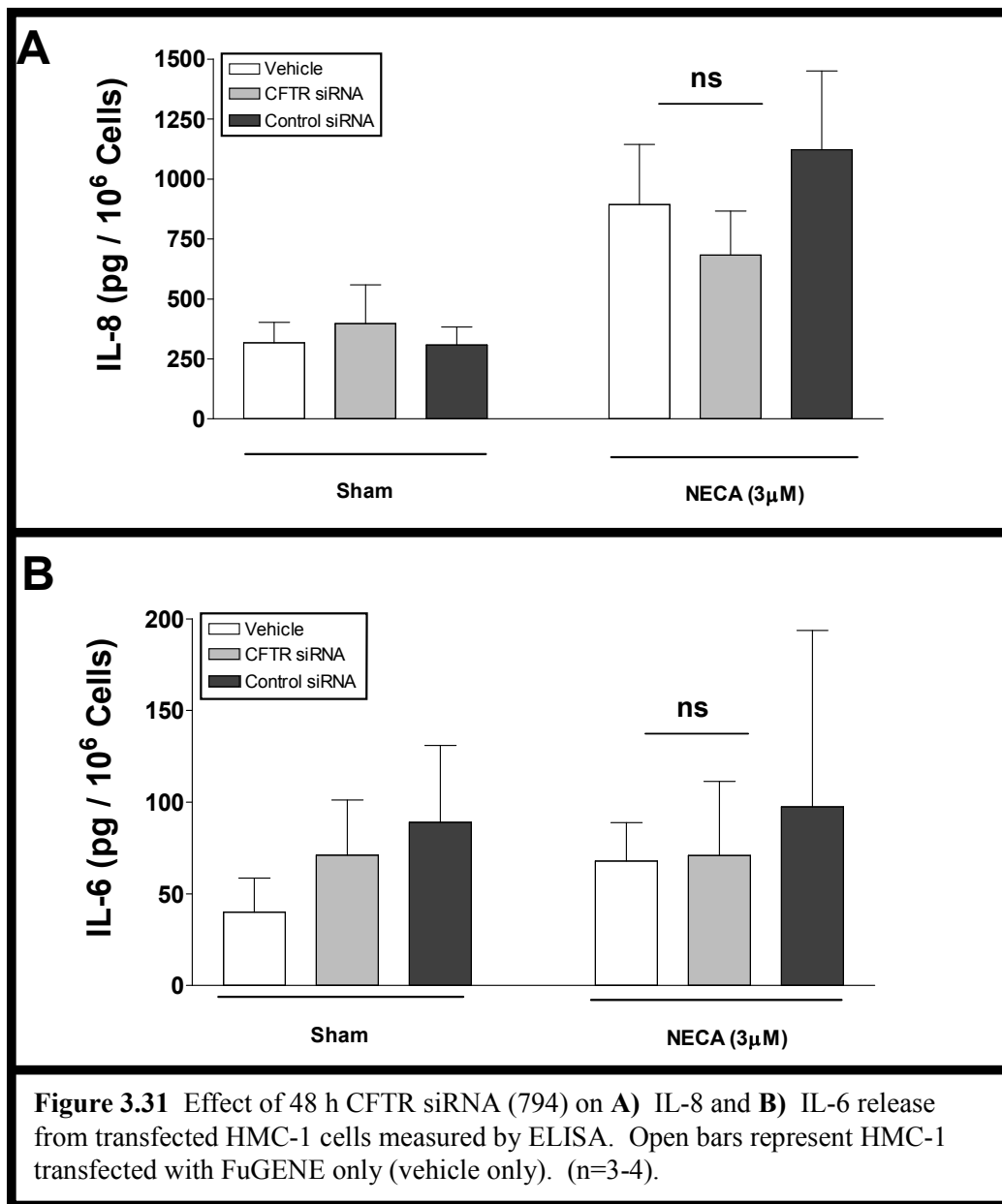


Background fluorescence in untransfected cells stained with isotype control antibody was 3% (Figure 3.30 A). When 24-1 antibody was used instead of isotype, untransfected cells were 89% positive for CFTR. We found no differences in staining between FuGene only (no siRNA), scrambled siRNA (SCR siRNA) or CFTR siRNA (794 siRNA) when we assessed percentage of FITC positive cells (89%, 89% and 90% respectively) (Figure 3.30 B, C and D). Western blot analysis of 794 as well as Ambion siRNA in HMC-1 cells suggests that CFTR was not knocked down by this method after 48 h (not shown).

4. CFTR siRNA 794 does not affect IL-8 or IL-6 secretion from HMC-1

After 48 h transfection with CFTR siRNA 794, cells were harvested and stimulated with NECA (3 μ M) for 24 h to assess the effect of CFTR siRNA on IL-6 and IL-8 secretion (Figure 3.31). Untransfected and unstimulated cells spontaneously released 316 ± 86 pg/10⁶ cells of IL-8, whereas missense or 794 siRNA treatment did not significantly alter spontaneous IL-8 release from the cells (308 ± 75 and 397 ± 161 pg/10⁶ cells respectively) (Figure 3.31 A). After 24 h treatment with NECA, untransfected HMC-1 released significantly more IL-8 than was spontaneously released (893 ± 250 pg/10⁶ cells). Neither SCR siRNA nor 794 siRNA significantly changed IL-8 release from the cells upon NECA stimulation (1122 ± 327 and 683 ± 183 pg/10⁶ cells respectively) (Figure 3.31 A).

Untransfected and unstimulated HMC-1 also spontaneously released IL-6 (40 ± 19 pg/10⁶) (Figure 3.31 B).



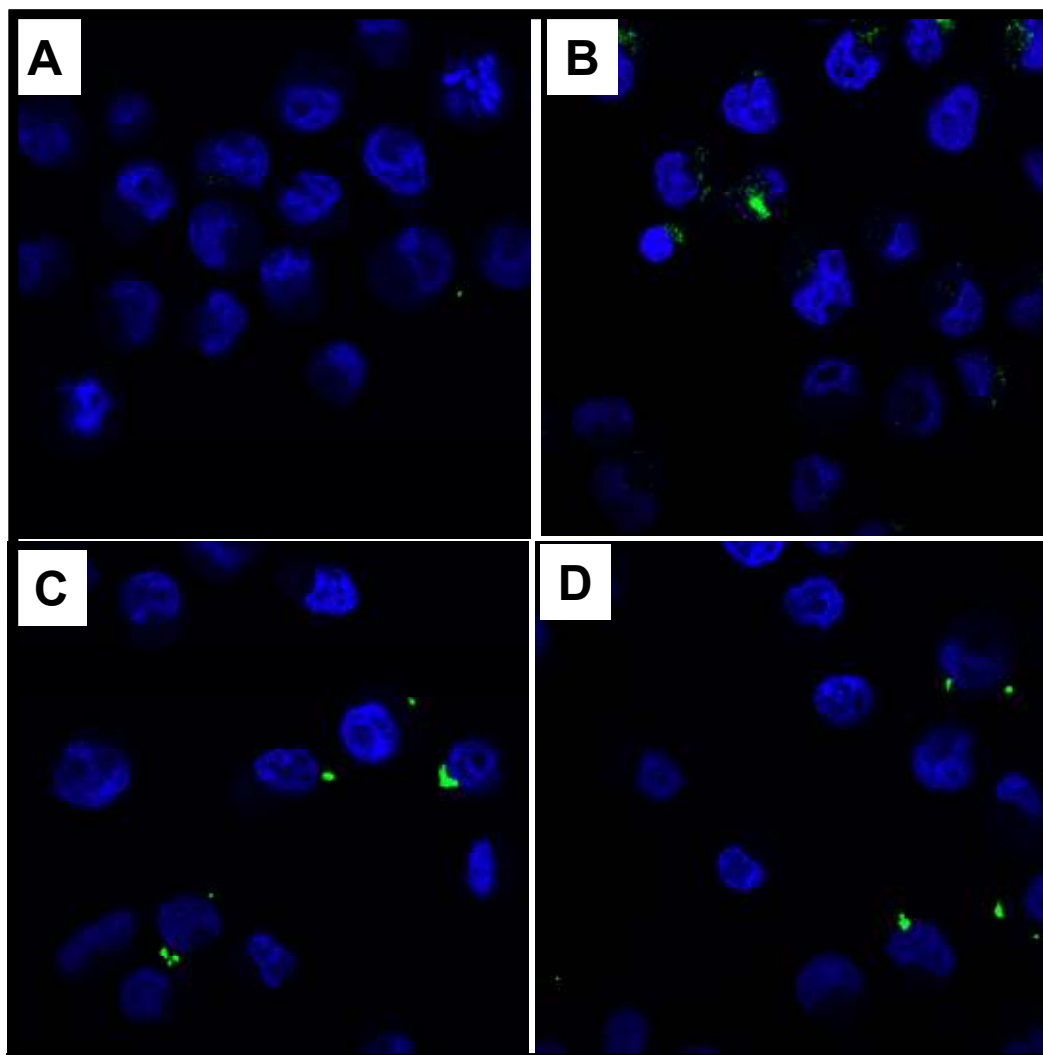


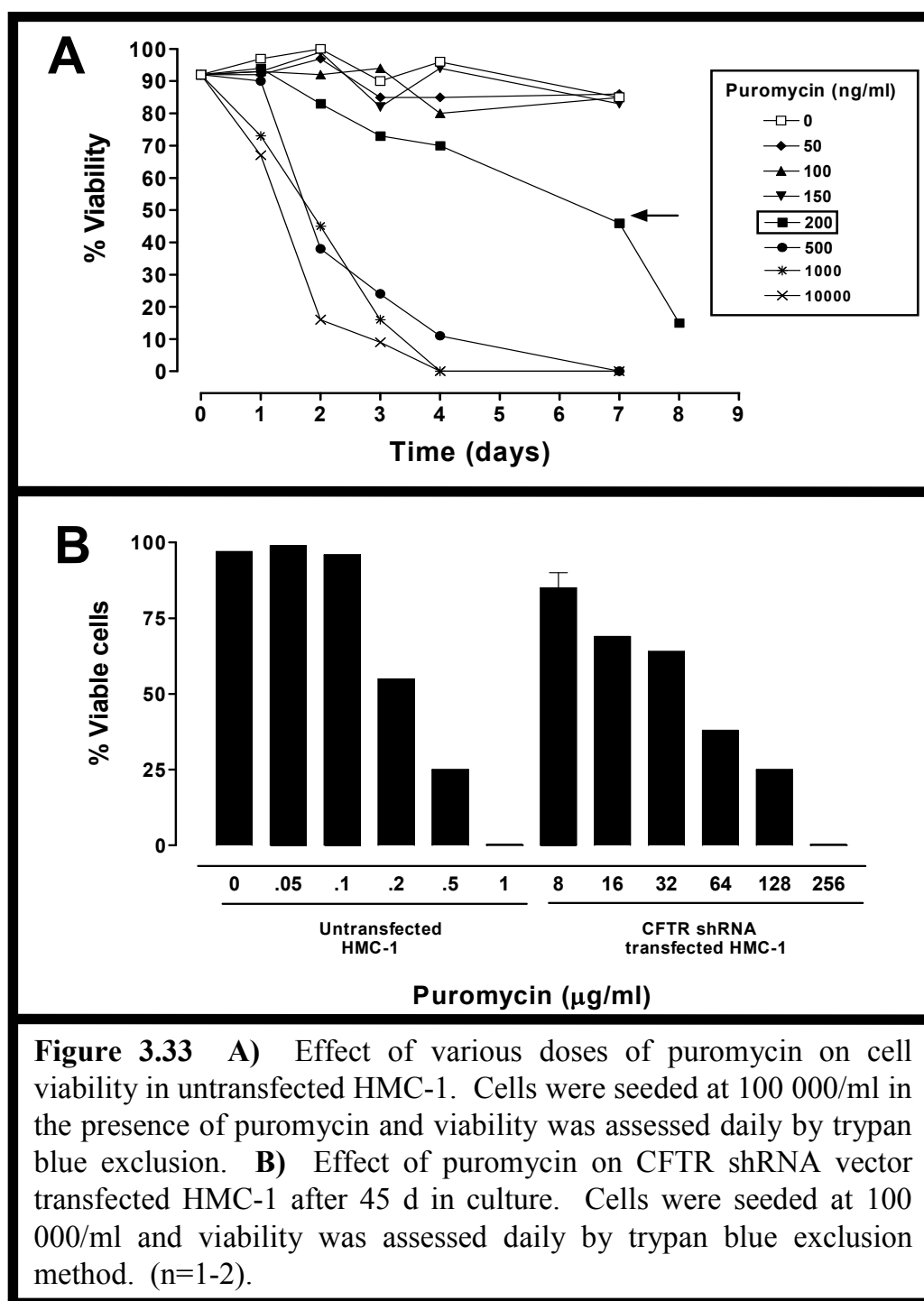
Figure 3.32 Confocal microscopy of experiments performed in Figure 3.28. Optimization of transfection efficiency in HMC-1 using various ratios of nucleic acid:lipid (nM BLOCK-iT siRNA:ml lipofectamine). **A)** 40:0 **B)** 40:0.5 **C)** 80:1 **D)** 160:1.5. Cells were transfected for 24 h at 37°C and confocal microscopy analysis was performed measuring BLOCK-iT (FITC) and nuclear stain 4',6-diamidino-2-phenylindole (DAPI). (n=1). Magnification= 400x

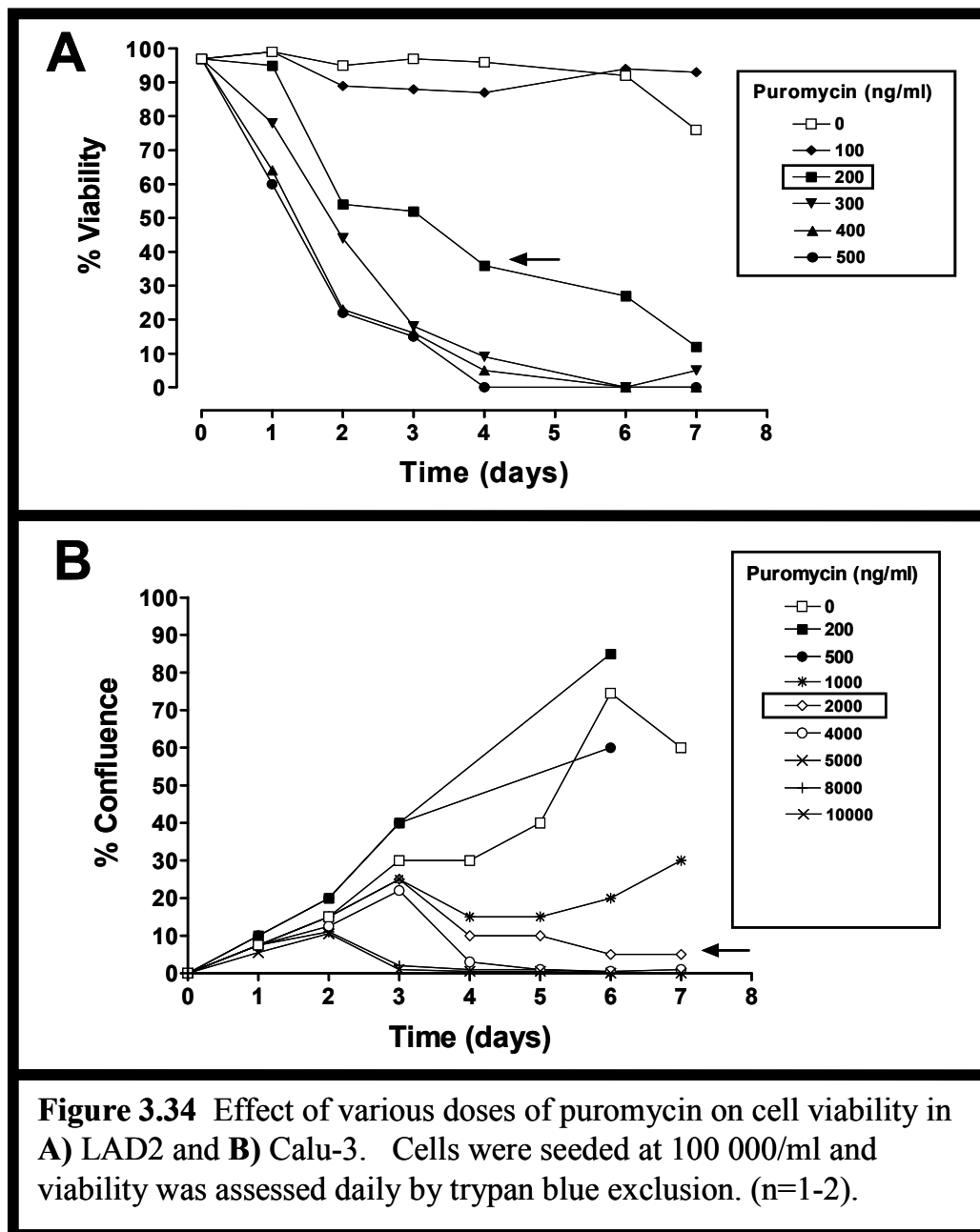
Neither treatment with SCR siRNA or 794 siRNA had any effect on spontaneous release of IL-6 from the cells (89 ± 42 pg/ 10^6 and 71 ± 40 pg/ 10^6 cells respectively). After 24 h stimulation with NECA, IL-6 release from untransfected HMC-1 increased to 68 ± 21 pg/ 10^6 cells. Neither missense nor 794 siRNA had any effect on IL-6 release from NECA stimulated HMC-1 cells (71 ± 40 pg/ 10^6 and 97 ± 96 pg/ 10^6 cells respectively) (Figure 3.31 B).

5. Confocal microscopy of BLOCK-iT transfected cells using short hairpin RNA (shRNA)

To investigate why the siRNA for CFTR was not reducing CFTR protein levels, we transfected HMC-1 with the BLOCK-iT:Lipofectamine ratios used previously and we performed confocal microscopy on the cells to determine the location of the fluorescent signal (Figure 3.28). Our results suggest that a large proportion of the BLOCK-iT fluorescent siRNA is stuck to the outside of the cells (Figure 3.32).

The siRNA data above suggest that little siRNA is getting inside the cells. This was also supported by an observation we made upon trypan blue staining of freshly transfected HMC-1 cells, which were viable, but had dark blue spots all around their periphery (not shown). At the time, we did not realize what this meant, but as trypan blue is a nucleic acid stain, we later realized that trypan blue was likely staining extracellular siRNA:lipid complexes.





I. Stable knockdown of CFTR in HMC-1

Having tried siRNA with several cell types and several different siRNA from different companies, and having had no success with CFTR knockdown, we suspected that most of the siRNA was not entering the cells. Moreover, transfection in HMC-1 was inefficient and CFTR siRNA was not being delivered in a manner to knock down the protein. Therefore, we attempted to stably transfect MC using a lentiviral vector system with a puromycin selection marker.

1. Determination of HMC-1, LAD2 and Calu-3 puromycin susceptibility

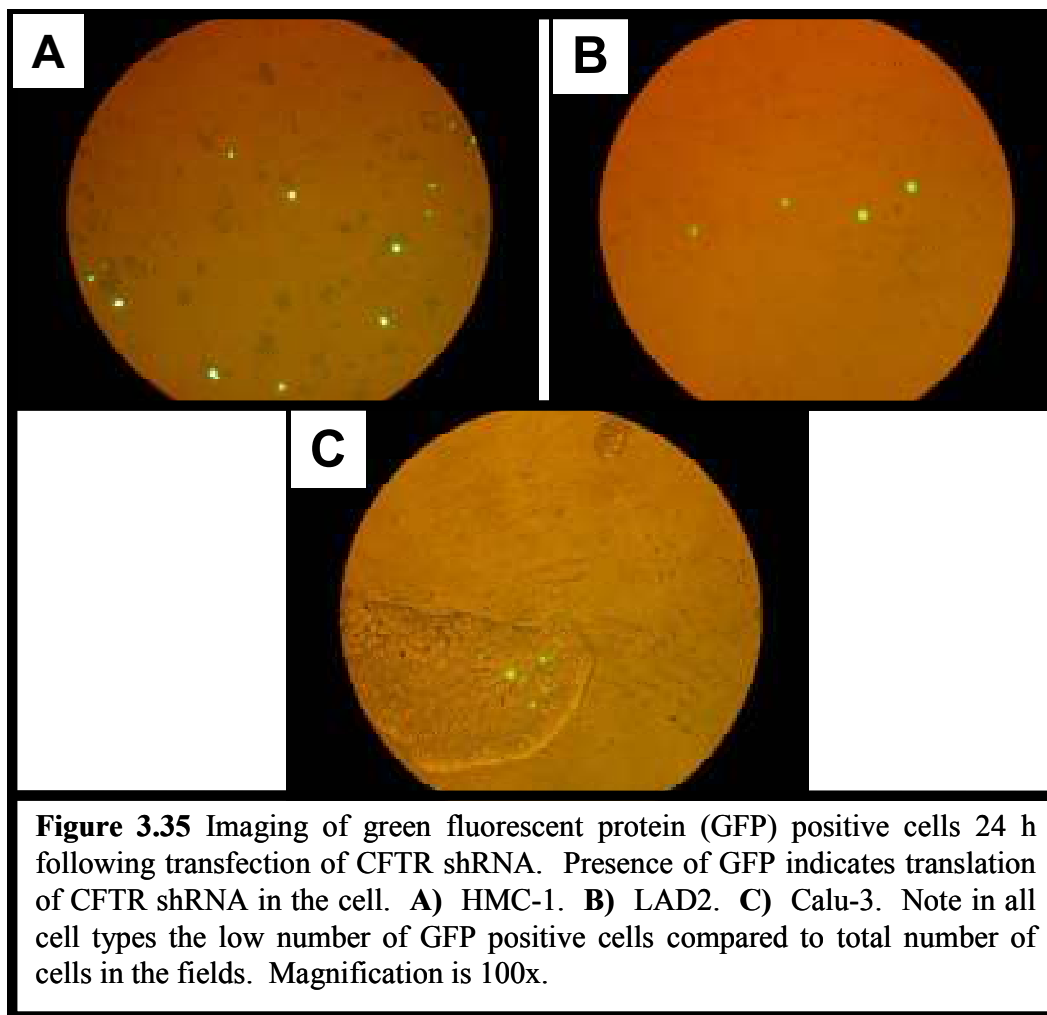
As described in chapter 2, puromycin is used to stop translation of mRNA into protein, and doses that interfere with metabolic processes kills cells within a few days. To determine the best dose of puromycin to use in our cell lines, we performed experiments to generate puromycin kill curves using untransfected cells as described in chapter 2. For HMC-1 as well as LAD2 cells, the presence of up to 150 ng/ml puromycin, had no effect and the cells proliferated until the flasks were overgrown and viability began to decline (Figure 3.33 A and 3.34 A). However, in the presence of 200 ng/ml puromycin, the cells began to die after 24 h and viability continued to decline until 7 d. In both cell types, higher doses of puromycin accelerated the decline of cell viability (figure 3.33 A and 3.34 A).

For Calu-3 cells, the presence of up to 500 ng/ml puromycin did not affect confluency of the flasks. When 1000 ng/ml puromycin was present, cell growth was slowed and confluence was delayed past 7 d. When 2000 ng/ml puromycin

was present, cells began to die at 3 d and were nearly all detached by 7 d (Figure 3.34 B). Remaining Calu-3 cells were unhealthy looking, sparse with clumps of cells still attached to the flask and confluence was estimated at 2-5%. Therefore, 200 ng/ml puromycin for HMC-1 and LAD2 and 2000 ng/ml puromycin for Calu-3 were chosen as initial doses of puromycin to add to transfected cells to establish stable transfected cell lines (Figure 3.33 and 3.34).

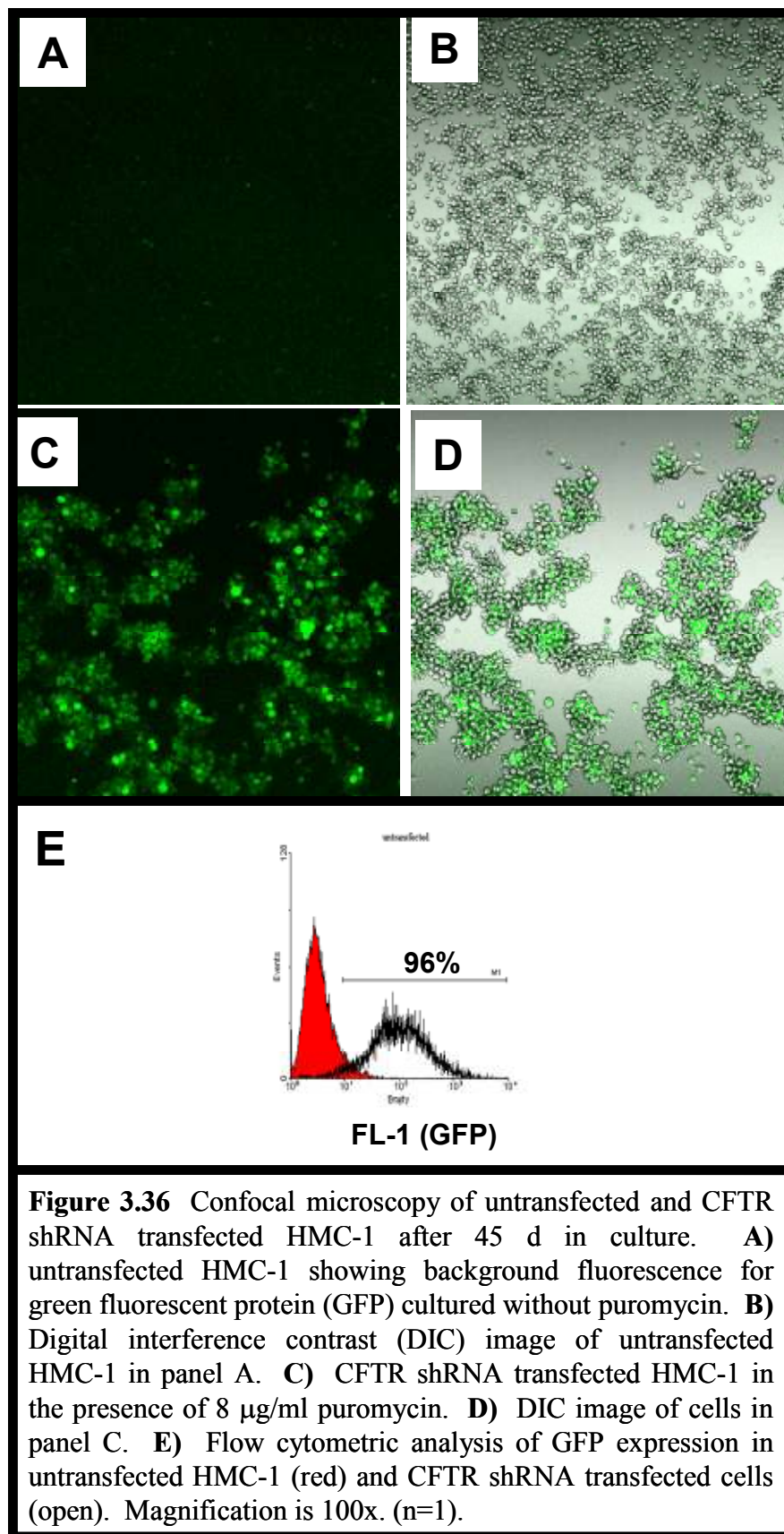
2. Transfection of HMC-1 with lentiviral CFTR shRNA vector

To transfect HMC-1, LAD2 and Calu-3 with the vector, we complexed 2 μ g/ml vector DNA according to manufacturer's recommendations, with 8 μ l FuGENE HD determined to be the best ratio in previous experiments (Figure 3.29). After 24 h transfection, few cells were positive for green fluorescent protein (GFP) in HMC-1, LAD2 and Calu-3, confirming our previous findings that the transfection efficiency is low in these cell types (Figure 3.35). For HMC-1 puromycin was added 48 h after transfection and the dose was gradually doubled weekly until 8 μ g/ml was reached over 7 wk (Figure 3.33 B). At 3 d in the presence of 200 ng/ml puromycin, untransfected HMC-1 viability had declined to 55%, and then to 15% by 7 d, but transfected cells were totally resistant to those doses (Figure 3.33 B). Transfected cells only began to die after the addition of 16 μ g/ml puromycin (Figure 3.33 B). After 7 wk in culture with puromycin (8 μ g/ml), scrambled control (SCR shRNA) and CFTR shRNA transfected cells were >90% viable, and 96% positive for GFP (Figure 3.36).



When 200 ng/ml puromycin was added to LAD2 cells, the culture seemed to be more sensitive than established by previous experiments, as the cells succumbed to the puromycin. Cells were retransfected, using 10 ng/ml starting dose of puromycin and dose was increased to 50 ng/ml over 6 wk. However, cells were lost due to an incubator failure after 12 wk in culture, and after starting a new LAD2 culture, cells had to be transfected once again. This caused a 6-8 month delay in our LAD2 work. After 2 wk in the presence of puromycin (100 ng/ml) only 3-4% of cells were positive for GFP in SCR shRNA and CFTR shRNA and only 14-15% of cells were positive for the dead cell stain propidium iodide. Thus, after retransfection of LAD2 cells, puromycin resistance seems to be the same as previously established and thus has recently been increased to 200 ng/ml. Transfected LAD2 cells are currently in the selection and expansion phase in the presence of increasing doses of puromycin and were not ready for use at the time of writing of this thesis.

Transfected Calu-3 cells also proved to be difficult to culture in the presence of puromycin. As we had determined in previous experiments (Figure 3.34 B), we seeded transfected Calu-3 cells in various doses of puromycin, including 1500 ng/ml, a dose which was between the survival and lethal doses of 1000 and 2000 ng/ml respectively. The transfected Calu-3 cells did not survive in 1500 or 2000 ng/ml puromycin, but survived in 1000 ng/ml. However, the untransfected Calu-3 also survived in 1000 ng/ml of puromycin. We attempted three separate transfections, but were not successful in generating a stable CFTR knockdown Calu-3 cell line.



3. CFTR shRNA but not scrambled control reduces CFTR mRNA expression in HMC-1

Having established a stably transfected HMC-1 cell line >96% positive for GFP, we proceeded to assess CFTR mRNA and protein expression levels. Our realtime PCR results show that CFTR mRNA is reduced 4 fold when comparing sham to CFTR shRNA, and when comparing SCR shRNA to CFTR shRNA (3.39 A). However, mRNA levels are unchanged when comparing sham vs SCR shRNA (Figure 3.37 A). SCR shRNA increased CFTR mRNA levels 0.5 fold compared to sham treatment (Figure 3.37 A). PCR products from this experiment were run on a gel to show that only one product was produced in the reaction (Figure 3.37 B black arrow). In lanes containing no template, primer dimers routinely form, and are <100 bp, which is smaller than the products observed in the other lanes (3.37 B). Specificity of the PCR product was also confirmed by melt curve analysis (Figure 3.37 C).

4. CFTR shRNA but not scrambled control reduces CFTR protein expression in HMC-1

When Western blot was performed on transfected HMC-1 cells, we were surprised to find that the CFTR shRNA did not knock down the 167 kDa band as expected, but rather increased the intensity of this band (Figure 3.38 band C). CFTR shRNA also reduced the intensity of two bands at 93 and 86 kDa, which was observed using both MA1-935 and 24-1 antibodies (Figure 3.38 D band B

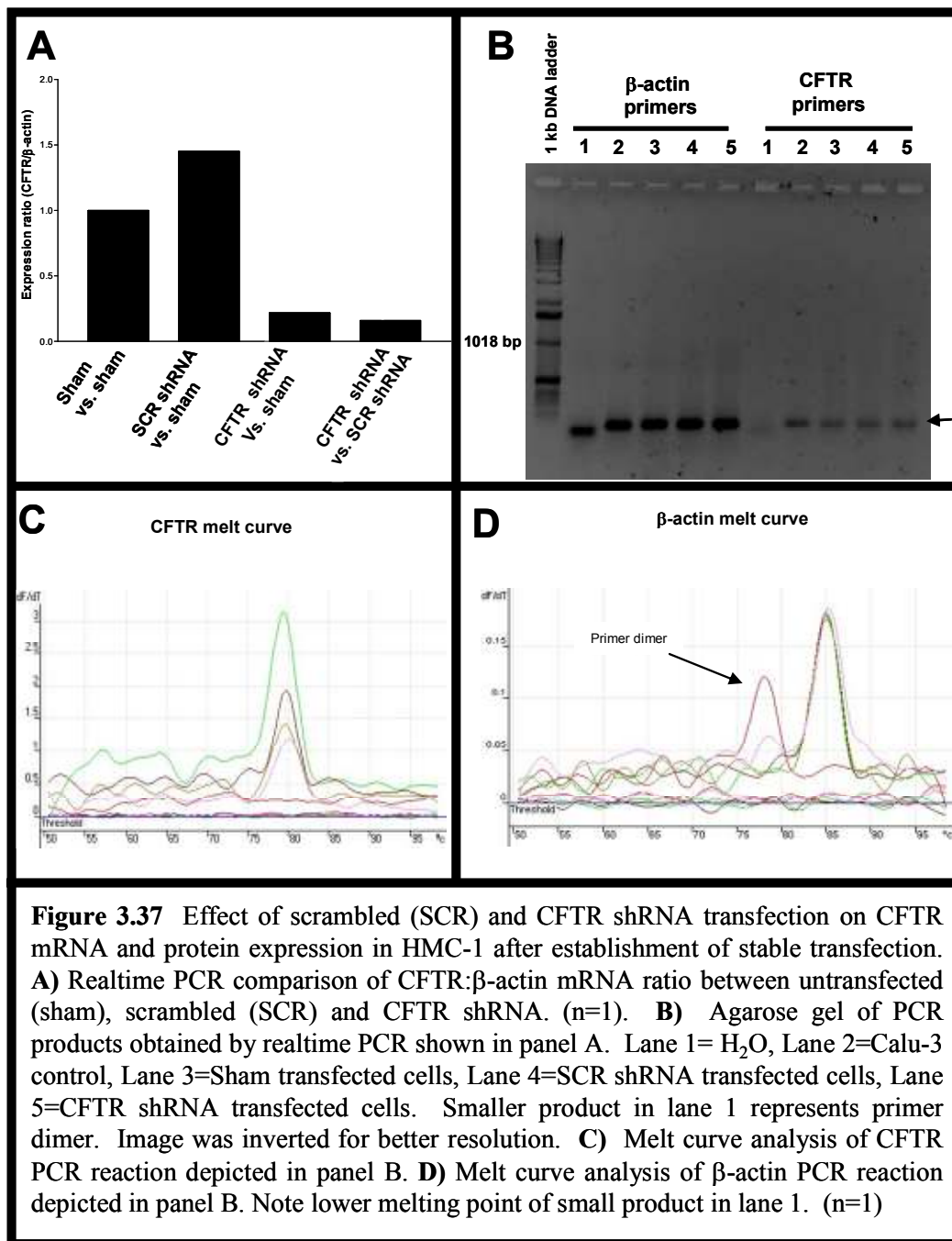
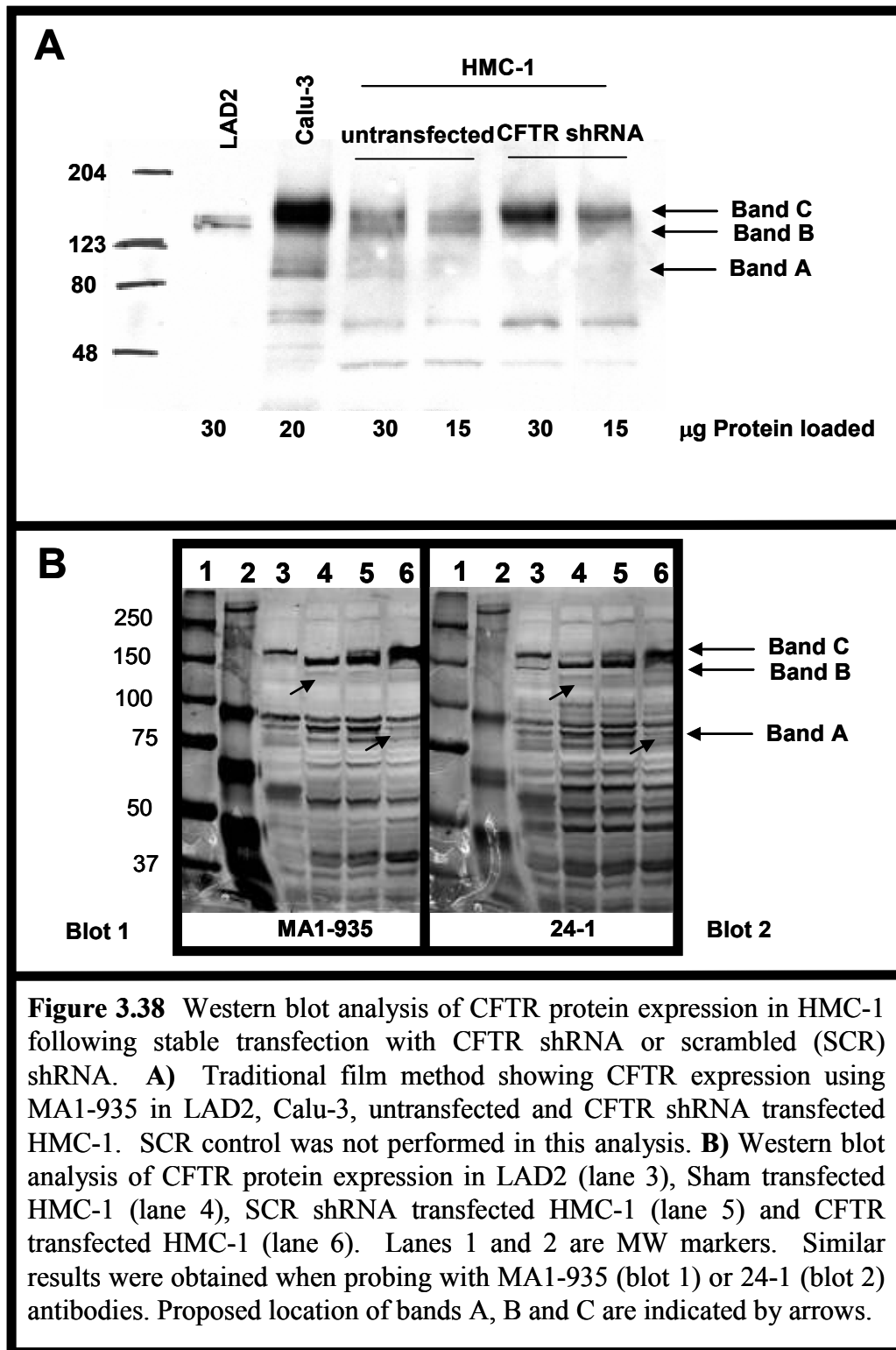


Figure 3.37 Effect of scrambled (SCR) and CFTR shRNA transfection on CFTR mRNA and protein expression in HMC-1 after establishment of stable transfection. **A)** Realtime PCR comparison of CFTR:β-actin mRNA ratio between untransfected (sham), scrambled (SCR) and CFTR shRNA. (n=1). **B)** Agarose gel of PCR products obtained by realtime PCR shown in panel A. Lane 1= H₂O, Lane 2=Calu-3 control, Lane 3=Sham transfected cells, Lane 4=SCR shRNA transfected cells, Lane 5=CFTR shRNA transfected cells. Smaller product in lane 1 represents primer dimer. Image was inverted for better resolution. **C)** Melt curve analysis of CFTR PCR reaction depicted in panel B. **D)** Melt curve analysis of β-actin PCR reaction depicted in panel B. Note lower melting point of small product in lane 1. (n=1)



and A). Furthermore, the doublet expressed at 167 and 145 kDa was shifted from strong lower band and weak upper band in the sham and SCR shRNA treatments, to weak lower band and strong upper band in the CFTR shRNA (Figure 3.38). This result was obtained using both MA1-935 and 24-1 antibodies as well as traditional film and Odyssey IR Western blot methods (Figure 3.38). This data suggests that CFTR is translated as a 90 kDa molecule in HMC-1, maturing to its final MW of 150-170 kDa. In untransfected cells, fully mature CFTR turnover results in little 167 kDa CFTR expression, which seems to be altered in CFTR shRNA HMC-1. Changes in intensity of the bands at 145 and 167 kDa suggests that knockdown of CFTR mRNA may increase stability of mature CFTR, resulting in more protein being expressed at 167 kDa in CFTR shRNA HMC-1. SCR shRNA Western blots also indicate that this stability effect may be partially mediated by transfection and/or by the vector as SCR shRNA cells had more 167 kDa CFTR than sham HMC-1, but less than CFTR shRNA HMC-1 (Figure 3.38). We believe that CFTR antibodies also detect cleaved CFTR fragments, some of which are undetectable using traditional film method, but appear when the more sensitive Odyssey IR imaging system is used. This hypothesis will be discussed in Chapter 4.

Having established that CFTR is knocked down in CFTR shRNA but not SCR transfected cells, we wanted to dissect the localization of the knocked down proteins. Thus, we performed flow cytometry on unpermeabilized HMC-1 using the extracellular epitope antibody MA1-935, to determine if CFTR knockdown resulted in reduction of plasma membrane CFTR (Figure 3.39 A-I).

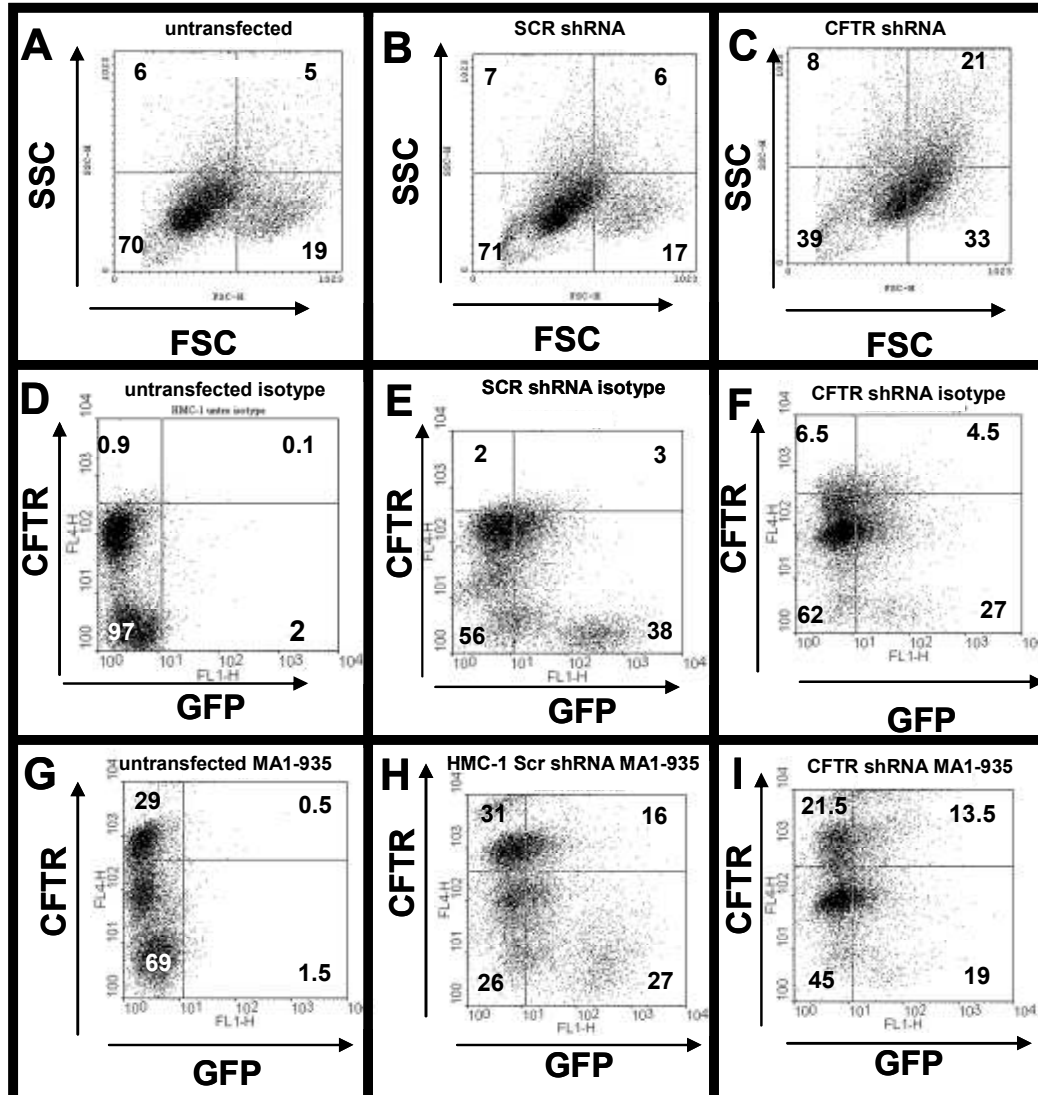


Figure 3.41 Flow cytometric analysis of CFTR expression in unpermeabilized HMC-1 using MA1-935 antibody. **A-C**) Forward (FSC) and side (SSC) scatter analysis of untransfected, scrambled (SCR) and CFTR shRNA transfected cells. **D-F**) Green fluorescent protein (GFP) and MA1-935 isotype control staining of untransfected, SCR and CFTR shRNA transfected cells. **G-I**) GFP and MA1-935 staining for CFTR expression in untransfected, SCR and CFTR shRNA transfected cells. Numbers in quadrants represent % positive cells in that quadrant. (n=1).

Untransfected and SCR shRNA HMC-1 had similar SSC and FSC profiles, whereas we observed that the CFTR shRNA transfected cells displayed an increase in FSC (33% vs 19% and 17% in lower right quadrant), and a slight increase in SSC (29% vs 11% and 13% in upper right quadrant) (Figure 3.39 A – C). Background fluorescence for GFP was set at 1.5% in untransfected cells. SCR shRNA and CFTR shRNA transfected cells were 41% and 31.5% positive for GFP, indicating the presence of the vector in these cells (Figure 3.39 E and F). Background fluorescence using isotype control IgM antibody staining was set as 0.9, 2 and 6.5% in untransfected, SCR shRNA and CFTR shRNA respectively (Figure 3.39 D-F). When cells were stained with MA1-935 CFTR antibody, untransfected and SCR shRNA transfected cells were 29% and 31% positive for CFTR, but CFTR shRNA transfected cells were only 21.5% positive for CFTR (Figure 3.39 G-I). In figure 3.39, quadrants are identical in all panels, but if quadrants were set so that background fluorescence for CFTR was 0 in each treatment, CFTR expression in untransfected, SCR shRNA and CFTR shRNA would actually be 28%, 29% and 15% respectively. This data shows that CFTR shRNA is reducing plasma membrane CFTR expression by approximately 35-50% compared to sham and SCR shRNA treatments. In SCR and CFTR shRNA transfected cells, 16% and 13 % of the cells were double positive for CFTR and GFP respectively. These cells may represent a subpopulation of cells in which the 167 kDa band is present at higher levels than in untransfected controls (see figure 3.39). Another explanation is that since double positive cells (upper right

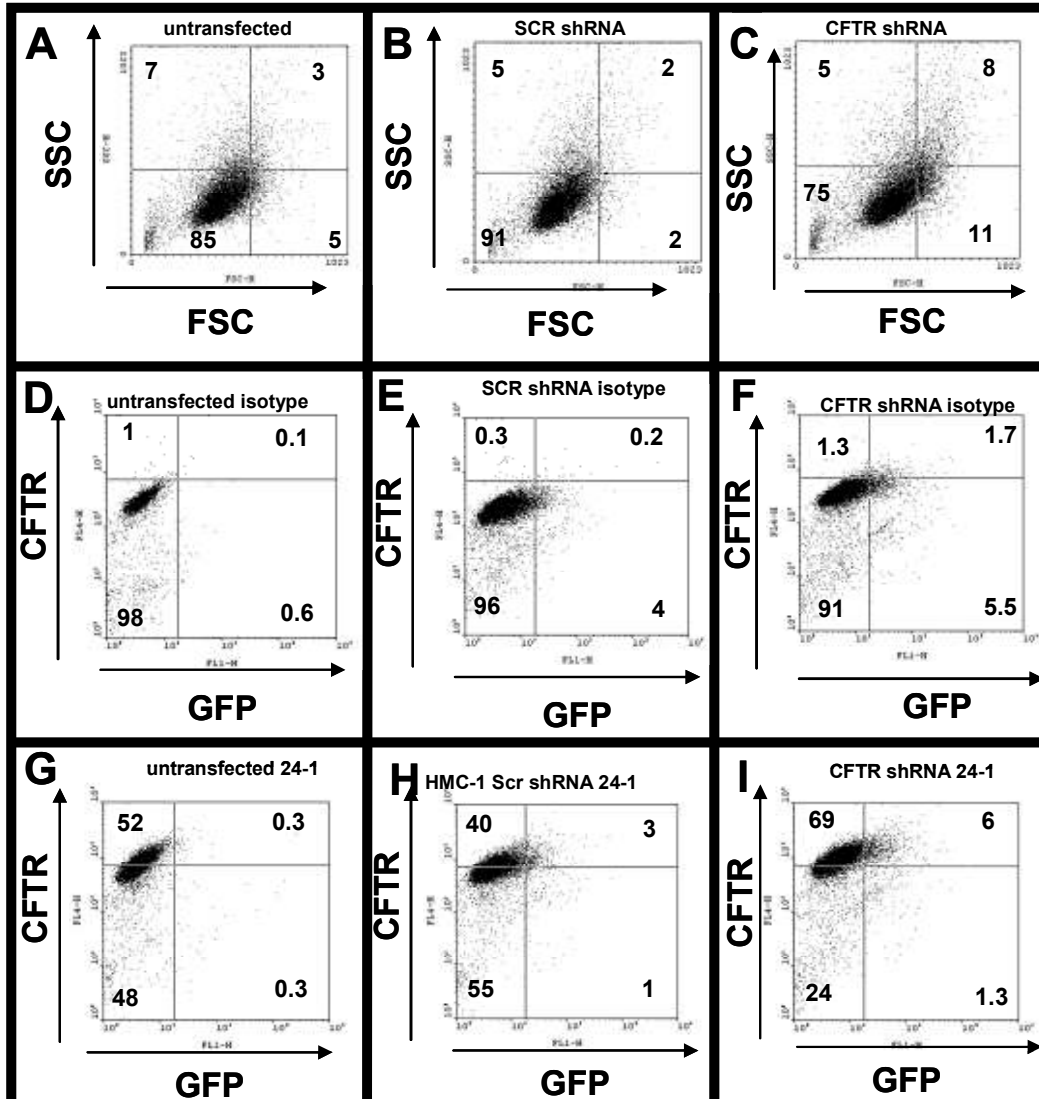
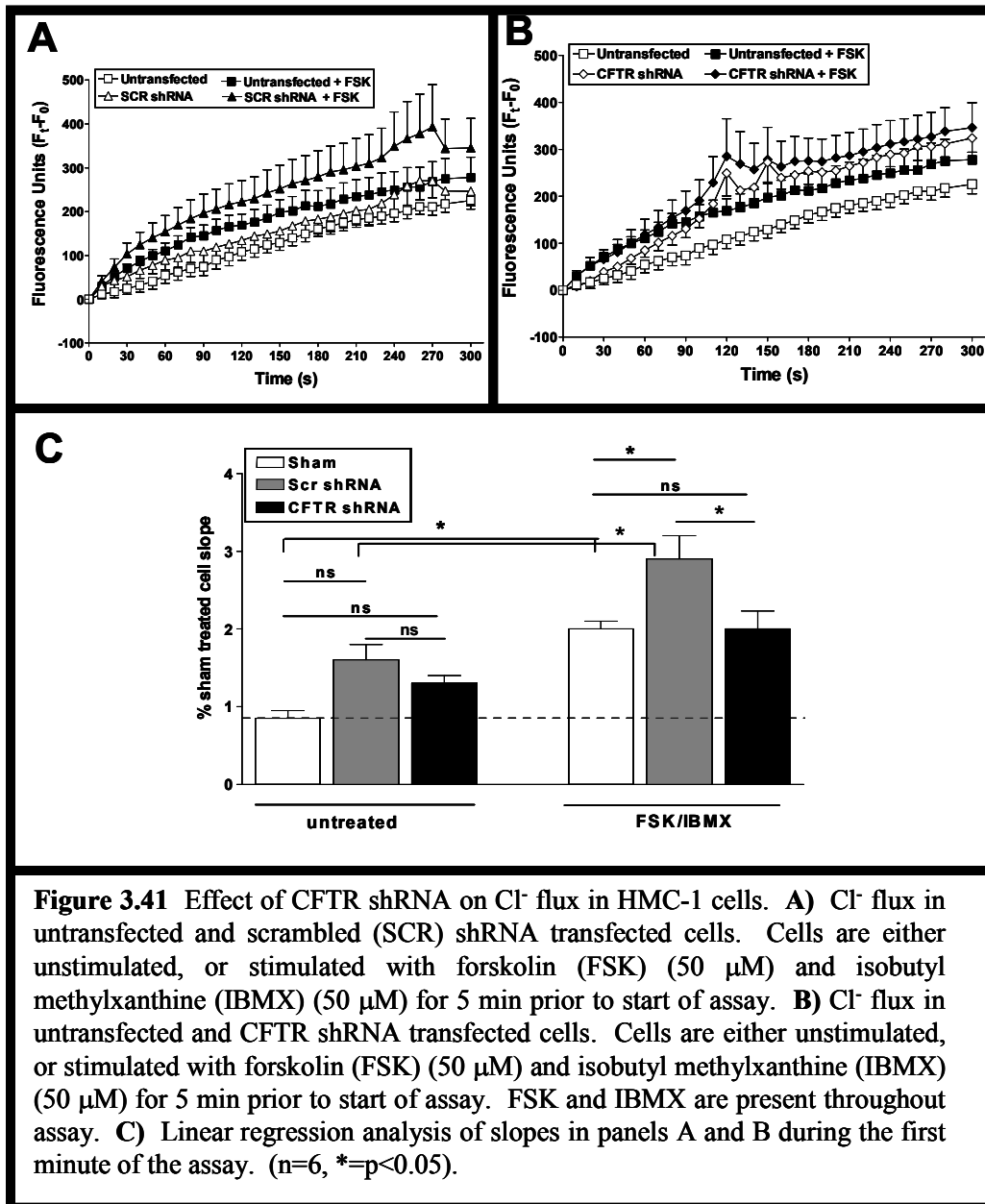


Figure 3.42 Flow cytometric analysis of CFTR expression in permeabilized HMC-1 using 24-1 antibody. **A-C)** Forward (FSC) and side (SSC) scatter analysis of untransfected, scrambled (SCR) and CFTR shRNA transfected cells. **D-F)** Green fluorescent protein (GFP) and 24-1 isotype control staining of untransfected, SCR and CFTR shRNA transfected cells. **G-I)** GFP and 24-1 staining for CFTR expression in untransfected, SCR and CFTR shRNA transfected cells. Numbers in quadrants represent % positive cells in that quadrant. (n=1).

quadrant) were weakly positive for GFP (compared to untransfected GFP), indicating that a small population of CFTR shRNA HMC-1 cells is transfected with a low abundance of vector making them GFP positive, but still capable of producing CFTR. Flow cytometry was also performed on permeabilized HMC-1 using 24-1 antibody to determine if CFTR knockdown resulted in reduction of intracellular CFTR (Figure 3.40 A-I). As observed in MA1-935 experiments, untransfected and SCR shRNA transfected cells had similar SSC and FSC profiles, whereas CFTR shRNA transfected cells displayed an increase in FSC (11% vs 5% and 2% in lower right quadrant), and a slight increase in SSC (8% vs 3% and 2% in upper right quadrant) (Figure 3.40 A – C). This shift in FSC indicates that CFTR shRNA cells are slightly bigger than their untransfected and SCR shRNA transfected counterparts. Background fluorescence for GFP was set at 0.6% in untransfected cells and CFTR background fluorescence was set at between 1 and 1.3 using isotype control IgG_{2a} antibody in the three treatments (Figure 3.40 D-F). GFP signal was low when using 24-1 antibody, but this may be attributed to fixation of the cells as previously described (7). When cells were stained with 24-1 antibody, untransfected and SCR shRNA transfected cells were 52% and 40% positive for CFTR respectively (figure 3.40 G and H). Unexpectedly, CFTR shRNA transfected cells were 69% positive for CFTR when stained with 24-1 antibody (Figure 3.40 I). This data suggests that the CFTR band at 90 kDa and at 145 kDa which are reduced in intensity in figure 3.38 D may be the forms of CFTR expressed at the plasma membrane, whereas the band



at 167 kDa which increases in intensity may be a form of CFTR which is expressed intracellularly. As these two experiments were some of the last experiments performed for this thesis, we only had time to perform the experiment once for each antibody.

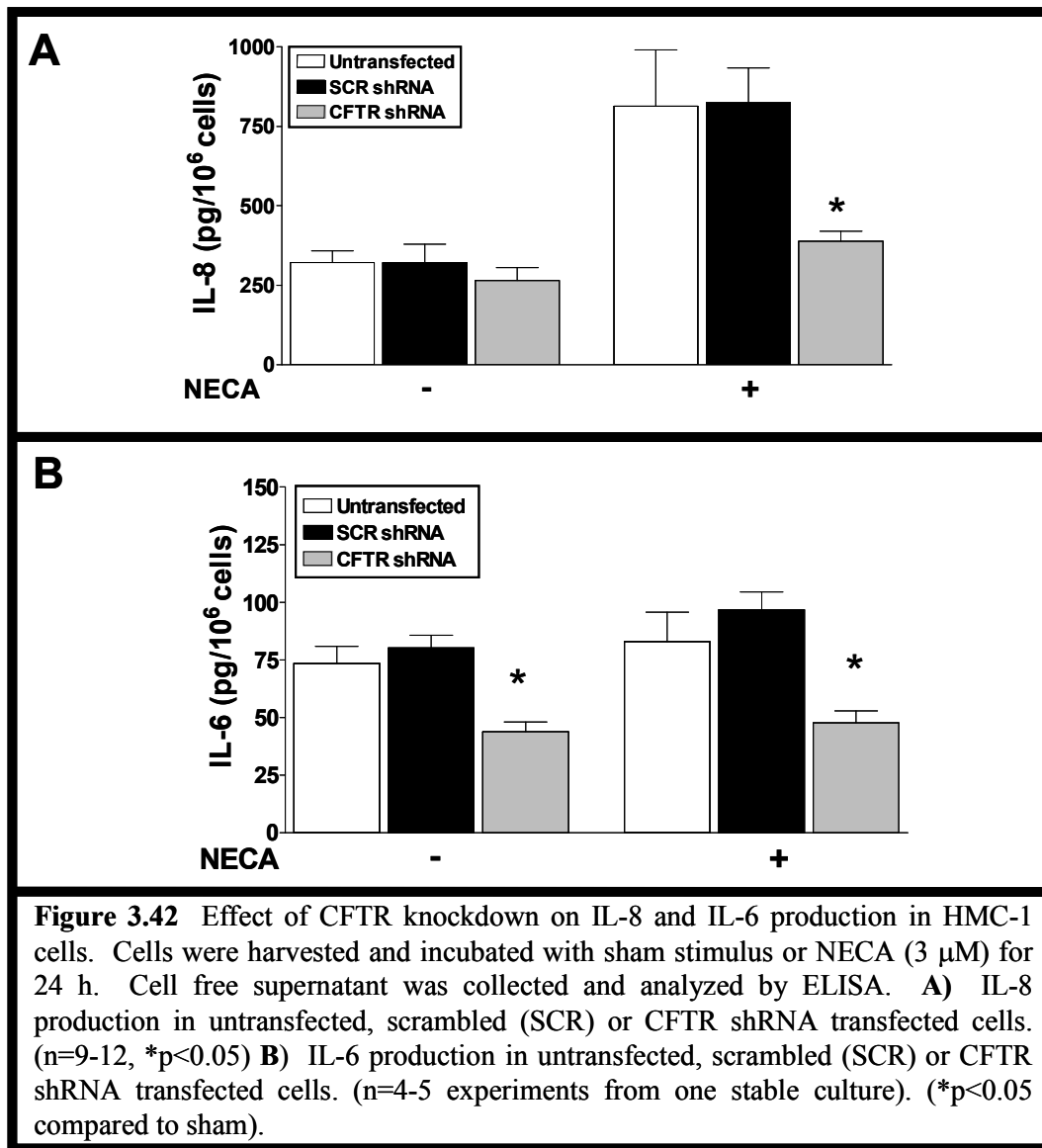
5. CFTR shRNA reduces cAMP-dependent Cl⁻ flux in HMC-1

Knowing that CFTR expression is reduced in CFTR shRNA treated HMC-1, we next examined the effect of CFTR shRNA on Cl⁻ flux in HMC-1 cells. SCR shRNA transfected HMC-1 displayed a basal Cl⁻ flux which was similar to basal Cl⁻ flux in untransfected cells during the entire assay. (Figure 3.41 A). Slopes for sham and SCR shRNA transfected HMC-1 during the 1st min of the assay were not statistically different (0.9 ± 0.13 vs. $1.6 \pm .16$, n=7) (Figure 3.41 C). The unstimulated Cl⁻ flux in CFTR shRNA transfected cells was also not statistically different to that observed in untransfected and SCR shRNA transfected HMC-1, but only during the 1st min of the assay (0.9 ± 0.13 vs. 1.3 ± 0.1 , n=7) (Figure 3.41 B and C). Interestingly, unlike in SCR shRNA transfected cells, unstimulated Cl⁻ flux in CFTR shRNA transfected cells, was significantly increased during the 2nd min of the assay compared to that of untransfected and SCR shRNA transfected HMC-1 (Figure 3.41 A and B). From the beginning of the 3rd min to the end of the assay, the Cl⁻ flux resumed its parallel increase in a similar fashion to untransfected and SCR shRNA transfected cells (Figure 3.41 B). This suggests that absence of CFTR upregulates other Cl⁻ channel function in HMC-1.

When FSK was added to cells, there was a significant increase of $45 \pm 11\%$ and $58 \pm 6\%$ and in Cl^- flux during the 1st min in both untransfected and SCR shRNA transfected HMC-1 respectively, compared to their respective unstimulated counterparts (Figure 3.41 A and C). In contrast, this 1st min increase in FSK-activated Cl^- flux was not significant in CFTR shRNA transfected cells when compared to its unstimulated counterpart (Figure 3.41 B and C). These data strengthen evidence that CFTR is expressed at the plasma membrane and show that CFTR shRNA reduces cAMP-dependent Cl^- flux in HMC-1. Furthermore, this evidence suggests that there may be some dysregulation of Cl^- flux by other channels after the first minute of the assay due to the absence of CFTR in CFTR shRNA transfected cells, as this phenomenon is not present in sham or SCR shRNA cells.

6. CFTR shRNA ablates HMC-1 response to A_{2b}R agonist NECA

Having established that CFTR plays a role in cAMP-dependent Cl^- flux in HMC-1, we wanted to determine whether CFTR also regulates secretion of newly synthesized cytokines in MC. To do this we used our stably transfected HMC-1 cells. When untransfected HMC-1 cells were stimulated with NECA, IL-8 secretion significantly increased from $321 \pm 37 \text{ pg}/10^6$ cells to $813 \pm 176 \text{ pg}/10^6$ cells (Figure 3.42 A). In SCR shRNA transfected cells, IL-8 secretion was similar to that in untransfected cells, going from $320 \pm 58 \text{ pg}/10^6$ cells to $824 \pm 109 \text{ pg}/10^6$ cells following NECA stimulation (Figure 3.42 A). However, in CFTR shRNA transfected cells, response to NECA was not significant, and IL-8



secretion was 264 ± 40 pg/ 10^6 and 388 ± 32 pg/ 10^6 cells in sham and NECA treated cells respectively (Figure 3.42 A). When untransfected, SCR or CFTR shRNA transfected cells were stimulated with NECA, IL-6 secretion was not significantly increased (Figure 3.42 B). Although IL-6 secretion did not seem to be increased by NECA stimulation, basal IL-6 secretion significantly decreased in CFTR shRNA transfected cells compared to untransfected or SCR transfected cells. (43 ± 4 pg/ 10^6 cells vs 73 ± 7 pg/ 10^6 to 83 ± 12 pg/ 10^6 cells respectively) (Figure 3.42 B). This data shows that CFTR is involved in cytokine secretion in HMC-1 in response to NECA, and also suggests that there is some dysregulation of

intracellular signaling pathways involved in cytokine secretion, as basal IL-6 secretion is decreased in response to removal of CFTR.

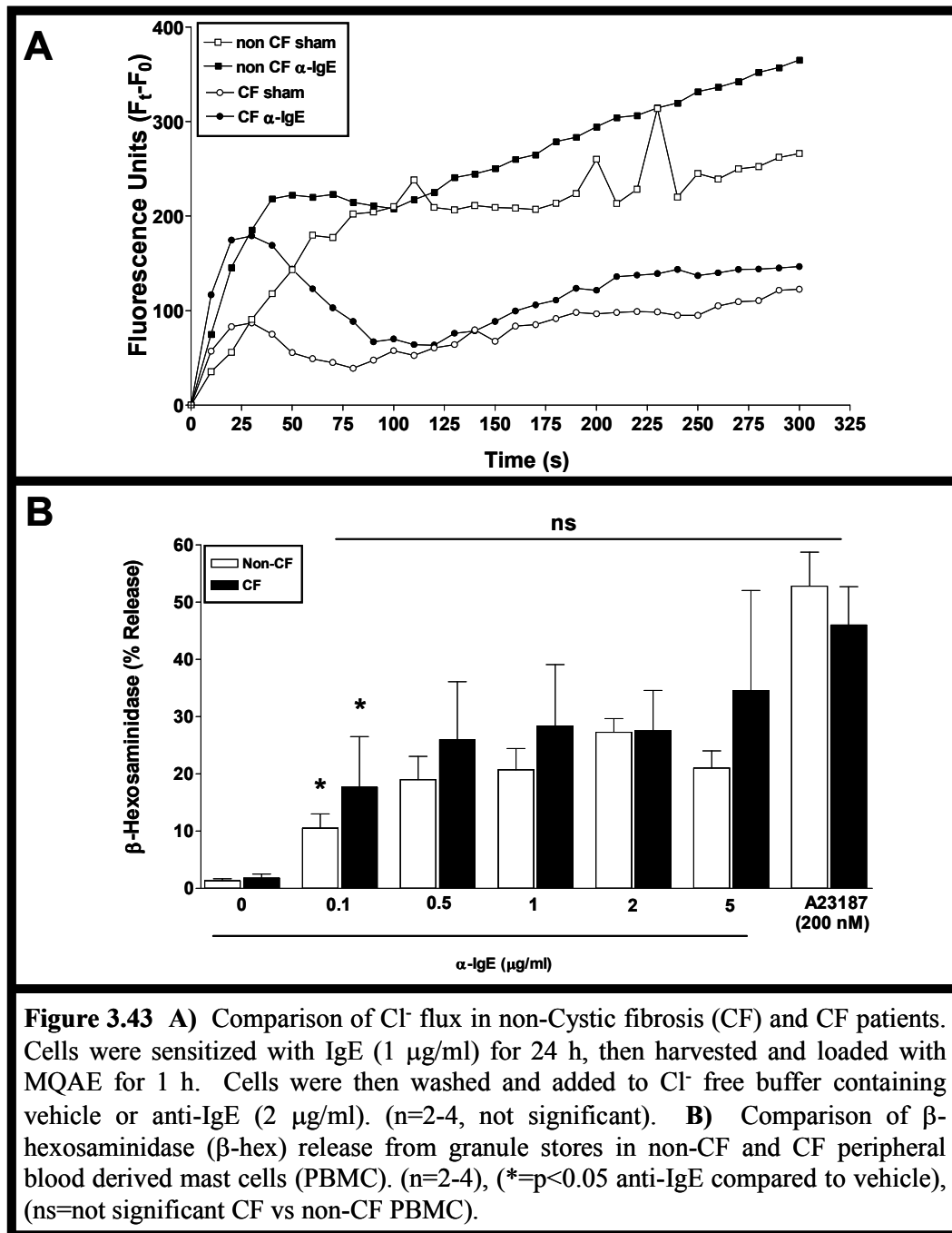
Thus, we have shown that CFTR expression is reduced by CFTR shRNA but not by SCR control. HMC-1 cells lacking CFTR seem to have a dysregulation of cAMP-dependent Cl⁻ flux, as well as a profound dysregulation of IL-8 and IL-6 secretion in response to NECA stimulation. We hypothesize that this loss of NECA response is due to downregulation of A_{2b}R which has been shown to associate with CFTR in EC. These data also suggest that there is a divergence in the CFTR related signalling pathway between IL-8 and IL-6 secretion downstream of NF-κB, as CFTR downregulation had no effect of basal IL-8 secretion, but reduced basal IL-6 secretion. We hypothesize that CFTR is acting at a transcriptional level, or that CFTR is dysregulating secretion of small secretory vesicles carrying IL-6 but not IL-8 in the absence of NECA

stimulation, which could explain this difference as well. These hypotheses remain to be tested and will be discussed further in chapter 4.

J. Comparison of Cystic Fibrosis and non-Cystic Fibrosis peripheral blood derived mast cells

1. CF PBMC may have dysregulated Cl⁻ efflux in response to IgE/anti-IgE stimulation

Having established that CFTR is involved in function of HMC-1, we wanted to examine the role of CFTR in primary MC cultures using peripheral blood CD34⁺ progenitor derived MC from non-CF and CF donors as described in chapter 2. When non-stimulated non-CF PBMC were loaded with MQAE and placed in Cl⁻ free buffer, the slope of Cl⁻ flux during the 1st min was 2.9 ± 0.6 , (n=5). A plateau was reached at 120 s (Figure 3.43 A). When non-CF PBMC were loaded with MQAE and placed in Cl⁻ free buffer containing anti-IgE (2 μ g/ml), the slope of Cl⁻ flux during the first min was significantly increased to 4.6 ± 0.6 ($p > 0.05$, n=3) (Figure 3.43 A). In stimulated non-CF PBMC, Cl⁻ flux reached a plateau at 60s, which lasted for 1 min and then Cl⁻ efflux began to increase again until the end of the assay (Figure 3.43 A). Cl⁻ flux in unstimulated CF PBMC exhibited a slope of 1.5 ± 0.4 (n=2) during the 1st min of the assay (Figure 3.43 A). The plateau of Cl⁻ flux was reached before the end of the 1st min in CF PBMC, and Cl⁻ flux was reversed during the 2nd min, a phenomenon which did not occur in sham treated non-CF PBMC. When CF PBMC were stimulated



with anti-IgE (2 $\mu\text{g/ml}$), increase in Cl^- flux was similar to that seen in anti-IgE-stimulated non-CF PBMC with a slope of 3.4 ± 0.9 ($n=2$). However, the Cl^- flux was reversed during the 2nd min, which did not occur in stimulated non-CF PBMC (Figure 3.43 A). ANOVA analysis of Cl^- flux in non-CF vs. CF PBMC revealed that this effect was not significant. We speculate that this is due to small sample size. These data suggest that CFTR has a role in Cl^- flux in PBMC and that the absence of CFTR in CF PBMC may promote re-uptake of secreted Cl^- by other Cl^- channels, which quenches the fluorescence.

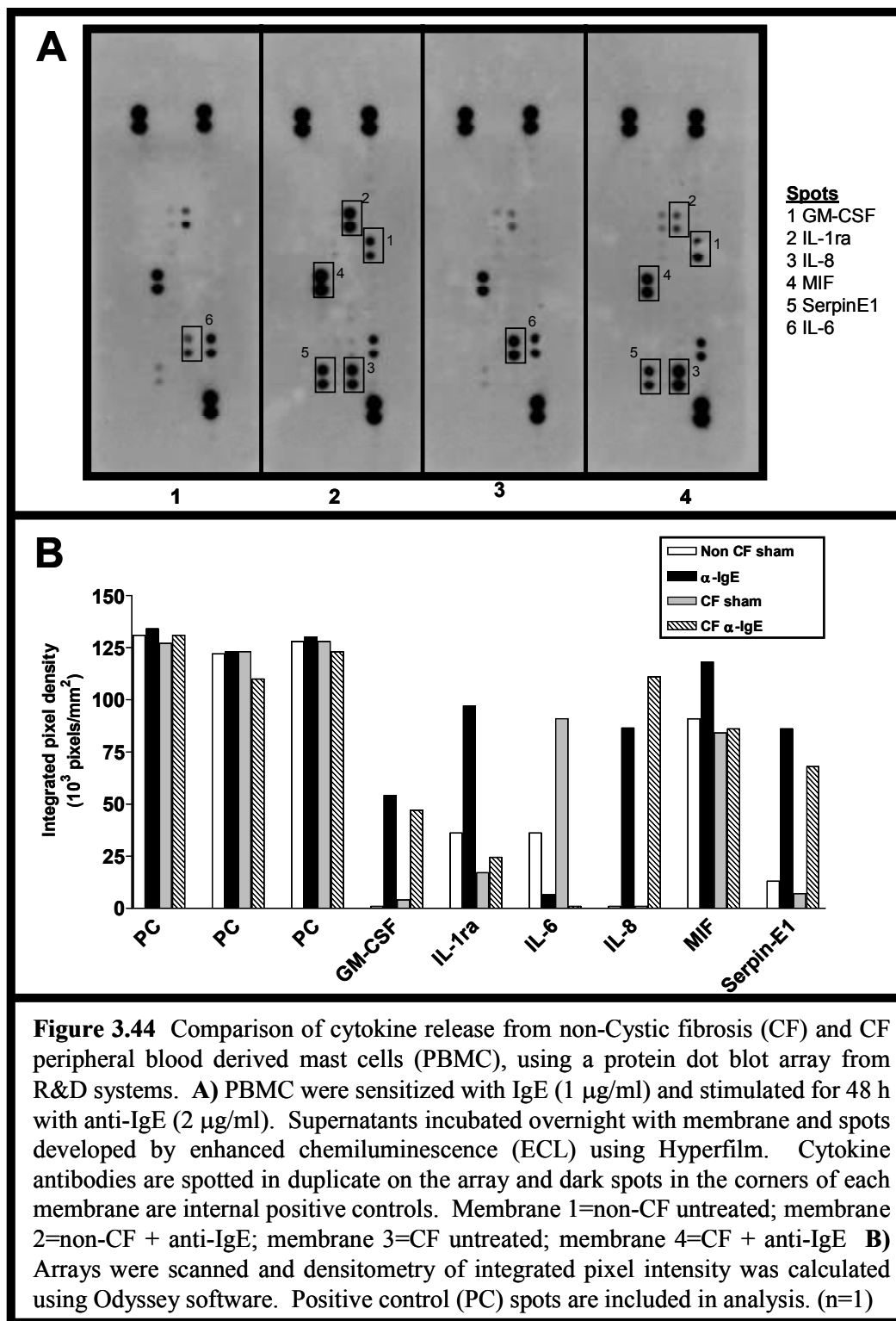
2. β -hex secretion from CF PBMC in response to IgE/anti-IgE stimulation is not affected by absence of plasma membrane CFTR

We next examined the capacity of CF PBMC to release β -hex in response to classical IgE/anti-IgE stimulation in comparison to non-CF PBMC (Figure 3.43 B). Unstimulated non-CF and CF PBMC spontaneously released $1.3 \pm 0.3\%$ and $1.7 \pm 0.7\%$ β -hex respectively (Figure 3.43 B). When stimulated with anti-IgE, non-CF PBMC showed a dose dependent increase in β -hex release from $11 \pm 2\%$, $19 \pm 4\%$, $21 \pm 4\%$, $27 \pm 2\%$, and $21 \pm 3\%$ with 0.1, 0.5, 1, 2 and 5 $\mu\text{g/ml}$ anti-IgE respectively (Figure 3.43 B). In CF PBMC, there was also a dose dependent increase in β -hex release in response to stimulation with anti-IgE going from $18 \pm 9\%$, $26 \pm 10\%$, $28 \pm 19\%$, $27 \pm 7\%$ and $35 \pm 18\%$ in response to 0.1, 0.5, 1, 2 and 5 $\mu\text{g/ml}$ anti-IgE respectively (Figure 3.43 B). The difference in β -hex secretion

between non-CF and CF PBMC was not significant, indicating that CFTR is not involved in release of β -hex from human PBMC (Figure 3.43 B).

3. PBMC from CF and non-CF donors exhibit differences in release of newly synthesized mediators in response to IgE/anti-IgE

The R&D protein array used for LAD2 was also used in non-CF and CF PBMC as an initial semi-quantitative screen to determine which cytokines were secreted by PBMC in response to anti-IgE treatment. This array was used to screen which cytokines are produced by PBMC following IgE/anti-IgE stimulation. The array includes three positive control spots on each membrane which give maximal obtainable signal in a reproducible way (Figure 3.44). This assay can be used to semi-quantify cytokine secretion by performing densitometric analysis of integrated pixel density. R&D Systems does not provide inter-assay variability data for their product, but we found that with proper technique, the array is very reproducible when following manufacturer's instructions. In a similar fashion to multiplex analysis of cytokine secretion, inter-assay variability is dependent on the samples themselves and not on the assay. Cytokines which appeared as a detectable spot on the array were later analyzed by Searchlight multiplex assay only if changes were observed between CF and non-CF PBMC following treatment with anti-IgE. When supernatants from sham treated non-CF and CF PBMC were placed on the array, several potential differences were apparent (Figure 3.44 A). Unstimulated non-CF PBMC appeared to secrete more GM-CSF but less IL-1 α , MIF and SerpinE1 than



unstimulated CF PBMC (Figure 3.44 A). When stimulated with anti-IgE (2 μ g/ml) for 48 h, non-CF PBMC appeared to secrete more GM-CSF, IL-1ra, MIF, and serpinE1, but less IL-6 and IL-8 than CF PBMC (Figure 3.44 B). This data indicates that there are some differences between non-CF and CF PBMC in the production and/or secretion of various cytokines and chemokines.

To validate these observations, three separate experiments for non-CF and three separate experiments for CF PBMC were performed as described in chapter 2 and samples were sent to Searchlight for analysis. By sending both supernatants and cell lysates for analysis, we were able to differentiate between synthesis and secretion of cytokines from PBMC. The data can be found in Appendix 1, Figures 1-9. The results have been tabulated for the reader (Table 3.5), and trends. Although the sample size is low this data suggests that there are several potential differences in both synthesis as well as secretion of several mediators from non-CF and CF PBMC. Basal synthesis of GM-CSF, IL-8, MIF, IL-1ra, IL-1 α , and CCL20 was higher in CF PBMC than in non-CF PBMC.. This data also suggests that CF PBMC also have increased basal secretion GM-CSF, IL-8 and CCL20 compared to basal secretion in non-CF PBMC. Interestingly, although basal synthesis of MIF, IL-1ra and IL-1 α was enhanced in CF PBMC, there were no differences in MIF and IL-1ra secretion. Interestingly, although basal synthesis of IL-1 α was higher in CF PBMC, basal secretion of IL-1 α from CF PBMC was significantly less IL-1 α is secreted from the cells compared to non-CF PBMC. This finding of increased synthesis of IL-1 α correlates with another study showing increased gene transcription of IL-1 α in CF tracheal glands (247).

Table 3.5 Differences in total and secreted cytokine from non-CF and CF PBMC in unstimulated and IgE/anti-IgE-stimulated cells

Cytokine	Unstimulated				IgE/anti-IgE			
	Total protein		% secretion		Total protein		% secretion	
	Non-CF	CF	Non-CF	CF	Non-CF	CF	Non-CF	CF
GM-CSF	-	+	+	++	+++	++	+++	+++
IL-8	-	+	+	++	+++	++	+++	+++
IL-6	+++	+++	+++	+++	+	-	+	-
MIF	+	++	+	+	+	++	+	++
IL-1ra	++	+++	+	+	++	++	+	++
PAI-1	++	+	+	++	+	+	+	+
IL-1 α	+	++*	++	++*	+	++	++	++
CCL4	+	+	++	++	++	++	++	++
CCL20	+	++	++	+++	+	++	++	++

* = p<0.05

Magnitude of response:

- = none
+ = low
++ = medium
+++ = high

This data, although not statistically significant due to small sample size, with the exception of IL-1 α secretion, suggests that there are some profound differences between CF and non-CF PBMC cytokine synthesis and ability to secrete these cytokines. These may be linked to CFTR protein interactions which may alter intracellular vesicle trafficking from the Golgi to the plasma membrane.

When CF and non-CF PBMC were stimulated with anti-IgE at various doses, there was a trend towards increased synthesis of GM-CSF, MIF, IL-1 α , CCL4 and CCL20 from non-CF PBMC compared to CF PBMC (Table 3.5). CF PBMC secreted more MIF and IL-1ra than non-CF PBMC. In contrast to our array data, the searchlight analysis suggests that anti-IgE-stimulated non-CF PBMC synthesize more IL-8, but no differences were observed in secretion. Interestingly, synthesis of SerpinE1 was lower in CF than in non-CF PBMC, but more SerpinE1 was released from the cells by CF-PBMC. Although not statistically significant due to small sample size, these trends show that non-CF and CF PBMC differentially synthesize and secrete cytokines and chemokines, which could contribute to inflammatory cytokine imbalance in CF lungs. Increasing sample size will be important before we can reach conclusions about the role of CFTR in cytokine synthesis and secretion from PBMC.

4. PBMC from CF and non-CF donors exhibit differences in release of newly synthesized mediators in response to *Pseudomonas aeruginosa*

In an attempt to discern between allergic and innate immune responses of MC we examined the response of non-CF and CF PBMC to innate immune stimulation by *P. aeruginosa* (PAO1) bacteria. The data for these experiments

can be found in Appendix 1, Figures 10-18, and the data has been tabulated for the reader (Table 3.6). When PBMC were exposed to killed PAO1 for 24 h, there was a trend toward increased synthesis of GM-CSF, IL-8, IL-6, MIF, IL-1ra, IL-1 α , CCL4 and CCL20 in CF PBMC compared to non-CF PBMC. Although synthesis of these cytokines was increased in CF PBMC, only GM-CSF, IL-1 α and CCL4 showed increased secretion from the cells. Also, there appeared to be no difference in the synthesis of PAI-1 between the two genotypes, but secretion of PAI-1 seemed to be increased in CF PBMC. These data suggest that PBMC are involved in response to bacterial invasion, and that this response may be dysregulated in CF and that CFTR deficiency may lead to an inappropriate preprogrammed microbial response signature as has been shown previously (247). However, sample size will need to be increased to confirm these findings statistically.

5. Absence of plasma membrane CFTR does not change LTC₄ and PGD₂ secretion in PBMC

Constitutive secretion of PGD₂ in CF PBMC was not detectable (Figure 3.45 A). When non-CF cells were stimulated with anti-IgE at 0.1, 0.5, 1, 5 and 10 μ g/ml respectively, there was a dose dependent increase in PGD₂ production which was not statistically different than that observed when CF PBMC were stimulated with the same doses of anti-IgE (Figure 3.45 A).

Constitutive secretion of LTC₄ in both non-CF and CF PBMC was not detectable (Figure 3.45 B). When non-CF cells were stimulated with anti-IgE, at 0.1, 0.5, 1, 2 and 10 μ g/ml, there was a dose dependent increase in LTC₄

Table 3.6 Differences in total and secreted cytokine from non-CF and CF PBMC in *P. aeruginosa*-stimulated cells

Cytokine	Total Protein		% Secretion	
	Non-CF	CF	Non-CF	CF
GM-CSF	+	++	++	++
IL-8	+	++	++	++
IL-6	+	++	++	++
MIF	+++	+++	+	+
IL-1ra	+	++	+	+
PAI-1	+	+	+	++
IL-1α	+	+++*	+	++
CCL4	-	+	+	+
CCL20	+	+++*	+	+

* = p<0.05

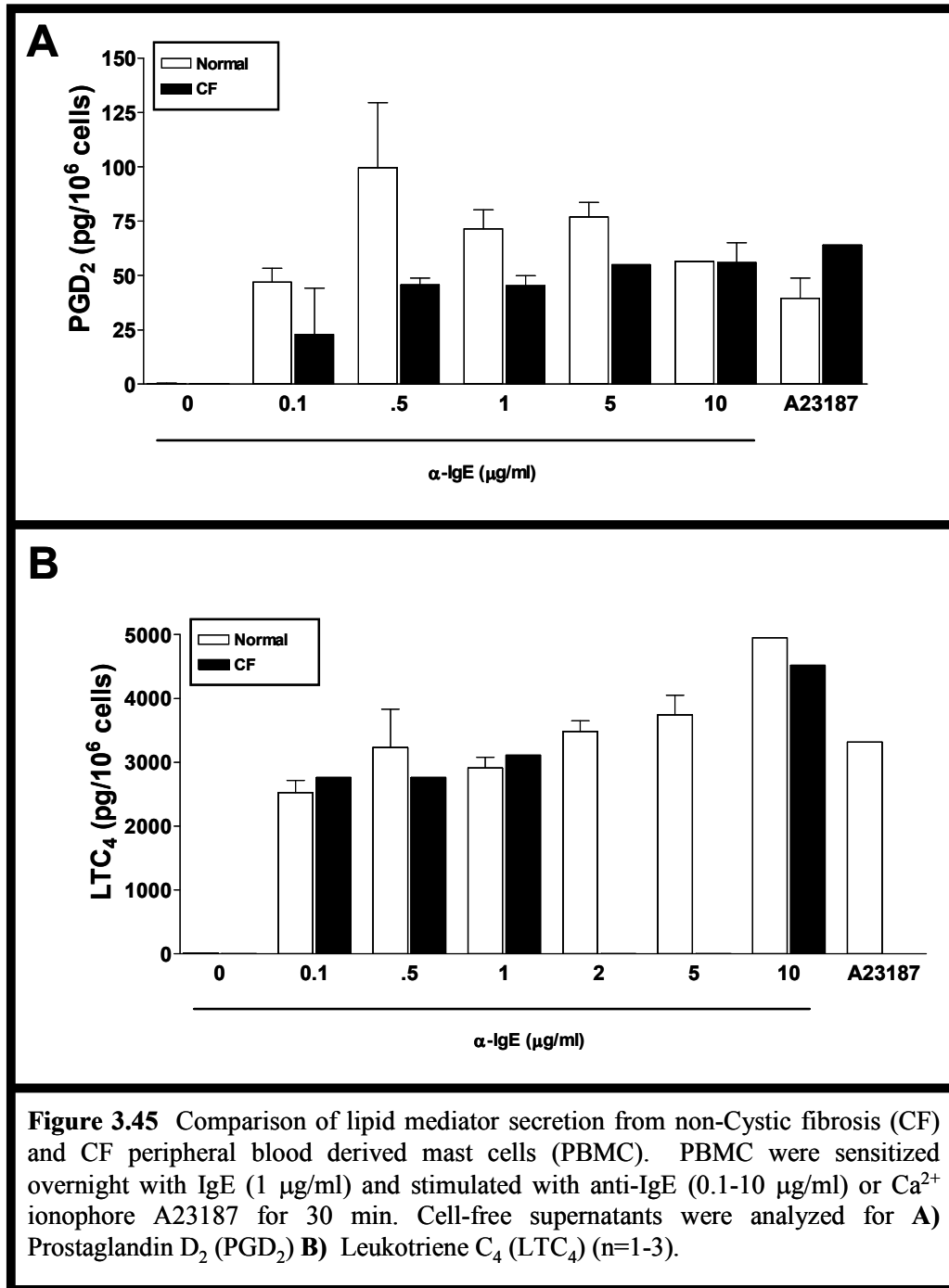
Magnitude of response:

- = none
+ = low
++ = medium
+++ = high

production which was not statistically different than that observed in CF PBMC stimulated with the same doses of anti-IgE. Although we have limited data due to small sample size, this data correlates with pharmacological inhibition of CFTR data in LAD2 (Figure 3.23 D) and suggests that absence or dysfunction of CFTR does not affect LTC₄ secretion from PBMC.

6. Summary

The data presented above suggests that the lack of CFTR at the plasma membrane in PBMC causes a dysregulation of both basal secretion, and also of the preprogrammed response to stimuli such as IgE/anti-IgE or *P. aeruginosa*. If one examines the CF literature, many of the same mediators shown to be dysregulated in CF PBMC are also dysregulated in CF EC. Thus, it would appear that CFTR regulates intracellular signalling pathways common to many of these



cytokines, but may also regulate their transport in small secretory vesicles once they are synthesized, which could explain the difference in basal secretion of many of these cytokines.

Chapter 4. Discussion and future directions

Since its discovery in 1989, CFTR has been extensively studied, and although some therapeutic advances have been made, we still do not fully understand its full functional responsibilities. There have been thousands of studies examining CFTR in EC, but only a handful of studies have examined the role of CFTR in other cell types. To compound the problem, the research community does not appreciate the full picture of CF and most CF reviews, although excellent, fail to acknowledge the role of many of these cells in the pathophysiology of CF, including MC (14, 200, 315, 316). Evidence about CFTR function in other cell types is beginning to emerge and be appreciated. Presently, most people do not think of MC in the context of CF because they are thought of primarily as cells involved in allergy. However, recent evidence shows that MC are critical innate immune cells, and can be key players in orchestrating the response to invading pathogens. In this thesis, I have attempted to address some of these gaps in our knowledge by examining the expression and functional significance of CFTR in human MC. This has been a challenging undertaking due to the low expression of CFTR in MC, together with the challenges associated with obtaining and maintaining human MC cell lines and primary cultures, and the painstaking process of optimization of CFTR RNA interference and pharmacological inhibition of CFTR in MC.

I have shown that the MW profile of CFTR is different in MC than it is in EC. These results, taken together with our previous work on CFTR regulation by IFN γ suggest that glycosylation may be different in MC, which could lead to trafficking and localization differences in CFTR between two cell types. These

differences could in turn lead to different functional roles for CFTR between MC and EC. The results show that CFTR regulates both Cl^- flux as well as mediator secretion in MC. Upon pharmacological inhibition or knockdown of CFTR, there is a disturbance of normal Cl^- flux through MC, which appears to involve both CFTR channel function, as well as regulation of other Cl^- channels. We have shown that the role of CFTR in MC mediator secretion does not apply to all mediators, but rather is stimulus and secretory compartment-specific. Pharmacological inhibition of CFTR in LAD2 cells, or absence of plasma membrane CFTR in CF PBMC does not affect β -hex release, suggesting that Cl^- flux through CFTR does not significantly influence secretion of mediators stored in granules, a process that involves hyperpolarization and Ca^{2+} entry. Initially, this was surprising because our previous work showed that β -hex release from rat PMC was inhibited by DPC, and that PMC appeared to express CFTR on their granules (Appendix 2) (107). These findings will be discussed further below.

Although inhibition or removal of CFTR does not affect release of stored mediators from human MC, it has a significant inhibitory effect on the release of certain newly synthesized cytokines and chemokines, but not on the release of lipid mediators LTC_4 and PGD_2 in response to the classical IgE/anti-IgE stimulus. CFTR may also be a key regulator of innate immune stimulation in MC, as differences appear to exist in non-CF and CF responses to *P. aeruginosa* stimulation. This would suggest that MC contribute to the pathophysiology of CF, and warrant further investigation for their role in this disease. These findings will be discussed in the sections that follow.

A. Characterization of CFTR expression in MC

1. CFTR mRNA expression in human mast cells

In our previous work, we showed that rat and human MC express CFTR mRNA (107, 201). In these experiments, we showed by regular RT-PCR that rat MC express CFTR mRNA, but human MC were not analyzed in this study. We wanted to identify CFTR transcripts in human PBMC by RT-PCR so we used human CFTR primers previously described (292). We optimized temperature and $MgCl_2$ concentration and detected CFTR expression in Calu-3, HMC-1 and LAD2 cells in our system. CFTR mRNA is present in MC lines in low abundance, which correlates with previous findings of low abundance CFTR mRNA (194, 195, 211, 212). We only had enough cells to perform one RNA extraction in PMBC. Nested RT-PCR results suggest that CFTR transcripts were not present at detectable levels in PBMC. As CFTR mRNA is expressed at low levels in MC degradation during the RNA extraction or DNase digestion phase may be a problem. Another possible explanation for our inability to detect CFTR mRNA in PBMC is that CFTR mRNA expression may be cyclical, and was not expressed at the time of cell lysis (317). Lack of mRNA does not always imply lack of protein, and these findings do not indicate that MC do not express CFTR protein. When more cells become available, these experiments should be repeated with RNA isolation at various time points during 8 wk culture of the

cells, to see if CFTR mRNA can be detected and might be regulated by MC maturation and culture conditions.

2. CFTR protein expression in human mast cells

The MW of the three reported forms of CFTR (bands A, B and C) is an issue under contention and varies widely in the literature. ProtParam ExPASy tools online reports fully mature CFTR (band C) as having a MW of 168 kDa based on the amino acid sequence and similarly, another study suggests that MW of fully mature CFTR is 160 kDa (149). Others have reported fully glycosylated CFTR to have a molecular mass of 180–200 kDa and others suggest a MW of 170 kDa for band C (160, 318). This sets the range for fully mature CFTR at anywhere between 160-200 kDa. Band B also has a wide reported MW range of 130-150 kDa, but the reported MW of band A is not as variable, and has been reported between 127-130 kDa (148, 152, 154-156). These discrepancies can be explained by variation in Western blotting protocols for CFTR. Most of these studies used gradient or non-gradient gels at different percentages, running buffers and MW standards, which can all have an impact on the reported MW of proteins. MW markers have different migration patterns in Tris-Glycine and Tris-HCl, and companies usually report MW in only one buffer and only 1 gel density. This complicates CFTR MW comparison between studies, and introduces significant variation in the literature. We carefully standardized our protocols and compared CFTR expression in MC and EC.

Our experiments confirmed that Calu-3 cells express CFTR in easily detectable levels. Both 24-1 and MA1-935 antibodies detected CFTR. Since these monoclonal antibodies recognize distinct epitopes of CFTR, detection by both antibodies reduces the possibility of nonspecific binding. CFTR in Calu-3 cells appeared as a distinct “doublet” pattern near 170 kDa with the higher band being 172 ± 3 kDa and the lower band 162 ± 3 kDa. This pattern was observed repeatedly with an average of 10 kDa separation between the two bands. This closely spaced doublet is consistent with bands C and B respectively, which have been reported near those MW ranges.

The characteristics of CFTR were different in MC than in EC when studied by Western blot. In both HMC-1 and LAD2 cells, CFTR expression was similar to that in Calu-3 cells, but the doublet bands reproducibly migrated at slightly different MW when run on the same gels (Figure 3.17). We routinely detected bands at 167 ± 6 and 145 ± 2 kDa, which is slightly below the reported MW range of bands C and B respectively in EC. In one gel, we saw the appearance of an additional band at 140 kDa, which is slightly higher than the reported MW of band A. LAD2 cells showed significant differences in the characteristics of CFTR compared to EC. In LAD2 cells, CFTR appeared as either a doublet at 159 ± 3 and 145 ± 2 kDa, or a single band at 155 ± 4 kDa. The upper band of the LAD2 doublet is consistently of equivalent MW to the lower band of the Calu-3 doublet when run on the same gel (Figure 3.17). When only a single band appeared, it was associated with reduced protein loading (≥ 30 μ g) as longer exposure time makes the LAD2 doublet appear, but obscures the Calu-3

doublet by overexposure (Figure 3.17). In rat PMC, we detected a single band at 137 ± 5 kDa, which is near the reported MW of band B. As MC populations can be heterogeneous, these differences in CFTR maturity in different MC may be associated with MC phenotype and expression or activity of glycosylation enzymes, which may change CFTR maturation and/or trafficking patterns. If this is true, then CFTR expression and maturation may be linked to cell maturation. This suggests that full glycosylation from band B to band C in more mature MC such as LAD2 and PMC does not occur, because of glycosylation pathway differences. Glycosylation differences for CFTR in different cell types have been previously reported (149). Also, because CFTR expression is lower in LAD2 and PMC relative to total protein in comparison to EC, it is also possible that band B glycosylation to band C occurs below detectable limits by Western blotting. Also, several atypical CFTR bands were detected by 24-1 and MA1-935 in our Western blots and will be discussed in a later section.

3. Atypical CFTR bands

It is interesting to note that all four cell types tested (Calu-3, LAD-2, HMC-1 and PMC) expressed other bands that were reactive for both monoclonal antibodies, but not isotype control antibody. These bands have not been routinely reported nor well characterized in the literature, although in the rare studies that show full gels for CFTR, some atypical CFTR bands are shown. For the purpose of this thesis, we named the two most reproducible atypical bands, band “D” and “E”. Band D occurred at MW of 94 ± 2 , 97 ± 6 and 85 ± 4 kDa in Calu-3, HMC-

1, LAD2 respectively, but did not occur in PMC. Band E occurred at a MW of 81 ± 2 , 77 ± 5 , 68 ± 4 , and 82 ± 4 kDa in Calu-3, HMC-1, LAD2 and PMC respectively. Since band A (unglycosylated CFTR) is reported as being 120-130 kDa, it is unlikely that bands D or E are analogous to band A. One possibility is that these bands represent proteolytically degraded fragments of CFTR. More recently, when we probed for CFTR using the more sensitive Odyssey IR imager, we detected more bands than when we used the traditional film method for Western blots. The fact that bands D and E were detected by both antibodies, but not by isotype control antibodies helps rule out the possibility that they are the result of non-specific binding. It is interesting to note that most reports on CFTR which use Western blotting, show only fragments of gels, usually cutting off what falls below 100 kDa or what is not of “interest” for their purposes. It has been reported in other cell types such as kidney cells, that CFTR exists not only in its full length form, but also as a truncated splice variant named TNF-CFTR. This altered form of CFTR is reported as a functional half CFTR molecule with a MW of 75-80 kDa (319, 320). TNF-CFTR is localized to endosomes and the functional role of TNF-CFTR has not been fully determined. It has also been reported that a truncated form of CFTR without exon 5 is present in cardiac tissue (156). This splice variant of CFTR has a 30 amino acid deletion in the first extracellular loop, and is expressed only as a core glycosylated form at 140 kDa (156). This exon 5 splice variant has lower conductance than wild type CFTR and was localized to intracellular membranes. Other functional roles of this splice variant are unknown. Our LAD2 Western blot data shows that a band at

approximately 140 kDa appears in MC when 24-1 is used, but not MA1-935 (figure 3.18 and 3.38 B lane 3). Since MA1-935, but not 24-1 binds to the first extracellular loop of CFTR, this suggests that the exon 5 splice variant is present in MC. This hypothesis does not preclude expression of differentially glycosylated wild type CFTR in MC. Furthermore, it is also possible that TNF-CFTR is expressed in MC as a band appears at 80-90 kDa, which is the reported MW of TNF-CFTR (153, 321). However, these hypotheses remain to be investigated.

One possible explanation for the number of bands we detect in our Western blots may lie in proteolytic cleavage of CFTR at proline-glutamic acid-serine-threonine (PEST) recognition motifs that act as proteolytic cleavage signals (322). It has been reported that there are at least 5 PEST sequences in CFTR (195, 323). However, when we ran the CFTR amino acid sequence through the PEST-FIND program (322), as many as 18 potential PEST sequences were returned by the algorithm (figure 4.1). The major PEST sequence between amino acid 716 and 733 would result in cleavage of CFTR into two roughly equal halves with MW at around 80 kDa (Figure 4.1). Other cleavage sites could potentially lead to peptide fragments of as little as 241 and 178 amino acids that could still be detected by MA1-935 and 24-1 respectively (Figure 4.1 arrows). These peptide fragments are roughly 12-16% of the total amino acid content and which would equate to a MW of approximately 20-27 kDa based on amino acid content. Differential regulation of PEST sequences by glycosylation or metabolic pathways may occur in various cell types, or under various activation states,

which may explain the multiple bands observed within as well as between cell types in our Western blot experiments (323). If the other atypical bands we detected using the Odyssey IR method or Western blotting are actually fragments of CFTR, what proteases are responsible for the cleavage? What regulates this degradation? Do these peptides have any function(s)? These are all interesting questions that require further investigation to answer. Interestingly, calpain is speculated to be one of the proteases responsible for PEST sequence degradation (324). We have previously shown that calpain activity is downregulated by IFN γ treatment in MC in a nitric oxide-dependent way (325). Thus, inhibition of calpain may be a mechanism by which IFN γ upregulates CFTR expression in MC. This hypothesis remains to be tested. It would also be informative to isolate protein from these bands by two-dimensional gel electrophoresis and sequence them to determine their nature. We were unable to determine the precise intracellular locations of CFTR in MC. Reliable detection of CFTR often requires experimental overexpression (266). We showed that rat PMC and PBMC from non-CF donors express CFTR on the plasma membrane. Moreover, much of the CFTR signal is intracellular in rat and human MC. There are interesting differences in MW and banding pattern of CFTR between

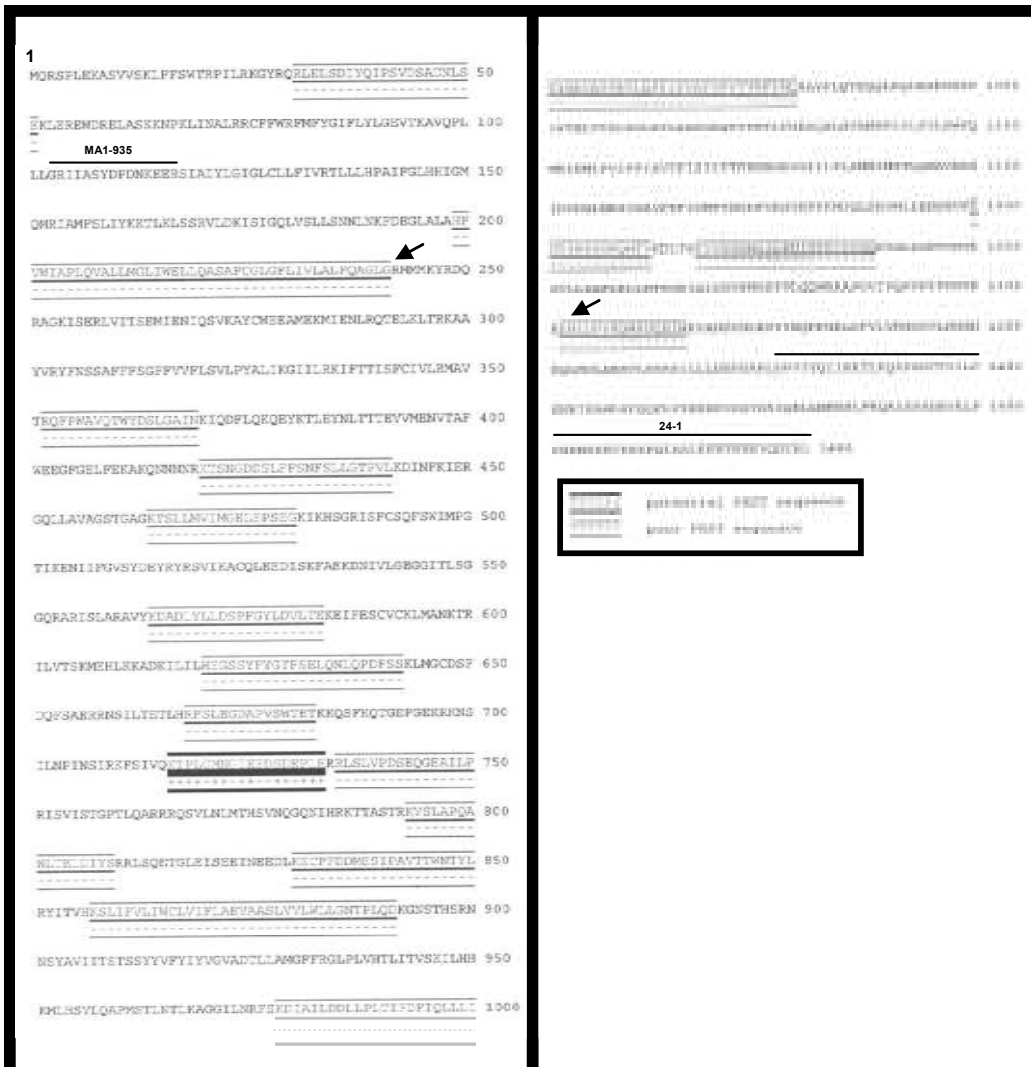


Figure 4.1 Potential proline-glutamic acid-serine-threonine (PEST) sequences in CFTR protein sequence. Dark PEST sequence, if active in mast cells (MC), could result in two equal halves of CFTR with molecular weight (MW) of approximately 80 kDa. Included are the actual amino acid binding sites for MA1-935 (103-117) and 24-1 (1377-1480). Black arrows represent smallest possible CFTR fragments that could be recognized by MA1-935 and 24-1.

MA1-935 and 24-1 antibodies, suggesting that at least some of the CFTR expressed in MC may be alternately spliced as previously reported (156). Although these results do not offer a clear picture of the differences in CFTR localization, processing, and trafficking between MC and EC, they do provide evidence that these processes vary among cells and represent novel information about CFTR in MC. Hopefully, further characterization of the glycosylation state, alternate splicing and localization of CFTR in MC can further elucidate the role of CFTR in MC. By understanding the differences in CFTR localization and processing pathways between these cell types we hope to gain further understanding of the basis of the pathophysiology of CF associated with a large spectrum of mutations in CFTR.

4. CFTR subcellular localization in rat peritoneal mast cells

To further explore subcellular localization of CFTR expression in MC, we studied *in vivo*-derived rat PMC as we had evidence that CFTR was associated with granules in these cells (Appendix 2). CFTR was found in PMC using both 24-1 and MA1-935 monoclonal antibodies. PMC display a single band for CFTR that has an average weight of 137 kDa. This band is 22 kDa smaller than the upper band and 8 kDa smaller than the lower band of the LAD2 doublet. The size differences observed between CFTR in MC and EC suggest that there could be different processing pathways, different localization in the cells, as well as different function(s) of CFTR.

When PMC were fractionated into granule, organelles and membranes (high speed pellet) and cytosol (high speed supernatant), CFTR was found in the

high-speed fraction pellet in only one experiment at a MW of 139 kDa (Figure 3.19), and was not found in the cytosolic fraction. Whole PMC lysate ran on the same gel expressed the same band. Controls were run to characterize the localization of plasma membrane and MC granule in the fractions. We used rat MCP-5 as a marker for granules (23). Rat MCP-5 localized to the granule fraction in a band corresponding to 25 kDa. We used c-Kit as a marker for MC membranes. This protein, a membrane bound MC cell growth factor receptor was found in the whole PMC and PMC high-speed fraction pellet, indicating that there is little membrane contamination in the cytosolic fraction (high speed fraction supernatant). The c-Kit signal appeared as a doublet of 145 kDa and 165 kDa (figure 3.19 C) in the high-speed fraction pellet, which is likely to contain plasma membrane proteins, as well as other membrane bound organelles such as the endoplasmic reticulum, Golgi, microsomes, and other small vesicles. Localizing CFTR to this fraction provides at least three possibilities for the subcellular location of CFTR. The first is that CFTR localizes to MC plasma membrane. This conclusion is consistent with CFTR localization in EC. This possibility does not contrast our initial confocal-microscopy based hypothesis suggesting vesicular/granular localization, as plasma membrane integrity was lost in this study due to fixation protocol (Appendix 2). The next possibility is that CFTR is present in MC in the ER/Golgi pathway and is localized to these organelles. Although it is likely that MC CFTR travels through these organelles as it is processed, it is unlikely that this is the final destination for CFTR. Finally, it is possible that CFTR localizes to some small membrane bound vesicles in the cell.

This observation would support our previous data (Appendix 2) and offer the possibility of a vesicular trafficking pathway from the Golgi to the plasma membrane in MC. Such a pool of CFTR has been observed in EC (326). One explanation for such a pathway could be linked to a recycling or storage compartment for CFTR. A proposed functional role for this CFTR trafficking pathway in MC is delivery of CFTR to the plasma membrane upon MC activation, which could help depolarize the cell and regulate subsequent mediator production, as a form of negative feedback mechanism. Localization of CFTR may be carbohydrate-dependent with the fully processed, larger, upper band in EC (172 ± 3 kDa) being targeted to the plasma membrane and the lower band (162 ± 3 kDa) being targeted to membrane bound vesicles. This hypothesis is supported by the fact that both forms of CFTR are found in EC (which exhibit both PM and endosomal localizations of CFTR) while only the smaller form is found in MC (154 ± 4 kDa). In our fractionation experiments, we were not able to detect CFTR in MC granules. At this time, we cannot explain lack of cross validation with our confocal studies (Appendix 2), other than to suggest that there are differences in sensitivity or epitope preservation between the two techniques that may allow detection of weak signals by confocal but not by Western blot.

Since MC consistently express CFTR of a lower molecular weight than EC, it is likely that the size difference seen between MC CFTR and Calu-3 CFTR is related to protein function. We know that CFTR is in the high-speed fraction of rat PMC which contains fragments of PM, but also intracellular organelles and their membranes. It would be valuable to perform more precise sub-cellular

fractionation procedures to obtain greater resolution, although this may prove to be a challenging undertaking. This data neither confirms nor rejects the hypothesis that CFTR is present in a different subcellular location in MC than in EC, and technical challenges of CFTR imaging in LAD2 cells restricted further analysis of CFTR subcellular localization in human MC by confocal microscopy. However, when our Western blot results are combined with previous confocal pictures the possibility of differential localization is likely and requires further study (Appendix 2).

In conclusion, I speculate that CFTR expression in MC is different than in EC. It appears that MC have similar bands A and B, but that band C is different than in EC which could be due to glycosylation differences. These differences could result in alternate CFTR trafficking in MC, and lead to different functions of CFTR in these cells.

B. Effect of pharmacological inhibition of CFTR on mast cell function

The role of CFTR in MC was studied using a spectrum of pharmacological inhibitors. CFTR regulates production and/or secretion of some newly synthesized mediators, but does not appear to affect stored mediator secretion from MC granules. Specificity and dosage have long been an issue with pharmacological agents used to block CFTR and we used several CFTR inhibitors with doses as low as possible to try to circumvent problems (see table 1.1). We used NPPB and DPC which have been shown to inhibit CFTR, but also have

some non-specific effects at higher doses (327, 328). We also used the newly characterized CFTR blockers CFTR_{inh-172} and GlyH-101, which have been shown to be more specific for CFTR than previous inhibitors. Furthermore, GlyH-101 is thought to be the most specific CFTR inhibitor and is unique because it possess a novel inhibition mechanism involving occlusion of CFTR near the extracellular pore (189). Inhibition of CFTR with NPPB and CFTR_{inh-172} significantly inhibited Cl⁻ flux, but only NPPB significantly inhibited IgE/anti-IgE-induced β -hex secretion in MC (LAD2, PBMC). We also showed that NPPB in HMC-1 potentiated adenosine-induced release of IL-8, and IL-6, whereas GlyH-101 inhibited cytokine release from HMC-1. We also have evidence suggesting that GlyH-101 and NPPB inhibited IL-13 and IL-16 release, but only GlyH-101 seemed to inhibit SerpinE1 and I-309 release from LAD2 cells. Our description of this difference is only semi-quantitative at present, but could be linked to specificity of the drugs or possibly to conformational changes in CFTR in response to the drugs which have different binding sites. These could change CFTR binding protein interactions leading to divergent downstream signaling. This has been shown in MC cytokine production in response to SCF and TNF, and is linked to activation of either MAPK or NF- κ B (329).

In addition, we showed that neither NPPB nor GlyH-101 had any effect on eicosanoid production in human MC (Figure 3.23 D). There is a report suggesting that NPPB inhibits COX enzymes with an IC₅₀ of 8 μ M in rat mesangial cells (330). It is possible that some degree of COX inhibition occurs in

MC, but that the IC_{50} is higher than in mesangial cells. Thus, our data suggests that CFTR is not involved in eicosanoid production in MC.

1. Cl^- flux

We began pharmacological studies of CFTR inhibition by measuring cAMP-induced Cl^- flux in HMC-1 and LAD2 treated with CFTR inhibitors. In all treatments, there was a linear increase in MQAE fluorescence associated with Cl^- efflux during the first minute. Treatment with CFTR inhibitors changed the slope of this increase during the first minute. Because this method measures activity of several Cl^- channels, we used two inhibitors of CFTR, NPPB and CFTR_{inh-172} to isolate the CFTR-dependent portion of Cl^- flux. At the dose used, neither NPPB nor CFTR_{inh-172} inhibited basal Cl^- efflux, which would indicate that these inhibitors are not blocking other Cl^- channels such as ClC or $Na^+/K^+/2Cl^-$ exchangers. As shown in the literature, NPPB in a dose range of 10-50 μM , inhibits CFTR-dependent Cl^- flux (331, 332). In preliminary experiments, GlyH-101 treatment (25-50 μM) appeared to inhibit a larger portion of Cl^- flux than did NPPB, including a portion of the basal Cl^- flux, and appeared to show strong inhibition of cAMP activated Cl^- flux. This corresponds with data showing that 50 μM GlyH-101 almost completely abrogates apical Cl^- currents in EC mounted in Ussing chambers (189). However, we established that GlyH-101 is a direct quencher of MQAE (Figure 3.21 D), and therefore, the effects on Cl^- flux in our study, are likely due to direct quenching of the fluorescent signal rather than CFTR inhibition. Thus, we stopped using this inhibitor in the MQAE assay and

replaced it with CFTR_{inh-172}. We did not see MQAE quenching when using CFTR_{inh-172}, but we did see inhibition of cAMP-mediated Cl⁻ flux.

2. β -hex secretion

Although it is not fully understood where Cl⁻ channels fit into the puzzle of stimulus-secretion coupling and MC activation, regulation of these channels appears to be closely linked to changes in intracellular Ca²⁺ concentrations and Ca²⁺ channel activation (93). One mechanism to explain this may be through cAMP dependent outward rectification of Cl⁻ ions through CFTR, which depolarizes the membrane, reducing the electrical gradient for Ca²⁺ entry (214, 333). A main obstacle to more precisely define the role of Cl⁻ channels in MC function is that the intracellular Cl⁻ concentration, which varies widely between cells (97, 334), is not known for mature human MC *in vivo* (93). In light of increasing evidence for non-Cl⁻ transport-related functions of CFTR in non-EC, Cl⁻ transport may not be the sole regulatory function of CFTR in MC.

In this study, β -hex results showed that NPPB decreased, whereas GlyH-101 had no effect on β -hex release from LAD2 MC. Furthermore, we showed that the Δ F508 mutation of CFTR in PBMC from CF patients had no effect on IgE/anti-IgE-mediated β -hex release. Our previous data shows that DPC inhibited β -hex release in rat PMC (107). In our experiments, DPC did not have an effect on β -hex release in LAD2 cells, but this could be attributed to lower dose used in comparison to our previous rat studies. To have greater confidence in specificity of action and due to difficulty in obtaining large numbers of cells to

study β -hex release in LAD2 cells, we chose a dose of DPC that was between the lowest and second lowest significant dose in our previous study, which is roughly twice the IC_{50} (Table 1.1) (107). Our results suggest that GlyH-101 and DPC may be more specific CFTR inhibitors than NPPB at the doses used. There is evidence that the dose range of DPC that maintains specificity for CFTR is greater than NPPB (335, 336). In EC there are reports that both DPC and NPPB have non-CFTR specific effects such as inhibition of cAMP (300 – 1000 μ M), inhibition of volume, Ca^{2+} , and outwardly rectifying Cl^- channels at doses ranging from 50-100 μ M (179, 183-185, 337-339). Taken together, this data suggests that 50 μ M NPPB may have inhibitory activity on inwardly rectifying Ca^{2+} activated Cl^- channels which reduces hyperpolarization and Ca^{2+} entry in MC (Figure 4.2). At the dose used, it appears that DPC did not have this effect. For β -hex release in human MC, DPC may have the same effect as NPPB when used at a higher dose, but may still be CFTR specific at 50 μ M, which explains why DPC and GlyH-101 both had no effect on β -hex secretion. As GlyH-101 is more specific and does not cross the plasma membrane, it only acted on CFTR, and caused no significant changes in MC degranulation. DIDS had similar effects as NPPB on degranulation, suggesting that NPPB is acting through a non-CFTR effect. Our data on β -hex release in non-CF and CF PBMC although not statistically significant due to small sample size, strengthens the evidence that CFTR does not play a significant role in MC degranulation (Figure 3.45B).

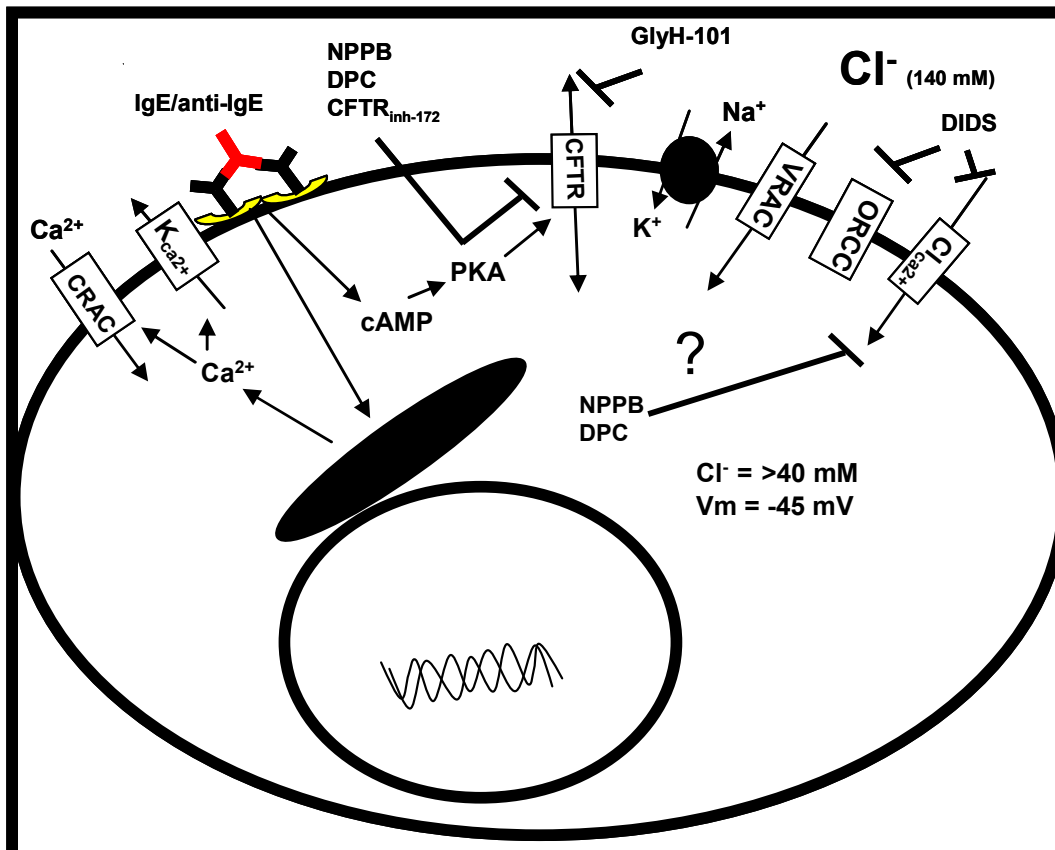


Figure 4.2 Potential mechanism of action of inhibitors NPPB, GlyH-101 and CFTR_{inh-172} on human mast cell (MC) degranulation. At rest, MC are electrically silent and the intracellular Cl⁻ concentration is between 0-40 mM. Upon stimulation with anti-IgE, Ca²⁺ is released from stores which triggers activation of inwardly rectifying Ca²⁺ release activated Ca²⁺ channels (CRAC), letting in extracellular Ca²⁺. Opening of Cl⁻ channels hyperpolarizes the membrane and increases MC degranulation. Activation also opens inwardly rectifying Ca²⁺ activated Cl⁻ channels and causes a transient cAMP increase which activates CFTR. NPPB may inhibit β-hex release through non-CFTR specific inhibition of Ca²⁺ gated Cl⁻ channel (Cl_{Ca²⁺}), an effect not observed when the more CFTR specific GlyH-101 is used. DPC may not have been used at a dose high enough to have the same effect in our experiments. DIDS blocked MC degranulation in a CFTR non-specific fashion. (See table 1.1 for full names of inhibitors). Inhibitors used at 50 μM.

3. IgE/anti-IgE-mediated cytokine secretion

Using these inhibitors, we assessed the effect of CFTR on newly synthesized mediator secretion in MC. In EC CFTR has previously been shown to regulate RANTES production (340), nitric oxide synthase expression (341), outwardly-rectifying Cl^- channels (342), the epithelial Na^+ channel (ENaC) (343) and aquaporin-3 water channels (344). CFTR also regulates intracellular acidification (225, 230) protein processing, IL-8 production and apoptosis (345-347). Similarly, in lymphocytes from CF patients a reduction in $\text{IFN}\gamma$ secretion has been reported (219), while EC in CF, enhanced intracellular accumulation of IL-6 and IL-8 has been reported (348). Reduced CFTR expression has been linked to impaired innate immune responses in CF, in particular defense mechanisms against *P. aeruginosa*, reduced production of nitric oxide through inducible nitric oxide synthase (NOS2) and gene expression associated with innate immune stimulus (247, 349, 350).

Recently, the effects of CFTR on secretion of mediators has been linked to channel function of CFTR, as well the presence of intact CFTR within lipid rafts (312, 351-353). When CFTR Cl^- channel function was blocked by CFTR_{inh-172}, EC secreted more IL-8 (312). The authors linked these events to CFTR channel function and increased proteasomal degradation of NF- κB inhibitor I- $\kappa\text{B}\alpha$ and this was attributed to loss of HCO_3^- and glutathione transport and imbalance of intracellular pH (312, 351, 352). However, since activation of CFTR by cAMP changes the conformation of the two NBD and the channel pore, one could speculate that CFTR inhibitors also prevent certain conformational changes that

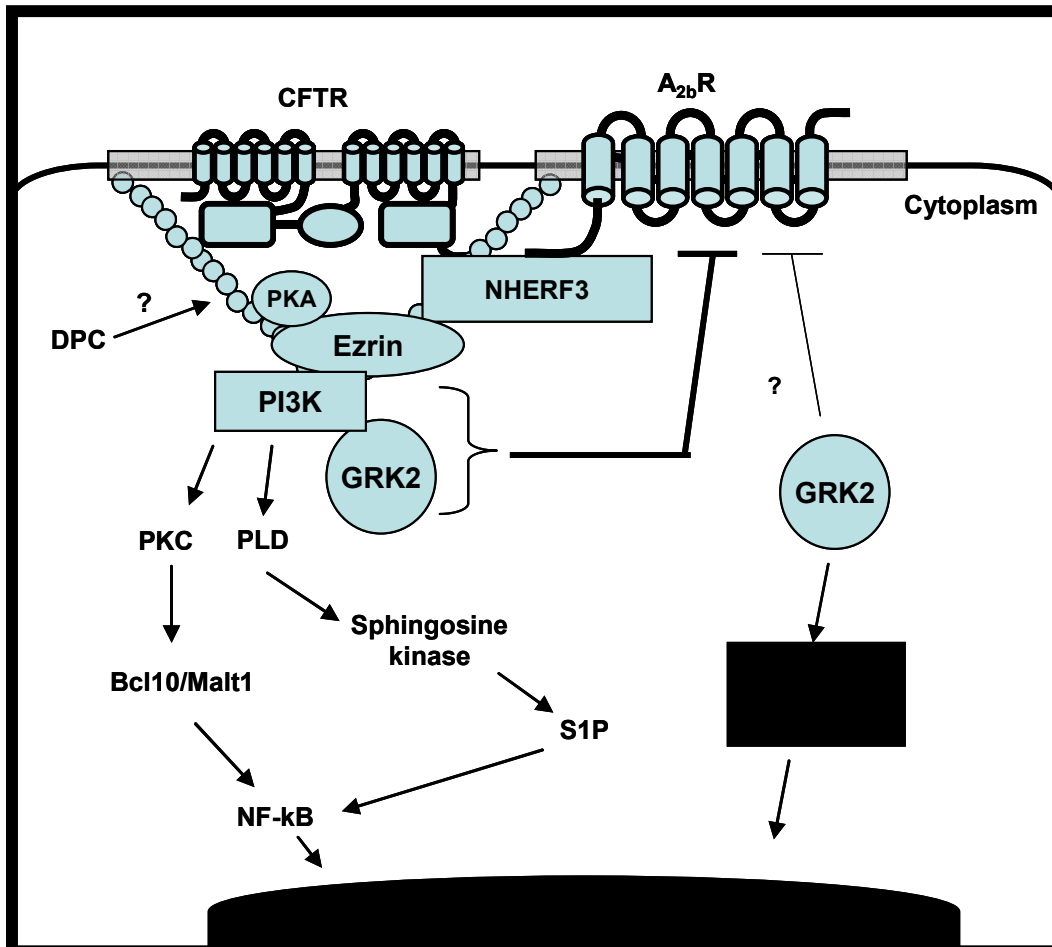


Figure 4.3 Proposed mechanism of CFTR-adenosine 2b receptor (A_{2b}R) interactions and regulation of IL-8 production. Both CFTR and A_{2b}R associate with lipid rafts (gray boxes) through cytoskeletal Na⁺-H⁺ exchange regulatory factor-3 (NHERF3)-ezrin binding. A_{2b}R is linked to CFTR by NHERF3-ezrin. GRK2 can phosphorylate PI3K which can then bind to ezrin and also associate with G-protein coupled receptor kinase-2 (GRK2). PI3K-GRK2 complex upregulates A_{2b}R desensitization when compared to uncoupled GRK2 as a negative feedback mechanism following CFTR activation. Potential mechanism of action of GlyH-101 is inhibition of ezrin-PI3K binding by preventing conformational change in CFTR, leading to increased receptor desensitization. PI3K can activate PKC and phospholipase D (PLD), which leads to phosphorylation of Bcl10/Malt1 and sphingosine 1 phosphate (S1P), which can activate NF-kB. GRK2 may also have "black box" effects which lead to hypersecretion of cytokines in CF due to uncoupling to PI3K-NHERF3.

promote CFTR association with its binding partners and downstream intracellular signaling. This idea is strengthened by a recent study showing that CFTR is associated with lipid rafts and regulation of cell stimulation (312). When the PDZ domain of CFTR was removed or inactivated, CFTR could no longer associate with lipid rafts resulting in a loss of negative regulation of TNF, IL-1 β and TLR mediated NF-kB signaling (312, 353). This suggests a significant role for CFTR protein interactions in regulation of cell stimulation, but the mechanism leading from CFTR to NF-kB activation is unclear and could be linked to CFTR conformational events that alter PDZ binding (Figure 4.3). Thus, CFTR is more than an ion channel, having functional roles through protein interactions and intracellular signaling. Given this information, MC in CF patients may be more responsive to certain stimuli than MC of non-CF patients. To test this hypothesis, I examined the role of CFTR in the production of secretory mediators by LAD2 and HMC-1 using the pharmacological inhibitors identified above. Although we showed in LAD2 that MC β -hex secretion is not impaired by pharmacological inhibition of CFTR, evidence suggests that CFTR balances whole cell currents in a delayed fashion, or has a channel-associated role on intracellular signaling that is not linked to Cl⁻ flux (351, 352). Stimulation of channel opening by cAMP changes intracellular CFTR conformation, such that differences in protein binding and intracellular signaling may occur as a result of CFTR activation, which are independent of ion transport. Our data on the effects of inhibitors on LAD2 shows that NPPB and DPC enhanced IL-8 secretion in response to IgE/anti-IgE, whereas DPC but not NPPB affected NECA-induced release of IL-8.

Enhancement or suppression of IL-8 release by NPPB and DPC may be linked to inhibition of non-CFTR Cl^- channels (Figure 4.4). Alternately, the enhancement of IL-8 by NPPB and DPC may be linked to inhibition of cAMP in LAD2 cells, which may lead to reduced expression of an early repressor gene, which suppresses MC synthesis and secretion of cytokines in response to IgE/anti-IgE stimulation (figure 4.4) (354, 355). Suppression of NECA-induced IL-8 release in LAD2 by DPC but not NPPB, is more difficult to interpret, and may not be linked to membrane hyperpolarization and Ca^{2+} entry, but rather to interactions with CFTR binding partners that are regulated by NECA stimulation (Figure 4.3). These interactions will be discussed below as we examine our HMC-1 data.

4. NECA-mediated cytokine secretion

DPC had no effect on NECA stimulated release of IL-8 and IL-6 in HMC-1 cells. In contrast, NPPB enhanced, whereas GlyH-101 decreased IL-8 secretion (Figure 3.23). Furthermore, the effects of NPPB and GlyH-101 on IL-6 secretion seemed to be unrelated to cell stimulation, as this enhancement also occurred in unstimulated cells (Figure 3.23). HMC-1 do not express $\text{Fc}\epsilon\text{R1}$, and thus do not respond to IgE/anti-IgE stimulation (276). However, they secrete IL-8 in response to the adenosine receptor agonist NECA (49, 356). To stimulate the cells, we used a relatively low dose of NECA (3 μM) for 24 h, and induced a significant release of IL-8 and IL-6. Our data suggests that under normal conditions, CFTR regulates release of these cytokines in MC, since inhibition of CFTR by NPPB potentiated, whereas GlyH-101 inhibited release of these

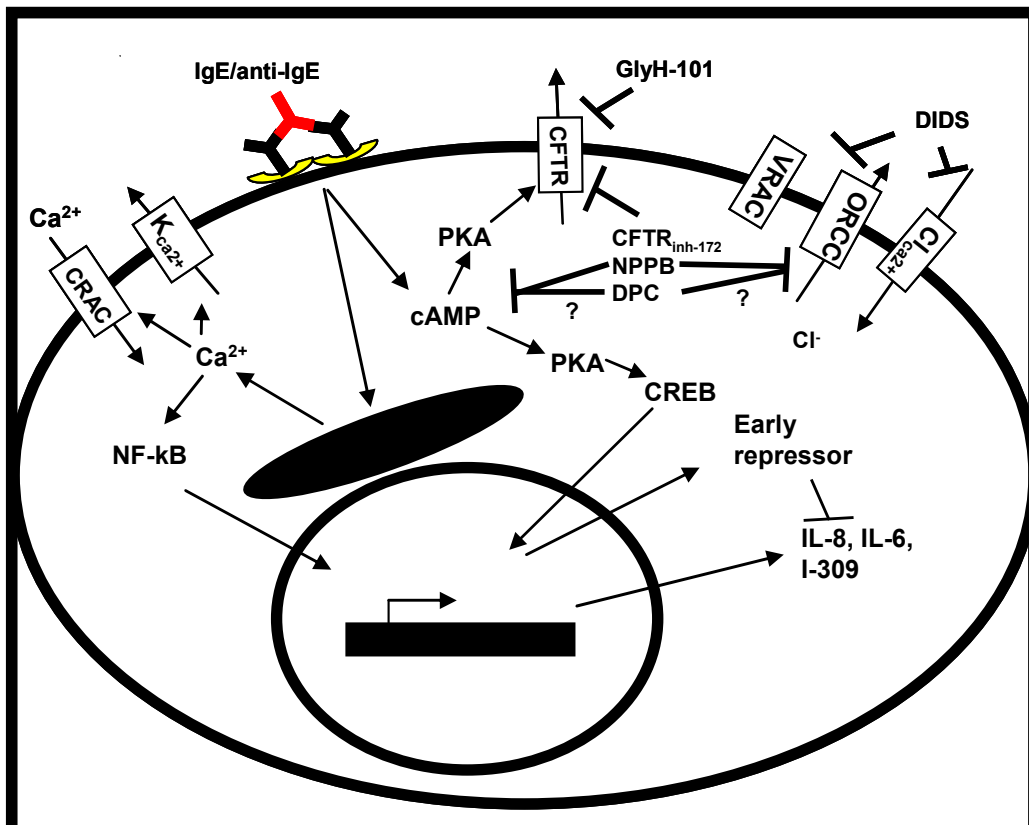


Figure 4.4 Potential mechanism of action of inhibitors NPPB, GlyH-101 and CFTR_{inh-172} on LAD2 mast cell (MC) cytokine release in response to IgE/anti-IgE. Upon stimulation with anti-IgE, Ca²⁺ is released from stores which triggers activation of inwardly rectifying Ca²⁺ release activated Ca²⁺ channels (CRAC), letting in extracellular Ca²⁺. Opening of Cl⁻ channels hyperpolarizes the membrane and increases Ca²⁺ influx. Activation also opens inwardly rectifying Ca²⁺ activated Cl⁻ channels and causes a transient cAMP increase which activates CFTR and also negatively regulates secretion by cAMP response element binding protein (CREB) activation which initiates transcription of early repressor gene. In LAD2, NPPB and DPC may enhance IL-8 and IL-6 release through non-CFTR specific inhibition of cAMP and reduced early repressor generation. DIDS blocked LAD2 cytokine release in a CFTR non-specific fashion. (See table 1.1 for full names of inhibitors). Inhibitors used at 50 μ M.

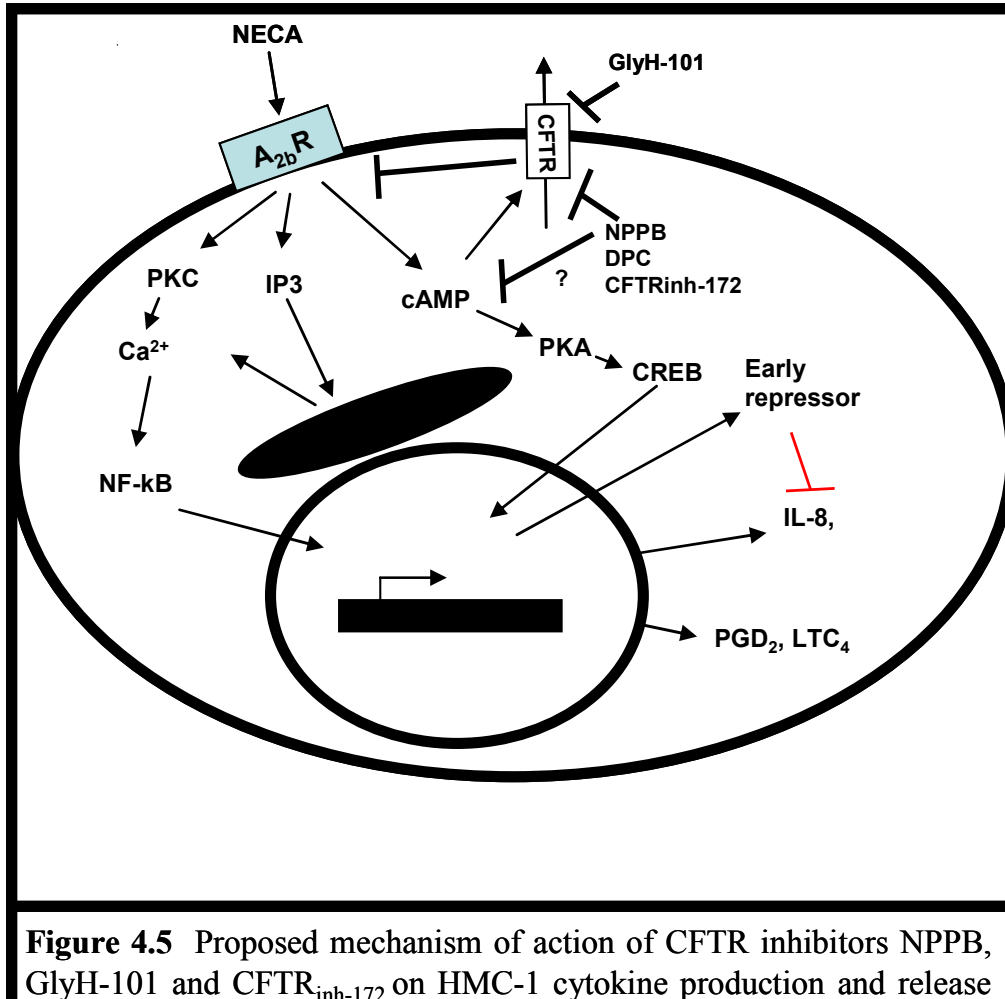


Figure 4.5 Proposed mechanism of action of CFTR inhibitors NPPB, GlyH-101 and CFTR_{inh-172} on HMC-1 cytokine production and release in response to adenosine 2b receptor (A_{2b}R) agonist NECA. Upon stimulation with NECA, there is activation of PKC and cAMP via G_{αq} and G_{αs} respectively. This leads to an increase in intracellular Ca²⁺, causing NF-κB activation, as well as increase in early repressor expression which regulates cytokine secretion. NPPB may enhance IL-8 production and release through non-CFTR specific inhibition of cAMP and reduced early repressor generation. GlyH-101 blocks CFTR conformational changes which alters the interactions of CFTR with its binding partners, leading to A_{2b}R desensitization and reduction in signalling. (See table 1.1 for full names of inhibitors).

cytokines. Assuming that GlyH-101 activity is CFTR specific, our data contrasts with previous reports that CFTR inhibition with CFTR_{inh-172} results in increased IL-8 secretion in EC (312). As we have demonstrated that CFTR is differentially regulated in MC and EC, this difference could be cell type-dependent and involve differences in expression and interaction of CFTR binding partners. This difference may also involve inhibition of cAMP and activation of an early repressor gene in a similar fashion as in IgE/anti-IgE stimulation (Figure 4.5).

It has been shown that G-protein coupled receptor kinase-2 (GRK2) can desensitize β_2 AR and suppress signaling through this receptor (Figure 4.3) (357). These events are mediated by phosphorylation, ubiquitination and endocytosis of the receptor. Interestingly, it has also been shown that GRK2 is upregulated in CF cells, and that this kinase can phosphorylate ezrin, which associates with CFTR through the PDZ binding protein NHERF1 (357, 358). PI3K has been linked to NF- κ B activation in MC through PKC activation and downstream phosphorylation of Bcl10 and Malt1 (359). Furthermore, PI3K can interact with both phospho-ezrin and GRK2, suggesting that there may be an association between β_2 adrenergic receptor (β_2) signaling and CFTR expression (357). Inhibition of PI3K/GRK2 binding markedly suppresses receptor desensitization and prolongs signaling through the β_2 AR (357). In addition to β_2 AR interaction with CFTR through NHERF1, there are reports of A_{2b}R association with CFTR through NHERF3 (E3KARP) (166). Thus, PI3K may sequester GRK2 and regulate the rate of G-protein coupled receptor desensitization (Figure 4.3). Inhibition of CFTR with pharmacological inhibitors may disrupt conformational

changes which promote NHERF3-ezrin-PI3K-GRK2 interactions, thus accelerating A_{2b}R desensitization and reducing IL-8 production/secretion. The non-NECA mediated effects of CFTR inhibitors on IL-6 production is difficult to interpret, but may be linked to threshold levels of NF-kB required for binding to various cytokine promoters, or to basal activation of the cell by these drugs which is not significant when IL-8 is measured, as release of IL-8 occurs at a much higher concentration.

In HMC-1 cells, there was a potentiation of IL-8 and IL-6 release, in response to NECA, which did not occur in the more mature LAD2 cell line. One explanation for this observation lies in potential differences in expression of A_{2a}R or A_{2b}R in the two cell lines, compounded by potential differences in G-protein signaling from the A_{2b}R. It has been shown that A_{2b}R can be coupled to both G_{αs} and/or G_{αq} depending on cell type. In HMC-1, the A_{2b}R couples to G_{αq} and G_{αs} which activates PLCγ and cAMP/PKA (360). We speculate that G-protein coupling may differ in LAD2, or that HMC-1 and LAD2 differentially express A_{2a}R and A_{2b}R, a hypothesis that may explain the differences in NECA responsiveness between the two cell types. HMC-1 and LAD2 MC may also possess differences in GRK expression. It has been shown that GRK2 is responsible for β₂AR ubiquitination and endocytosis (357). Combinations of all of these factors may be involved in the differences in secretion between HMC-1 and LAD2 depending on readout and experimental design.

In conclusion, CFTR may be an important molecule in the regulation of non-epithelial cells such as MC. Whether it exerts its functions directly via

regulation of Cl^- flux and Ca^{2+} entry, or indirectly via receptor desensitization or activation of other pathways is still unclear. We attempted to address the issue of inhibitor specificity by using several CFTR inhibitors, but the picture of the role of these inhibitors on MC secretion is unclear. Our data suggests that these inhibitors have differing effects on CFTR depending on the stimulus used and the secretory compartment examined. Thus, while pharmacological inhibition of CFTR yields some important clues as to its function with regards to Cl^- flux, it also poses new questions as to the role of channel function in MC intracellular signaling.

C. CFTR knockdown in mast cells

1. Antisense oligonucleotides (ASO)

To complement our data with pharmacological inhibitors, we examined secretion from CFTR deficient HMC-1 and PBMC from CF and non-CF patients. When we used ASO, to knock down CFTR we were not able to detect differences in CFTR protein levels by Western blot, but we did show reduction in Cl^- flux in HMC-1 (Figure 3.25). However, we did not use FSK activation in these experiments, so the decrease in Cl^- flux we observed may be linked to non-specific effects of ASO and not a specific CFTR deficiency. We also unable to show differences in β -hex release from HMC-1 using Ca^{2+} ionophore A23187. When we used the physiological stimulus NECA to stimulate ASO and MSO treated cells rather than A23187, we saw the appearance of non-specific effects of

the ASO and MSO, as the MSO treatment resulted in as much potentiation of the IL-8 and IL-6 secretion as the ASO (Figure 3.26). As our ASO and MSO are phosphorothioate modified oligonucleotides, they could potentially enhance HMC-1 response to CpG motifs through TLR-9 as has been demonstrated (361, 362). As a result, we abandoned the ASO strategy and moved to CFTR inhibition by siRNA, a more state-of-the-art method of RNA interference.

2. CFTR small inhibitory RNA (siRNA)

At this point in our studies, the use of ASO was beginning to decrease as the discovery of siRNA to knock down proteins was proving to be a better and more physiological methodology. It did not use chemically modified nucleic acids and had been shown to be an elegant mechanism to downregulate gene expression (363). In our hands, although we attempted to optimize transfection conditions using BLOCK-iT fluorescent siRNA, transfection experiments with CFTR siRNA only modestly reduced CFTR expression in Calu-3 cells and did not reduce CFTR expression in HMC-1 (Figure 3.28, 3.30 and 3.31). Incubation of the cells with siRNA for 48 h should have been sufficient to reduce CFTR mRNA and protein expression, as CFTR half life has been estimated at 10-12 h (283, 284). When we probed deeper into this puzzling result using confocal microscopy, we found that the siRNA appeared to be sticking to the outside of the cells and insufficient siRNA transfection for CFTR knockdown (Figure 3.32). After struggling with siRNA transfection into MC for a long time, we decided to adopt a stable transfection system using a CFTR short hairpin (CFTR sh) RNA

transfection system with a lentiviral vector containing a puromycin resistance gene.

3. CFTR short hairpin RNA (shRNA)

Using CFTR shRNA, we were successful in knocking down CFTR mRNA and protein expression in HMC-1 cells. Knockdown is not 100% effective, but seems to have reduced CFTR transcript levels and expression of the 100 kDa anti-CFTR reactive protein (Figure 3.37 and 3.38). Interestingly, our CFTR shRNA treated cells displayed a shift in expression of two bands at 167 and 145 kDa. In untransfected and SCR transfected cells, a weak band at 167 kDa and a strong lower band at 145 kDa is visible. The intensity of the band at 167 kDa increases slightly with SCR shRNA treatment, but there is a complete reversal in intensity when cells are transfected with CFTR shRNA (Figure 38. B lane 6). Furthermore, two other bands at 93 and 86 kDa have lower intensity in CFTR shRNA, but not SCR shRNA treatment. These results were obtained on two different transfected HMC-1 preparations, performed 2 y apart and the second experiment gave very similar results using both CFTR antibodies, which strengthens the data (Figure 3.38). The band at 96 kDa which disappears in shRNA CFTR could in fact be band A. The difference between the MW in this gel and the reported MW of band A in EC could be attributed to gel density, running buffer and MW marker differences, as we have shown that the MW of CFTR band A is very similar in HMC and Calu-3 cells (Figure 3.17). This 96 kDa band was also similar to Calu-3 band A in our previous result, but we did not run a Calu-3 lysate in the latest gel (Figure 3.38 B).

This data is difficult to interpret. It has been widely accepted that only fully glycosylated CFTR migrates to the plasma membrane, but this has come under some debate (364, 365). Thus, we should not take for granted that the highest MW form of CFTR is found at the plasma membrane in MC. Our data showing inhibition of cAMP-dependent Cl^- flux and NECA-induced secretion of IL-8 and IL-6 with CFTR shRNA treatment suggest that some form of CFTR is not present on the plasma membrane of CFTR shRNA-treated cells (Figure 4.3). Thus this data argues that either the 93, 86 or 145 kDa form of CFTR are expressed at the plasma membrane and expression of one or more of these bands is reduced at the cell surface by CFTR shRNA. It is unlikely that the 167 kDa form which is upregulated by CFTR shRNA is expressed at the plasma membrane, as we did not see enhancement of cAMP-mediated Cl^- flux in CFTR shRNA during the 1st min of the assay. We saw potentiation of FSK-induced Cl^- flux in CFTR shRNA transfected cells after 1 min, but it is more likely that this increase in Cl^- flux comes from loss of CFTR regulation of other Cl^- channels in MC, and that the 167 kDa band represents some form of intracellular pool of CFTR (Figure 4.6). One possible explanation is that this pool of CFTR could be an endosomal recycling pathway of CFTR that has become blocked by the disruption of the rab11b endosomal recycling pathway (Figure 4.6) (326, 366). We hypothesize that 167 kDa CFTR is removed from the cell surface by endocytosis, but that it does not recycle to the plasma membrane in CFTR shRNA, becoming trapped inside the cell where it accumulates and is not

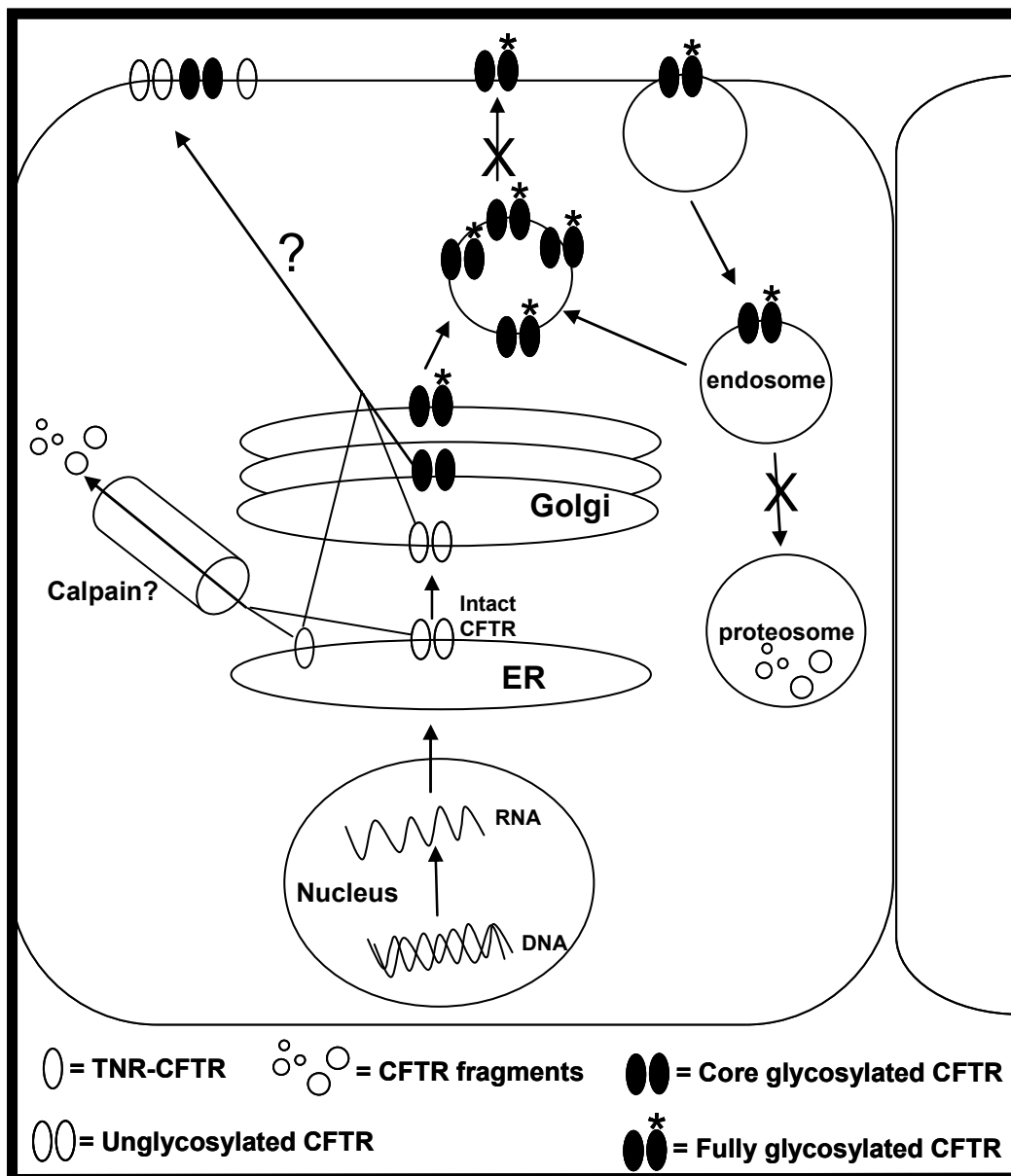


Figure 4.6 Proposed synthesis and processing pathways of CFTR in MC. Following synthesis, a pool of unglycosylated, fully mature CFTR or TNF-CFTR migrate to the plasma membrane by passing through the Golgi apparatus. Recycling of CFTR occurs at the plasma membrane, regulating expression and proteolytic degradation of CFTR. Other degradation pathways may occur through other proteases such as calpain. Following CFTR shRNA treatment, endosomal recycling as well as proteasomal degradation may be inhibited, such that fully mature CFTR accumulates inside the cells. Reduction in mature CFTR at the surface may upregulate synthesis and trafficking of TNR-CFTR or unglycosylated CFTR which may be expressed at the surface in an attempt to compensate for the loss of mature CFTR at the plasma membrane.

degraded (Figure 4.6). Alternately, there could be a pool of fully glycosylated CFTR within the Golgi that is also protected from proteolytic degradation, but is unable to migrate to the cell surface by disruption of CFTR trafficking. These hypotheses attempt to explain these findings, but remain to be tested. These results suggest that the 96 and 83 kDa bands in HMC-1 may represent functional TNF-CFTR. TNR-CFTR may be expressed in MC and get to the plasma membrane where it forms functional channels as previously described (Figure 4.6) (319, 320, 367). TNR-CFTR may dimerize and loss of dimerized TNR-CFTR could give the impression of a reduction of 167 kDa band. The shift in band intensity at 150 kDa between sham, SCR and CFTR shRNA could be attributed to changes in turnover rate of CFTR induced either by the vector or by the reduction of unglycosylated CFTR production. The lower band at 150 kDa may also represent band B, and the upper band represent band C, which indicates changes in CFTR glycosylation pathways by CFTR shRNA treatment. Such changes are difficult to interpret, but could be attributed to upregulation of glycosyltransferase and glycosylation of CFTR.

So far we have assumed that knockdown of CFTR is homogeneous in our HMC-1 population. However, our flow cytometry using MA1-935 antibody in unpermeabilized cells suggests that this is not the case. When we stained with MA1-935, we detected the presence of HMC-1 with various amounts of plasma membrane CFTR expression based on the intensity of the signal. This suggests that not all the cells are transfected equally, and are expressing various amounts of CFTR protein (Figure 3.39). When we stained permeabilized cells with 24-1

antibody, we saw an increase in CFTR signal in CFTR shRNA transfected cells. Using these two antibodies in tandem, we can deduce that CFTR shRNA transfected cells have more CFTR signal than the untransfected and SCR shRNA transfected cells (Figure 3.40 H and I), but that less CFTR is present at the plasma membrane (Figure 3.39 H and I). This data strengthens our hypothesis that there is an internal pool of CFTR that is sequestered from degradation by the transfection of CFTR shRNA.

D. Cystic Fibrosis vs non-Cystic Fibrosis peripheral blood derived mast cells

Having established that CFTR has a role in Cl^- flux and secretion in MC, we wanted to investigate CFTR in primary MC cultures. To do this we obtained consent of the University of Alberta Health Research Ethics Board to obtain peripheral blood from non-CF and CF donors in collaboration with Dr. Neil Brown, Director of the University of Alberta Hospital's CF clinic. In total, 4 CF and 4 non-CF patients were recruited into the pilot study and MC were cultured from their peripheral blood progenitors as described in chapter 2. We compared numbers of CD34^+ cells in peripheral blood of CF and non-CF donors and found no differences (Figure 3.3). After 8 weeks in culture, CF and non-CF PBMC were compared head to head in a battery of functional tests including tryptase chymase staining, expression of c-Kit and $\text{Fc}\epsilon\text{R1}$, β -hex release, cytokine production and secretion, and production of lipid mediators. These tests were conducted in response to IgE/anti-IgE stimulation, but cytokine release was also

assessed in response to innate immune stimulation. For some comparisons, we only had enough cells to perform one experiment as we used most of the cells for analysis of secretion. Here we show that there is no significant difference in tryptase chymase staining, expression of c-Kit and FcεR1, β-hex release and lipid mediator synthesis between CF and non-CF PBMC. Our data shows that CF PBMC do not express plasma membrane CFTR, are bigger than non-CF PBMC (Figure 3.12 B-D), and differentially synthesize and secrete cytokines. These results will be discussed below.

CFTR expression in PBMC could not be assessed by Western blot, as our Ponceau S data suggests that the cells are laden with low molecular weight protein, which precludes analysis of CFTR by this method (Figure 3.13). We therefore analyzed CFTR expression by flow cytometry using MA1-935 and 24-1 for surface and intracellular expression respectively. Because of our small sample size, we only had enough cells to perform one experiment. When we stained PBMC for surface expression of CFTR using MA1-935 in unpermeabilized cells, we saw that CF PBMC had lower surface expression than non-CF PBMC. However, intracellular staining with 24-1 revealed that CF and non-CF PBMC had similar CFTR expression. Although we did not do it because of sample size and technical difficulties, it would be interesting to compare CFTR expression in PBMC to that in LAD2 and HMC-1 by Western blot to determine if the same banding patterns occur in these cells. This may give additional clues as to the molecular characterization of CFTR in primary human MC.

Interestingly, when we performed flow cytometry on CF and non-CF PBMC as well as on CFTR shRNA HMC-1, we made the observation that CF deficient MC have increased FSC compared to untransfected, SCR shRNA of non-CF PBMC counterparts (Figures 3.12 insets, 3.39 and 3.40 panels A-C). This observation indicates that CFTR deficient MC are larger than CFTR sufficient cells, suggesting that CFTR has some role in regulation of cell volume. It has reported that airway cells from CF patients are swollen, but this has been attributed to edema and infection (368). One report has shown that CF null mutant mice intestinal crypts do not undergo volume reduction in response to secretagogues as do wild type mouse crypts (369). This is not confined to the gut, as others have reported that loss of CFTR results in loss of volume control in airway (370). Other reports have associated CFTR with cell volume and shown that CFTR deficient cells lose regulatory volume decrease (RVD) function and appear different than their CFTR sufficient counterparts (368). In mammalian cells, RVD occurs through simultaneous activation of K^+ and Cl^- channels accompanied osmotically by H_2O (371). It was recently found that in EC, RVD is initiated by TRPV4, a non-selective cation channel that is responsive to mechanical stress, heat, pH changes, endogenous ligands and cell volume (372). When cells swell, TRPV4 is activated and allows Ca^{2+} entry which triggers Ca^{2+} sensing outwardly rectifying K^+ channels. Loss of K^+ through these channels is accompanied by vectorial Cl^- transport and osmotic H_2O loss, thus reducing cell volume (368, 372). It was shown that the TRPV4-mediated Ca^{2+} influx is absent in CF EC (372). This effect is not associated with reduced TRPV4 expression,

and is still not clearly understood. A similar process may be occurring in PBMC, accounting for increased cell size in CF PBMC. This observation requires further study as loss of RVD response in CF PBMC may be a source of cell hyperpolarization and activation and cytokine hypersecretion upon activation.

When we compared cytokine secretion from these cells using the R&D Systems protein array, several differences were apparent between non-CF and CF cells (Figure 3.44). This data suggested that CF PBMC secreted more IL-8 and serpinE1, but less IL-1ra, IL-6, and MIF when stimulated with anti-IgE. We repeated the experiment with three separate CF and three separate non-CF PBMC cultures and sent the samples to Aushon Biosystems for Searchlight analysis. The Searchlight data showed that CF-PBMC appear to have higher basal secretion of GM-CSF, IL-8, IL-1ra, CCL4 and CCL20 than non-CF PBMC (Table 3.5). Interestingly, unstimulated CF PBMC synthesized significant more but secreted significantly less IL-1 α than non-CF PBMC. A recent study showed that CF tracheal glands synthesized and secreted more IL-1 α than their non-CF counterparts (247). CF PBMC also showed a trend toward increased synthesis of IL-6, MIF, IL-1ra, and CCL20. When stimulated with anti-IgE, CF PBMC secreted more GM-CSF, MIF, IL-1ra, CCL4 and CCL20 than their non-CF counterparts (Table 3.5). This increase in GM-CSF, IL-6, CCL4 in CF has been previously reported (147). In contrast to a previous report in EC (198), CF PBMC seemed to secrete more IL-1ra than non-CF PBMC. CF PBMC also appear to secrete less IL-8 than non-CF PBMC, which correlates with our data in HMC-1 where CFTR shRNA transfected cells do not secrete IL-8 in response to NECA

(Figure 3.42 A). Taken together, this data shows that PBMC from CF patients show a trend towards differences in secretion, as well as synthesis in most of the cytokines tested. Although the data showed that these differences were not statistically significant, we believe that this was due to small sample size. Since lack of CFTR does not affect degranulation from MC, these data suggest that absence of CFTR may act downstream of Ca^{2+} on transcription factors such as NF- κ B (Figure 1.3). Another possibility is that absence of CFTR dysregulates the MC secretory compartments in some way such that various cytokines such as IL-8 or IL-6 may be differentially released from MC following activation (Figure 1.6). Thus, absence of CFTR at the plasma membrane may affect either synthesis of cytokines (total protein) or % release of the total protein (secretion) through dysregulation of secretory vesicle trafficking. Therefore, it is important to repeat this experiment to increase sample size. In our opinion, this will further highlight differences in cytokine synthesis and secretion between CF and non-CF PBMC

As CF patients have chronic *P. aeruginosa* infections, we also wanted to determine whether CF MC respond differently than non-CF MC to innate immune stimulation. We stimulated the cells with a selected dose of fixed and killed *P. aeruginosa* PAO1 strain. As we had limited numbers of cells, we selected one dose (multiplicity of infection (MOI) of 25:1 *P. aeruginosa*) and one stimulation time point (24 h), based on previous reports as well as personal communication with Dr. Tong-Jun Lin at Dalhousie University (294-297). In our experiments, when stimulated with *P. aeruginosa*, CF PBMC secreted more GM-CSF, IL-8, MIF, IL-1ra, CCL4, CCL20 and significantly more IL-1 α than non-CF PBMC

(Table 3.6). Furthermore, CF PBMC had increased synthesis of CCL20 when stimulated with *P. aeruginosa*. Although IL-8 secretion was lower in CF PBMC, overall differences in cytokine synthesis and secretion suggest that CF MC possess a pro-inflammatory phenotype compared to non-CF PBMC, both in response to classical allergic as well as innate immune stimulation. Thus, although further investigation is required, this data supports the hypothesis that MC contribute to the pathophysiology of CF.

E. Future directions

During the course of this work, we have also made several observations which we did not have time to pursue. These observations relate to the regulation of CFTR expression in MC and EC. We have shown in Appendix 2 that IFN γ upregulates CFTR mRNA and protein expression in MC, whereas it has the opposite effect in EC and we hypothesize that there are at least two potential mechanisms for this regulation by IFN γ . These will be discussed in the next section.

1. mRNA stability

Many proteins are translated from mRNA containing 3'-untranslated regions (3'UTR) that possess Adenine/Uracil-Rich Elements (ARE) (373, 374). These motifs are binding sites for ARE binding proteins (AREbp), which are under the regulation of MAP kinases (375, 376).

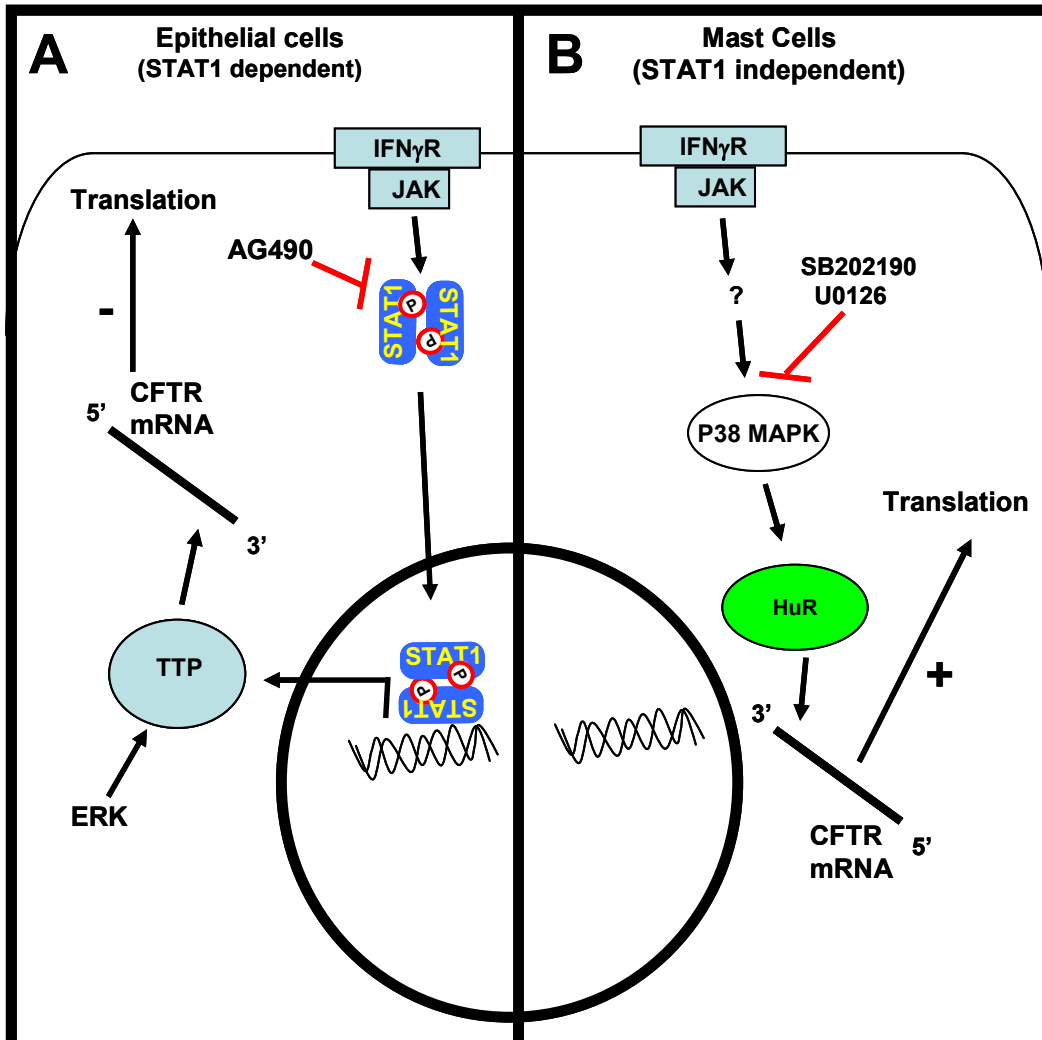


Figure 4.7 A) Proposed mechanism of CFTR regulation in EC and MC by IFN γ . In EC, IFN γ stimulation activates JAK phosphorylation of STAT1, which dimerizes, migrates to the nucleus and initiates gene transcription including extracellular regulated kinase (ERK). ERK can phosphorylate AU rich element (ARE) binding protein (AREbp) tristetraprolin (TTP). When phosphorylated, TTP can bind to 3'untranslated regions of mRNA transcripts and promote their degradation through destabilization. **B)** In MC, IFN γ stimulation upregulates CFTR through a STAT1 independent mechanism probably by inducing p38 MAPK kinase (p38 MAPK) activation which phosphorylates AREbp HuR. HuR can bind to 3'UTR of mRNA transcripts and inhibit their degradation (ie., enhanced stability).

Regulation of AREbp activity by MAPK is a way for cells to regulate mRNA stability through increased or decreased stability of the transcript. It has been shown in EC that CFTR mRNA has a 3' untranslated region (3'UTR), and that this region contains several ARE which act as recognition motifs for mRNA stabilizing or destabilizing AREbp (145). Regulation of mRNA stability is complex, involving many AREbp, the expression of which is cell type specific, such that in T84 and Calu-3 EC, CFTR mRNA expression is differentially regulated by treatment with IL-1 β or TNF (145).

In our previous work (Appendix 2), we have shown that CFTR is upregulated in MC, but downregulated in EC by 24 h IFN γ treatment (201). We showed that regulation of CFTR expression by IFN γ is STAT1-dependent in EC, and p38 MAPK-dependent in MC (Figure 4.7). We propose that the mechanism of IFN γ CFTR downregulation in EC may involve STAT1 phosphorylation and transcription of new genes, among which is the mRNA destabilizing AREbp tristetraprolin (TTP). We propose that when phosphorylated by ERK, TTP can bind to CFTR mRNA, reducing its stability (Figure 4.7 A). IFN γ has been shown to upregulate transcription of TTP, and ERK phosphorylation of TTP has been described in mature dendritic cells (377, 378). In MC, however, the JAK/STAT inhibitor AG490 had no effect on CFTR mRNA expression in MC, suggesting that the ERK/TTP pathway was is not involved.

However, when MC were treated with p38 MAPK inhibitors prior to IFN γ treatment, CFTR expression was reduced, suggesting that a stabilizing AREbp is being phosphorylated through a STAT-1 independent pathway, as JAK inhibitors

had no effect of CFTR expression in MC. We hypothesize that the AREbp involved in IFN γ regulation of MC CFTR expression is a member of the HuR family, as these proteins stabilize mRNA (373).

It would be interesting to determine which AREbp are expressed in human MC, and which ones are regulated by IFN γ . Doing this would allow us to dissect this pathway and to elucidate the precise mechanism of the regulation of CFTR expression in MC. If we can find novel ways to enhance CFTR expression through these mechanisms, this may provide new therapeutic strategies to treat CF.

2. WT-1

It is interesting that several reports suggest that the first intron of CFTR contains a DHS site which is thought to be a transcriptional regulatory element (139, 140, 143, 144). The identity and role of this regulatory element is not fully understood. We ran the sequence of the first intron of CFTR through an online program called Transcriptional Element Search System (TESS) and discovered that a 30 nucleotide thymine guanine (TG) repeat segment is a putative binding site for the Wilm's Tumor-1 (WT-1) protein (Figure 4.8). Coincidentally, a previous student in our lab studied the role of WT-1 on MMP-9 transcription in EC (379). WT-1 is a repressor of MMP-9, which translocates from the nucleus to the cytoplasm upon phosphorylation in a nitric oxide (NO) dependent pathway. The effects of NO on WT-1 translocation were attributed to soluble guanylate cyclase (sGC)-dependent PKA activation.

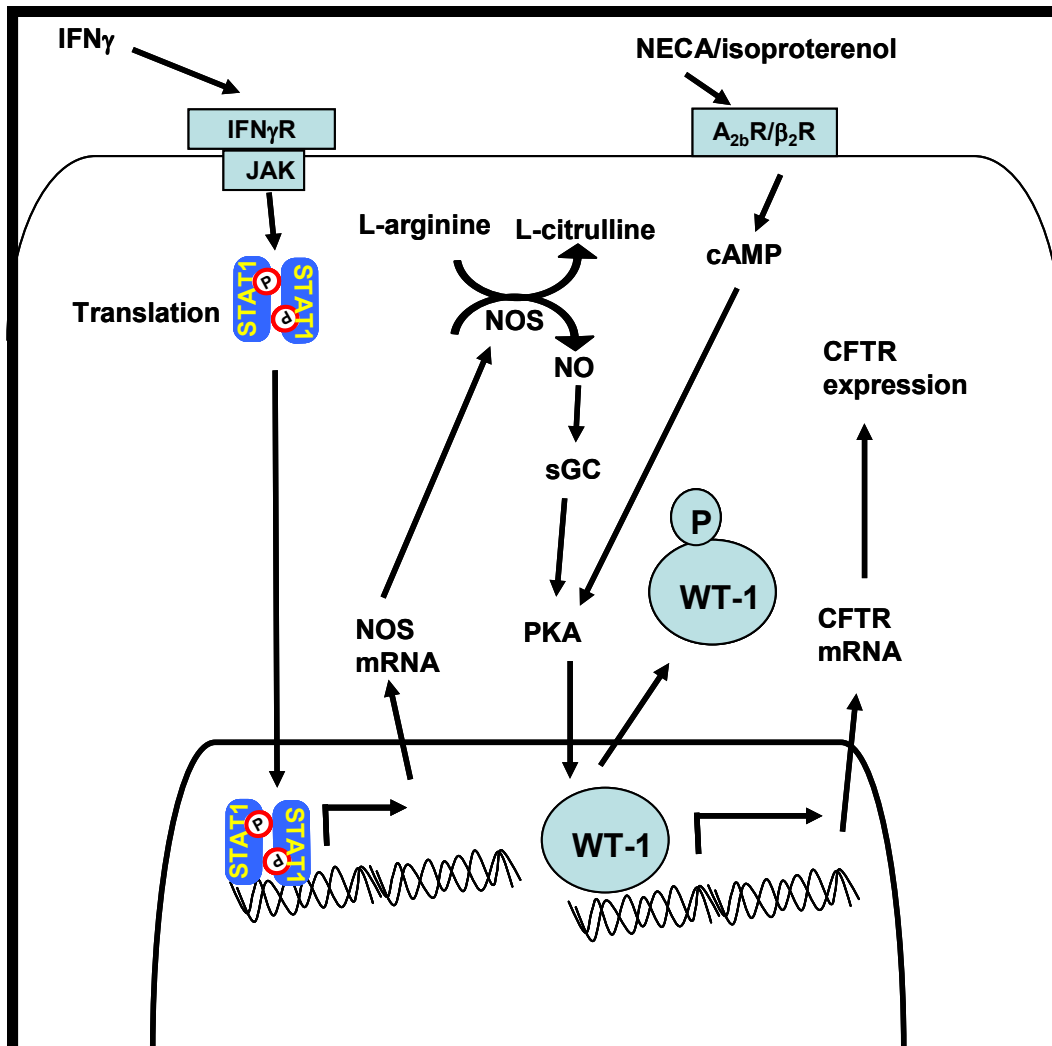


Figure 4.9 Proposed mechanism of WT-1 regulation of CFTR mRNA expression in EC and MC through nitric oxide (NO) soluble guanylate cyclase (sGC) activation of PKA. STAT1 initiates nitric oxide synthase (NOS) expression which makes NO from L-arginine. NO activates sGC which in turn upregulates PKA phosphorylation of WT-1 in the nucleus, releasing it from the first intron of CFTR. Inhibition of WT-1-CFTR interaction by phosphorylation leads to derepression of CFTR and transcription of mRNA. Similar de-repression of WT-1 may also occur as a result of $G_{\alpha s}$ protein coupled receptor activation. Stimulation of adenosine 2b receptor (A $_{2b}$ R) or β_2 adrenergic receptor (β_2 R) may result in PKA activation which leads to CFTR upregulation through WT-1 interactions.

We hypothesize that NO synthesis by NOS enzymes causes activation of PKA through sGC activation and that PKA phosphorylates WT-1 which de-represses CFTR expression (Figure 4.9). Alternately, CFTR de-repression by WT-1 phosphorylation may occur through activation of A_{2b}R or β_2 AR G_{αs} protein coupled receptors. It has been shown that β_2 AR activation upregulates CFTR expression in human EC (380). The authors claim that this effect is post-transcriptional, but this does not rule out transcriptional events which are being masked by changes in mRNA stability. If WT-1 binds to and represses transcription of the CFTR gene, a better understanding of the regulation of WT-1 phosphorylation is necessary which will shed more light on the regulation of CFTR expression and may uncover more therapeutic strategies for the treatment of CF.

F. Conclusion

In this thesis, we attempted to dissect the localization and functional role of CFTR in human MC using CFTR pharmacological inhibitors and RNA interference. These experiments have shown that CFTR is expressed in MC, but at low levels compared to EC. The fact that expression of a protein is low does not preclude its functional significance, as T-cells express CFTR at levels 400-1000 fold lower than EC, but yet CFTR is functional in these cells (195). We have shown that CFTR deficient MC exhibit different cytokine secretion profiles, which may be a contributing factor to the cytokine imbalance seen in CF. The differences in cytokine synthesis and secretion between IgE/anti-IgE and PAO1 stimulated PBMC underscores the complexity of receptor-coupled secretion.

With over 31,000 published articles on CF, and over 5900 published articles on CFTR, it is surprising that many of the functions of this complex protein are not well understood and still controversial. Thus, we need to expand our horizons when it comes to CFTR study, as it is now well accepted that Cl^- channel dysfunction in EC is not the only cause of CF. Continued study of the effects of CFTR on MC function is necessary to help us better understand CF, and to continue to move towards a cure.

Endnotes

The work on CFTR inhibitors in HMC-1 and LAD2 has been submitted for publication to the Journal of Pharmacology and Experimental Therapeutics, September 2009

References

1. Rao, K.N., and M.A. Brown. 2008. Mast cells: multifaceted immune cells with diverse roles in health and disease. *Ann N Y Acad Sci* 1143:83-104.
2. Beaven, M.A. 2009. Our perception of the mast cell from Paul Ehrlich to now. *Eur J Immunol* 39:11-25.
3. Dvorak, A.M. 2005. Ultrastructural studies of human basophils and mast cells. *J Histochem Cytochem* 53:1043-1070.
4. Kirshenbaum, A.S., and D.D. Metcalfe. 2006. Growth of human mast cells from bone marrow and peripheral blood-derived CD34+ pluripotent progenitor cells. *Methods Mol Biol* 315:105-112.
5. Stevens, R.L., M.E. Rothenberg, F. Levi-Schaffer, and K.F. Austen. 1987. Ontogeny of in vitro-differentiated mouse mast cells. *Fed Proc* 46:1915-1919.
6. Yong, L.C., S. Watkins, and D.L. Wilhelm. 1975. The mast cell: distribution and maturation in the peritoneal cavity of the adult rat. *Pathology* 7:307-318.
7. Gurish, M.F., and J.A. Boyce. 2006. Mast cells: ontogeny, homing, and recruitment of a unique innate effector cell. *J Allergy Clin Immunol* 117:1285-1291.
8. Arinobu, Y., H. Iwasaki, and K. Akashi. 2009. Origin of basophils and mast cells. *Allergol Int* 58:21-28.
9. Lappalainen, J., K.A. Lindstedt, and P.T. Kovanen. 2007. A protocol for generating high numbers of mature and functional human mast cells from peripheral blood. *Clin Exp Allergy* 37:1404-1414.
10. Galli, S.J., J. Kalesnikoff, M.A. Grimbaldston, A.M. Piliponsky, C.M. Williams, and M. Tsai. 2005. Mast cells as "tunable" effector and immunoregulatory cells: recent advances. *Annu Rev Immunol* 23:749-786.
11. Kalesnikoff, J., and S.J. Galli. 2008. New developments in mast cell biology. *Nat Immunol* 9:1215-1223.
12. Kitamura, Y., and A. Ito. 2005. Mast cell-committed progenitors. *Proc.Natl.Acad.Sci.U.S.A* 102:11129-11130.

13. Kulka, M., C.H. Sheen, B.P. Tancowny, L.C. Grammer, and R.P. Schleimer. 2008. Neuropeptides activate human mast cell degranulation and chemokine production. *Immunology* 123:398-410.
14. Matthews, G., E. Neher, and R. Penner. 1989. Chloride conductance activated by external agonists and internal messengers in rat peritoneal mast cells. *J Physiol* 418:131-144.
15. Tkaczyk, C., Y. Okayama, D.D. Metcalfe, and A.M. Gilfillan. 2004. Fcγ receptors on mast cells: activatory and inhibitory regulation of mediator release. *Int Arch Allergy Immunol* 133:305-315.
16. Dawicki, W., and J.S. Marshall. 2007. New and emerging roles for mast cells in host defence. *Curr Opin Immunol* 19:31-38.
17. Galli, S.J., J. Kalesnikoff, M.A. Grimaldeston, A.M. Piliponsky, C.M. Williams, and M. Tsai. 2005. Mast cells as "tunable" effector and immunoregulatory cells: recent advances. *Annu.Rev.Immunol.* 23:749-786.
18. Mogensen, T.H. 2009. Pathogen recognition and inflammatory signaling in innate immune defenses. *Clin Microbiol Rev* 22:240-273, Table of Contents.
19. Redegeld, F.A., and F.P. Nijkamp. 2003. Immunoglobulin free light chains and mast cells: pivotal role in T-cell-mediated immune reactions? *Trends Immunol.* 24:181-185.
20. Bellou, A., B. Schaub, L. Ting, and P.W. Finn. 2003. Toll receptors modulate allergic responses: interaction with dendritic cells, T cells and mast cells. *Curr.Opin.Allergy Clin.Immunol* 3:487-494.
21. Forsythe, P., and M. Ennis. 1999. Adenosine, mast cells and asthma. *Inflamm.Res.* 48:301-307.
22. Miller, H.R., and A.D. Pemberton. 2002. Tissue-specific expression of mast cell granule serine proteinases and their role in inflammation in the lung and gut. *Immunology* 105:375-390.
23. Befus, A.D., B. Chin, J. Pick, S. Evans, S. Osborn, and J. Forstrom. 1995. Proteinases of rat mast cells. Peritoneal but not intestinal mucosal mast cells express mast cell proteinase 5 and carboxypeptidase A. *J Immunol* 155:4406-4411.
24. Lutzelschwab, C., G. Pejler, M. Aveskogh, and L. Hellman. 1997. Secretory granule proteases in rat mast cells. Cloning of 10 different serine

- proteases and a carboxypeptidase A from various rat mast cell populations. *J Exp Med* 185:13-29.
25. Ide, H., H. Itoh, M. Tomita, Y. Murakumo, T. Kobayashi, H. Maruyama, Y. Osada, and Y. Nawa. 1995. Cloning of the cDNA encoding a novel rat mast-cell proteinase, rMCP-3, and its expression in comparison with other rat mast-cell proteinases. *Biochem J* 311 (Pt 2):675-680.
 26. Lutzelschwab, C., M.R. Huang, M.C. Kullberg, M. Aveskog, and L. Hellman. 1998. Characterization of mouse mast cell protease-8, the first member of a novel subfamily of mouse mast cell serine proteases, distinct from both the classical chymases and tryptases. *Eur J Immunol* 28:1022-1033.
 27. Kovanen, P.T. 1997. Chymase-containing mast cells in human arterial intima: implications for atherosclerotic disease. *Heart Vessels Suppl* 12:125-127.
 28. Kitamura, Y., Y. Kanakura, S. Sonoda, H. Asai, and T. Nakano. 1987. Mutual phenotypic changes between connective tissue type and mucosal mast cells. *Int Arch Allergy Appl Immunol* 82:244-248.
 29. Puxeddu, I., A.M. Piliponsky, I. Bachelet, and F. Levi-Schaffer. 2003. Mast cells in allergy and beyond. *Int J Biochem Cell Biol* 35:1601-1607.
 30. Luckasen, J.R., J.G. White, and J.H. Kersey. 1974. Mitogenic properties of a calcium ionophore, A23187. *Proc Natl Acad Sci U S A* 71:5088-5090.
 31. Higashijima, T., S. Uzu, T. Nakajima, and E.M. Ross. 1988. Mastoparan, a peptide toxin from wasp venom, mimics receptors by activating GTP-binding regulatory proteins (G proteins). *J Biol Chem* 263:6491-6494.
 32. Higashijima, T., J. Burnier, and E.M. Ross. 1990. Regulation of Gi and Go by mastoparan, related amphiphilic peptides, and hydrophobic amines. Mechanism and structural determinants of activity. *J Biol Chem* 265:14176-14186.
 33. Maggi, C.A. 1995. The mammalian tachykinin receptors. *Gen Pharmacol* 26:911-944.
 34. Mousli, M., T.E. Hugli, Y. Landry, and C. Bronner. 1994. Peptidergic pathway in human skin and rat peritoneal mast cell activation. *Immunopharmacology* 27:1-11.

35. Pfaar, O., U. Raap, M. Holz, K. Hormann, and L. Klimek. 2009. Pathophysiology of itching and sneezing in allergic rhinitis. *Swiss Med Wkly* 139:35-40.
36. Kopec, A., B. Panaszek, and A.M. Fal. 2006. Intracellular signaling pathways in IgE-dependent mast cell activation. *Arch Immunol Ther Exp (Warsz)* 54:393-401.
37. Chen, X.J., and L. Enerback. 2000. Regulation of IgE-receptor expression, IgE occupancy and secretory capacity of mast cells. *Apmis* 108:633-641.
38. Blank, U., and J. Rivera. 2004. The ins and outs of IgE-dependent mast-cell exocytosis. *Trends Immunol* 25:266-273.
39. Marshall, J.S., and D.M. Jawdat. 2004. Mast cells in innate immunity. *Journal of Allergy & Clinical Immunology* 114:21-27.
40. Marshall, J.S. 2004. Mast-cell responses to pathogens. *Nat Rev Immunol* 4:787-799.
41. Marshall, J.S., C.A. King, and J.D. McCurdy. 2003. Mast cell cytokine and chemokine responses to bacterial and viral infection. *Curr Pharm Des* 9:11-24.
42. Kulka, M., and D.D. Metcalfe. 2006. TLR3 activation inhibits human mast cell attachment to fibronectin and vitronectin. *Mol Immunol* 43:1579-1586.
43. Zanker, K.S. 2008. General introduction to innate immunity: Dr. Jekyll/Mr. Hyde quality of the innate immune system. *Contrib Microbiol* 15:12-20.
44. Hasko, G., and B.N. Cronstein. 2004. Adenosine: an endogenous regulator of innate immunity. *Trends Immunol* 25:33-39.
45. Meade, C.J., I. Dumont, and L. Worrall. 2001. Why do asthmatic subjects respond so strongly to inhaled adenosine? *Life Sci* 69:1225-1240.
46. Brown, R.A., D. Spina, and C.P. Page. 2008. Adenosine receptors and asthma. *Br J Pharmacol* 153 Suppl 1:S446-456.
47. Thiel, M., C.C. Caldwell, and M.V. Sitkovsky. 2003. The critical role of adenosine A2A receptors in downregulation of inflammation and immunity in the pathogenesis of infectious diseases. *Microbes.Infect.* 5:515-526.

48. Polosa, R. 2002. Adenosine-receptor subtypes: their relevance to adenosine-mediated responses in asthma and chronic obstructive pulmonary disease. *Eur.Respir.J.* 20:488-496.
49. Meade, C.J., L. Worrall, D. Hayes, and U. Protin. 2002. Induction of interleukin 8 release from the HMC-1 mast cell line: synergy between stem cell factor and activators of the adenosine A(2b) receptor. *Biochem.Pharmacol* 64:317-325.
50. Vliagoftis, H., and A.D. Befus. 2005. Mast cells at mucosal frontiers. *Curr Mol Med* 5:573-589.
51. Vliagoftis, H., and A.D. Befus. 2005. Rapidly changing perspectives about mast cells at mucosal surfaces. *Immunol Rev* 206:190-203.
52. Bissonnette, E.Y., and A.D. Befus. 1998. Mast cells in asthma. *Can Respir J* 5:23-24.
53. Kulka, M., and A.D. Befus. 2003. The dynamic and complex role of mast cells in allergic disease. *Arch.Immunol Ther.Exp (Warsz.)* 51:111-120.
54. Gurish, M.F., and K.F. Austen. 2001. The diverse roles of mast cells. *J Exp Med* 194:F1-5.
55. Okayama, Y., and T. Kawakami. 2006. Development, migration, and survival of mast cells. *Immunol Res* 34:97-115.
56. Okayama, Y., C. Tkaczyk, D.D. Metcalfe, and A.M. Gilfillan. 2003. Comparison of Fc epsilon RI- and Fc gamma RI-mediated degranulation and TNF-alpha synthesis in human mast cells: selective utilization of phosphatidylinositol-3-kinase for Fc gamma RI-induced degranulation. *Eur J Immunol* 33:1450-1459.
57. Nigo, Y.I., M. Yamashita, K. Hirahara, R. Shinnakasu, M. Inami, M. Kimura, A. Hasegawa, Y. Kohno, and T. Nakayama. 2006. Regulation of allergic airway inflammation through Toll-like receptor 4-mediated modification of mast cell function. *Proc Natl Acad Sci U S A* 103:2286-2291.
58. Forsythe, P., M. Gilchrist, M. Kulka, and A.D. Befus. 2001. Mast cells and nitric oxide: control of production, mechanisms of response. *Int Immunopharmacol* 1:1525-1541.
59. Tachimoto, H., M. Ebisawa, T. Hasegawa, T. Kashiwabara, C. Ra, B.S. Bochner, K. Miura, and H. Saito. 2000. Reciprocal regulation of cultured

- human mast cell cytokine production by IL-4 and IFN-gamma. *J Allergy Clin Immunol* 106:141-149.
60. Okayama, Y., D.D. Hagan, and D.D. Metcalfe. 2001. A comparison of mediators released or generated by IFN-gamma-treated human mast cells following aggregation of Fc gamma RI or Fc epsilon RI. *J Immunol* 166:4705-4712.
 61. Theoharides, T.C., D. Kempuraj, M. Tager, P. Conti, and D. Kalogeromitros. 2007. Differential release of mast cell mediators and the pathogenesis of inflammation. *Immunol Rev* 217:65-78.
 62. Miller, H.R. 1996. Mucosal mast cells and the allergic response against nematode parasites. *Vet Immunol Immunopathol* 54:331-336.
 63. Theoharides, T.C., and W.W. Douglas. 1978. Secretion in mast cells induced by calcium entrapped within phospholipid vesicles. *Science* 201:1143-1145.
 64. Pickett, J.A., and J.M. Edwardson. 2006. Compound exocytosis: mechanisms and functional significance. *Traffic* 7:109-116.
 65. Benado, A., Y. Nasagi-Atiya, and R. Sagi-Eisenberg. 2009. Protein trafficking in immune cells. *Immunobiology* 214:403-421.
 66. Luster, A.D., and A.M. Tager. 2004. T-cell trafficking in asthma: lipid mediators grease the way. *Nat Rev Immunol* 4:711-724.
 67. Frossi, B., M. De Carli, and C. Pucillo. 2004. The mast cell: an antenna of the microenvironment that directs the immune response. *J Leukoc Biol* 75:579-585.
 68. Maurer, M., T. Theoharides, R.D. Granstein, S.C. Bischoff, J. Bienenstock, B. Henz, P. Kovanen, A.M. Piliponsky, N. Kambe, H. Vliagoftis, F. Levi-Schaffer, M. Metz, Y. Miyachi, D. Befus, P. Forsythe, Y. Kitamura, and S. Galli. 2003. What is the physiological function of mast cells? *Exp Dermatol* 12:886-910.
 69. Noli, C., and A. Miolo. 2001. The mast cell in wound healing. *Vet Dermatol* 12:303-313.
 70. Metcalfe, D.D., D. Baram, and Y.A. Mekori. 1997. Mast cells. *Physiol Rev* 77:1033-1079.
 71. Kulka, M., N. Fukuishi, M. Rottem, Y.A. Mekori, and D.D. Metcalfe. 2006. Mast cells, which interact with *Escherichia coli*, up-regulate genes

associated with innate immunity and become less responsive to Fc(epsilon)RI-mediated activation. *J Leukoc Biol* 79:339-350.

72. Okumura, S., J. Kashiwakura, H. Tomita, K. Matsumoto, T. Nakajima, H. Saito, and Y. Okayama. 2003. Identification of specific gene expression profiles in human mast cells mediated by Toll-like receptor 4 and FcepsilonRI. *Blood* 102:2547-2554.
73. Hosoda, M., M. Yamaya, T. Suzuki, N. Yamada, M. Kamanaka, K. Sekizawa, J.H. Butterfield, T. Watanabe, H. Nishimura, and H. Sasaki. 2002. Effects of rhinovirus infection on histamine and cytokine production by cell lines from human mast cells and basophils. *J Immunol* 169:1482-1491.
74. Kirshenbaum, A.S., E. Swindle, M. Kulka, Y. Wu, and D.D. Metcalfe. 2008. Effect of lipopolysaccharide (LPS) and peptidoglycan (PGN) on human mast cell numbers, cytokine production, and protease composition. *BMC Immunol* 9:45.
75. Galli, S.J., S. Nakae, and M. Tsai. 2005. Mast cells in the development of adaptive immune responses. *Nat Immunol* 6:135-142.
76. McNeil, H.P., R. Adachi, and R.L. Stevens. 2007. Mast cell-restricted tryptases: structure and function in inflammation and pathogen defense. *J Biol Chem* 282:20785-20789.
77. Chen, R., G. Ning, M.L. Zhao, M.G. Fleming, L.A. Diaz, Z. Werb, and Z. Liu. 2001. Mast cells play a key role in neutrophil recruitment in experimental bullous pemphigoid. *J Clin Invest* 108:1151-1158.
78. Nelson, K.C., M. Zhao, P.R. Schroeder, N. Li, R.A. Wetsel, L.A. Diaz, and Z. Liu. 2006. Role of different pathways of the complement cascade in experimental bullous pemphigoid. *J Clin Invest* 116:2892-2900.
79. Varadaradjalou, S., F. Feger, N. Thieblemont, N.B. Hamouda, J.M. Pleau, M. Dy, and M. Arock. 2003. Toll-like receptor 2 (TLR2) and TLR4 differentially activate human mast cells. *Eur J Immunol* 33:899-906.
80. McCurdy, J.D., T.J. Olynych, L.H. Maher, and J.S. Marshall. 2003. Cutting edge: distinct Toll-like receptor 2 activators selectively induce different classes of mediator production from human mast cells. *J Immunol* 170:1625-1629.
81. Supajatura, V., H. Ushio, A. Nakao, S. Akira, K. Okumura, C. Ra, and H. Ogawa. 2002. Differential responses of mast cell Toll-like receptors 2 and 4 in allergy and innate immunity. *J Clin Invest* 109:1351-1359.

82. Najib, U., and J. Sheikh. 2009. The spectrum of chronic urticaria. *Allergy Asthma Proc* 30:1-10.
83. Brown, J.M., T.M. Wilson, and D.D. Metcalfe. 2008. The mast cell and allergic diseases: role in pathogenesis and implications for therapy. *Clin Exp Allergy* 38:4-18.
84. Bunimovich, O., M. Grassi, and M.R. Baer. 2009. Systemic mastocytosis: classification, pathogenesis, diagnosis, and treatment. *Cutis* 83:29-36.
85. Wasiuk, A., V.C. de Vries, K. Hartmann, A. Roers, and R.J. Noelle. 2009. Mast cells as regulators of adaptive immunity to tumours. *Clin Exp Immunol* 155:140-146.
86. Fairweather, D., and S. Frisancho-Kiss. 2008. Mast cells and inflammatory heart disease: potential drug targets. *Cardiovasc Hematol Disord Drug Targets* 8:80-90.
87. He, S.H. 2004. Key role of mast cells and their major secretory products in inflammatory bowel disease. *World J Gastroenterol* 10:309-318.
88. Bradding, P., J.A. Roberts, K.M. Britten, S. Montefort, R. Djukanovic, R. Mueller, C.H. Heusser, P.H. Howarth, and S.T. Holgate. 1994. Interleukin-4, -5, and -6 and tumor necrosis factor-alpha in normal and asthmatic airways: evidence for the human mast cell as a source of these cytokines. *Am J Respir Cell Mol Biol* 10:471-480.
89. Pawankar, R. 2001. Mast cells as orchestrators of the allergic reaction: the IgE-IgE receptor mast cell network. *Curr Opin Allergy Clin Immunol* 1:3-6.
90. Vass, G., and I. Horvath. 2008. Adenosine and adenosine receptors in the pathomechanism and treatment of respiratory diseases. *Curr Med Chem* 15:917-922.
91. Huszar, E., G. Vass, E. Vizi, Z. Csoma, E. Barat, V.G. Molnar, I. Herjavec, and I. Horvath. 2002. Adenosine in exhaled breath condensate in healthy volunteers and in patients with asthma. *Eur.Respir.J.* 20:1393-1398.
92. Nilius, B., and G. Droogmans. 2003. Amazing chloride channels: an overview. *Acta Physiol Scand.* 177:119-147.
93. Bradding, P., and E.C. Conley. 2002. Human mast cell ion channels. *Clin Exp Allergy* 32:979-983.

94. Romanin, C., M. Reinsprecht, I. Pecht, and H. Schindler. 1991. Immunologically activated chloride channels involved in degranulation of rat mucosal mast cells. *Embo J* 10:3603-3608.
95. Seebeck, J., S. Tritschler, T. Roloff, M.L. Kruse, W.E. Schmidt, and A. Ziegler. 2002. The outwardly rectifying chloride channel in rat peritoneal mast cells is regulated by serine/threonine kinases and phosphatases. *Pflugers Arch* 443:558-564.
96. Duffy, S.M., W.J. Lawley, E.C. Conley, and P. Bradding. 2001. Resting and activation-dependent ion channels in human mast cells. *J Immunol* 167:4261-4270.
97. Duffy, S.M., M.L. Leyland, E.C. Conley, and P. Bradding. 2001. Voltage-dependent and calcium-activated ion channels in the human mast cell line HMC-1. *J Leukoc Biol* 70:233-240.
98. Dietrich, J., and M. Lindau. 1994. Chloride channels in mast cells: block by DIDS and role in exocytosis. *J Gen Physiol* 104:1099-1111.
99. Redrup, A.C., J.C. Foreman, N.A. Hayes, and F.L. Pearce. 1997. Fc epsilon RI-mediated chloride uptake by rat mast cells: modulation by chloride transport inhibitors in relation to histamine secretion. *Br J Pharmacol* 122:1188-1194.
100. Meyer, G., S. Doppiero, P. Vallin, and L. Daffonchio. 1996. Effect of frusemide on Cl⁻ channel in rat peritoneal mast cells. *Eur Respir J* 9:2461-2467.
101. Bradding, P., Y. Okayama, N. Kambe, and H. Saito. 2003. Ion channel gene expression in human lung, skin, and cord blood-derived mast cells. *J Leukoc Biol* 73:614-620.
102. Wu, Y., J. Hu, R. Zhang, C. Zhou, Y. Xu, X. Guan, and S. Li. 2008. Enhanced intracellular calcium induced by urocortin is involved in degranulation of rat lung mast cells. *Cell Physiol Biochem* 21:173-182.
103. Mark Duffy, S., P. Berger, G. Cruse, W. Yang, S.J. Bolton, and P. Bradding. 2004. The K⁺ channel iKCA1 potentiates Ca²⁺ influx and degranulation in human lung mast cells. *J Allergy Clin Immunol* 114:66-72.
104. Ratner, P.H., P.M. Ehrlich, S.M. Fineman, E.O. Meltzer, and D.P. Skoner. 2002. Use of intranasal cromolyn sodium for allergic rhinitis. *Mayo Clin Proc* 77:350-354.

105. Kay, A.B., G.M. Walsh, R. Moqbel, A.J. MacDonald, T. Nagakura, M.P. Carroll, and H.B. Richerson. 1987. Disodium cromoglycate inhibits activation of human inflammatory cells in vitro. *J Allergy Clin Immunol* 80:1-8.
106. Altounyan, R.E. 1980. Review of clinical activity and mode of action of sodium cromoglycate. *Clin Allergy* 10 Suppl:481-489.
107. Kulka, M., M. Gilchrist, M. Duszyk, and A.D. Befus. 2002. Expression and functional characterization of CFTR in mast cells. *J.Leukoc.Biol* 71:54-64.
108. Foskett, J.K. 1998. ClC and CFTR chloride channel gating. *Annu Rev Physiol* 60:689-717.
109. Jentsch, T.J. 2008. CLC chloride channels and transporters: from genes to protein structure, pathology and physiology. *Crit Rev Biochem Mol Biol* 43:3-36.
110. Mohammad-Panah, R., C. Ackerley, J. Rommens, M. Choudhury, Y. Wang, and C.E. Bear. 2002. The chloride channel ClC-4 co-localizes with cystic fibrosis transmembrane conductance regulator and may mediate chloride flux across the apical membrane of intestinal epithelia. *J Biol Chem* 277:566-574.
111. Kulka, M., A. Schwingshackl, and A.D. Befus. 2002. Mast cells express chloride channels of the ClC family. *Inflamm Res* 51:451-456.
112. Suzuki, M., T. Morita, and T. Iwamoto. 2006. Diversity of Cl(-) channels. *Cell Mol Life Sci* 63:12-24.
113. Kulka, M. 2002. IFN γ modulates Chloride in Mast Cells. In *Medicine*. University of Alberta, Edmonton. 258.
114. Mendoza, J.L., and P.J. Thomas. 2007. Building an understanding of cystic fibrosis on the foundation of ABC transporter structures. *J Bioenerg Biomembr* 39:499-505.
115. Hanrahan, J.W., and M.A. Wioland. 2004. Revisiting Cystic Fibrosis Transmembrane Conductance Regulator Structure and Function. In *Proceedings of the American Thoracic Society*. 17-21.
116. Ostedgaard, L.S., O. Baldursson, and M.J. Welsh. 2001. Regulation of the cystic fibrosis transmembrane conductance regulator Cl⁻ channel by its R domain. *J Biol Chem* 276:7689-7692.

117. Muallem, D., and P. Vergani. 2009. Review. ATP hydrolysis-driven gating in cystic fibrosis transmembrane conductance regulator. *Philos Trans R Soc Lond B Biol Sci* 364:247-255.
118. Berger, H.A., S.M. Travis, and M.J. Welsh. 1993. Regulation of the cystic fibrosis transmembrane conductance regulator Cl⁻ channel by specific protein kinases and protein phosphatases. *J Biol Chem* 268:2037-2047.
119. Chappe, V., D.A. Hinkson, L.D. Howell, A. Evagelidis, J. Liao, X.B. Chang, J.R. Riordan, and J.W. Hanrahan. 2004. Stimulatory and inhibitory protein kinase C consensus sequences regulate the cystic fibrosis transmembrane conductance regulator. *Proc Natl Acad Sci U S A* 101:390-395.
120. Chappe, V., D.A. Hinkson, T. Zhu, X.B. Chang, J.R. Riordan, and J.W. Hanrahan. 2003. Phosphorylation of protein kinase C sites in NBD1 and the R domain control CFTR channel activation by PKA. *J Physiol* 548:39-52.
121. Chen, Y., B. Button, G.A. Altenberg, and L. Reuss. 2004. Potentiation of effect of PKA stimulation of *Xenopus* CFTR by activation of PKC: role of NBD2. *Am J Physiol Cell Physiol* 287:C1436-1444.
122. Dulhanty, A.M., and J.R. Riordan. 1994. Phosphorylation by cAMP-dependent protein kinase causes a conformational change in the R domain of the cystic fibrosis transmembrane conductance regulator. *Biochemistry* 33:4072-4079.
123. Fischer, H., B. Illek, and T.E. Machen. 1998. Regulation of CFTR by protein phosphatase 2B and protein kinase C. *Pflugers Arch* 436:175-181.
124. Thelin, W.R., M. Kesimer, R. Tarran, S.M. Kreda, B.R. Grubb, J.K. Sheehan, M.J. Stutts, and S.L. Milgram. 2005. The cystic fibrosis transmembrane conductance regulator is regulated by a direct interaction with the protein phosphatase 2A. *J Biol Chem* 280:41512-41520.
125. Choo-Kang, L.R., and P.L. Zeitlin. 2000. Type I, II, III, IV, and V cystic fibrosis transmembrane conductance regulator defects and opportunities for therapy. *Curr Opin Pulm Med* 6:521-529.
126. Rowe, S.M., K. Varga, A. Rab, Z. Bebok, K. Byram, Y. Li, E.J. Sorscher, and J.P. Clancy. 2007. Restoration of W1282X CFTR activity by enhanced expression. *Am J Respir Cell Mol Biol* 37:347-356.

127. Howard, M., R.A. Frizzell, and D.M. Bedwell. 1996. Aminoglycoside antibiotics restore CFTR function by overcoming premature stop mutations. *Nat Med* 2:467-469.
128. Thomas, P.J., and P.L. Pedersen. 1993. Effects of the delta F508 mutation on the structure, function, and folding of the first nucleotide-binding domain of CFTR. *J Bioenerg Biomembr* 25:11-19.
129. Ward, C.L., and R.R. Kopito. 1994. Intracellular turnover of cystic fibrosis transmembrane conductance regulator. Inefficient processing and rapid degradation of wild-type and mutant proteins. *J Biol Chem* 269:25710-25718.
130. Ward, C.L., S. Omura, and R.R. Kopito. 1995. Degradation of CFTR by the ubiquitin-proteasome pathway. *Cell* 83:121-127.
131. Brown, C.R., L.Q. Hong-Brown, and W.J. Welch. 1997. Correcting temperature-sensitive protein folding defects. *J Clin Invest* 99:1432-1444.
132. Brown, C.R., L.Q. Hong-Brown, J. Biwersi, A.S. Verkman, and W.J. Welch. 1996. Chemical chaperones correct the mutant phenotype of the delta F508 cystic fibrosis transmembrane conductance regulator protein. *Cell Stress Chaperones* 1:117-125.
133. Yang, Y., J.F. Engelhardt, and J.M. Wilson. 1994. Ultrastructural localization of variant forms of cystic fibrosis transmembrane conductance regulator in human bronchial epithelial of xenografts. *Am J Respir Cell Mol Biol* 11:7-15.
134. Yang, Y., D.C. Devor, J.F. Engelhardt, S.A. Ernst, T.V. Strong, F.S. Collins, J.A. Cohn, R.A. Frizzell, and J.M. Wilson. 1993. Molecular basis of defective anion transport in L cells expressing recombinant forms of CFTR. *Hum Mol Genet* 2:1253-1261.
135. Reenstra, W.W., K. Yurko-Mauro, A. Dam, S. Raman, and S. Shorten. 1996. CFTR chloride channel activation by genistein: the role of serine/threonine protein phosphatases. *Am J Physiol* 271:C650-657.
136. Kelley, T.J., L. Al-Nakkash, C.U. Cotton, and M.L. Drumm. 1996. Activation of endogenous deltaF508 cystic fibrosis transmembrane conductance regulator by phosphodiesterase inhibition. *J Clin Invest* 98:513-520.
137. Chiba-Falek, O., E. Kerem, T. Shoshani, M. Aviram, A. Augarten, L. Bentur, A. Tal, E. Tullis, A. Rahat, and B. Kerem. 1998. The molecular

basis of disease variability among cystic fibrosis patients carrying the 3849+10 kb C->T mutation. *Genomics* 53:276-283.

138. Maitra, R., C.M. Shaw, B.A. Stanton, and J.W. Hamilton. 2001. Functional enhancement of CFTR expression by mitomycin C. *Cell Physiol Biochem* 11:93-98.
139. McCarthy, V.A., and A. Harris. 2005. The CFTR gene and regulation of its expression. *Pediatr.Pulmonol.* 40:1-8.
140. Paul, T., S. Li, S. Khurana, N.S. Leleiko, and M.J. Walsh. 2007. The epigenetic signature of CFTR expression is co-ordinated via chromatin acetylation through a complex intronic element. *Biochem J* 408:317-326.
141. Trezise, A.E., C.C. Linder, D. Grieger, E.W. Thompson, H. Meunier, M.D. Griswold, and M. Buchwald. 1993. CFTR expression is regulated during both the cycle of the seminiferous epithelium and the oestrous cycle of rodents. *Nat Genet* 3:157-164.
142. White, N.L., C.F. Higgins, and A.E. Trezise. 1998. Tissue-specific in vivo transcription start sites of the human and murine cystic fibrosis genes. *Hum Mol Genet* 7:363-369.
143. Rowntree, R.K., G. Vassaux, T.L. McDowell, S. Howe, A. McGuigan, M. Phylactides, C. Huxley, and A. Harris. 2001. An element in intron 1 of the CFTR gene augments intestinal expression in vivo. *Hum Mol Genet* 10:1455-1464.
144. Smith, A.N., M.L. Barth, T.L. McDowell, D.S. Moulin, H.N. Nuthall, M.A. Hollingsworth, and A. Harris. 1996. A regulatory element in intron 1 of the cystic fibrosis transmembrane conductance regulator gene. *J Biol Chem* 271:9947-9954.
145. Baudouin-Legros, M., A. Hinzpeter, A. Jaulmes, F. Brouillard, B. Costes, P. Fanen, and A. Edelman. 2005. Cell-specific posttranscriptional regulation of CFTR gene expression via influence of MAPK cascades on 3'UTR part of transcripts. *Am.J.Physiol Cell Physiol* 289:C1240-C1250.
146. Barreau, C., L. Paillard, and H.B. Osborne. 2005. AU-rich elements and associated factors: are there unifying principles? *Nucleic Acids Res* 33:7138-7150.
147. Hartl, D., M. Griesse, M. Kappler, G. Zissel, D. Reinhardt, C. Rebhan, D.J. Schendel, and S. Krauss-Etschmann. 2006. Pulmonary T(H)2 response in *Pseudomonas aeruginosa*-infected patients with cystic fibrosis. *J Allergy Clin Immunol* 117:204-211.

148. Gregory, R.J., S.H. Cheng, D.P. Rich, J. Marshall, S. Paul, K. Hehir, L. Ostedgaard, K.W. Klinger, M.J. Welsh, and A.E. Smith. 1990. Expression and characterization of the cystic fibrosis transmembrane conductance regulator. *Nature* 347:382-386.
149. O'Riordan, C.R., A.L. Lachapelle, J. Marshall, E.A. Higgins, and S.H. Cheng. 2000. Characterization of the oligosaccharide structures associated with the cystic fibrosis transmembrane conductance regulator. *Glycobiology* 10:1225-1233.
150. Kopito, R.R. 1999. Biosynthesis and degradation of CFTR. *Physiol Rev* 79:S167-173.
151. Zeitlin, P.L., I. Crawford, L. Lu, S. Woel, M.E. Cohen, M. Donowitz, M.H. Montrose, A. Hamosh, G.R. Cutting, D. Gruenert, and et al. 1992. CFTR protein expression in primary and cultured epithelia. *Proc Natl Acad Sci U S A* 89:344-347.
152. Mulberg, A.E., E.B. Wiedner, X. Bao, J. Marshall, D.M. Jefferson, and S.M. Altschuler. 1994. Cystic fibrosis transmembrane conductance regulator protein expression in brain. *Neuroreport* 5:1684-1688.
153. Devuyst, O., C.R. Burrow, E.M. Schwiebert, W.B. Guggino, and P.D. Wilson. 1996. Developmental regulation of CFTR expression during human nephrogenesis. *Am J Physiol* 271:F723-735.
154. Devuyst, O., P.E. Golstein, M.V. Sanches, K. Piontek, P.D. Wilson, W.B. Guggino, J.E. Dumont, and R. Beauwens. 1997. Expression of CFTR in human and bovine thyroid epithelium. *Am J Physiol* 272:C1299-1308.
155. Luo, Y., K. McDonald, and J.W. Hanrahan. 2009. Trafficking of immature DeltaF508-CFTR to the plasma membrane and its detection by biotinylation. *Biochem J* 419:211-219, 212 p following 219.
156. Xie, J., M.L. Drumm, J. Zhao, J. Ma, and P.B. Davis. 1996. Human epithelial cystic fibrosis transmembrane conductance regulator without exon 5 maintains partial chloride channel function in intracellular membranes. *Biophys J* 71:3148-3156.
157. Bradbury, N.A., J.A. Clark, S.C. Watkins, C.C. Widnell, H.S.t. Smith, and R.J. Bridges. 1999. Characterization of the internalization pathways for the cystic fibrosis transmembrane conductance regulator. *Am J Physiol* 276:L659-668.

158. Nichols, D., J. Chmiel, and M. Berger. 2008. Chronic inflammation in the cystic fibrosis lung: alterations in inter- and intracellular signaling. *Clin Rev Allergy Immunol* 34:146-162.
159. Devuyst, O., and W.B. Guggino. 2002. Chloride channels in the kidney: lessons learned from knockout animals. *Am J Physiol Renal Physiol* 283:F1176-1191.
160. Scanlin, T.F., and M.C. Glick. 1999. Terminal glycosylation in cystic fibrosis. *Biochim Biophys Acta* 1455:241-253.
161. Li, C., and A.P. Naren. 2005. Macromolecular complexes of cystic fibrosis transmembrane conductance regulator and its interacting partners. *Pharmacol Ther* 108:208-223.
162. Cormet-Boyaka, E., A. Di, S.Y. Chang, A.P. Naren, A. Tousson, D.J. Nelson, and K.L. Kirk. 2002. CFTR chloride channels are regulated by a SNAP-23/syntaxin 1A complex. *Proc Natl Acad Sci U S A* 99:12477-12482.
163. Chang, S.Y., A. Di, A.P. Naren, H.C. Palfrey, K.L. Kirk, and D.J. Nelson. 2002. Mechanisms of CFTR regulation by syntaxin 1A and PKA. *J Cell Sci* 115:783-791.
164. Naren, A.P., B. Cobb, C. Li, K. Roy, D. Nelson, G.D. Heda, J. Liao, K.L. Kirk, E.J. Sorscher, J. Hanrahan, and J.P. Clancy. 2003. A macromolecular complex of beta 2 adrenergic receptor, CFTR, and ezrin/radixin/moesin-binding phosphoprotein 50 is regulated by PKA. *Proc Natl Acad Sci U S A* 100:342-346.
165. Short, D.B., K.W. Trotter, D. Reczek, S.M. Kreda, A. Bretscher, R.C. Boucher, M.J. Stutts, and S.L. Milgram. 1998. An apical PDZ protein anchors the cystic fibrosis transmembrane conductance regulator to the cytoskeleton. *J Biol Chem* 273:19797-19801.
166. Sitaraman, S.V., L. Wang, M. Wong, M. Bruewer, M. Hobert, C.H. Yun, D. Merlin, and J.L. Madara. 2002. The adenosine 2b receptor is recruited to the plasma membrane and associates with E3KARP and Ezrin upon agonist stimulation. *J Biol Chem* 277:33188-33195.
167. Moyer, B.D., J. Denton, K.H. Karlson, D. Reynolds, S. Wang, J.E. Mickle, M. Milewski, G.R. Cutting, W.B. Guggino, M. Li, and B.A. Stanton. 1999. A PDZ-interacting domain in CFTR is an apical membrane polarization signal. *J.Clin.Invest* 104:1353-1361.

168. Bissonnette, E.Y., and A.D. Befus. 1997. Anti-inflammatory effect of beta 2-agonists: inhibition of TNF-alpha release from human mast cells. *Journal of Allergy & Clinical Immunology* 100:825-831.
169. Li, C., and A.P. Naren. 2005. Macromolecular complexes of cystic fibrosis transmembrane conductance regulator and its interacting partners. *Pharmacol.Ther.* 108:208-223.
170. Weixel, K.M., and N.A. Bradbury. 2000. The carboxyl terminus of the cystic fibrosis transmembrane conductance regulator binds to AP-2 clathrin adaptors. *J Biol Chem* 275:3655-3660.
171. Hallows, K.R., V. Raghuram, B.E. Kemp, L.A. Witters, and J.K. Foskett. 2000. Inhibition of cystic fibrosis transmembrane conductance regulator by novel interaction with the metabolic sensor AMP-activated protein kinase. *J Clin Invest* 105:1711-1721.
172. Knorre, A., M. Wagner, H.E. Schaefer, W.H. Colledge, and H.L. Pahl. 2002. DeltaF508-CFTR causes constitutive NF-kappaB activation through an ER-overload response in cystic fibrosis lungs. *Biol Chem.* 383:271-282.
173. Venkatakrishnan, A., A.A. Stecenko, G. King, T.R. Blackwell, K.L. Brigham, J.W. Christman, and T.S. Blackwell. 2000. Exaggerated activation of nuclear factor-kappaB and altered IkappaB-beta processing in cystic fibrosis bronchial epithelial cells. *Am.J.Respir.Cell Mol.Biol* 23:396-403.
174. Estell, K., G. Braunstein, T. Tucker, K. Varga, J.F. Collawn, and L.M. Schwiebert. 2003. Plasma membrane CFTR regulates RANTES expression via its C-terminal PDZ-interacting motif. *Mol Cell Biol* 23:594-606.
175. Weber, A.J., G. Soong, R. Bryan, S. Saba, and A. Prince. 2001. Activation of NF-kappaB in airway epithelial cells is dependent on CFTR trafficking and Cl- channel function. *Am J Physiol Lung Cell Mol Physiol* 281:L71-78.
176. Bonfield, T.L., M.W. Konstan, P. Burfeind, J.R. Panuska, J.B. Hilliard, and M. Berger. 1995. Normal bronchial epithelial cells constitutively produce the anti-inflammatory cytokine interleukin-10, which is downregulated in cystic fibrosis. *Am J Respir Cell Mol Biol* 13:257-261.
177. Chin, K.V., W.L. Yang, R. Ravatn, T. Kita, E. Reitman, D. Vettori, M.E. Cvijic, M. Shin, and L. Iacono. 2002. Reinventing the wheel of cyclic AMP: novel mechanisms of cAMP signaling. *Ann.N.Y.Acad.Sci.* 968:49-64.

178. Linsdell, P. 2005. Location of a common inhibitor binding site in the cytoplasmic vestibule of the cystic fibrosis transmembrane conductance regulator chloride channel pore. *J Biol Chem* 280:8945-8950.
179. Schultz, B.D., A.K. Singh, D.C. Devor, and R.J. Bridges. 1999. Pharmacology of CFTR chloride channel activity. *Physiol Rev* 79:S109-144.
180. McCarty, N.A. 2000. Permeation through the CFTR chloride channel. *J Exp Biol* 203:1947-1962.
181. Quinton, P.M., and M.M. Reddy. 2000. CFTR, a rectifying, non-rectifying anion channel? *J Korean Med Sci* 15 Suppl:S17-20.
182. Li, H., I.A. Findlay, and D.N. Sheppard. 2004. The relationship between cell proliferation, Cl⁻ secretion, and renal cyst growth: a study using CFTR inhibitors. *Kidney Int* 66:1926-1938.
183. Reddy, M.M., and P.M. Quinton. 2002. Effect of anion transport blockers on CFTR in the human sweat duct. *J Membr Biol* 189:15-25.
184. Keeling, D.J., A.G. Taylor, and P.L. Smith. 1991. Effects of NPPB (5-nitro-2-(3-phenylpropylamino)benzoic acid) on chloride transport in intestinal tissues and the T84 cell line. *Biochim Biophys Acta* 1115:42-48.
185. Lukacs, G.L., A. Nanda, O.D. Rotstein, and S. Grinstein. 1991. The chloride channel blocker 5-nitro-2-(3-phenylpropyl-amino) benzoic acid (NPPB) uncouples mitochondria and increases the proton permeability of the plasma membrane in phagocytic cells. *FEBS Lett* 288:17-20.
186. Stutts, M.J., D.C. Henke, and R.C. Boucher. 1990. Diphenylamine-2-carboxylate (DPC) inhibits both Cl⁻ conductance and cyclooxygenase of canine tracheal epithelium. *Pflügers Arch* 415:611-616.
187. Sheppard, D.N. 2004. CFTR channel pharmacology: novel pore blockers identified by high-throughput screening. *J Gen Physiol* 124:109-113.
188. Wang, X.F., M.M. Reddy, and P.M. Quinton. 2004. Effects of a new cystic fibrosis transmembrane conductance regulator inhibitor on Cl⁻ conductance in human sweat ducts. *Exp Physiol* 89:417-425.
189. Muanprasat, C., N.D. Sonawane, D. Salinas, A. Taddei, L.J. Galletta, and A.S. Verkman. 2004. Discovery of glycine hydrazide pore-occluding CFTR inhibitors: mechanism, structure-activity analysis, and in vivo efficacy. *J Gen Physiol* 124:125-137.

190. Al-Awqati, Q. 2002. Alternative treatment for secretory diarrhea revealed in a new class of CFTR inhibitors. *J Clin Invest* 110:1599-1601.
191. Taddei, A., C. Folli, O. Zegarra-Moran, P. Fanen, A.S. Verkman, and L.J. Galiotta. 2004. Altered channel gating mechanism for CFTR inhibition by a high-affinity thiazolidinone blocker. *FEBS Lett* 558:52-56.
192. Thiagarajah, J.R., Y. Song, P.M. Haggie, and A.S. Verkman. 2004. A small molecule CFTR inhibitor produces cystic fibrosis-like submucosal gland fluid secretions in normal airways. *Faseb J* 18:875-877.
193. Ma, T., J.R. Thiagarajah, H. Yang, N.D. Sonawane, C. Folli, L.J. Galiotta, and A.S. Verkman. 2002. Thiazolidinone CFTR inhibitor identified by high-throughput screening blocks cholera toxin-induced intestinal fluid secretion. *J Clin Invest* 110:1651-1658.
194. Yoshimura, K., H. Nakamura, B.C. Trapnell, C.S. Chu, W. Dalemans, A. Pavirani, J.P. Lecocq, and R.G. Crystal. 1991. Expression of the cystic fibrosis transmembrane conductance regulator gene in cells of non-epithelial origin. *Nucleic Acids Res.* 19:5417-5423.
195. Krauss, R.D., G. Berta, T.A. Rado, and J.K. Bubien. 1992. Antisense oligonucleotides to CFTR confer a cystic fibrosis phenotype on B lymphocytes. *Am J Physiol* 263:C1147-1151.
196. Hernandez-Gonzalez, E.O., C.L. Trevino, L.E. Castellano, J.L. de la Vega-Beltran, A.Y. Ocampo, E. Wertheimer, P.E. Visconti, and A. Darszon. 2007. Involvement of cystic fibrosis transmembrane conductance regulator in mouse sperm capacitation. *J Biol Chem* 282:24397-24406.
197. Stutts, M.J., S.E. Gabriel, J.C. Olsen, J.T. Gatzky, T.L. O'Connell, E.M. Price, and R.C. Boucher. 1993. Functional consequences of heterologous expression of the cystic fibrosis transmembrane conductance regulator in fibroblasts. *J Biol Chem* 268:20653-20658.
198. Courtney, J.M., M. Ennis, and J.S. Elborn. 2004. Cytokines and inflammatory mediators in cystic fibrosis. *J Cyst Fibros* 3:223-231.
199. Dong, Y.J., A.C. Chao, K. Kouyama, Y.P. Hsu, R.C. Bocian, R.B. Moss, and P. Gardner. 1995. Activation of CFTR chloride current by nitric oxide in human T lymphocytes. *Embo J* 14:2700-2707.
200. Brennan, S. 2008. Innate immune activation and cystic fibrosis. *Paediatr Respir Rev* 9:271-279; quiz 279-280.

201. Kulka, M., R. Dery, D. Nahirney, M. Duszyk, and A.D. Befus. 2005. Differential regulation of cystic fibrosis transmembrane conductance regulator by interferon gamma in mast cells and epithelial cells. *J Pharmacol Exp Ther* 315:563-570.
202. Painter, R.G., V.G. Valentine, N.A. Lanson, Jr., K. Leidal, Q. Zhang, G. Lombard, C. Thompson, A. Viswanathan, W.M. Nauseef, G. Wang, and G. Wang. 2006. CFTR Expression in human neutrophils and the phagolysosomal chlorination defect in cystic fibrosis. *Biochemistry* 45:10260-10269.
203. Tirouvanziam, R., Y. Gernez, C.K. Conrad, R.B. Moss, I. Schrijver, C.E. Dunn, Z.A. Davies, L.A. Herzenberg, and L.A. Herzenberg. 2008. Profound functional and signaling changes in viable inflammatory neutrophils homing to cystic fibrosis airways. *Proc Natl Acad Sci U S A* 105:4335-4339.
204. Painter, R.G., R.W. Bonvillain, V.G. Valentine, G.A. Lombard, S.G. LaPlace, W.M. Nauseef, and G. Wang. 2008. The role of chloride anion and CFTR in killing of *Pseudomonas aeruginosa* by normal and CF neutrophils. *J Leukoc Biol* 83:1345-1353.
205. Morris, M.R., I.J. Doull, S. Dewitt, and M.B. Hallett. 2005. Reduced iC3b-mediated phagocytotic capacity of pulmonary neutrophils in cystic fibrosis. *Clin.Exp.Immunol.* 142:68-75.
206. Tirouvanziam, R., I. Khazaal, and B. Peault. 2002. Primary inflammation in human cystic fibrosis small airways. *Am.J.Physiol Lung Cell Mol.Physiol* 283:L445-L451.
207. Schroeder, T.H., N. Reiniger, G. Meluleni, M. Grout, F.T. Coleman, and G.B. Pier. 2001. Transgenic cystic fibrosis mice exhibit reduced early clearance of *Pseudomonas aeruginosa* from the respiratory tract. *Journal of Immunology* 166:7410-7418.
208. Thomas, C., N. Yuki, and B. Fertil. 2001. Influence of gangliosides or LPS-like gangliosides on the tumoricidal activity of adherent leukocytes. *C.R.Acad.Sci.III* 324:115-122.
209. Pan, P., Y. Guo, and J. Gu. 2008. Expression of cystic fibrosis transmembrane conductance regulator in ganglion cells of the hearts. *Neurosci Lett* 441:35-38.
210. Solbach, T.F., B. Paulus, M. Weyand, T. Eschenhagen, O. Zolk, and M.F. Fromm. 2008. ATP-binding cassette transporters in human heart failure. *Naunyn Schmiedebergs Arch Pharmacol* 377:231-243.

211. Gao, Z., H.Y. Sun, C.P. Lau, P. Chin-Wan Fung, and G.R. Li. 2007. Evidence for cystic fibrosis transmembrane conductance regulator chloride current in swine ventricular myocytes. *J Mol Cell Cardiol* 42:98-105.
212. Yajima, T., H. Nagashima, R. Tsutsumi-Sakai, N. Hagiwara, S. Hosoda, T. Quertermous, H. Kasanuki, and M. Kawana. 1997. Functional activity of the CFTR Cl⁻ channel in human myocardium. *Heart Vessels* 12:255-261.
213. Robert, R., J.P. Savineau, C. Norez, F. Becq, and C. Guibert. 2007. Expression and function of cystic fibrosis transmembrane conductance regulator in rat intrapulmonary arteries. *Eur Respir J* 30:857-864.
214. Michoud, M.C., R. Robert, M. Hassan, B. Moynihan, C. Haston, V. Govindaraju, P. Ferraro, J.W. Hanrahan, and J.G. Martin. 2008. Role of the CFTR Channel in Human Airway Smooth Muscle. *Am J Respir Cell Mol Biol*
215. Vandebrouck, C., P. Melin, C. Norez, R. Robert, C. Guibert, Y. Mettey, and F. Becq. 2006. Evidence that CFTR is expressed in rat tracheal smooth muscle cells and contributes to bronchodilation. *Respir Res* 7:113.
216. Noe, J., D. Petrusca, N. Rush, P. Deng, M. Vandemark, E. Berdyshev, Y. Gu, P. Smith, K. Schweitzer, J. Pilewsky, V. Natarajan, Z. Xu, A.G. Obhukov, and I. Petrache. 2009. CFTR Regulation of Intracellular pH and Ceramides is Required for Lung Endothelial Cell Apoptosis. *Am J Respir Cell Mol Biol*
217. Sun, X.C., and J.A. Bonanno. 2002. Expression, localization, and functional evaluation of CFTR in bovine corneal endothelial cells. *Am J Physiol Cell Physiol* 282:C673-683.
218. Bubien, J.K. 2001. CFTR may play a role in regulated secretion by lymphocytes: a new hypothesis for the pathophysiology of cystic fibrosis. *Pflugers Arch.* 443 Suppl 1:S36-S39.
219. Moss, R.B., Y.P. Hsu, and L. Olds. 2000. Cytokine dysregulation in activated cystic fibrosis (CF) peripheral lymphocytes. *Clin Exp Immunol* 120:518-525.
220. Moss, R.B., R.C. Bocian, Y.P. Hsu, Y.J. Dong, M. Kemna, T. Wei, and P. Gardner. 1996. Reduced IL-10 secretion by CD4⁺ T lymphocytes expressing mutant cystic fibrosis transmembrane conductance regulator (CFTR). *Clin Exp Immunol* 106:374-388.

221. McDonald, T.V., P.T. Nghiem, P. Gardner, and C.L. Martens. 1992. Human lymphocytes transcribe the cystic fibrosis transmembrane conductance regulator gene and exhibit CF-defective cAMP-regulated chloride current. *J Biol Chem* 267:3242-3248.
222. Kostyk, A.G., K.M. Dahl, M.W. Wynes, L.A. Whittaker, D.J. Weiss, R. Loi, and D.W. Riches. 2006. Regulation of chemokine expression by NaCl occurs independently of cystic fibrosis transmembrane conductance regulator in macrophages. *Am J Pathol* 169:12-20.
223. Pfeffer, K.D., T.P. Huecksteadt, and J.R. Hoidal. 1993. Expression and regulation of tumor necrosis factor in macrophages from cystic fibrosis patients. *Am J Respir Cell Mol Biol* 9:511-519.
224. Thomas, G.R., E.A. Costelloe, D.P. Lunn, K.J. Stacey, S.J. Delaney, R. Passey, E.C. McGlinn, B.J. McMorran, A. Ahadizadeh, C.L. Geczy, B.J. Wainwright, and D.A. Hume. 2000. G551D cystic fibrosis mice exhibit abnormal regulation of inflammation in lungs and macrophages. *J Immunol* 164:3870-3877.
225. Swanson, J. 2006. CFTR: helping to acidify macrophage lysosomes. *Nat Cell Biol* 8:908-909.
226. Di, A., M.E. Brown, L.V. Deriy, C. Li, F.L. Szeto, Y. Chen, P. Huang, J. Tong, A.P. Naren, V. Bindokas, H.C. Palfrey, and D.J. Nelson. 2006. CFTR regulates phagosome acidification in macrophages and alters bactericidal activity. *Nat Cell Biol* 8:933-944.
227. Poschet, J.F., J. Skidmore, J.C. Boucher, A.M. Firoved, R.W. Van Dyke, and V. Deretic. 2002. Hyperacidification of cellubrevin endocytic compartments and defective endosomal recycling in cystic fibrosis respiratory epithelial cells. *J Biol Chem* 277:13959-13965.
228. Haggie, P.M., and A.S. Verkman. 2009. Defective Organellar Acidification as a Cause of Cystic Fibrosis Lung Disease - Re-Examination of a Recurring Hypothesis. *Am J Physiol Lung Cell Mol Physiol*
229. Haggie, P.M., and A.S. Verkman. 2007. Cystic fibrosis transmembrane conductance regulator-independent phagosomal acidification in macrophages. *J Biol Chem* 282:31422-31428.
230. Poschet, J.F., J.A. Fazio, G.S. Timmins, W. Ornatowski, E. Perkett, M. Delgado, and V. Deretic. 2006. Endosomal hyperacidification in cystic fibrosis is due to defective nitric oxide-cyclic GMP signalling cascade. *EMBO Rep* 7:553-559.

231. Poschet, J.F., G.S. Timmins, J.L. Taylor-Cousar, W. Ornatowski, J. Fazio, E. Perkett, K.R. Wilson, H.D. Yu, H.R. de Jonge, and V. Deretic. 2007. Pharmacological modulation of cGMP levels by phosphodiesterase 5 inhibitors as a therapeutic strategy for treatment of respiratory pathology in cystic fibrosis. *Am J Physiol Lung Cell Mol Physiol* 293:L712-719.
232. Weyler, R.T., K.A. Yurko-Mauro, R. Rubenstein, W.J. Kollen, W. Reenstra, S.M. Altschuler, M. Egan, and A.E. Mulberg. 1999. CFTR is functionally active in GnRH-expressing GT1-7 hypothalamic neurons. *Am.J.Physiol* 277:C563-C571.
233. Bradbury, N.A. 1999. Intracellular CFTR: localization and function. *Physiol Rev.* 79:S175-S191.
234. Strausbaugh, S.D., and P.B. Davis. 2007. Cystic fibrosis: a review of epidemiology and pathobiology. *Clin Chest Med* 28:279-288.
235. Boucher, R.C. 2002. An overview of the pathogenesis of cystic fibrosis lung disease. *Adv.Drug Deliv.Rev.* 54:1359-1371.
236. Terheggen-Lagro, S.W., G.T. Rijkers, and C.K. van der Ent. 2005. The role of airway epithelium and blood neutrophils in the inflammatory response in cystic fibrosis. *J Cyst Fibros* 4 Suppl 2:15-23.
237. Muhlebach, M.S., and T.L. Noah. 2002. Endotoxin activity and inflammatory markers in the airways of young patients with cystic fibrosis. *Am J Respir Crit Care Med* 165:911-915.
238. Moraes, T.J., J. Plumb, R. Martin, E. Vachon, V. Cherepanov, A. Koh, C. Loeve, J. Jongstra-Bilen, J.H. Zurawska, J.V. Kus, L.L. Burrows, S. Grinstein, and G.P. Downey. 2006. Abnormalities in the pulmonary innate immune system in cystic fibrosis. *American Journal of Respiratory Cell & Molecular Biology* 34:364-374.
239. Heijerman, H. 2005. Infection and inflammation in cystic fibrosis: a short review. *J.Cyst.Fibros.* 4 Suppl 2:3-5.
240. Davies, J.C. 2002. *Pseudomonas aeruginosa* in cystic fibrosis: pathogenesis and persistence. *Paediatr.Respir.Rev* 3:128-134.
241. Armstrong, D.S., K. Grimwood, J.B. Carlin, R. Carzino, J.P. Gutierrez, J. Hull, A. Olinsky, E.M. Phelan, C.F. Robertson, and P.D. Phelan. 1997. Lower airway inflammation in infants and young children with cystic fibrosis. *Am.J.Respir.Crit Care Med.* 156:1197-1204.

242. Dakin, C.J., A.H. Numa, H. Wang, J.R. Morton, C.C. Vertzyas, and R.L. Henry. 2002. Inflammation, infection, and pulmonary function in infants and young children with cystic fibrosis. *Am.J.Respir.Crit Care Med.* 165:904-910.
243. Hull, J., W. Skinner, C. Robertson, and P. Phelan. 1998. Elemental content of airway surface liquid from infants with cystic fibrosis. *Am J Respir Crit Care Med* 157:10-14.
244. Mak, J.C., T.T. Chuang, C.A. Harris, and P.J. Barnes. 2002. Increased expression of G protein-coupled receptor kinases in cystic fibrosis lung. *Eur J Pharmacol* 436:165-172.
245. Augarten, A., G. Paret, I. Avneri, H. Akons, M. Aviram, L. Bentur, H. Blau, O. Efrati, A. Szeinberg, A. Barak, E. Kerem, and J. Yahav. 2004. Systemic inflammatory mediators and cystic fibrosis genotype. *Clin Exp Med* 4:99-102.
246. Venkatakrisnan, A., A.A. Stecenko, G. King, T.R. Blackwell, K.L. Brigham, J.W. Christman, and T.S. Blackwell. 2000. Exaggerated activation of nuclear factor-kappaB and altered IkappaB-beta processing in cystic fibrosis bronchial epithelial cells. *Am J Respir Cell Mol Biol* 23:396-403.
247. Bastonero, S., Y. Le Priol, M. Armand, C.S. Bernard, M. Reynaud-Gaubert, D. Olive, D. Parzy, S. de Bentzmann, C. Capo, and J.L. Mege. 2009. New microbicidal functions of tracheal glands: defective anti-infectious response to *Pseudomonas aeruginosa* in cystic fibrosis. *PLoS One* 4:e5357.
248. Becker, M.N., M.S. Sauer, M.S. Muhlebach, A.J. Hirsh, Q. Wu, M.W. Verghese, and S.H. Randell. 2004. Cytokine secretion by cystic fibrosis airway epithelial cells. *Am.J.Respir.Crit Care Med.* 169:645-653.
249. Ramirez, J.C., G.A. Patterson, T.L. Winton, A.L. de Hoyos, J.D. Miller, and J.R. Maurer. 1992. Bilateral lung transplantation for cystic fibrosis. The Toronto Lung Transplant Group. *J.Thorac.Cardiovasc.Surg.* 103:287-293.
250. Nunley, D.R., W. Grgurich, A.T. Iacono, S. Yousem, N.P. Otori, R.J. Keenan, and J.H. Dauber. 1998. Allograft colonization and infections with *pseudomonas* in cystic fibrosis lung transplant recipients. *Chest* 113:1235-1243.
251. Krishnaswamy, G., O. Ajitawi, and D.S. Chi. 2006. The human mast cell: an overview. *Methods Mol Biol* 315:13-34.

252. Marshall, J.S., and D.M. Jawdat. 2004. Mast cells in innate immunity. *J Allergy Clin Immunol* 114:21-27.
253. Sawynok, J., and X.J. Liu. 2003. Adenosine in the spinal cord and periphery: release and regulation of pain. *Prog.Neurobiol.* 69:313-340.
254. Baldwin, S.A., J.R. Mackey, C.E. Cass, and J.D. Young. 1999. Nucleoside transporters: molecular biology and implications for therapeutic development. *Mol.Med.Today* 5:216-224.
255. Casado, F.J., M.P. Lostao, I. Aymerich, I.M. Larrayoz, S. Duflot, S. Rodriguez-Mulero, and M. Pastor-Anglada. 2002. Nucleoside transporters in absorptive epithelia. *J Physiol Biochem* 58:207-216.
256. Beju, D., W.D. Meek, and J.C. Kramer. 2004. The ultrastructure of the nasal polyps in patients with and without cystic fibrosis. *J Submicrosc Cytol Pathol* 36:155-165.
257. Henderson, W.R., Jr., and E.Y. Chi. 1992. Degranulation of cystic fibrosis nasal polyp mast cells. *J.Pathol.* 166:395-404.
258. Hubeau, C., E. Puchelle, and D. Gaillard. 2001. Distinct pattern of immune cell population in the lung of human fetuses with cystic fibrosis. *J.Allergy Clin.Immunol* 108:524-529.
259. Norkina, O., S. Kaur, D. Ziemer, and R.C. De Lisle. 2004. Inflammation of the cystic fibrosis mouse small intestine. *Am.J.Physiol Gastrointest.Liver Physiol* 286:G1032-G1041.
260. Pawel, B.R., J.P. de Chadarevian, and M.E. Franco. 1997. The pathology of fibrosing colonopathy of cystic fibrosis: a study of 12 cases and review of the literature. *Hum.Pathol.* 28:395-399.
261. Hsieh, F.H., P. Sharma, A. Gibbons, T. Goggans, S.C. Erzurum, and S.J. Haque. 2005. Human airway epithelial cell determinants of survival and functional phenotype for primary human mast cells. *Proc.Natl.Acad.Sci.U.S.A* 102:14380-14385.
262. Birrer, P. 1995. Proteases and antiproteases in cystic fibrosis: pathogenetic considerations and therapeutic strategies. *Respiration* 62 Suppl 1:25-28.
263. Weldon, S., and C.C. Taggart. 2007. Innate host defense functions of secretory leucoprotease inhibitor. *Exp Lung Res* 33:485-491.
264. Feoktistov, I., and I. Biaggioni. 1996. Role of adenosine in asthma. *Drug Dev Res* 39:333-336.

265. Jacob, C., P.C. Yang, D. Darmoul, S. Amadesi, T. Saito, G.S. Cottrell, A.M. Coelho, P. Singh, E.F. Grady, M. Perdue, and N.W. Bunnett. 2005. Mast cell tryptase controls paracellular permeability of the intestine. Role of protease-activated receptor 2 and beta-arrestins. *J Biol Chem* 280:31936-31948.
266. Bertrand, C.A., and R.A. Frizzell. 2003. The role of regulated CFTR trafficking in epithelial secretion. *Am J Physiol Cell Physiol* 285:C1-18.
267. Denning, G.M., L.S. Ostedgaard, S.H. Cheng, A.E. Smith, and M.J. Welsh. 1992. Localization of cystic fibrosis transmembrane conductance regulator in chloride secretory epithelia. *J Clin Invest* 89:339-349.
268. Denning, G.M., L.S. Ostedgaard, and M.J. Welsh. 1992. Abnormal localization of cystic fibrosis transmembrane conductance regulator in primary cultures of cystic fibrosis airway epithelia. *J Cell Biol* 118:551-559.
269. Swieter, M., T.D. Lee, R.H. Stead, H. Fujimaki, and D. Befus. 1987. Mast cell pleomorphism: properties of intestinal mast cells. *Adv Exp Med Biol* 216A:613-623.
270. Boucher, R.C. 2002. An overview of the pathogenesis of cystic fibrosis lung disease. *Adv Drug Deliv Rev* 54:1359-1371.
271. Berger, M. 2002. Inflammatory mediators in cystic fibrosis lung disease. *Allergy Asthma Proc* 23:19-25.
272. Kitamura, Y., K. Oboki, and A. Ito. 2006. Molecular mechanisms of mast cell development. *Immunol Allergy Clin North Am* 26:387-405; v.
273. Greene, C.M., T.P. Carroll, S.G. Smith, C.C. Taggart, J. Devaney, S. Griffin, J. O'Neill S, and N.G. McElvaney. 2005. TLR-induced inflammation in cystic fibrosis and non-cystic fibrosis airway epithelial cells. *J Immunol* 174:1638-1646.
274. Tomioka, M., T. Goto, T.D. Lee, J. Bienenstock, and A.D. Befus. 1989. Isolation and characterization of lung mast cells from rats with bleomycin-induced pulmonary fibrosis. *Immunology* 66:439-444.
275. Benyon, R.C., J.A. Enciso, and A.D. Befus. 1993. Analysis of human skin mast cell proteins by two-dimensional gel electrophoresis. Identification of tryptase as a sialylated glycoprotein. *J Immunol* 151:2699-2706.

276. Nilsson, G., T. Blom, M. Kusche-Gullberg, L. Kjellen, J.H. Butterfield, C. Sundstrom, K. Nilsson, and L. Hellman. 1994. Phenotypic characterization of the human mast-cell line HMC-1. *Scand J Immunol* 39:489-498.
277. Kirshenbaum, A.S., C. Akin, Y. Wu, M. Rottem, J.P. Goff, M.A. Beaven, V.K. Rao, and D.D. Metcalfe. 2003. Characterization of novel stem cell factor responsive human mast cell lines LAD 1 and 2 established from a patient with mast cell sarcoma/leukemia; activation following aggregation of FcepsilonRI or FcgammaRI. *Leuk Res* 27:677-682.
278. Theoharides, T.C., D. Kempuraj, M. Tagen, M. Vasiadi, and C.L. Cetrulo. 2006. Human umbilical cord blood-derived mast cells: a unique model for the study of neuro-immuno-endocrine interactions. *Stem Cell Rev* 2:143-154.
279. Andersen, H.B., M. Holm, T.E. Hetland, C. Dahl, S. Junker, P.O. Schiotz, and H.J. Hoffmann. 2008. Comparison of short term in vitro cultured human mast cells from different progenitors - Peripheral blood-derived progenitors generate highly mature and functional mast cells. *J Immunol Methods* 336:166-174.
280. Lam, R.S., E.M. App, D. Nahirney, A.J. Szkotak, M.A. Vieira-Coelho, M. King, and M. Duszyk. 2003. Regulation of Cl⁻ secretion by alpha2-adrenergic receptors in mouse colonic epithelium. *J Physiol* 548:475-484.
281. Moon, T.C., and A.D. Befus. 2008. Exogenous nitric oxide regulates cyclooxygenase-2 expression and prostaglandin D(2) generation through p38 MAPK in mouse bone marrow-derived mast cells. *Free Radic Biol Med* 45:780-788.
282. Wagner, J.A., T.V. McDonald, P.T. Nghiem, A.W. Lowe, H. Schulman, D.C. Gruenert, L. Stryer, and P. Gardner. 1992. Antisense oligodeoxynucleotides to the cystic fibrosis transmembrane conductance regulator inhibit cAMP-activated but not calcium-activated chloride currents. *Proc Natl Acad Sci U S A* 89:6785-6789.
283. Cantin, A.M., G. Bilodeau, C. Ouellet, J. Liao, and J.W. Hanrahan. 2006. Oxidant stress suppresses CFTR expression. *Am J Physiol Cell Physiol* 290:C262-270.
284. Bartoszewski, R., A. Rab, G. Twitty, L. Stevenson, J. Fortenberry, A. Piotrowski, J.P. Dumanski, and Z. Bebok. 2008. The mechanism of cystic fibrosis transmembrane conductance regulator transcriptional repression during the unfolded protein response. *J Biol Chem* 283:12154-12165.

285. Darken, M.A. 1964. Puromycin Inhibition of Protein Synthesis. *Pharmacol Rev* 16:223-243.
286. Gomez Lahoz, E., M.S. Lopez de Haro, A. Nieto, and P. Esponda. 1991. Use of puromycin N-acetyltransferase (PAC) as a new reporter gene in transgenic animals. *Nucleic Acids Res* 19:3465.
287. Chomczynski, P., and N. Sacchi. 1987. Single-step method of RNA isolation by acid guanidinium thiocyanate-phenol-chloroform extraction. *Anal Biochem* 162:156-159.
288. Gilchrist, M., A.J. MacDonald, I. Neverova, B. Ritchie, and A.D. Befus. 1997. Optimization of the isolation and effective use of mRNA from rat mast cells. *J Immunol Methods* 201:207-214.
289. Tsai, M., M. Miyamoto, S.Y. Tam, Z.S. Wang, and S.J. Galli. 1995. Detection of mouse mast cell-associated protease mRNA. Heparinase treatment greatly improves RT-PCR of tissues containing mast cell heparin. *Am J Pathol* 146:335-343.
290. Glaum, M.C., Y. Wang, D.G. Raible, and E.S. Schulman. 2001. Degranulation influences heparin-associated inhibition of RT-PCR in human lung mast cells. *Clin Exp Allergy* 31:1631-1635.
291. Pfaffl, M.W. 2001. A new mathematical model for relative quantification in real-time RT-PCR. *Nucleic Acids Res* 29:e45.
292. Ramalho, A.S., S. Beck, C.M. Farinha, L.A. Clarke, G.D. Heda, B. Steiner, J. Sanz, S. Gallati, M.D. Amaral, A. Harris, and M. Tzetis. 2004. Methods for RNA extraction, cDNA preparation and analysis of CFTR transcripts. *J Cyst Fibros* 3 Suppl 2:11-15.
293. West, M.R., and C.R. Molloy. 1996. A microplate assay measuring chloride ion channel activity. *Anal Biochem* 241:51-58.
294. Lin, T.J., L.H. Maher, K. Gomi, J.D. McCurdy, R. Garduno, and J.S. Marshall. 2003. Selective early production of CCL20, or macrophage inflammatory protein 3alpha, by human mast cells in response to *Pseudomonas aeruginosa*. *Infect Immun* 71:365-373.
295. Sun, G., F. Liu, and T.J. Lin. 2005. Identification of *Pseudomonas aeruginosa*-induced genes in human mast cells using suppression subtractive hybridization: up-regulation of IL-8 and CCL4 production. *Clin Exp Immunol* 142:199-205.

296. Lin, T.J., R. Garduno, R.T. Boudreau, and A.C. Issekutz. 2002. *Pseudomonas aeruginosa* activates human mast cells to induce neutrophil transendothelial migration via mast cell-derived IL-1 alpha and beta. *J Immunol* 169:4522-4530.
297. Jenkins, C.E., A. Swiatoniowski, M.R. Power, and T.J. Lin. 2006. *Pseudomonas aeruginosa*-induced human mast cell apoptosis is associated with up-regulation of endogenous Bcl-xS and down-regulation of Bcl-xL. *J Immunol* 177:8000-8007.
298. Shim, J.U., and K.T. Lim. 2009. Inhibitory effect of glycoprotein isolated from *Cudrania tricuspidata* bureau on expression of inflammation-related cytokine in bisphenol A-treated HMC-1 cells. *Inflammation* 32:211-217.
299. Ko, J., C.Y. Yun, J.S. Lee, D.H. Kim, J.E. Yuk, and I.S. Kim. 2006. Differential regulation of CC chemokine receptors by 9-cis retinoic acid in the human mast cell line, HMC-1. *Life Sci* 79:1293-1300.
300. Pernas-Sueiras, O., A. Alfonso, M.R. Vieytes, and L.M. Botana. 2006. PKC and cAMP positively modulate alkaline-induced exocytosis in the human mast cell line HMC-1. *J Cell Biochem* 99:1651-1663.
301. Gage, M.C., J.N. Keen, A.T. Buxton, M.K. Bedi, and J.B. Findlay. 2009. Proteomic Analysis of IgE-Mediated Secretion by LAD2 Mast Cells. *J Proteome Res*
302. Kassel, O., C. da Silva, and N. Frossard. 2001. The stem cell factor, its properties and potential role in the airways. *Pulm Pharmacol Ther* 14:277-288.
303. Ochi, H., N.H. De Jesus, F.H. Hsieh, K.F. Austen, and J.A. Boyce. 2000. IL-4 and -5 prime human mast cells for different profiles of IgE-dependent cytokine production. *Proc Natl Acad Sci U S A* 97:10509-10513.
304. Tsai, M., L.S. Shih, G.F. Newlands, T. Takeishi, K.E. Langley, K.M. Zsebo, H.R. Miller, E.N. Geissler, and S.J. Galli. 1991. The rat c-kit ligand, stem cell factor, induces the development of connective tissue-type and mucosal mast cells in vivo. Analysis by anatomical distribution, histochemistry, and protease phenotype. *J Exp Med* 174:125-131.
305. Gurish, M.F., N. Ghildyal, H.P. McNeil, K.F. Austen, S. Gillis, and R.L. Stevens. 1992. Differential expression of secretory granule proteases in mouse mast cells exposed to interleukin 3 and c-kit ligand. *J Exp Med* 175:1003-1012.

306. Kulka, M., R. Dery, D. Nahirney, M. Duszyk, and A.D. Befus. 2005. Differential regulation of cystic fibrosis transmembrane conductance regulator by interferon gamma in mast cells and epithelial cells. *J.Pharmacol.Exp.Ther.* 315:563-570.
307. Abe, T., M. Swieter, T. Imai, N.D. Hollander, and A.D. Befus. 1990. Mast cell heterogeneity: two-dimensional gel electrophoretic analyses of rat peritoneal and intestinal mucosal mast cells. *Eur J Immunol* 20:1941-1947.
308. Blume-Jensen, P., L. Ronnstrand, I. Gout, M.D. Waterfield, and C.H. Heldin. 1994. Modulation of Kit/stem cell factor receptor-induced signaling by protein kinase C. *J Biol Chem* 269:21793-21802.
309. Koma, Y., A. Ito, K. Watabe, T. Hirata, M. Mizuki, H. Yokozaki, T. Kitamura, Y. Kanakura, and Y. Kitamura. 2005. Distinct role for c-kit receptor tyrosine kinase and SgIGSF adhesion molecule in attachment of mast cells to fibroblasts. *Lab Invest* 85:426-435.
310. Krop, M., R. van Veghel, I.M. Garrelds, R.J. de Bruin, J.M. van Gool, A.H. van den Meiracker, M. Thio, P.L. van Daele, and A.H. Danser. 2009. Cardiac Renin levels are not influenced by the amount of resident mast cells. *Hypertension* 54:315-321.
311. Weston, M.C., N. Anderson, and P.T. Peachell. 1997. Effects of phosphodiesterase inhibitors on human lung mast cell and basophil function. *Br J Pharmacol* 121:287-295.
312. Vij, N., S. Mazur, and P.L. Zeitlin. 2009. CFTR is a negative regulator of NFkappaB mediated innate immune response. *PLoS One* 4:e4664.
313. Kahr, H., R. Schindl, R. Fritsch, B. Heinze, M. Hofbauer, M.E. Hack, M.A. Mortelmaier, K. Groschner, J.B. Peng, H. Takanaga, M.A. Hediger, and C. Romanin. 2004. CaT1 knock-down strategies fail to affect CRAC channels in mucosal-type mast cells. *J Physiol* 557:121-132.
314. Heinonen, J.E., C.I. Smith, and B.F. Nore. 2002. Silencing of Bruton's tyrosine kinase (Btk) using short interfering RNA duplexes (siRNA). *FEBS Lett* 527:274-278.
315. Ratjen, F.A. 2009. Cystic fibrosis: pathogenesis and future treatment strategies. *Respir Care* 54:595-605.
316. Rottner, M., J.M. Freyssinet, and M.C. Martinez. 2009. Mechanisms of the noxious inflammatory cycle in cystic fibrosis. *Respir Res* 10:23.

317. Englmann, A., L.A. Clarke, S. Christan, M.D. Amaral, D. Schindelhauer, and D. Zink. 2005. The replication timing of CFTR and adjacent genes. *Chromosome Res* 13:183-194.
318. Ostedgaard, L.S., and M.J. Welsh. 1992. Partial purification of the cystic fibrosis transmembrane conductance regulator. *J Biol Chem* 267:26142-26149.
319. de Andrade Pinto, A.C., C.M. Barbosa, D.S. Ornellas, H.J. Novaira, J. de Souza-Menezes, T.M. Ortega-Carvalho, P. Fong, and M.M. Morales. 2007. Thyroid hormones stimulate renal expression of CFTR. *Cell Physiol Biochem* 20:83-90.
320. Souza-Menezes, J., D.N. Tukaye, H.J. Novaira, W.B. Guggino, and M.M. Morales. 2008. Small nuclear RNAs U11 and U12 modulate expression of TNR-CFTR mRNA in mammalian kidneys. *Cell Physiol Biochem* 22:93-100.
321. Morales, M.M., T.P. Carroll, T. Morita, E.M. Schwiebert, O. Devuyst, P.D. Wilson, A.G. Lopes, B.A. Stanton, H.C. Dietz, G.R. Cutting, and W.B. Guggino. 1996. Both the wild type and a functional isoform of CFTR are expressed in kidney. *Am J Physiol* 270:F1038-1048.
322. Rechsteiner, M., and S.W. Rogers. 1996. PEST sequences and regulation by proteolysis. *Trends Biochem Sci* 21:267-271.
323. Riordan, J.R., J.M. Rommens, B. Kerem, N. Alon, R. Rozmahel, Z. Grzelczak, J. Zielenski, S. Lok, N. Plavsic, J.L. Chou, and et al. 1989. Identification of the cystic fibrosis gene: cloning and characterization of complementary DNA. *Science* 245:1066-1073.
324. Rogers, S., R. Wells, and M. Rechsteiner. 1986. Amino acid sequences common to rapidly degraded proteins: the PEST hypothesis. *Science* 234:364-368.
325. Forsythe, P., and A.D. Befus. 2003. Inhibition of calpain is a component of nitric oxide-induced down-regulation of human mast cell adhesion. *J Immunol* 170:287-293.
326. Ameen, N., M. Silvis, and N.A. Bradbury. 2007. Endocytic trafficking of CFTR in health and disease. *J Cyst Fibros* 6:1-14.
327. Gojkovic-Bukarica, L., A. Hambrock, C. Loffler-Walz, U. Quast, and U. Russ. 2002. Mg²⁺ sensitizes KATP channels to inhibition by DIDS: dependence on the sulphonylurea receptor subunit. *Br J Pharmacol* 137:429-440.

328. O'Neill, E.R., M.M. Sakowska, and D.R. Laver. 2003. Regulation of the calcium release channel from skeletal muscle by suramin and the disulfonated stilbene derivatives DIDS, DBDS, and DNDS. *Biophys J* 84:1674-1689.
329. Wong, C.K., C.M. Tsang, W.K. Ip, and C.W. Lam. 2006. Molecular mechanisms for the release of chemokines from human leukemic mast cell line (HMC)-1 cells activated by SCF and TNF-alpha: roles of ERK, p38 MAPK, and NF-kappaB. *Allergy* 61:289-297.
330. Breuer, W., and K.L. Skorecki. 1989. Inhibition of prostaglandin E2 synthesis by a blocker of epithelial chloride channels. *Biochem Biophys Res Commun* 163:398-405.
331. Haws, C., W.E. Finkbeiner, J.H. Widdicombe, and J.J. Wine. 1994. CFTR in Calu-3 human airway cells: channel properties and role in cAMP-activated Cl- conductance. *Am J Physiol* 266:L502-512.
332. Ito, Y., M. Aoyama, N. Yamada, Y. Mizuno, H. Kume, and K. Yamaki. 2001. [(Dihydroindenyl)oxy]alkonic acid inhibits the cystic fibrosis transmembrane conductance regulator. *Eur J Pharmacol* 426:175-178.
333. Robert, R., V. Thoreau, C. Norez, A. Cantereau, A. Kitzis, Y. Mettey, C. Rogier, and F. Becq. 2004. Regulation of the cystic fibrosis transmembrane conductance regulator channel by beta-adrenergic agonists and vasoactive intestinal peptide in rat smooth muscle cells and its role in vasorelaxation. *J Biol Chem* 279:21160-21168.
334. Friis, U.G., T. Johansen, N.A. Hayes, and J.C. Foreman. 1994. IgE-receptor activated chloride uptake in relation to histamine secretion from rat mast cells. *British Journal of Pharmacology* 111:1179-1183.
335. Gosling, M., J.W. Smith, and D.R. Poyner. 1995. Characterization of a volume-sensitive chloride current in rat osteoblast-like (ROS 17/2.8) cells. *J Physiol* 485 (Pt 3):671-682.
336. Kubo, M., and Y. Okada. 1992. Volume-regulatory Cl- channel currents in cultured human epithelial cells. *J Physiol* 456:351-371.
337. Alton, E.W., S.D. Manning, P.J. Schlatter, D.M. Geddes, and A.J. Williams. 1991. Characterization of a Ca(2+)-dependent anion channel from sheep tracheal epithelium incorporated into planar bilayers. *J Physiol* 443:137-159.

338. Alton, E.W., and A.J. Williams. 1992. Modification of gating of an airway epithelial chloride channel by 5-nitro-2-(3-phenylpropylamino)benzoic acid (NPPB). *J Membr Biol* 128:141-151.
339. Kreusel, K.M., M. Fromm, J.D. Schulzke, and U. Hegel. 1991. Cl-secretion in epithelial monolayers of mucus-forming human colon cells (HT-29/B6). *Am J Physiol* 261:C574-582.
340. Schwiebert, L.M., K. Estell, and S.M. Propst. 1999. Chemokine expression in CF epithelia: implications for the role of CFTR in RANTES expression. *Am J Physiol* 276:C700-710.
341. Dotsch, J., J. Puls, T. Klimek, and W. Rascher. 2002. Reduction of neuronal and inducible nitric oxide synthase gene expression in patients with cystic fibrosis. *Eur Arch Otorhinolaryngol* 259:222-226.
342. Hryciw, D.H., and W.B. Guggino. 2000. Cystic fibrosis transmembrane conductance regulator and the outwardly rectifying chloride channel: a relationship between two chloride channels expressed in epithelial cells. *Clin Exp Pharmacol Physiol* 27:892-895.
343. Hopf, A., R. Schreiber, M. Mall, R. Greger, and K. Kunzelmann. 1999. Cystic fibrosis transmembrane conductance regulator inhibits epithelial Na⁺ channels carrying Liddle's syndrome mutations. *J Biol Chem* 274:13894-13899.
344. Schreiber, R., R. Nitschke, R. Greger, and K. Kunzelmann. 1999. The cystic fibrosis transmembrane conductance regulator activates aquaporin 3 in airway epithelial cells. *J Biol Chem* 274:11811-11816.
345. Schwiebert, E.M., D.J. Benos, M.E. Egan, M.J. Stutts, and W.B. Guggino. 1999. CFTR is a conductance regulator as well as a chloride channel. *Physiol Rev* 79:S145-166.
346. Gottlieb, R.A., and A. Dosanjh. 1996. Mutant cystic fibrosis transmembrane conductance regulator inhibits acidification and apoptosis in C127 cells: possible relevance to cystic fibrosis. *Proc Natl Acad Sci U S A* 93:3587-3591.
347. Tabary, O., J.M. Zahm, J. Hinnrasky, J.P. Couetil, P. Cornillet, M. Guenounou, D. Gaillard, E. Puchelle, and J. Jacquot. 1998. Selective up-regulation of chemokine IL-8 expression in cystic fibrosis bronchial gland cells in vivo and in vitro. *Am J Pathol* 153:921-930.
348. Stecenko, A.A., G. King, K. Torii, R.M. Breyer, R. Dworski, T.S. Blackwell, J.W. Christman, and K.L. Brigham. 2001. Dysregulated

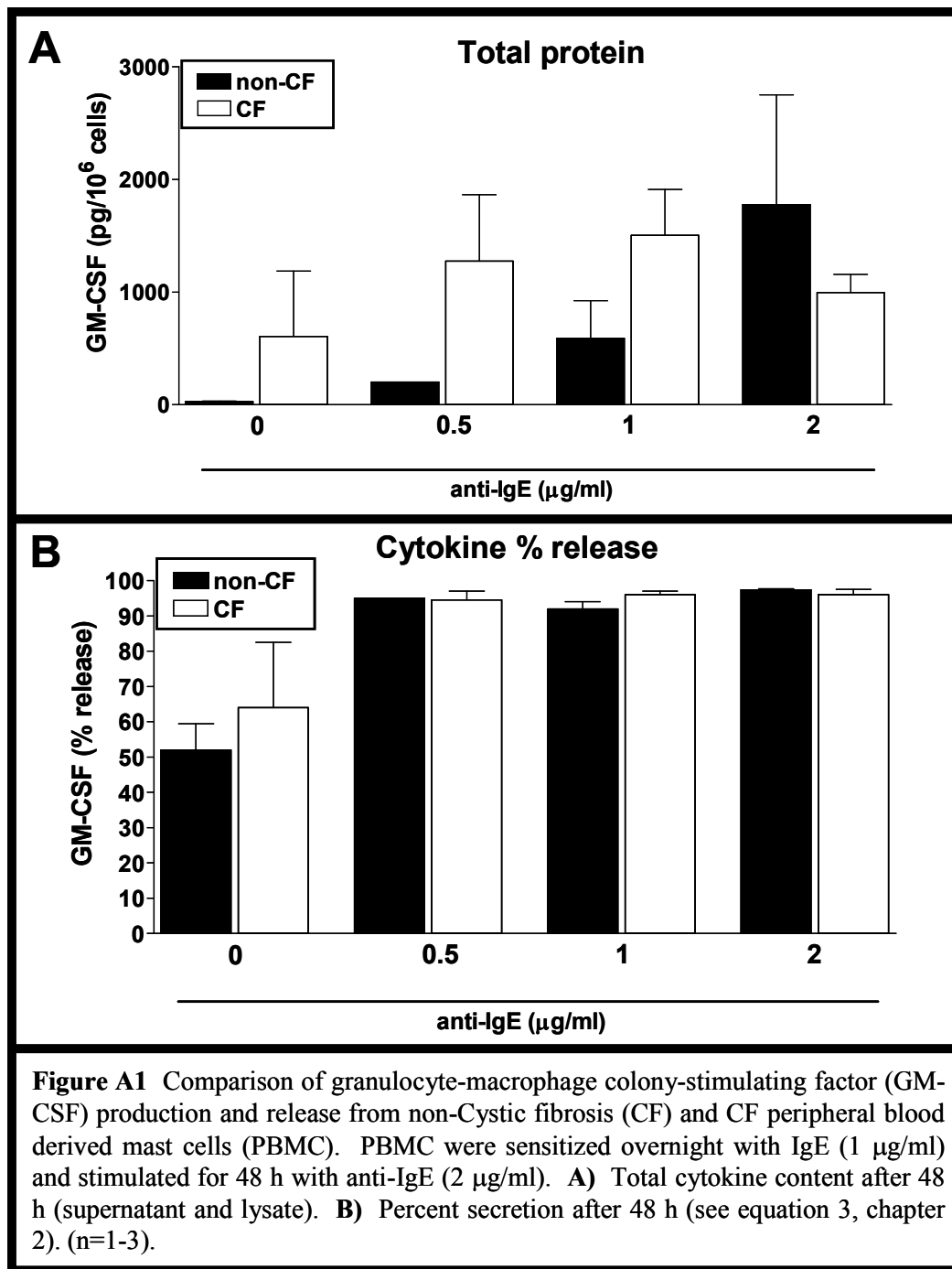
- cytokine production in human cystic fibrosis bronchial epithelial cells. *Inflammation* 25:145-155.
349. Kelley, T.J., and M.L. Drumm. 1998. Inducible nitric oxide synthase expression is reduced in cystic fibrosis murine and human airway epithelial cells. *J Clin Invest* 102:1200-1207.
 350. Yu, H., S.Z. Nasr, and V. Deretic. 2000. Innate lung defenses and compromised *Pseudomonas aeruginosa* clearance in the malnourished mouse model of respiratory infections in cystic fibrosis. *Infect Immun* 68:2142-2147.
 351. Machen, T.E. 2006. Innate immune response in CF airway epithelia: hyperinflammatory? *Am J Physiol Cell Physiol* 291:C218-230.
 352. Boncoeur, E., T. Roque, E. Bonvin, V. Saint-Criq, M. Bonora, A. Clement, O. Tabary, A. Henrion-Caude, and J. Jacquot. 2008. Cystic fibrosis transmembrane conductance regulator controls lung proteasomal degradation and nuclear factor-kappaB activity in conditions of oxidative stress. *Am J Pathol* 172:1184-1194.
 353. Perez, A., A.C. Issler, C.U. Cotton, T.J. Kelley, A.S. Verkman, and P.B. Davis. 2007. CFTR inhibition mimics the cystic fibrosis inflammatory profile. *Am J Physiol Lung Cell Mol Physiol* 292:L383-395.
 354. Kuehn, H.S., and A.M. Gilfillan. 2007. G protein-coupled receptors and the modification of FcepsilonRI-mediated mast cell activation. *Immunol Lett* 113:59-69.
 355. Feng, C., A.G. Mery, E.M. Beller, C. Favot, and J.A. Boyce. 2004. Adenine nucleotides inhibit cytokine generation by human mast cells through a Gs-coupled receptor. *J Immunol* 173:7539-7547.
 356. Feoktistov, I., and I. Biaggioni. 1995. Adenosine A2b receptors evoke interleukin-8 secretion in human mast cells. An enprofylline-sensitive mechanism with implications for asthma. *J Clin Invest* 96:1979-1986.
 357. Ribas, C., P. Penela, C. Murga, A. Salcedo, C. Garcia-Hoz, M. Jurado-Pueyo, I. Aymerich, and F. Mayor, Jr. 2007. The G protein-coupled receptor kinase (GRK) interactome: role of GRKs in GPCR regulation and signaling. *Biochim Biophys Acta* 1768:913-922.
 358. Cha, B., and M. Donowitz. 2008. The epithelial brush border Na⁺/H⁺ exchanger NHE3 associates with the actin cytoskeleton by binding to ezrin directly and via PDZ domain-containing Na⁺/H⁺ exchanger regulatory factor (NHERF) proteins. *Clin Exp Pharmacol Physiol* 35:863-871.

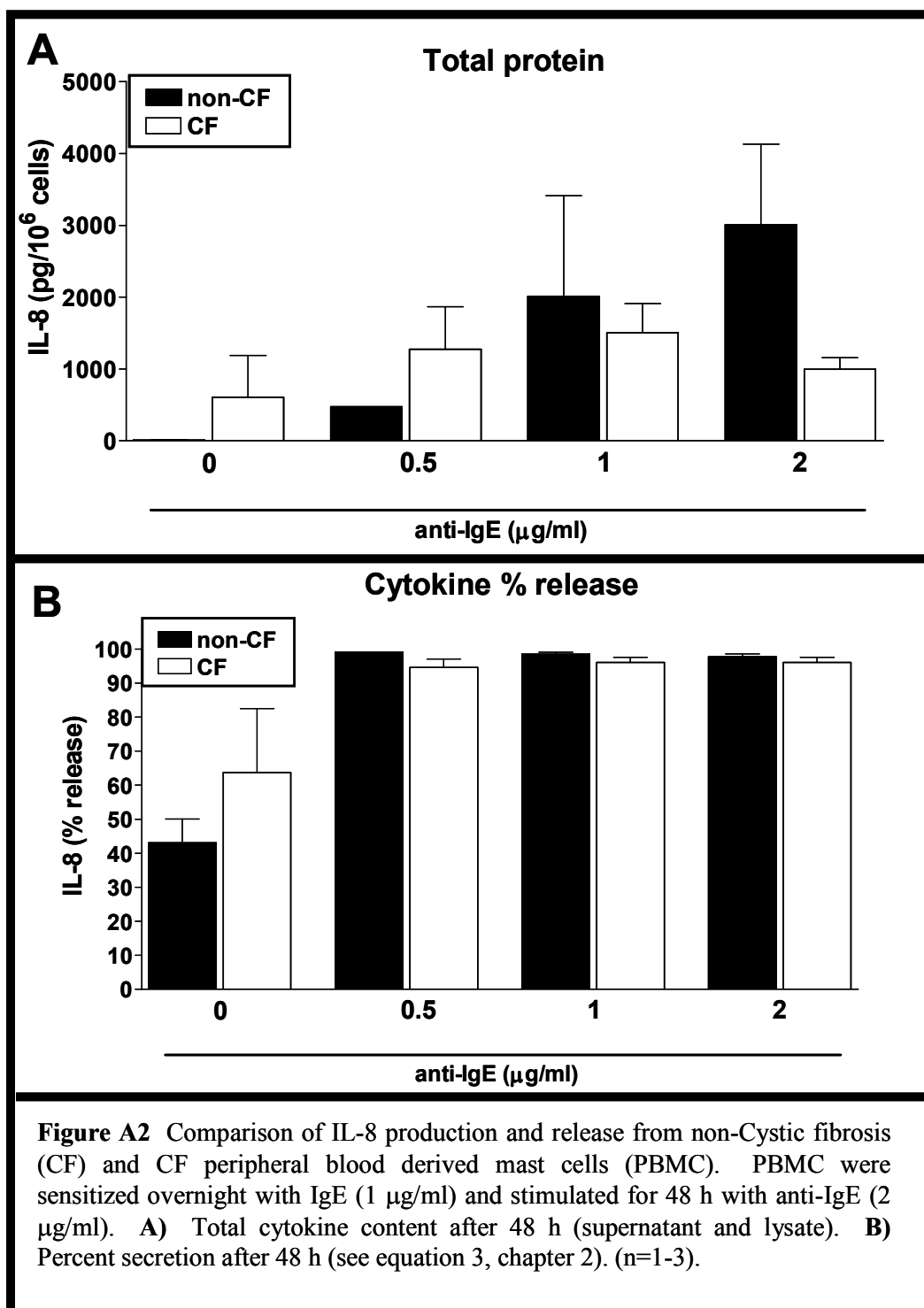
359. Roth, K., W.M. Chen, and T.J. Lin. 2008. Positive and negative regulatory mechanisms in high-affinity IgE receptor-mediated mast cell activation. *Arch Immunol Ther Exp (Warsz)* 56:385-399.
360. Feoktistov, I., A.E. Goldstein, and I. Biaggioni. 1999. Role of p38 mitogen-activated protein kinase and extracellular signal-regulated protein kinase kinase in adenosine A2B receptor-mediated interleukin-8 production in human mast cells. *Mol Pharmacol* 55:726-734.
361. Sester, D.P., K. Brion, A. Trieu, H.S. Goodridge, T.L. Roberts, J. Dunn, D.A. Hume, K.J. Stacey, and M.J. Sweet. 2006. CpG DNA activates survival in murine macrophages through TLR9 and the phosphatidylinositol 3-kinase-Akt pathway. *J Immunol* 177:4473-4480.
362. Sester, D.P., S. Naik, S.J. Beasley, D.A. Hume, and K.J. Stacey. 2000. Phosphorothioate backbone modification modulates macrophage activation by CpG DNA. *J Immunol* 165:4165-4173.
363. Fire, A., S. Xu, M.K. Montgomery, S.A. Kostas, S.E. Driver, and C.C. Mello. 1998. Potent and specific genetic interference by double-stranded RNA in *Caenorhabditis elegans*. *Nature* 391:806-811.
364. Denning, G.M., M.P. Anderson, J.F. Amara, J. Marshall, A.E. Smith, and M.J. Welsh. 1992. Processing of mutant cystic fibrosis transmembrane conductance regulator is temperature-sensitive. *Nature* 358:761-764.
365. Scanlin, T.F., and M.C. Glick. 2001. Glycosylation and the cystic fibrosis transmembrane conductance regulator. *Respir Res* 2:276-279.
366. Silvis, M.R., C.A. Bertrand, N. Ameen, F. Golin-Bisello, M.B. Butterworth, R.A. Frizzell, and N.A. Bradbury. 2009. Rab11b regulates the apical recycling of the cystic fibrosis transmembrane conductance regulator in polarized intestinal epithelial cells. *Mol Biol Cell* 20:2337-2350.
367. Wilson, P.D. 1999. Cystic fibrosis transmembrane conductance regulator in the kidney: clues to its role? *Exp Nephrol* 7:284-289.
368. Treharne, K.J., R.M. Crawford, and A. Mehta. 2006. CFTR, chloride concentration and cell volume: could mammalian protein histidine phosphorylation play a latent role? *Exp Physiol* 91:131-139.
369. Valverde, M.A., E. Vazquez, F.J. Munoz, M. Nobles, S.J. Delaney, B.J. Wainwright, W.H. Colledge, and D.N. Sheppard. 2000. Murine CFTR channel and its role in regulatory volume decrease of small intestine crypts. *Cell Physiol Biochem* 10:321-328.

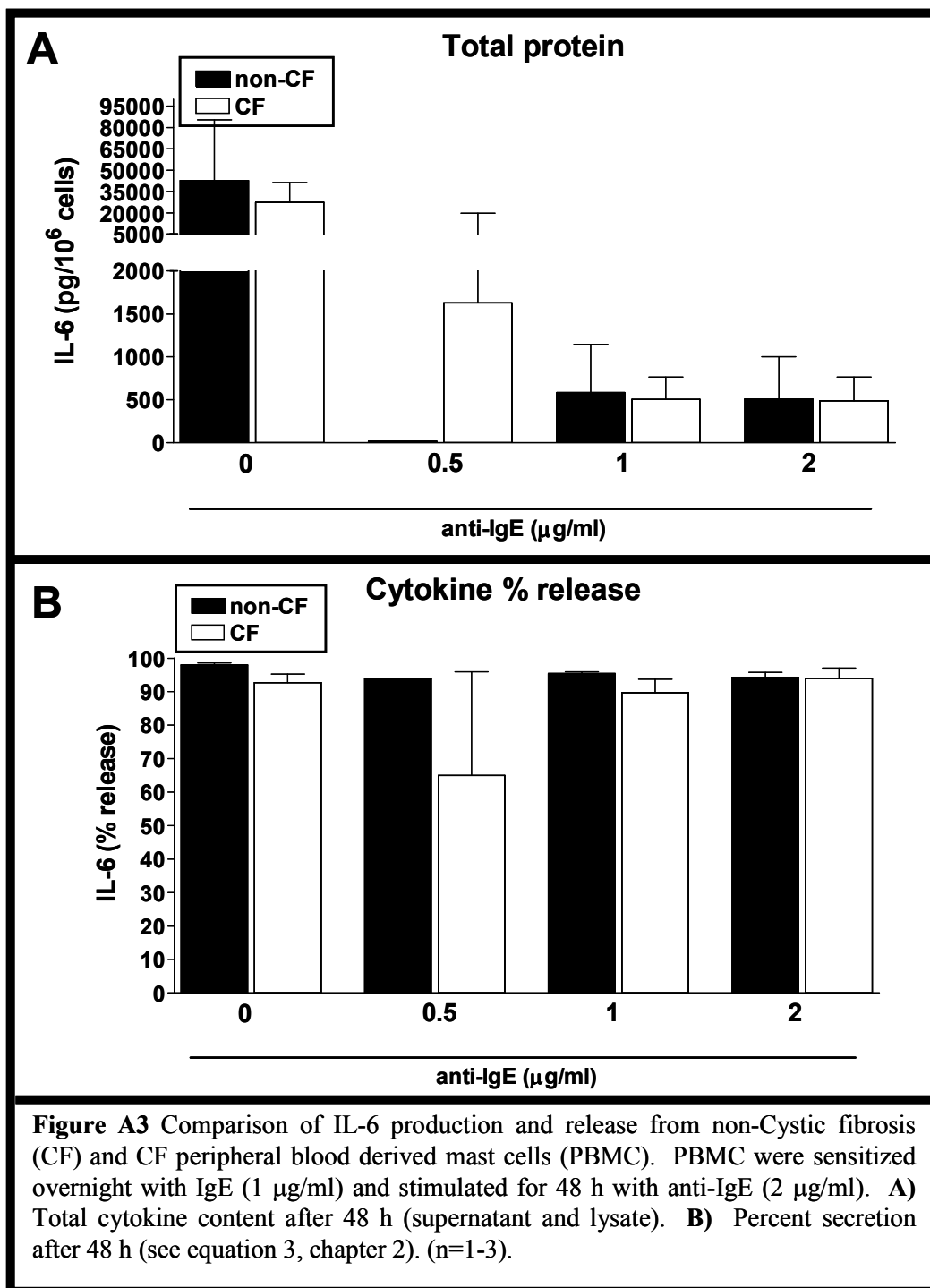
370. Vazquez, E., M. Nobles, and M.A. Valverde. 2001. Defective regulatory volume decrease in human cystic fibrosis tracheal cells because of altered regulation of intermediate conductance Ca^{2+} -dependent potassium channels. *Proc Natl Acad Sci U S A* 98:5329-5334.
371. Okada, Y., E. Maeno, T. Shimizu, K. Dezaki, J. Wang, and S. Morishima. 2001. Receptor-mediated control of regulatory volume decrease (RVD) and apoptotic volume decrease (AVD). *J Physiol* 532:3-16.
372. Arniges, M., E. Vazquez, J.M. Fernandez-Fernandez, and M.A. Valverde. 2004. Swelling-activated Ca^{2+} entry via TRPV4 channel is defective in cystic fibrosis airway epithelia. *J Biol Chem* 279:54062-54068.
373. Clark, A., J. Dean, C. Tudor, and J. Saklatvala. 2009. Post-transcriptional gene regulation by MAP kinases via AU-rich elements. *Front Biosci* 14:847-871.
374. Asirvatham, A.J., W.J. Magner, and T.B. Tomasi. 2009. miRNA regulation of cytokine genes. *Cytokine* 45:58-69.
375. Hinman, M.N., and H. Lou. 2008. Diverse molecular functions of Hu proteins. *Cell Mol Life Sci* 65:3168-3181.
376. Sandler, H., and G. Stoecklin. 2008. Control of mRNA decay by phosphorylation of tristetraprolin. *Biochem Soc Trans* 36:491-496.
377. Sauer, I., B. Schaljo, C. Vogl, I. Gattermeier, T. Kolbe, M. Muller, P.J. Blackshear, and P. Kovarik. 2006. Interferons limit inflammatory responses by induction of tristetraprolin. *Blood* 107:4790-4797.
378. Kummer, M., A.T. Prechtel, P. Muhl-Zurbes, N.M. Turza, and A. Steinkasserer. 2009. HSV-1 upregulates the ARE-binding protein tristetraprolin in a STAT1- and p38-dependent manner in mature dendritic cells. *Immunobiology*
379. Marcet-Palacios, M., M. Ulanova, F. Duta, L. Puttagunta, S. Munoz, D. Gibbings, M. Radomski, L. Cameron, I. Mayers, and A.D. Befus. 2007. The transcription factor Wilms tumor 1 regulates matrix metalloproteinase-9 through a nitric oxide-mediated pathway. *J Immunol* 179:256-265.
380. Taouil, K., J. Hinnrasky, C. Hologne, P. Corlieu, J.M. Klossek, and E. Puchelle. 2003. Stimulation of beta 2-adrenergic receptor increases cystic fibrosis transmembrane conductance regulator expression in human airway epithelial cells through a cAMP/protein kinase A-independent pathway. *J Biol Chem* 278:17320-17327.

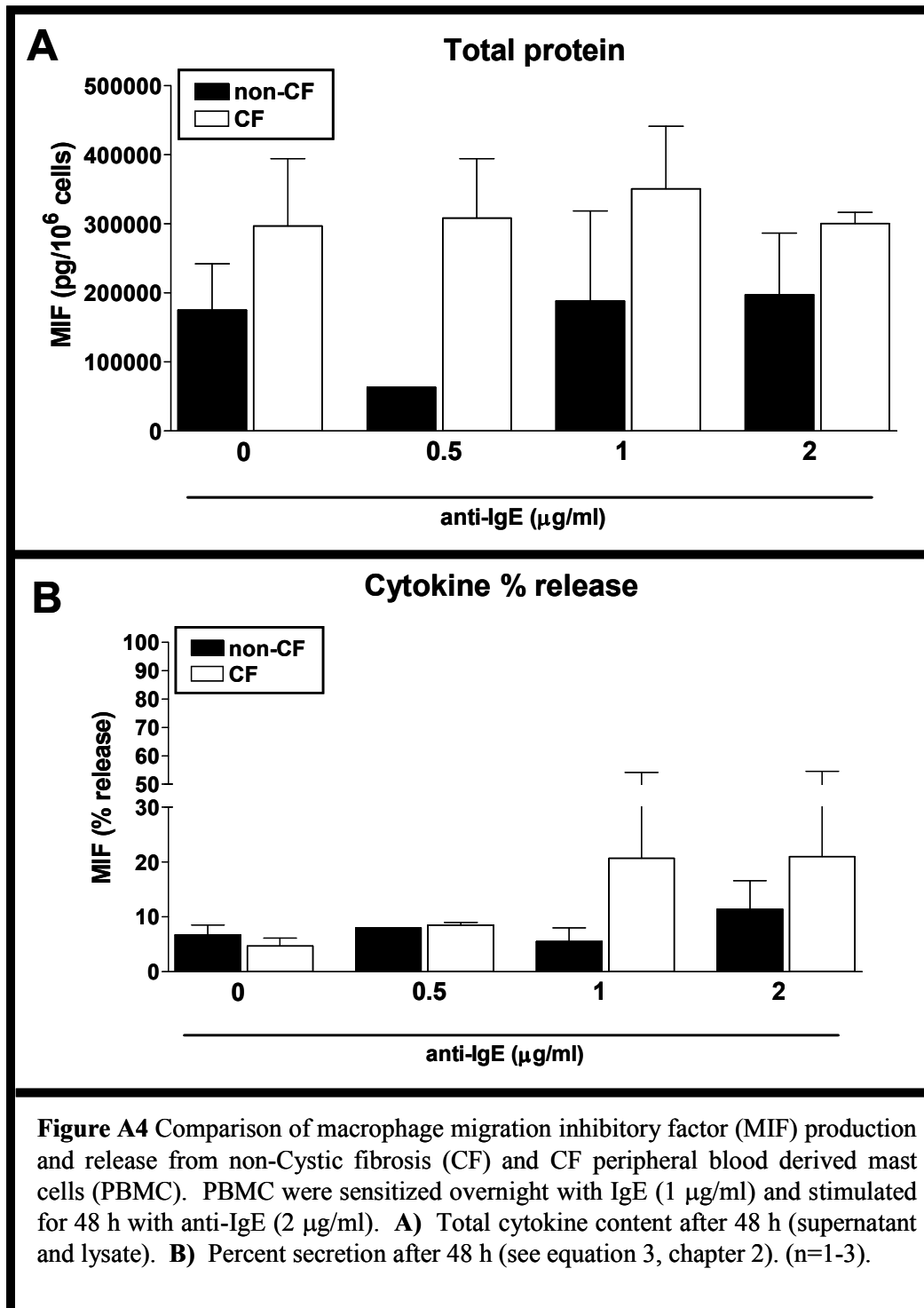
Appendix 1

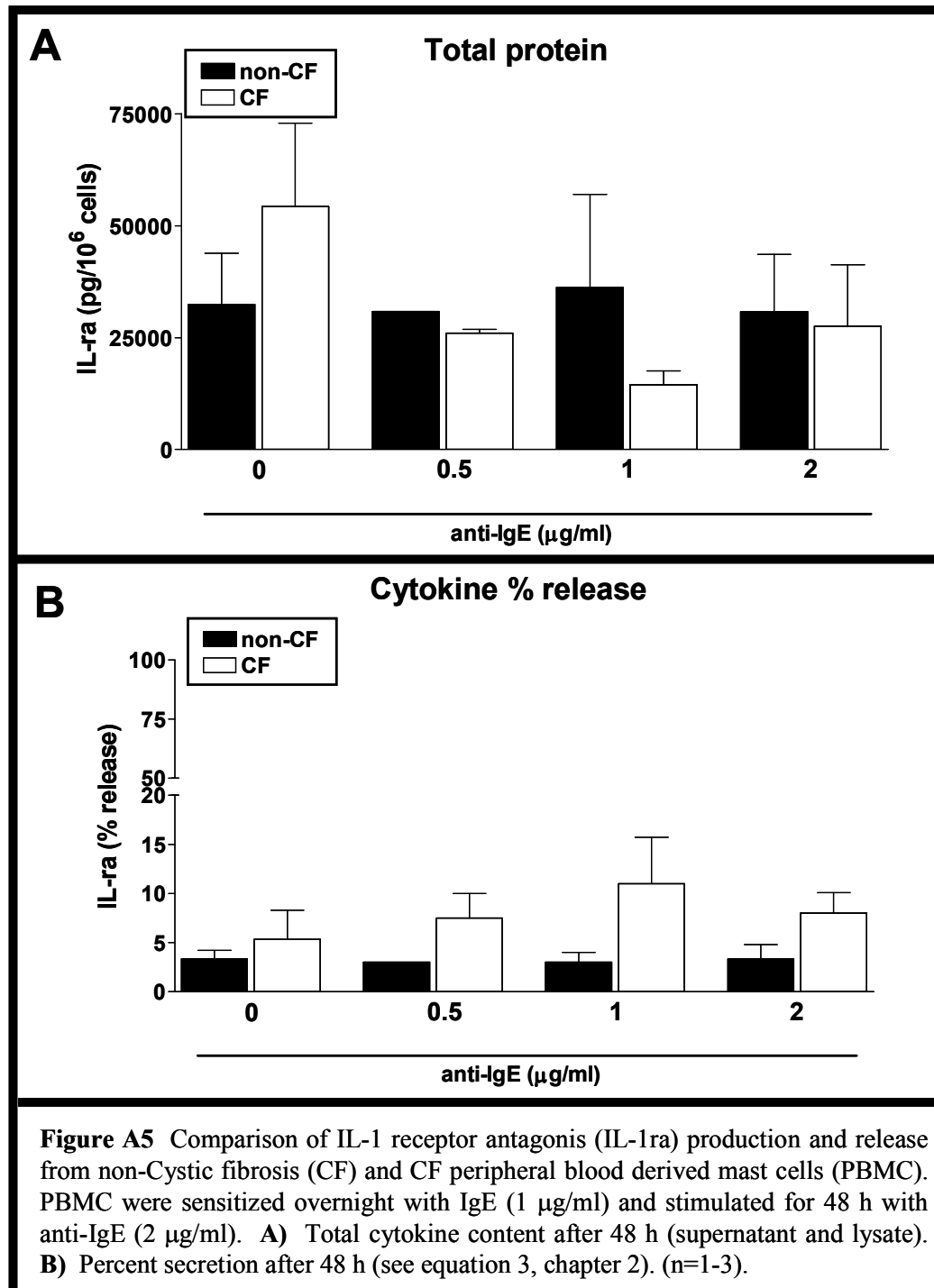
Cytokine and Chemokine Synthesis and Secretion by Cystic Fibrosis
and Non-Cystic Fibrosis Donor Peripheral Blood-Derived Mast Cells

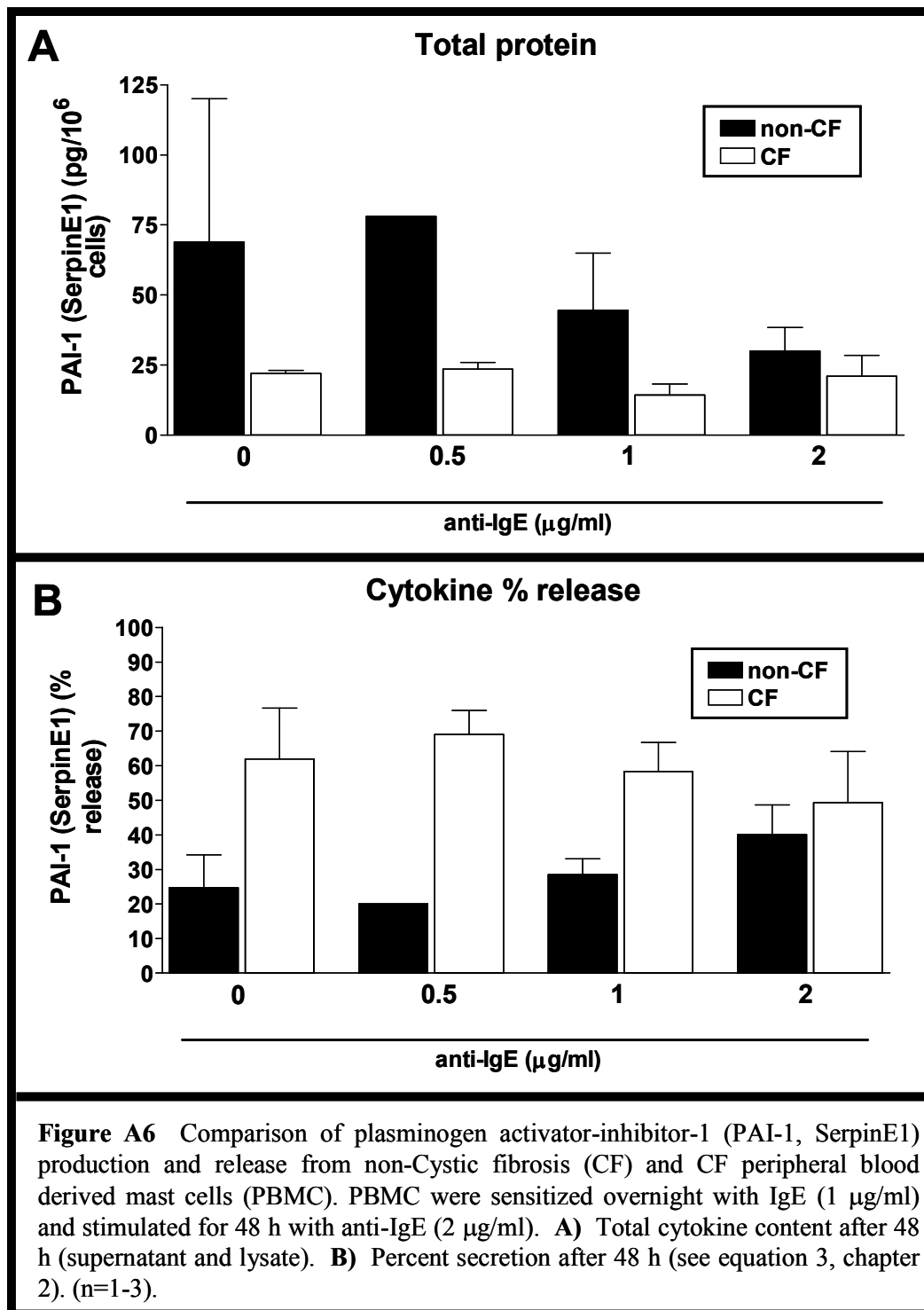


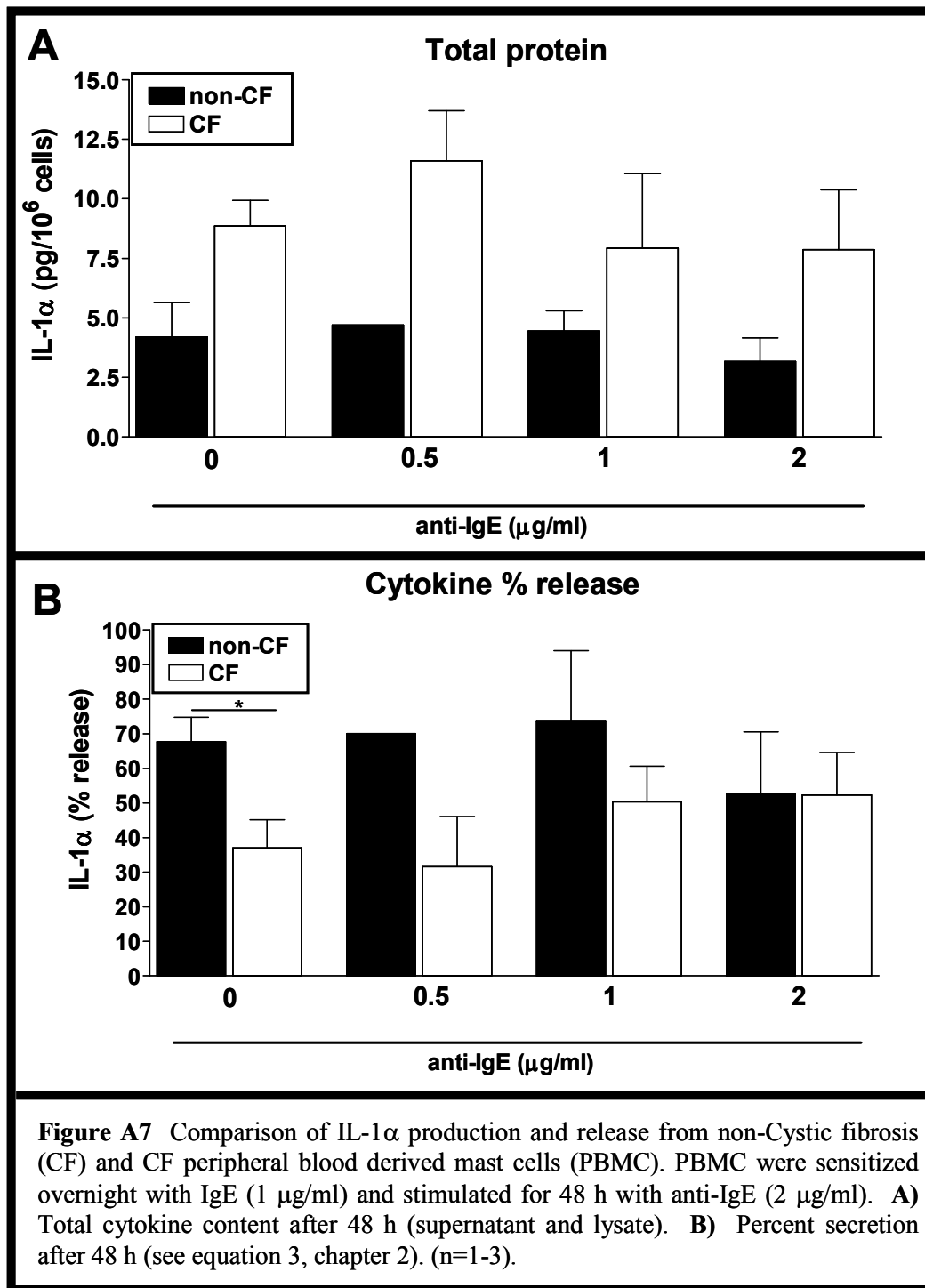


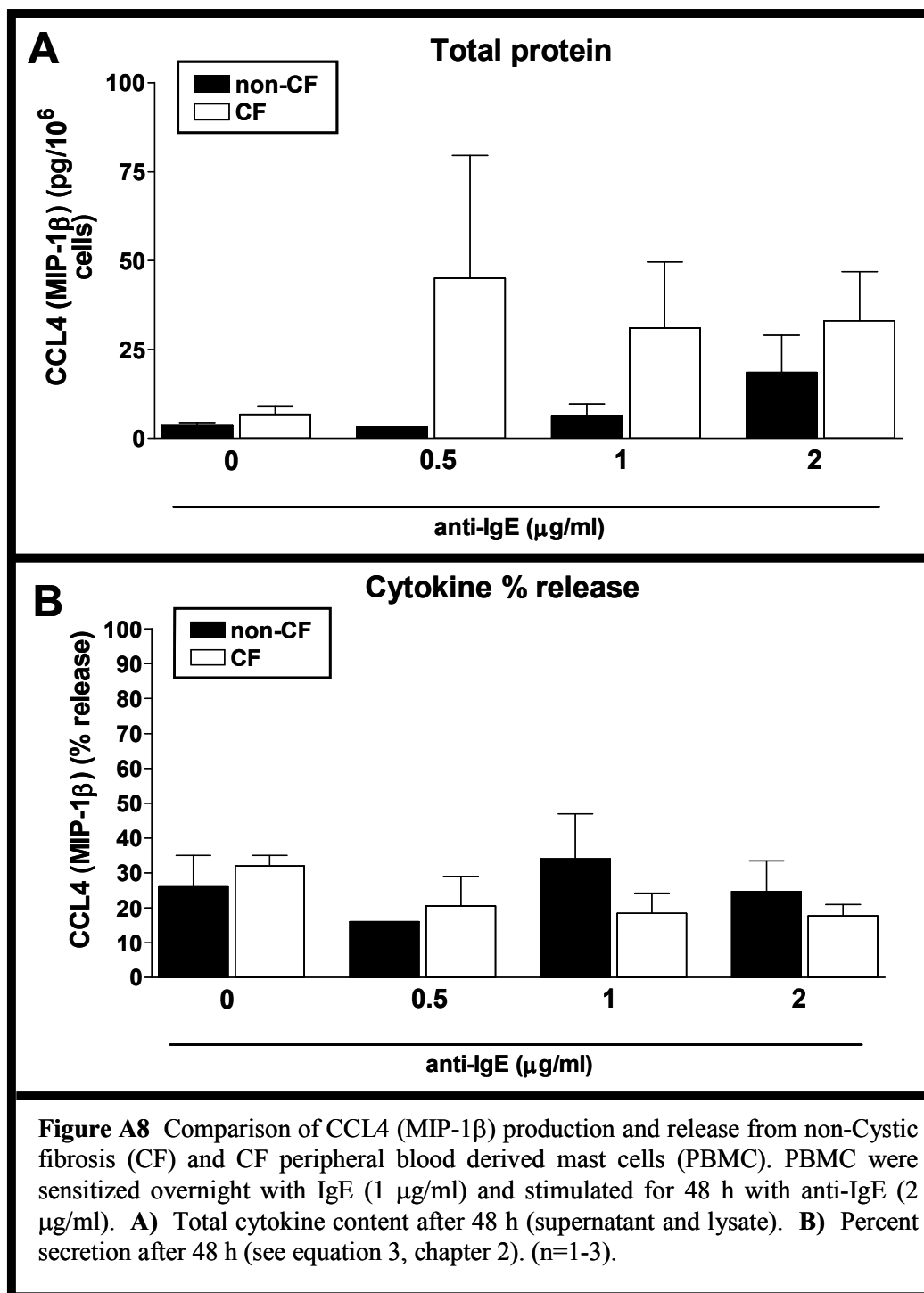


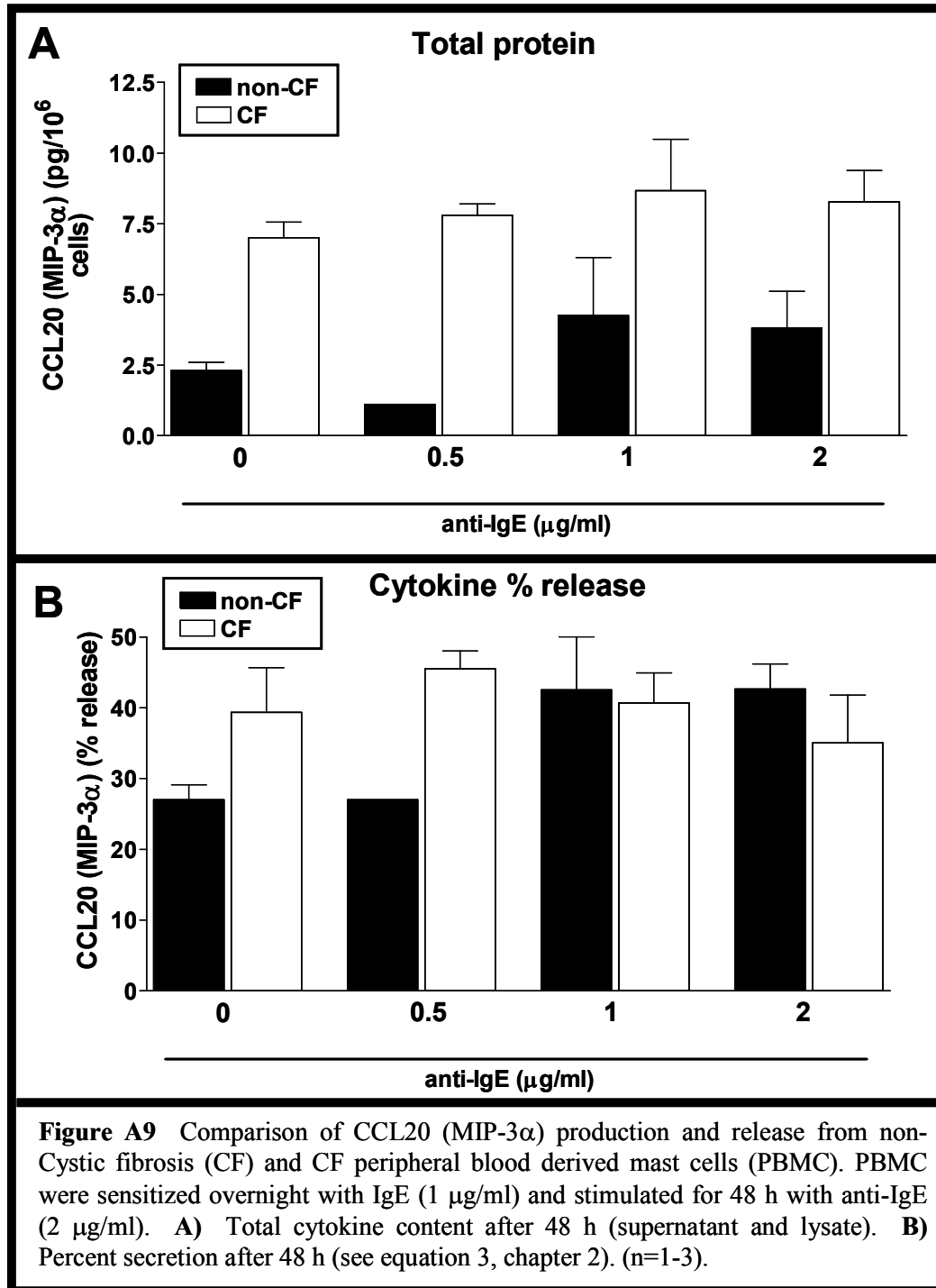


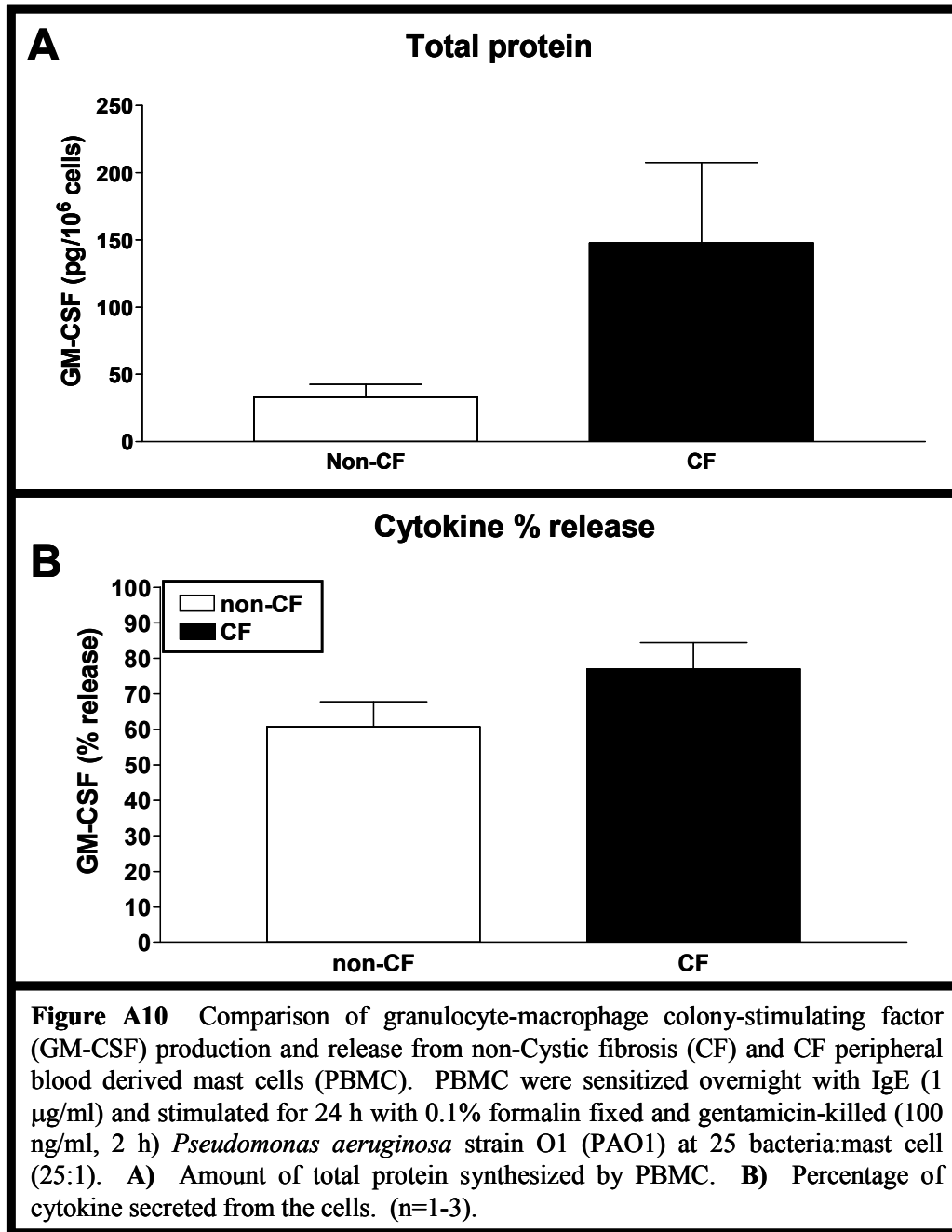


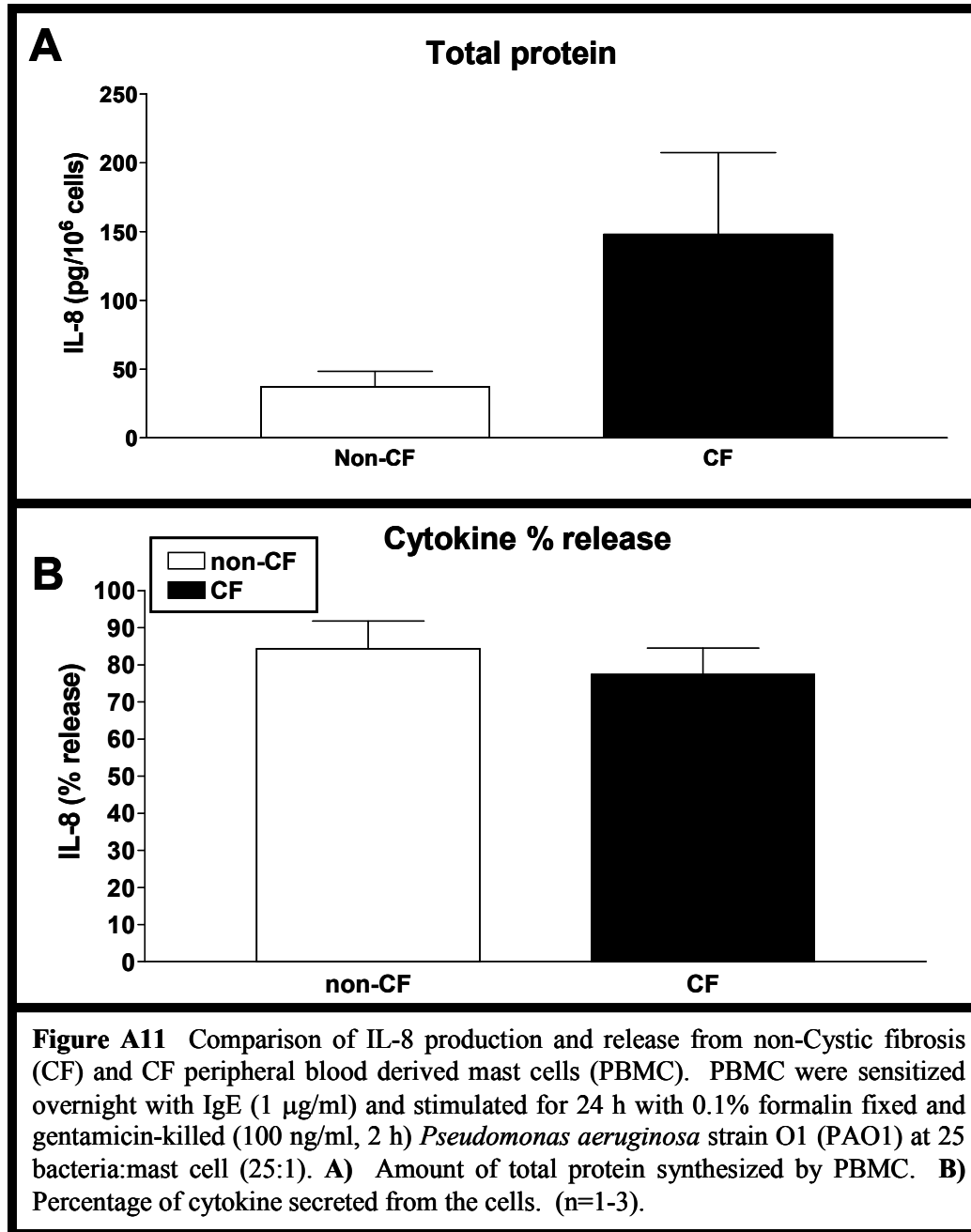


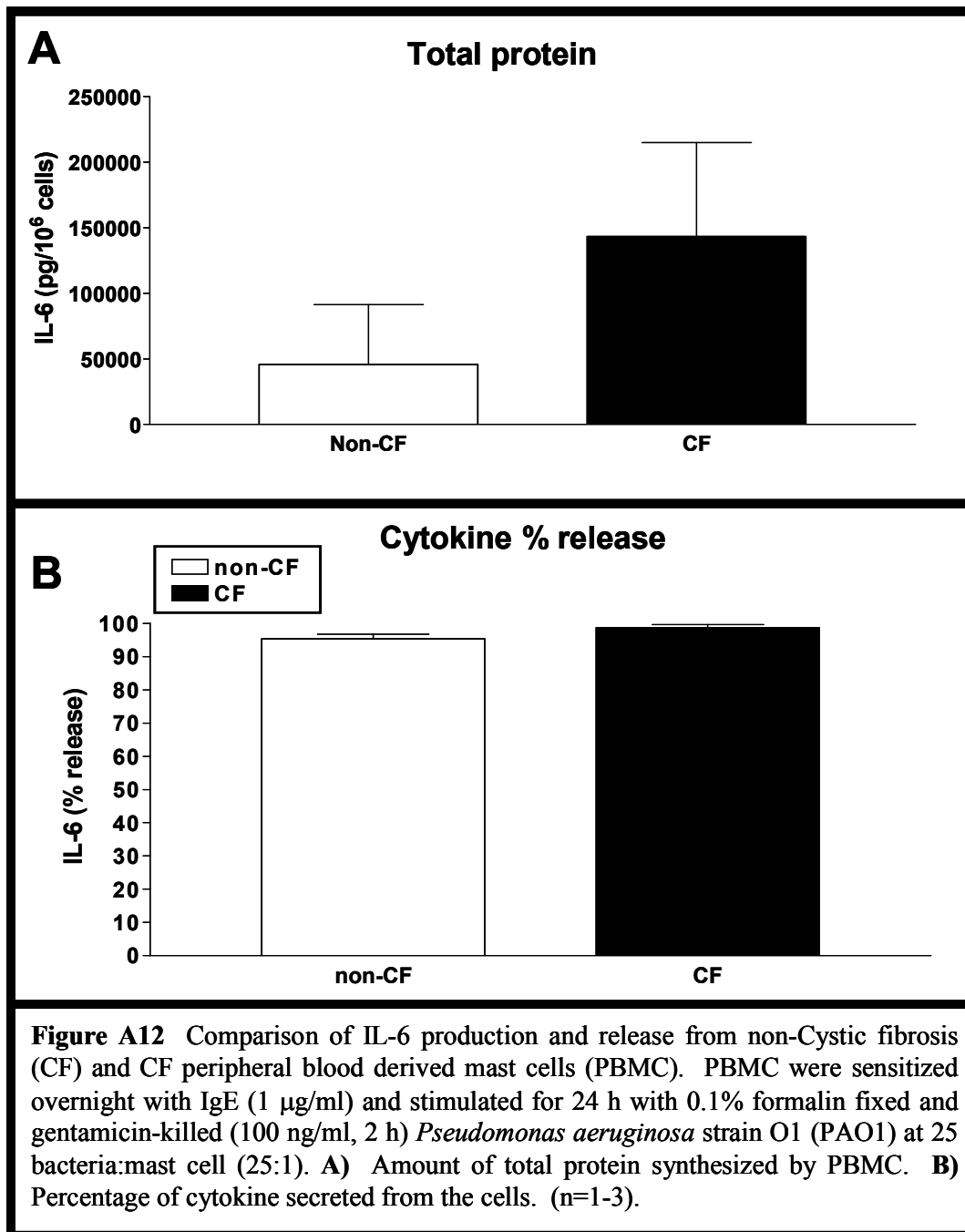


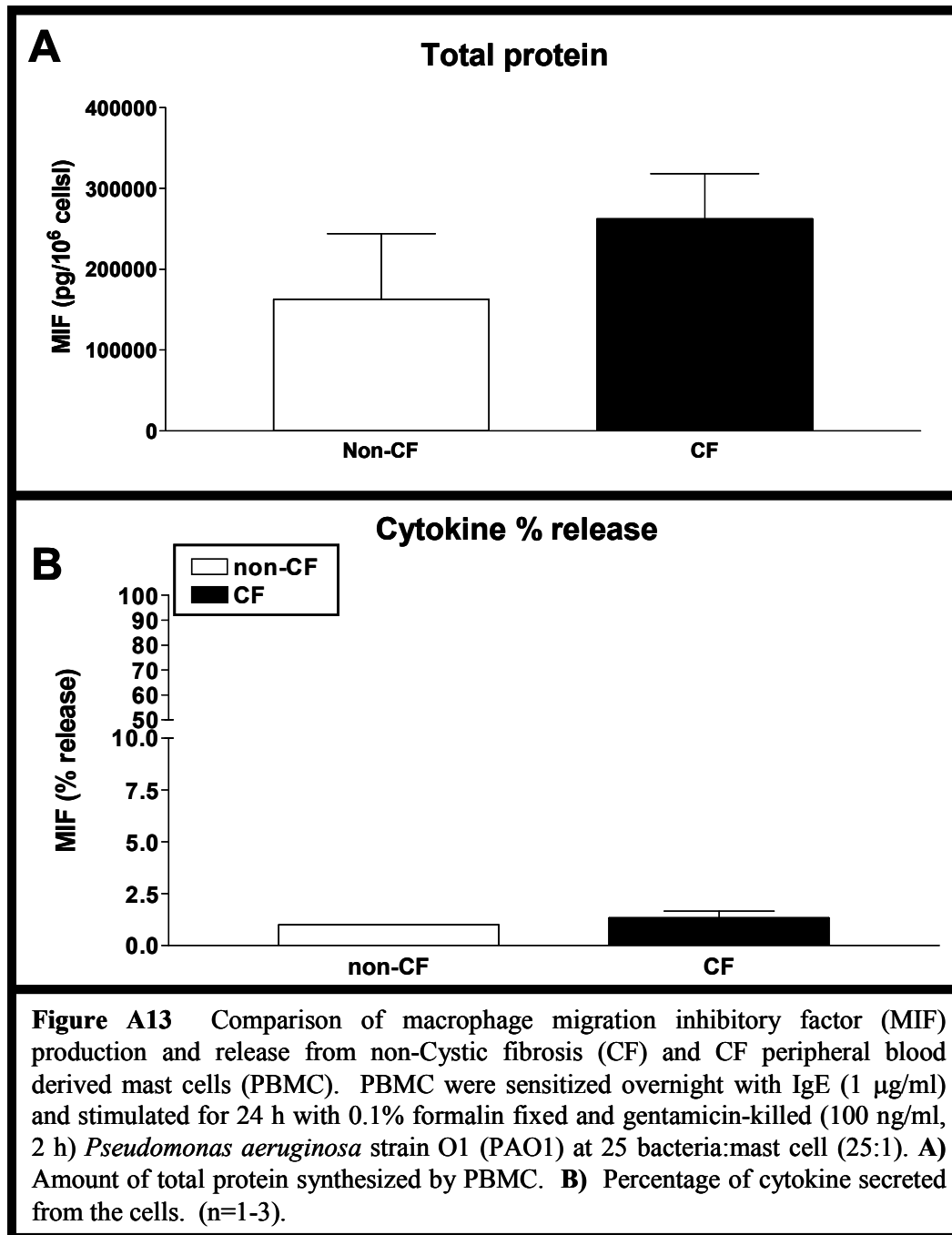


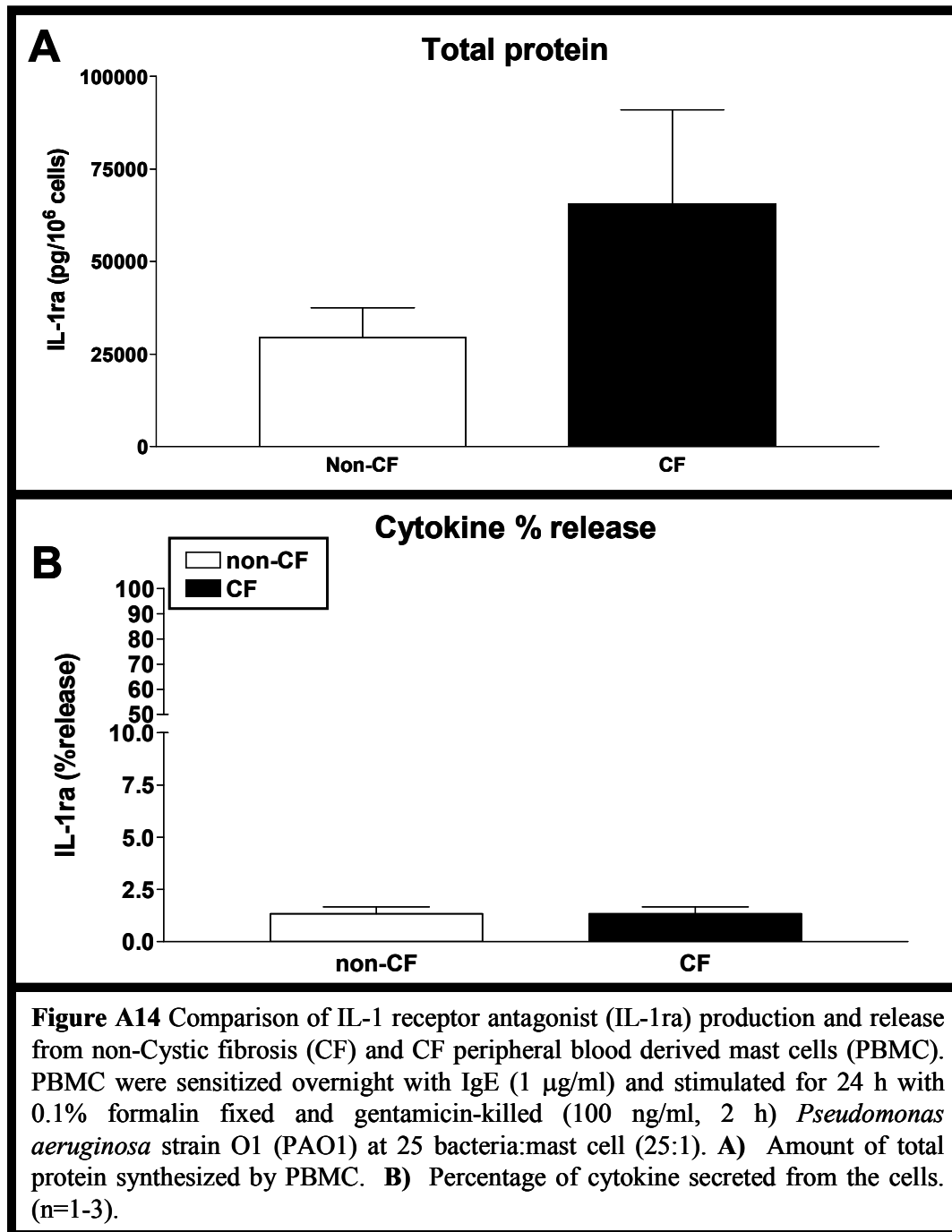


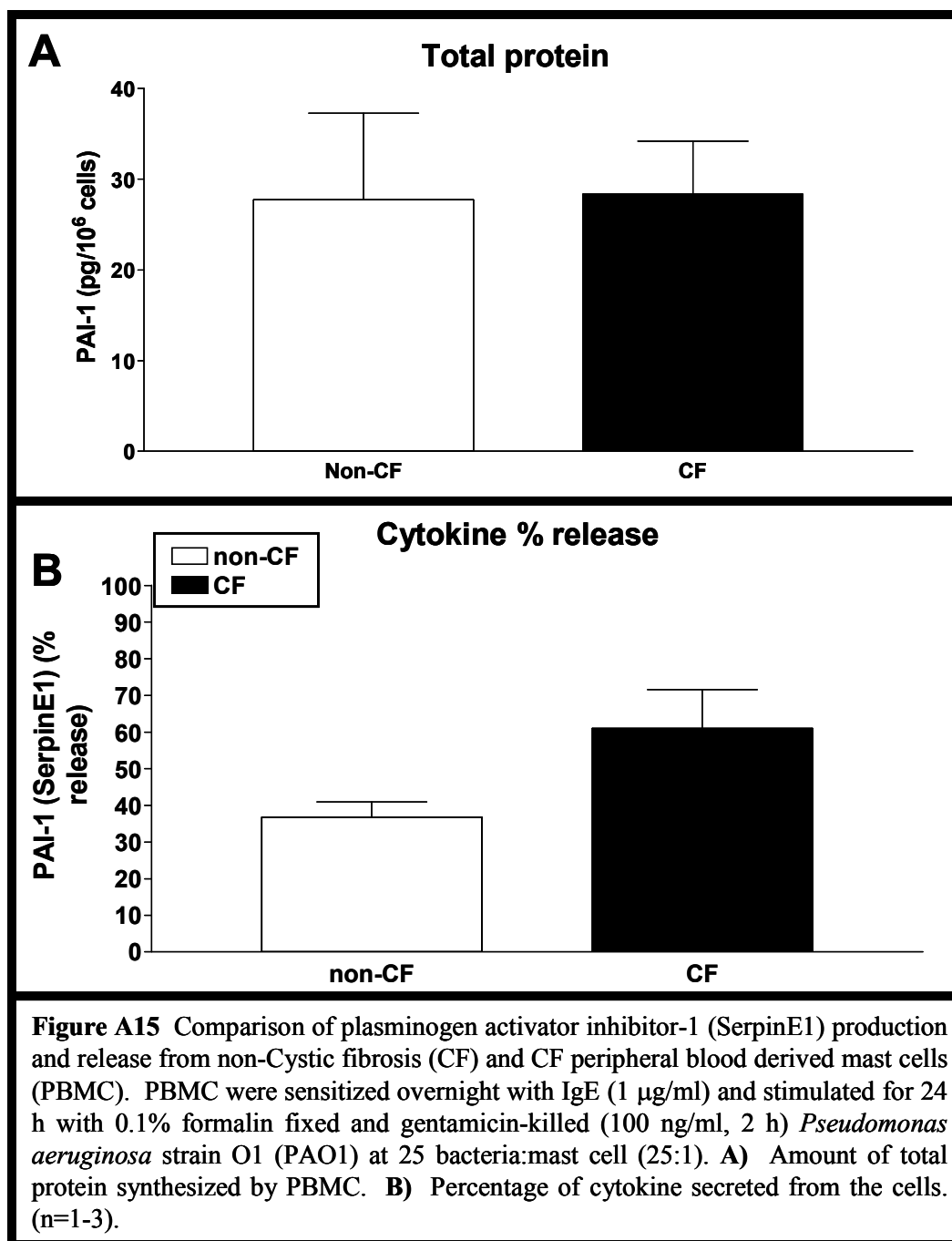


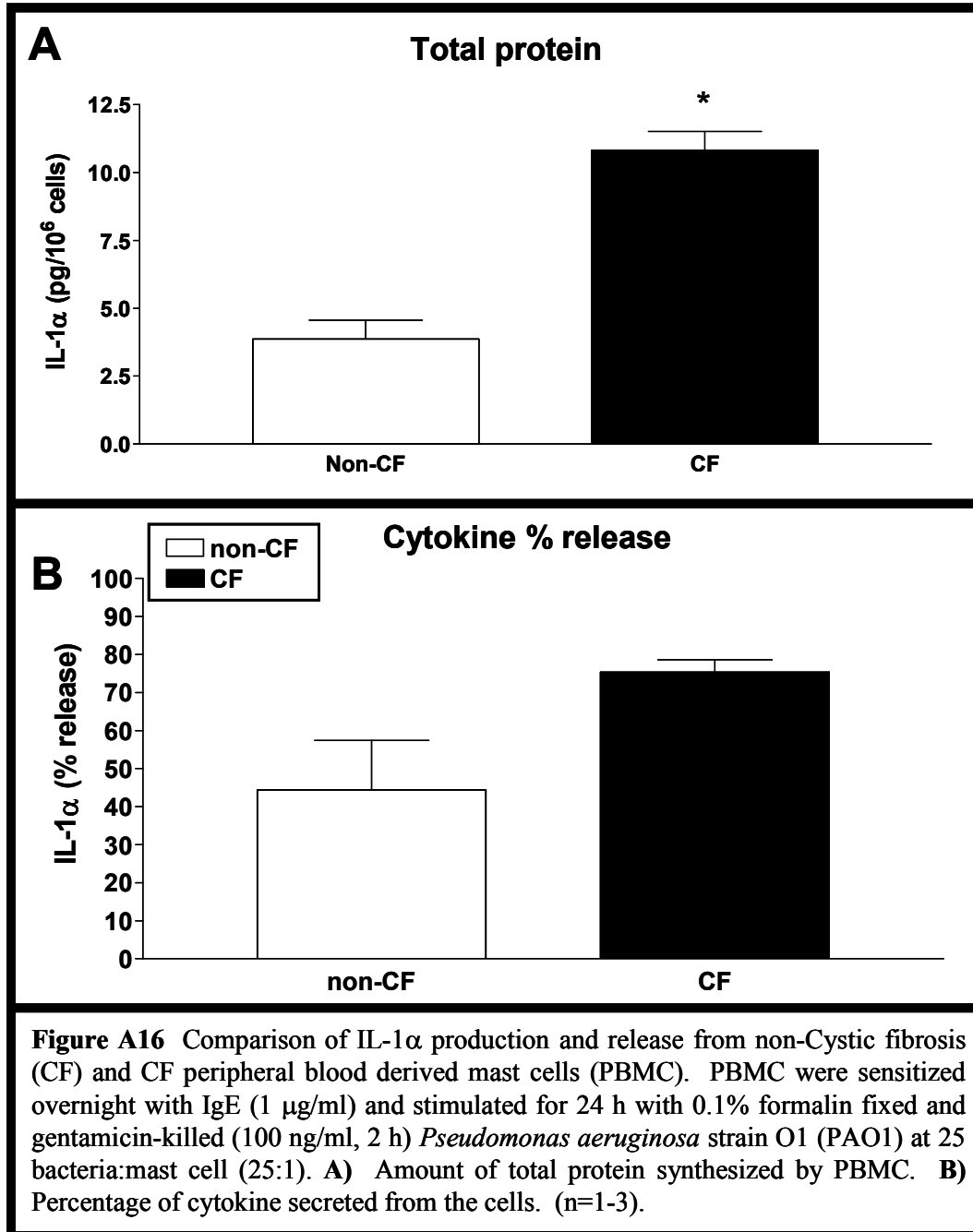


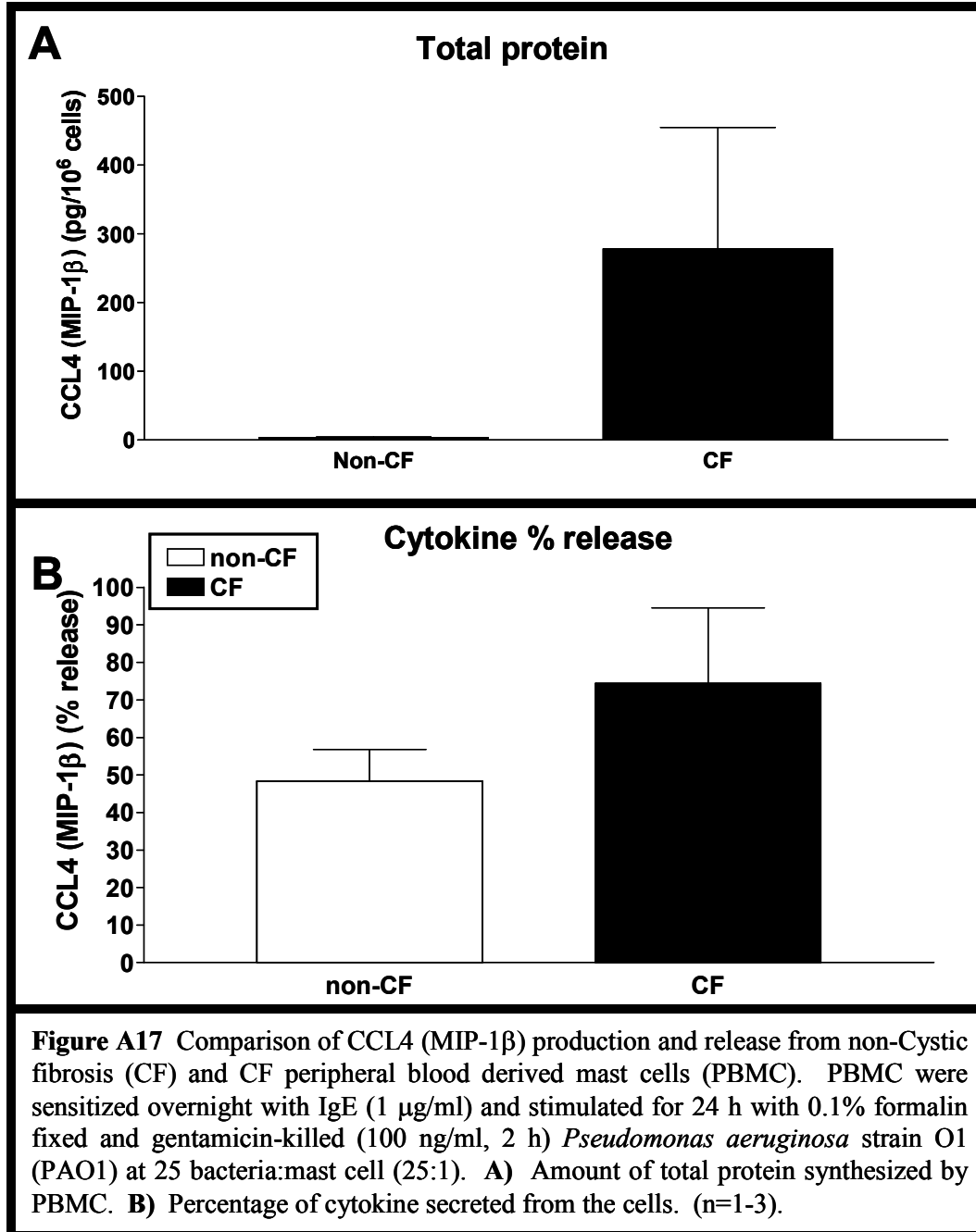


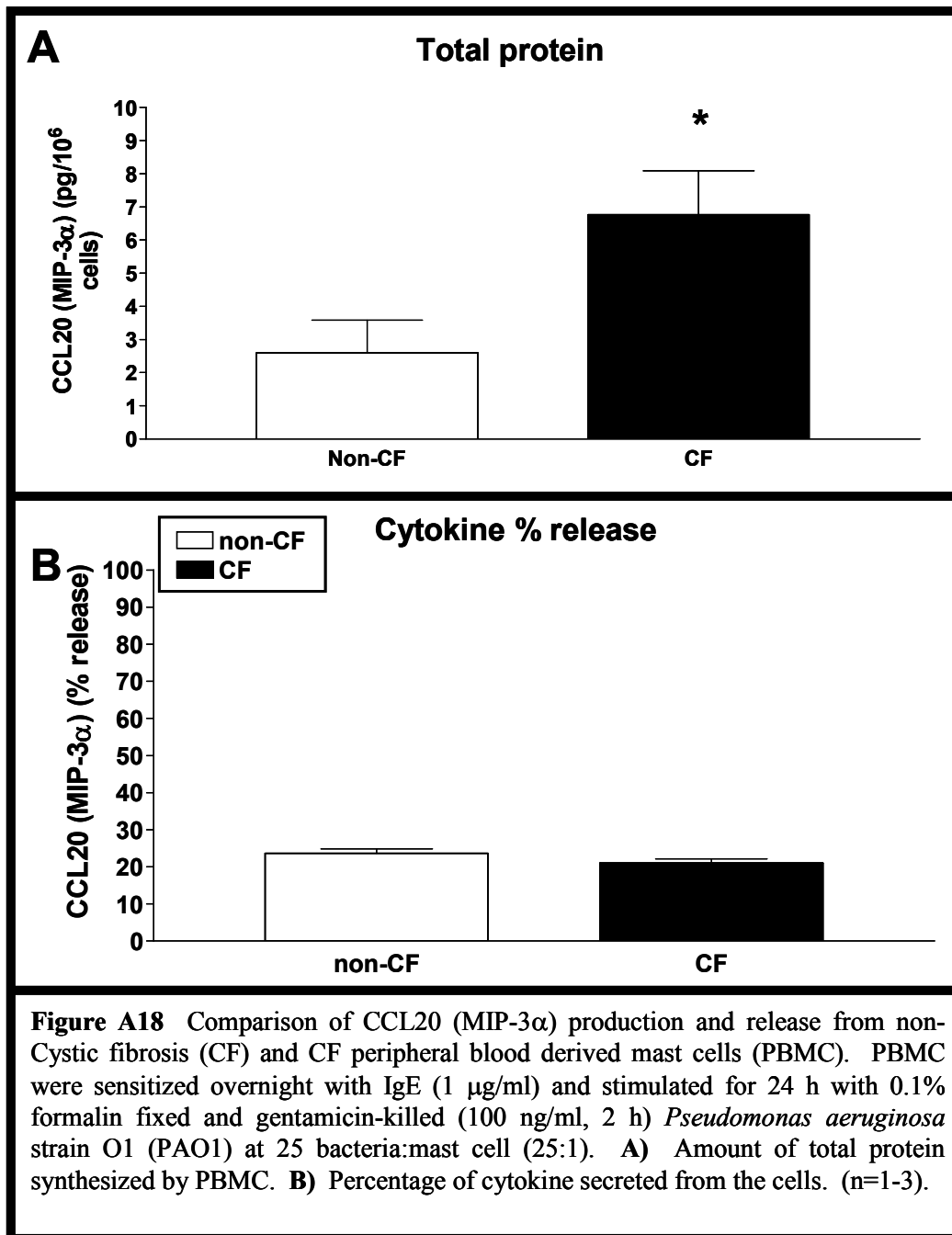












Appendix 2

Differential Regulation of CFTR by Interferon- γ in Mast Cells and Epithelial Cells

Marianna Kulka, Rene Dery, Drew Nahirney, Marek Duszyk and A. Dean Befus

Pulmonary Research Group
550B HMRC
University of Alberta
Edmonton, Alberta

Running title: “Cell type specific regulation of CFTR by IFN γ ”

Corresponding author:

A. Dean Befus

Room 550A HMRC

Pulmonary Research Group, Department of Medicine,

University of Alberta, Edmonton, Alberta, Canada

T6G 2S2

Phone (780)492-1909

Fax (780)492-5329

dean.befus@ualberta.ca

LIST OF ABBREVIATIONS

C/EBP, CCAAT-enhancer binding protein

ClC, voltage-gated Cl⁻ channel

CFTR, cystic fibrosis transmembrane conductance regulator

CREB, cAMP response element binding protein

DPC, diphenylamine-2-carboxylate

JAK, Janus kinase

ERK, extracellular signal-regulated kinase

HTB, Hepes Tyrode's buffer

PMC, peritoneal mast cells

JNK, c-Jun NH₂-terminal kinase

LAD2, Laboratory of Allergic Diseases mast cell line 2

MAPK, mitogen-activated protein kinase

MQAE, N-(ethoxycarbonylmethyl)-6-methoxyquinolinium bromide

NF- κ B, nuclear transcription factor kappaB

NPPB, 5-nitro-2-(3-phenylpropylamino) benzoic acid

PMA, phorbol 12 myristate 13 acetate

PMC, rat peritoneal mast cells

RCMC, rat cultured mast cells

STAT, signal transduction and activator of transcription

Recommended Section Assignment: Inflammation and Immunopharmacology

ABSTRACT

Cystic fibrosis transmembrane conductance regulator (CFTR) is a cAMP-dependent chloride channel in epithelial cells; recently we identified it in mast cells. Previous work that we confirmed showed that IFN γ downregulated CFTR expression in epithelial cells (T84), but by contrast, we found that IFN γ upregulated CFTR mRNA and protein expression in rat and human mast cells. IFN γ upregulation of CFTR in mast cells was inhibited by p38 and ERK kinase inhibitors but not a JAK2 inhibitor, whereas in T84 cells IFN γ -mediated downregulation of CFTR was JAK2 dependent, and ERK and p38 independent. Furthermore, IFN γ downregulation of CFTR in T84 epithelial cells was STAT1 dependent, but upregulation of CFTR in mast cells was STAT1 independent. Thus, differential regulatory pathways of CFTR expression in mast cells and epithelial cells exist that are dependent upon either p38/ERK or JAK/STAT pathways, respectively. Surprisingly, IFN γ treatment of mast cells inhibited Cl⁻ efflux, in contrast to upregulation of CFTR/mRNA and protein expression. However, downregulation of Cl⁻ flux correlated with IFN γ -mediated inhibition of mediator secretion. This and other work suggests that the effect of IFN γ on CFTR expression in mast cells is important for their function.

Introduction:

The cystic fibrosis transmembrane conductance regulator (CFTR) is a cAMP-dependent Cl^- channel that controls transepithelial electrolyte transport, fluid flow and ion concentrations in the intestine, lungs, pancreas and sweat glands (Gibson et al., 2003). Over 1,200 disease-associated mutations in the cystic fibrosis gene have been reported to the Cystic Fibrosis Genetic Analysis Consortium database (www.genet.sickkids.on.ca/cftr/). About 70% of patients with the disease have a deletion of phenylalanine at amino acid position 508 ($\Delta 508$) that severely decreases CFTR expression in the plasma membrane and compromises permeability to Cl^- . CFTR expression in epithelial cells is temporally and spatially complex and can be regulated by many factors including the cytokine IFN- γ (Besancon et al, 1994). Non-epithelial cells such as cardiac myocytes (Davies et al, 2004), lymphocytes and mast cells also express CFTR (Kraus et al, 1992; Dong et al, 1995; Kulka et al, 2002a).

In mast cells, several specific Cl^- conductances have been identified and linked with degranulation. Following antigen stimulation of rat peritoneal mast cells (PMC), there is an increase in Cl^- uptake (Romanin et al, 1991; Friis et al, 1994). Cl^- channel blockers such as 5-nitro-2-(3-phenylpropylamino) benzoic acid (NPPB) inhibit both mast cell Cl^- current and degranulation (Romanin et al, 1991), while diphenylamine-2-carboxylate (DPC), blocks Fc ϵ RI-stimulated degranulation and forskolin-induced Cl^- current in PMC (Kulka et al, 2002a). Moreover, mast cell stabilizing compounds, cromolyn and nedocromil inhibit mast cell degranulation, as well as Cl^- ion flux (Alton and Norris, 1996). We have

identified CFTR and voltage-gated chloride channel (ClC) family members ClC-2,3,4,5,7 in rat mast cells (Kulka et al, 2002a; Kulka et al, 2002b), and others have identified ClC3, 5 and 7 in human mast cells (Duffy et al, 2001; Bradding et al, 2003). Thus, given that CFTR in mast cells may be important for their functions, we have studied the regulation of CFTR expression in mast cells.

In epithelial cells, IFN γ downregulates expression of CFTR resulting in a significant decrease in CFTR-mediated Cl $^-$ current (Besancon et al, 1994). IFN γ is a member of a family of inducible secretory proteins produced largely by activated T lymphocytes and natural killer cells (Schroder et al, 2004). IFN γ modulates gene expression by activating Janus Kinase (JAK) resulting in signal transducer and activator of transcription (STAT) 1 binding and phosphorylation. Phosphorylated STAT1 dimerizes and translocates into the nucleus where it binds to γ -activated sequence (GAS) elements and initiates transcription (Schroder et al, 2004). In addition to the JAK/STAT pathway, IFN γ activates other signal-transduction proteins such as p38 mitogen-activated protein kinases (MAPK) and extracellular signal-regulated kinase (ERK) 1/2 MAPK (14). With regard to mast cells, IFN γ can inhibit proliferation, TNF-mediated cytotoxicity, cell differentiation and mediator release (Bissonnette and Befus, 1990; Holliday et al, 1994; Kirshenbaum et al, 1988). We hypothesized that IFN γ may downregulate CFTR expression in mast cells by a JAK/STAT1 dependent pathway, as in epithelial cells. However, in contrast to epithelial cells, we found that IFN γ upregulated CFTR expression in both rat and human mast cells and in a JAK/STAT1 independent manner. Surprisingly, Cl $^-$ flux measurements indicate

that IFN γ treatment of mast cells reduces Cl $^-$ flux despite the upregulation of CFTR levels.

Materials and Methods:

Materials

The JAK2 inhibitor, AG-490 (α -Cyano-(3,4-dihydroxy)-N-benzylcinnamide tyrphostin B42), was obtained from Calbiochem (La Jolla, CA), the p38 inhibitor SB202190 ($C_{20}H_{14}FN_3O$) and the ERK inhibitor U0126 (1,4-Diamino-2,3-dicyano-1,4-bis(2-aminophenylthio)-butadiene) were from Cell Signaling (Beverly, MA). Phorbol 12 myristate 13 acetate (PMA) was obtained from Sigma-Aldrich (St. Louis, MO). Stem cell factor, TNF and IFN γ (rat and human) were purchased from PeproTech (Rocky Hill, NJ).

Rats and PMC Isolation

Male Sprague Dawley rats (300-350 g; Charles River, St. Constant, Quebec, Canada) were housed in a pathogen-free viral antibody-free facility. Rats were sacrificed by cervical dislocation under anesthesia and PMC were isolated as previously described (Kulka et al, 2002a). Briefly, 20 mL of HEPES Tyrode's buffer (HTB, containing (mM): 137 NaCl, 5.5 glucose, 2.7 KCl, 0.5 NaH_2PO_4 , 1 $CaCl_2$, 12 HEPES (pH 7.2), and 1% BSA) was injected into the peritoneal cavity and massaged gently for 30 sec; the peritoneal cavity was opened, the buffer collected and kept at 4°C. Following centrifugation at 200 g for 5 min the cell pellet was resuspended in 5 mL of HTB, layered on top of a 30%/80% Percoll gradient, centrifuged at 500 g for 20 min, and the MC were collected from the pellet. PMC were >98% pure and >96% viable as measured by trypan blue exclusion.

Nippostrongylus brasiliensis Sensitization

Sprague Dawley rats were sensitized to *Nippostrongylus brasiliensis* by a single subcutaneous injection of 3000 L3 larvae (Befus et al, 1982). The adult worms were expelled after 10 days, but the mast cells remained sensitized with worm antigen specific IgE for several weeks. The rats were used for experiments 30-40 days post infection.

Cell Culture

The rat cultured MC line (RCMC) 1.11.2 (kindly provided by B. Chan and A. Froese, Winnipeg, Manitoba) was cultured in RPMI 1640 medium containing 5% FBS (Invitrogen, Grand Island, NY), 100 U/mL penicillin, 100 µg/mL streptomycin and 10 mM HEPES (Sigma-Aldrich). The recently established human mast cell line, Laboratory for Allergic Diseases (LAD) 2 (Kirschenbaum et al, 2003) (a generous gift from Drs. Kirschenbaum, Akin and Metcalfe, NIH), was cultured in serum free media (StemPro-34 SFM, Invitrogen) supplemented with 2 mM L-glutamine, 100 U/mL penicillin, 50 µg/mL streptomycin and 100 ng/mL stem cell factor. The T84 epithelial cell line was cultured in F-12/DMEM media (Invitrogen) containing 5% FBS, 100 U/mL penicillin and 100 µg/mL streptomycin. All cells were incubated in a humidified atmosphere of 5% CO₂ in air at 37°C.

Quantitative real-time polymerase chain reaction

Our previous study (Kulka et al, 2002a) established that mast cells express mRNA for CFTR and confirmed that the sequence was authentic CFTR. In the current study RNA was isolated as described previously (Gilchrist et al, 1997) and quantitative real-time PCR assay of transcripts was performed using gene-specific fluorescently-labeled primers and a 7700 Sequence Detector (Applied Biosystems, Foster City, CA). All primers and reagents were obtained from Invitrogen. Primers were designed using the LUX[®] primer design tool, and are listed along with their Invitrogen reference code (Table 1). Each primer set consisted of one labeled (6-carboxy fluorescein (FAM) fluorescent reporter at the 5' end) and one unlabeled primer. Lower case nucleotides in the labeled primer sequence represent hairpin-generating segments of the labeled primer. Data was collected during the annealing/extension phase of PCR and analyzed using the comparative C_t method (Nazarenko et al, 2002).

Western blot

Cells were washed with PBS and 1×10^6 cells lysed in buffer containing loading dye solution (Lithium dodecyl sulphate [LDS]) sample buffer (Invitrogen), 10% β -mercaptoethanol (Sigma-Aldrich), 0.1 M dithiothreitol (DTT; Sigma-Aldrich) and protease inhibitor cocktail (Roche, Indianapolis, IN). Whole cell lysates (30 μ g) were separated on 4-12% Bis-Tris SDS-PAGE gels (Invitrogen) and transferred onto nitrocellulose membranes. The membranes were blocked with 3% milk in TBS-0.05% Tween for 1 hr and then probed with primary antibodies against CFTR (clone H-182) and STAT1 (Santa Cruz

Biotechnology, Santa Cruz, CA), phosphoSTAT1 (BD Transduction Labs, Chicago, IL), phospho-stress-activated MAPK (SAPK) /c-Jun NH2-terminal kinase (JNK) (Thr183/Tyr185; Cell Signaling Technology), phospho-p38 MAPK (Thr180/Tyr182; Cell Signaling Technology), and phospho ERK1/2 (Thr202/Tyr204; Cell Signaling Technology), or anti-actin (Sigma-Aldrich) in 4% BSA/PBS for 1 hr at room temp. The membranes were washed with TBS-Tween 3X and then incubated with the horseradish peroxidase-linked secondary antibody (sheep anti-rabbit, Jackson ImmunoResearch Laboratories, West Grove, PA, or goat anti-mouse, Santa Cruz Biotechnology) for 1 hr. The nitrocellulose membranes were developed with chemiluminescence reagent (Invitrogen) for 1 min and exposed to high performance chemiluminescence film for 1-5 min.

Confocal microscopy

IFN γ treated (80 ng/ml), 24 h) rat PMCs and human T84. After incubation, T84 cells were detached by 10 min incubation with trypsin-EDTA at room temperature and 50 000 PMCs or T84 were then cytocentrifuged onto Superfrost plus charged slides using a Shandon Cytospin 2 (Fisher Scientific, Mississauga, ON, Canada) at 5g for 6 min in PBS containing 20% FBS. Cells were then air-dried overnight and fixed in 75% acetone/25% absolute ethanol for 15 min at -20°C. Non-specific binding sites were blocked by incubation in blocking buffer (PBS containing 3% BSA and 10% normal goat serum) for 2 h at room temperature. Slides were then incubated with mouse anti-human CFTR primary antibody (MA1-935; Affinity Bioreagents, Golden, CO) at 1/50 dilution in

blocking buffer for 2 h at room temperature. After three washes in PBS, specific antibody binding was detected using Alexa 568-conjugated goat anti-mouse IgM (Molecular Probes, Eugene, OR) at 1/2000 dilution in blocking buffer for 1 h at room temperature. Cell images were obtained using an Olympus FV1000 laser scanning confocal microscope (Carsen Group, Markham, ON, Canada) with 400x magnification.

³⁶Cl⁻ Flux Measurements

Changes in [Cl⁻] were measured by incubating 1 x 10⁶ cells/mL with 8.7 mM Na³⁶Cl (ICN, Aurora, OH) in flux buffer (137 mM NaCl, 4 mM KCl, 1 mM MgSO₄, 1 mM CaCl₂, 20 mM HEPES, 1 mg/mL BSA, 1 mg/mL glucose) at 37°C for 30 min (Friis et al, 1994). The incubation was terminated by transferring 100 µL of the cell suspension onto 120 µL of silicone oil in long, thin Eppendorf tubes. The tubes were centrifuged at 18,000 g for 30 s and then placed into a freezing methanol bath. The bottom of each tube was cut off and placed into a scintillation vial with 48 mM NaOH. Each scintillation vial was vortexed for 1 min after which 5 mL of scintillation fluid was added and the vial was counted using a Beckman scintillation counter. ³⁶Cl⁻ uptake was calculated based on the specific activity of ³⁶Cl⁻ in the extracellular medium, calculated as the sum of extracellular Cl⁻ and added ³⁶Cl⁻ concentrations (in nmol) divided by the radioactivity of the added ³⁶Cl⁻ (in cpm). All values of ³⁶Cl⁻ uptake were corrected for ³⁶Cl⁻ trapped in the extracellular space, which was determined by measuring cpm immediately after ³⁶Cl⁻ addition (50 ± 10.2 cpm).

MQAE Measurements

Fluorescence measurements were performed in HTB. Gluconate, Br⁻, or I⁻ buffers were identical to HTB except that 137 mM NaCl was replaced by equivalent amounts of sodium gluconate, NaBr, or NaI, respectively. One million cells/mL were incubated with 5 mM of the Cl⁻-sensitive dye N-(ethoxycarbonylmethyl)-6-methoxyquinolinium bromide (MQAE, Molecular Probes, Eugene, OR) in 1 mL HTB for 30 min at 37°C. Cells were washed twice and resuspended in 50 µl HTB. MQAE is quenched by Cl⁻ anions and thus, when Cl⁻ leaves the cell, it dissociates from MQAE and fluorescence increases. MQAE fluorescence was excited at 350 nm and the emission was measured at 450 nm with a PTI spectrofluorimeter (Photon Technology Int., London, Ontario), using Felix software (version 1.42). All experiments were performed at 37°C. To produce a driving force for Cl⁻ efflux, the cells were added to 1 mL of gluconate buffer and MQAE fluorescence was monitored for up to 10 min. Cl⁻ efflux was calculated as the initial rate of change of MQAE fluorescence after addition of cells to the gluconate buffer. For quantitative analysis, the data collected in the first 60 sec were fitted using linear regression, and the slope was used as a measure of Cl⁻ efflux. All traces were normalized to initial baseline reading (buffer, no cells).

In some experiments 10 worm equivalents/mL of *Nippostrongylus brasiliensis* antigen (Befus et al, 1982) was added to the cell suspension, and changes in fluorescence were monitored for up to 10 min.

Statistics

All data is presented as mean of at least three independent experiments with standard error of the mean (SEM). Where indicated, data was analysed using a paired *t*-test for sample means, ANOVA or the Tukey-Kramer multiple comparisons test.

Results:

Interferon- γ upregulates CFTR mRNA and protein expression in rat and human mast cells

PMA, TNF and IFN γ downregulate CFTR expression in epithelial cells (Nakamura et al, 1992; Sen et al, 1993; Besancon et al, 1994). To determine if CFTR in mast cells was similarly regulated, rat RCMC were treated with PMA, TNF or IFN γ for 24 hr and CFTR expression was identified by western blotting as we have done previously (confirmed using isotype controls for flow cytometry, western blot and immunohistochemistry, Kulka et al, 2002a). As expected, TNF and IFN γ decreased CFTR expression in T84 cells (Fig 1A). Surprisingly, however, TNF and IFN γ upregulated CFTR expression in RCMC. PMA had no detectable effect on CFTR expression in RCMC or T84 (Fig 1B). Because IFN γ upregulates STAT1 expression (Hu et al, 2002), membranes were stripped and re-probed with anti-STAT1. As expected, STAT1 protein (visible as a double band, representing STAT1 α and STAT1 β) was upregulated in both RCMC and T84 by PMA, TNF and IFN γ .

Confocal analysis of CFTR expression in T84 cells showed a largely cytoplasmic distribution and as expected from the results of Western blot analysis, the intensity of CFTR staining was decreased after IFN γ treatment (80 ng/ml, 24 h; Fig. 1C). By contrast, CFTR expression in rat PMC was increased after IFN γ treatment and seemed to be associated with granules (Fig. 1D). Studies of nonpermeabilized cells identified some CFTR in a plasma membrane-like

distribution on T84, but there was no obvious CFTR with such a distribution on PMC (not shown).

To further characterize upregulation of CFTR in mast cells, CFTR mRNA expression following IFN γ dose response and time course treatments was analyzed in RCMC, human LAD2 and T84 cells (Fig 2). Quantitative PCR analysis confirmed that IFN γ (10 ng/mL) significantly ($p < 0.05$) upregulated CFTR mRNA expression in RCMC by 3 hr following treatment and the magnitude of this upregulation was 39 ± 13 % at 12 hr. In LAD2 MC the upregulation of CFTR was statistically significant by 8 hr of IFN γ treatment and by 12 hr was 54 ± 17 % greater than in untreated cells (Fig 2A). Significant upregulation of CFTR was induced in mast cells within 8 hr with as little as 1 ng/mL (RCMC) or 10 ng/mL (LAD2) of IFN γ (Fig 2B).

By contrast, IFN γ significantly decreased CFTR mRNA expression in T84 cells within 3 hr (Fig 2A and B) and by 12 hr the magnitude of decrease was 49 ± 4 % at 12 hr of treatment. The IFN γ effect was dose dependent such that 1, 10 and 100 ng/mL of IFN γ decreased CFTR mRNA expression in T84 cells by 23, 50 and 83 % after 8 hr (all statistically significant decreases compared to the untreated group).

Western blot analysis showed that by 6 hr, CFTR expression was increased compared to untreated RCMC and by 24 hr, CFTR expression was significantly upregulated (Fig 2C). In T84 cells, decrease in CFTR protein expression was observable at 6 hr and remained low at 24 hr (Fig 2D). In both

T84 and RCMC, STAT1 protein was upregulated after 6 hr of treatment and remained elevated up to 24 hr.

IFN γ upregulation of CFTR is inhibited by MAP kinase inhibitors

To determine which IFN γ signalling pathways were activated in mast cells as compared to epithelial cells, RCMC were treated with IFN γ and whole cell lysates were analysed for phosphorylated STAT1, p38, ERK, and JNK (Fig 3). IFN γ activated STAT1, ERK and p38, but not JNK phosphorylation. STAT1 was activated at 5 min and remained activated for up to 30 min. ERK2 (bottom band) was constitutively activated, but phosphorylation of both ERK1 (top band) and ERK2 (bottom band) was induced after 5 min. p38 was activated at 15 min, later than STAT1 or ERK.

To determine if JAK/STAT1, p38 or ERK signalling pathways were involved in IFN γ -mediated upregulation of CFTR, RCMC, LAD2 and T84 cells were treated with IFN γ in the presence of a JAK2 inhibitor (AG-490), a p38 kinase inhibitor (SB202190) that blocks its phosphorylation (Marone et al, 2002) and an ERK MAP kinase inhibitor (U0126). In RCMC and LAD2, AG-490 did not affect IFN γ -mediated upregulation of CFTR protein expression, but both SB202190 and U0126 partially inhibited IFN γ -mediated upregulation of CFTR (Fig 4). By contrast, in T84 cells, AG-490 blocked IFN γ -mediated downregulation of CFTR. Membranes were stripped and reblotted with anti-STAT1 to compare regulation of another IFN γ responsive protein. STAT1 upregulation in RCMC was sensitive to AG-490 but in human LAD2 cells,

STAT1 upregulation was inhibited by AG-490, SB202190 and U0126. T84 cells were similar to the RCMC in that STAT1 upregulation was only blocked by AG-490 but not SB202190 and U0126. Densitometry analysis of three independent blotting experiments confirmed that AG-490 did not affect IFN γ -mediated upregulation of CFTR protein expression in both LAD2 and RCMC cells (Fig. 5, $p < 0.05$).

To confirm the actions of AG-490, SB202190 and U0126, RCMC were treated with IFN γ (10 ng/mL) in the presence of these inhibitors and STAT1, p38 and ERK1/2 phosphorylation was assessed by western blotting (Fig 6). As expected, AG-490 but not SB202190 or U0126 inhibited STAT1 constitutive and IFN γ -induced phosphorylation (Fig. 6A). U0126 inhibited ERK1/2 constitutive and IFN γ -induced phosphorylation (Fig. 6B). SB202190 inhibited IFN γ induced p38 phosphorylation (Fig. 6C).

IFN γ inhibits both constitutive and antigen-induced Cl $^-$ flux in mast cells

To determine the effect of IFN γ on Cl $^-$ flux in resting and antigen-IgE activated mast cells, we employed two methods: measurement of $^{36}\text{Cl}^-$ uptake and assessment of Cl $^-$ sensitive fluorescence using MQAE. Studies with $^{36}\text{Cl}^-$ have shown that IFN γ treatment decreases Cl $^-$ uptake of PMC (Fig 7A, $p < 0.01$). A time-course of PMC Cl $^-$ uptake shows that IFN γ did not have an effect at the earlier treatment points (less than 2 hr) but decreased Cl $^-$ uptake at 20 and 24 hr (Fig 7B). Similar results were obtained with $^{36}\text{Cl}^-$ uptake measurements in RCMC (data not shown).

Fluorescence measurements were performed with mast cells loaded with MQAE in HTB solution and chloride efflux was measured after placing cells in gluconate buffer. Figure 7C shows that IFN γ treatment significantly reduced Cl $^-$ flux in sensitized PMC not challenged with antigen ($P < 0.05$; $n = 8$ and 11 , control and IFN γ treated cells, respectively). Following antigen challenge (10 WE/mL) the magnitude of the IFN γ mediated depression in Cl $^-$ efflux was reduced (Fig. 7D). Although antigen challenge in the absence of IFN γ treatment showed a trend towards reduced Cl $^-$ efflux, this was not statistically significant ($P > 0.5$, $n = 3$). Identical results were obtained in both PMC and RCMC under conditions when the cells were loaded in gluconate buffer and placed in HTB to measure Cl $^-$ influx (data not shown).

Measurements of halide permeabilities indicated that Br $^-$ was more permeable than Cl $^-$ and I $^-$ in PMC cells ($\text{Br}^-(1.34) > \text{Cl}^-(1.00) \geq \text{I}^- (0.68)$, $n = 3$ in each set). Similar results were obtained with RCMC ($\text{Br}^-(1.19) \geq \text{Cl}^-(1.00) > \text{I}^- (0.61)$, $n = 3$ in each set). The halide permeability sequence, $\text{Br}^- \geq \text{Cl}^- > \text{I}^-$, is characteristic of CFTR Cl $^-$ channels (Illek et al, 1999), and suggests that CFTR channels are an important component of Cl $^-$ flux in mast cells.

Discussion:

This is the first study demonstrating that CFTR expression is regulated differently in epithelial and non-epithelial cells. Moreover, we show that IFN γ -induced upregulation of CFTR in MC involved MAPK signalling pathways, whereas IFN γ -induced downregulation of CFTR in epithelial cells involved JAK/STAT pathways. Paradoxically we also show that despite IFN γ upregulation of CFTR in mast cells, IFN γ treatment depressed mast cell Cl⁻ flux in multiple assay systems.

It is now well established that CFTR gene expression is regulated in a complex, cell- and stimulus-specific manner that may involve both transcriptional and posttranscriptional mechanisms. For example, TNF decreases CFTR mRNA in human colonic epithelial cells but not in airway epithelial cells, whereas IL-1 β increases it only in airway epithelial cells (Beaudouin-Legros et al., 2005). Although stimulation of CFTR gene expression by IL-1 β involves activation of the CFTR promoter (Brouillard et al., 2001), downregulation of CFTR by TNF and IFN γ involves mainly posttranscriptional mechanisms (Beaudouin-Legros et al., 2005). The results of this study show that in mast cells both TNF and IFN γ increase CFTR mRNA, but whether this process affects CFTR gene transcription and/or mRNA stability is presently unknown. However, the fact that IFN γ increased CFTR protein levels to a greater extent than the mRNA suggests that IFN γ treatment may increase mRNA stability rather than CFTR gene transcription.

IFN γ modulation of gene expression is mediated by both STAT1-dependent and independent pathways. Microarray analysis shows that IFN γ regulates the expression of at least 150 genes in STAT1 null mice (Gil et al, 2001). Therefore, IFN γ activates STAT1 independent pathways that can also modulate gene expression. Certainly, our results show that IFN γ activates STAT1, ERK1/2 and p38 but not JNK, suggesting that these pathways are also induced in mast cells. Using inhibitors to JAK/STAT, ERK and p38, we determined that in both rat and human mast cells, CFTR upregulation is JAK/STAT independent but requires activation of the MAPK pathways mediated by ERK and p38. In T84 cells, IFN γ -mediated downregulation of CFTR is inhibited by AG-490, but is unaffected by the p38 and ERK inhibitors. STAT1 expression, by comparison, is upregulated by IFN γ in both mast cells and T84 epithelial cells and is inhibited by AG-490, suggesting that STAT1 upregulation is a positive feedback mechanism that sensitizes mast cells to IFN γ as previously observed in human macrophages (Duffy et al, 2001). AG-490 is a member of the tyrphostin family of tyrosine kinase inhibitors that blocks JAK2 phosphorylation (Valdembri et al, 2002) and can therefore inhibit the JAK/STAT signalling pathway. Our results show that AG-490 does not inhibit ERK or p38 activation, suggesting that these pathways are not dependent upon JAK2 phosphorylation. In human LAD2 cells, IFN γ -mediated upregulation of STAT1 is also sensitive to ERK and p38 inhibitors perhaps indicating the importance of MAPK pathways in IFN γ signalling. Therefore, IFN γ activates at least two pathways in mast cells -

the JAK/STAT pathway responsible for upregulation of STAT1 and the p38/ERK pathway(s) that is responsible for upregulation of CFTR.

Although ERK activation is involved in CFTR upregulation, PMA activates ERK but does not upregulate CFTR (Fig 1). This suggests that ERK activation requires activation of other molecules, perhaps p38, for initiation of CFTR transcription. The CFTR promoter contains several elements involved in regulation of transcription, which include potential binding sites for the ubiquitous transcription factor Sp1, and activator protein-1, (Denamur and Chehab, 1994). Phorbol esters induce activator protein-1 activation and downregulate CFTR expression. The cAMP response element binding protein (CREB) binds an element in the 5' region of the CFTR promoter, directly upstream from the transcription initiation site (Matthews and McKnight, 1996). CREB has been linked with IFN γ signalling, although the nature of their interaction is poorly understood. A CREB-binding protein acts synergistically with STAT1 and nuclear transcription factor kappaB (NF- κ B) to activate transcription of CXC chemokines in response to IFN γ (30) demonstrating that IFN γ may influence CREB activity and thereby activate CFTR transcription. However, the role of transcription factors in initiating CFTR transcription in epithelial cells is still poorly understood. For example, the CCAAT-enhancer binding protein (C/EBP) also binds an element on the CFTR promoter (Valdembri et al, 2002), and IFN γ induces expression and activation of C/EBP β in T84 epithelial cells (Salmenperä et al, 2003). Since IFN γ downregulates CFTR

expression in T84 cells, C/EBP β activation may inhibit CFTR transcription by an unknown mechanism.

The mechanisms controlling the complex developmental and tissue-specific expression of CFTR are not well understood. Distinct, tissue-specific patterns of CFTR transcription start sites have been identified in both human and mouse (White et al, 1998). The fact that CFTR is controlled by a weak, “house keeping” promoter (Yoshimura et al, 1991) and that CFTR is expressed in a variety of cell types suggests that CFTR may play a role in cellular homeostasis (Shen et al, 1993). If so, modulation of CFTR expression by cytokines may have consequences for cell function and response to stimuli. The exact role of CFTR in mast cell function is unknown and is the subject of other work in our lab. To date we have established that DPC, a drug known to inhibit CFTR, but to also have other activities, blocks Fc ϵ RI-stimulated degranulation of PMC (Kulka et al, 2002a). Moreover, knockdown of CFTR expression by antisense oligonucleotides in the human mast cell line HMC-1 reduces Cl⁻ flux, adhesion to fibronectin and calcium ionophore A23187 induced degranulation and IL-6 production (A. Schwingshackl and R. Dery, unpublished results). Our working hypothesis is that CFTR in mast cells is an important component of Cl⁻ flux and perhaps of other activities, as recognized for epithelial cells (Rowe et al, 2005).

In turn, the role of mast cells in cystic fibrosis is unclear. Recently, mast cells have been recognized as important players in innate and acquired immune responses (Marshall, 2004). Moreover, there are increased numbers of mast cells in nasal polyps from cystic fibrosis patients compared to non-cystic fibrosis

patients and many show signs of activation in cystic fibrosis (Henderson and Chi, 1992). Differences have also been found in mast cell numbers in human fetal trachea between cystic fibrosis and non-cystic fibrosis specimens (Hubeau et al, 2001). Interestingly, mast cell numbers and mast cell specific genes and others genes associated with innate immunity are upregulated in the intestine in CFTR null mice that show a severe intestinal phenotype (Norkina et al, 2004). Thus, the role of mast cells in cystic fibrosis warrants further investigation.

The finding of IFN- γ mediated increase in CFTR expression and decrease in Cl⁻ flux could be explained in several ways. For example, if IFN γ treatment leads to cell depolarization, this would tend to reduce Cl⁻ flux under our experimental conditions, perhaps by channels other than CFTR. Alternately, IFN γ may modulate expression of other proteins involved in Cl⁻ flux, e.g other Cl⁻ channels; SNARE proteins, which inhibit CFTR activity by decreasing channel open probability (Cormet-Boyaka et al, 2002). It is also possible that although IFN γ increases CFTR expression in mast cells, this may not involve maturation of CFTR and its translocation to the plasma membrane, where it could be fully functional. We are pursuing studies to elucidate the mechanism involved.

The role of IFN γ -mediated upregulation of CFTR in mast cell physiology is difficult to determine. Further studies are required to characterize the functional effects of increased CFTR on mast cell functions such as Cl⁻ transport, degranulation and mediator release in response to stimuli such as allergens. Furthermore, the transcription factors involved in CFTR upregulation in mast cells must also be examined to provide insight into regulation of the CFTR

promoter. The mechanisms that modulate CFTR gene expression through extracellular and intracellular signals may ultimately provide targets for therapy in cystic fibrosis where CFTR expression is abnormal.

ACKNOWLEDGEMENTS

We thank Lynelle Watt for her help in the preparation of this manuscript and Dr.

Dean D. Metcalfe for helpful advice.

REFERENCES

- Alton EW and Norris AA (1996) Chloride transport and the actions of nedocromil sodium and cromolyn sodium in asthma. *J Allergy Clin Immunol.* 98:S102-105; discussion S105-106.
- Befus AD, Pearce FL, Gauldie J, Horsewood P and Bienenstock J (1982) Mucosal mast cells. I. Isolation and functional characteristics of rat intestinal mast cells. *J Immunol.* 128:2475-2480.
- Besancon F, Przewlocki G, Baro I, Hongre AS, Escande D and Edelman A (1994) Interferon-gamma downregulates CFTR gene expression in epithelial cells. *Am J Physiol.* 267:C1398-C1404.
- Bissonnette EY and Befus AD (1990) Inhibition of mast cell-mediated cytotoxicity by IFN α /beta and -gamma. *J Immunol.* 145:3385-3390.
- Bradding P, Okayama Y, Kambe N and Saito H (2003) Ion channel gene expression in human lung, skin, and cord blood derived mast cells. *J Leukoc Biol.* 73:614-620.
- Cormet-Boyaka E, Di A, Chang SY, Naren AP, Tousson A, Nelson DJ, Kirk KL (2002) CFTR chloride channels are regulated by a SNAP-23/syntaxin 1A complex. *Proc Natl Acad Sci USA.* 99:12477-12482.

Davies WL, Vandenberg JL, Sayeed RA and Trezise AE (2004) Post-transcriptional regulation of the cystic fibrosis gene in cardiac development and hypertrophy. *Biochem Biophys Res Commun.* 319:410-418.

Denamur E, Chehab FF (1994) Analysis of the mouse and rat CFTR promoter regions. *Hum Mol Genet.* 3:1089-1094.

Dong YJ, Chao AC, Kouyama K, Hsu YP, Bocian RC, Moss RB and Gardner P (1995) Activation of CFTR chloride current by nitric oxide in human T lymphocytes. *EMBO J.* 14:2700-2707.

Duffy SM, Leyland ML, Conley EC and Bradding P (2001) Voltage-dependent and calcium-activated ion channels in the human mast cell line HMC-1. *J Leukoc Biol.* 70:233-240.

Friis UG, Johansen T, Hayes NA and Foreman JC (1994) IgE-receptor activated chloride uptake in relation to histamine secretion from rat mast cells. *Br J Pharmacol.* 111:1179-1183.

Gibson RL, Burns JL and Ramsey BW (2003) Pathophysiology and management of pulmonary infections in cystic fibrosis. *Am J Respir Crit Care Med.* 168:918-951.

Gil MP, Bohn E, O'Guin AK, Ramana CV, Levine B, Stark GR, Virgin HW, Schreiber RD (2001) Biologic consequences of Stat1-independent IFN signaling. *Proc Natl Acad Sci USA.* 98:6680-6685.

Gilchrist M, MacDonald AJ, Neverova I, Ritchie B and Befus AD (1997) Optimization of the isolation and effective use of mRNA from rat mast cells. *J Immunol Methods.* 201:207-214.

Henderson WR Jr, Chi EY (1992) Degranulation of cystic fibrosis nasal polyp mast cells. *J Pathol.* 166:395-404.

Hiroi M, Ohmori Y (2003) The transcriptional coactivator CREB-binding protein cooperates with STAT1 and NF-kappa B for synergistic transcriptional activation of the CXC ligand 9/monokine induced by interferon-gamma gene. *J Biol Chem.* 278:651-660.

Holliday MR, Banks EM, Dearman RJ, Kimber I, Coleman JW (1994)

Interactions of IFN γ with IL-3 and IL-4 in the regulation of serotonin and arachidonate release from mouse peritoneal mast cells. *Immunology*. 82:70-74.

Hu X, Herrero C, Li WP, Antoniv TT, Falck-Pedersen E, Koch AE, Woods JM, Haines GK, Ivashkiv LB (2002) Sensitization of IFN γ Jak-STAT signaling during macrophage activation. *Nat Immunol*. 3:859-866.

Hubeau C, Puchelle E, Gaillard D (2001) Distinct pattern of immune cell population in the lung of human fetuses with cystic fibrosis. *J Allergy Clin Immunol*. 108:524-529.

Illek B, Tam AWK, Fischer H, Machen TE (1999) Anion selectivity of apical membrane conductance of Calu 3 human airway epithelium. *Pflugers Arch*. 437:812-822.

Kirschenbaum AS, Akin C, Wu Y, Rottem M, Goff JP, Beaven MA, Rao VK and Metcalfe DD (2003) Characterization of novel stem cell factor responsive human mast cell lines LAD 1 and 2 established from a patient with mast cell sarcoma/leukemia; activation following aggregation of Fc ϵ RI or Fc γ RI. *Leuk Res*. 27:677-682.

Kirschenbaum AS, Worobec AS, Davis A, Goff JP, Semere T, Metcalfe DD (1988) Inhibition of human mast cell growth and differentiation by interferon gamma-1b. *Exp Hematol.* 26:245-51.

Krauss R, Berta DG, Rado TA and Bubien JK (1992) Antisense oligonucleotides to CFTR confer a cystic fibrosis phenotype on B lymphocytes. *Am J Physiol.* 263:C1147-51.

Kulka M, Gilchrist M, Duszyk M and Befus AD (2002a) Expression and functional characterization of CFTR in mast cells. *J Leukoc Biol.* 71:54-64.

Kulka M, Schwingshackl A and Befus AD (2002b) Mast cells express chloride channels of the ClC family. *Inflamm Res.* 51:451-456.

Marone M, Scambia G, Bonanno G, Rutella S, de Ritis D, Guidi F, Leon G and Pierelli L (2002). Transforming growth factor-beta1 transcriptionally activates CD34 and prevents induced differentiation of TF-1 cells in the absence of any cell-cycle effects. *Leukemia.* 16:94-105.

Marshall JS (2004) Mast-cell responses to pathogens. *Nat Rev Immunol.* 4:787-99.

Matthews RP, McKnight GS (1996) Characterization of the cAMP response element of the cystic fibrosis transmembrane conductance regulator gene promoter. *J Biol Chem.* 271:31869-31877.

Nakamura H, Yoshimura K, Bajocchi G, Trapnell BC, Pavirani A, Crystal RG (1992) Tumor necrosis factor modulation of expression of the cystic fibrosis transmembrane conductance regulator gene. *FEBS Lett.* 314:366-70.

Nazarenko I, Lowe B, Darfler M, Ikononi P, Schuster D and Rashtchian A (2002) Multiplex quantitative PCR using self-quenched primers labeled with a single fluorophore. *Nucleic Acids Res.* 30-37

Norkina O, Kaur S, Ziemer D, De Lisle RC (2004) Inflammation of the cystic fibrosis mouse small intestine. *Am J Physiol Gastrointest Liver Physiol.* 286:G1032-1041.

Ramana CV, Gil MP, Schreiber RD and Stark GR (2002) Stat-1 dependent and – independent pathways in IFN-gamma-dependent signaling. *Trends Immunol.* 23:96-101.

Romanin C, Reinsprecht M, Pecht I and Schindler H (1991) Immunologically activated chloride channels involved in degranulation of rat mucosal mast cells. *EMBO J.* 10:3603-3608.

Rowe SM, Miller S and Sorscher EJ (2005) Cystic fibrosis. *New Engl J Med.* 352:1992-2001.

Salmenperä P, Hämäläinen S, Hukkanen M and Kankuri E (2003) Interferon- γ induces C/EBP β expression and activity through MEK/ERK and p38 in T84 colon epithelial cells. *Am J Physiol Cell Physiol.* 284:C1133-C1139.

Schroder K, Hertzog PJ, Ravasi T and Hume DA (2004) Interferon-gamma: an overview of signals, mechanisms and functions. *J Leukoc Biol.* 75:163-189.

Shen BQ, Barthelson RA, Skach W, Gruenert DC, Sigal E, Mrsny RJ, Widdicombe JH (1993) Mechanism of inhibition of cAMP-dependent epithelial chloride secretion by phorbol esters. *J Biol Chem.* 268:19070-19075.

Valdembri D, Serini G, Vacca A, Ribatti D, Bussolino F (2002) In vivo activation of JAK2/STAT-3 pathway during angiogenesis induced by GM-CSF. *FASEB J.* 16:225-227.

White NL, Higgins CF, Trezise AE (1998) Tissue-specific in vivo transcription start sites of the human and murine cystic fibrosis genes. *Hum Mol Genet.* 7:363-369.

Yoshimura K, Nakamura H, Trapnell BC, Dalemans W, Pavirani A, Lecocq JP, Crystal RG (1991) The cystic fibrosis gene has a "housekeeping"-type promoter and is expressed at low levels in cells of epithelial origin. *J Biol Chem.* 266:9140-9144.

Footnotes:

This work was funded by grants to AD Befus from the Canadian Institutes of Health Research (CIHR) and to M Duszyk from the Canadian Cystic Fibrosis Foundation. Dr. Kulka was supported by a student voucher from CIHR; * current address: Allergy-Immunology Division, Feinberg School of Medicine, Northwestern University, Chicago, Illinois.

Reprint Requests: A. Dean Befus
Room 550A HMRC
Pulmonary Research Group, Department of Medicine,
University of Alberta, Edmonton, Alberta, Canada
T6G 2S2
Phone (780)492-1909
Fax (780)492-5329
dean.befus@ualberta.ca

Figure Legends

Figure 1. Western blot analysis of CFTR and STAT1 expression in untreated (lane 1), PMA treated (lane 2), TNF treated (lane 3) and IFN γ treated (lane 4) T84 (panel **A**) and RCMC (panel **B**). T84 cells were treated with PMA (10 ng/mL), human recombinant TNF (10 ng/mL) or IFN γ (10 ng/mL) for 24 hr. RCMC were treated with PMA (10 ng/mL) or rat recombinant TNF (10 ng/mL) or IFN γ (10 ng/mL) for 24 hr. Cell lysates were resolved on an 4-12% SDS-PAGE and blotted with anti-CFTR, anti-STAT1 or anti-actin antibody. Western blots shown represent three independent experiments. The effect of 24 h IFN γ treatment (80 ng/ml) on CFTR expression was characterized in T84 cells (C) and rat peritoneal mast cells (D), using confocal laser scanning microscopy (bar on the figure represents 10 μ M)

Figure 2. Quantitative PCR analysis of CFTR expression in RCMC LAD2 and T84 cells following different times and doses of IFN γ treatment (A and B). Asterisks represent statistical significance as determined by student t test, compared to untreated sample (time=0) in each case ($p < 0.05$). The dose used in Fig. 2A was 10 ng/mL, and in Fig. 2B treatment was for 8 hr. Western blot analysis of CFTR, STAT and actin expression in RCMC and T84 following a timecourse (hr) of 10 ng/mL IFN γ treatment (C and D). (n=3)

Figure 3. Western blot analysis of STAT1 and MAP kinase activation following IFN γ treatment. RCMC were treated with 10 ng/mL of IFN γ for indicated times and cell lysates were probed with antibodies to phosphorylated STAT1, p38, ERK or JNK. Blots were stripped and probed with anti-actin to show equal loading. Representative of three independent experiments.

Figure 4. IFN γ -mediated upregulation of mast cell CFTR protein requires activation of JAK2 and/or p38 and ERK. RCMC, LAD2 and T84 cells were treated with IFN γ (10 ng/mL) with or without JAK2 inhibitor (AG-490; 30 mg/mL), p38 inhibitor (SB202190; 30 mg/mL), or ERK MAPK inhibitor (U0126; 30 mg/mL) for 24 hr. Representative of three independent experiments.

Figure 5. Densitometry summary of data in Fig. 4. RCMC were treated with IFN γ (10 ng/mL) with or without JAK2 inhibitor (AG-490; 30 mg/mL), p38 inhibitor (SP202190; 30 mg/mL), or ERK inhibitor (U0126; 30 mg/mL) for 24 hr and expression of CFTR (black bars) and STAT1 (grey bars) was analysed by western blot. Numbers on the X-axis represent the treatment groups in Fig. 4. (n=3 independent experiments; error bars represent SEM). Asterisks represent statistical significance as determined by student t test ($p < 0.05$).

Figure 6. RCMC were treated with IFN γ (10 ng/mL) alone (IFN) or pretreated with AG-490 (IFN+A; 30 mg/mL), SB202190 (IFN+S ; 30 mg/mL) or U0126 (IFN+U ; 30 mg/mL) for 10 min, then stimulated with IFN γ (10 ng/mL) and for 1

to 30 min. Cell lysates were analyzed for phosphorylation of STAT1 (A), ERK1/2 (B) or p38 (C) and β -actin (D) was assessed as a loading control. Representative of three independent experiments.

Figure 7. IFN γ decreases Cl $^-$ flux. Rat peritoneal mast cells were purified (>95%) and treated with IFN γ at various doses (A; 24hr) or for various times (B; 80 ng/mL). After treatment, mast cells were washed and incubated with $^{36}\text{Cl}^-$ for 30 min. Mast cells were spun through oil and radioactivity of cell pellets was measured in a scintillation counter (n=5 independent experiments; $p<0.01$ compared to untreated). Effects of IFN γ on Cl $^-$ flux in PMC as measured by MQAE (7C,D). Effects of IFN γ (80 ng/mL, 24 hr pretreatment) on Cl $^-$ efflux from sensitized rat peritoneal mast cells. After IFN γ pretreatment cells were loaded with the Cl $^-$ sensitive dye N-(ethoxycarbonylmethyl)-6-methoxyquinolinium bromide (MQAE) and the driving force for Cl $^-$ efflux involved placing them in gluconate buffer with or without antigen challenge (10 worm equivalents/mL); (n=8 to 11 independent experiments; $p<0.01$).

Figure 1

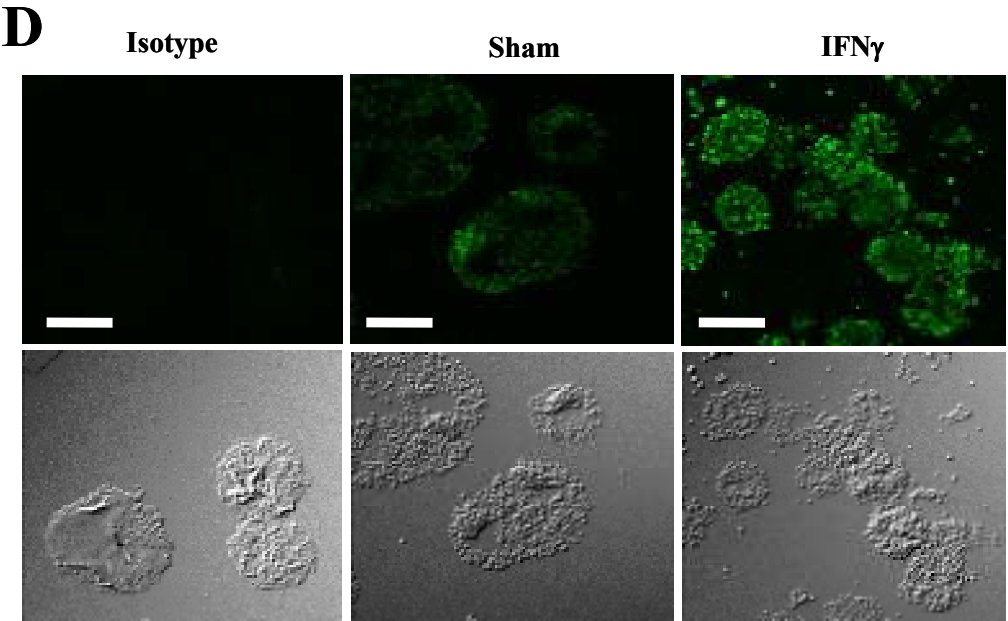
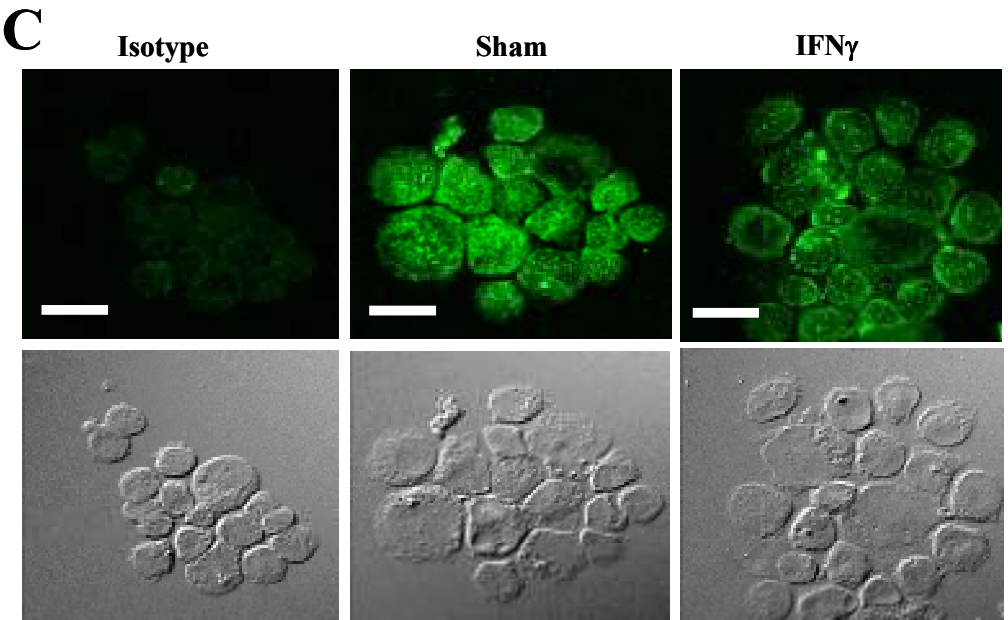
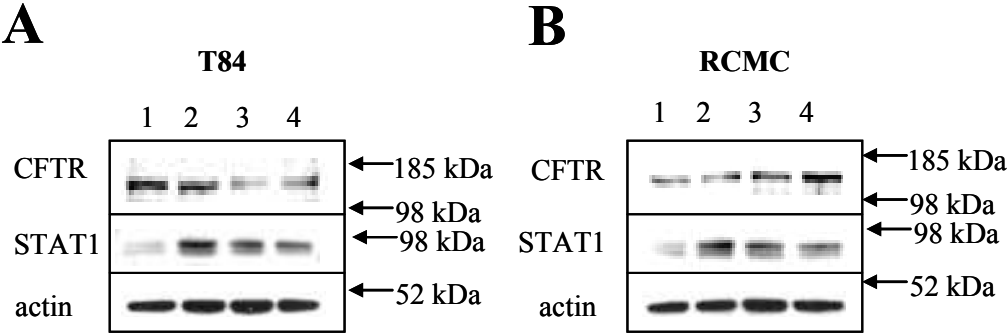
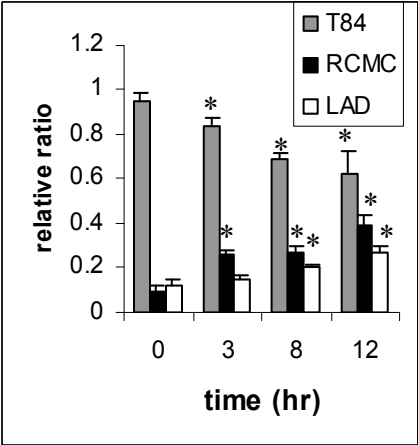
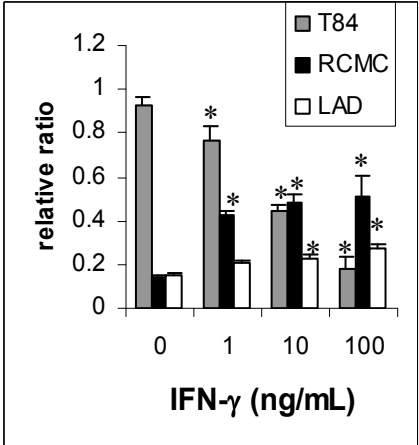


Figure 2

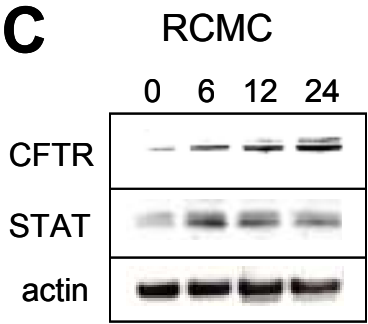
A



B



C



D

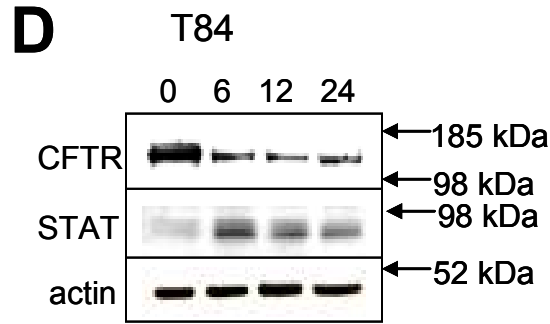
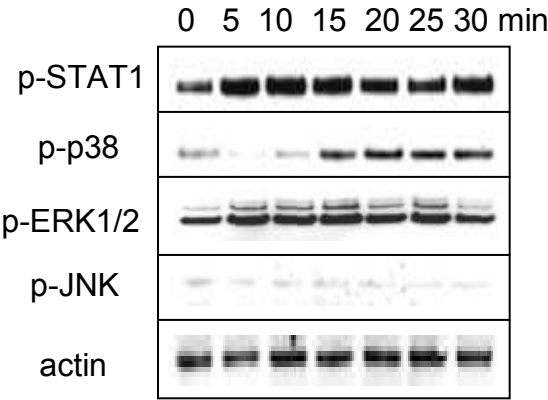


Figure 3



A

	1	2	3	4	5	6	7	8
IFN- γ	-	-	-	-	+	+	+	+
AG-490	-	+	-	-	-	+	-	-
SB202190	-	-	+	-	-	-	+	-
U0126	-	-	-	+	-	-	-	+

B

Cell Type	Condition	CFTR Band Intensity	STAT1 Band Intensity
RCMC	1	~0.2	~1.1
	2	~0.2	~1.1
	3	~0.3	~1.1
	4	~0.3	~1.1
	5	~1.1	~2.5
	6	~1.0	~1.3
	7	~0.4	~2.2
	8	~0.5	~2.3
LAD	1	~0.1	~0.8
	2	~0.1	~0.9
	3	~0.1	~1.0
	4	~0.2	~0.9
	5	~1.0	~2.1
	6	~0.9	~0.9
	7	~0.4	~0.8
	8	~0.5	~1.0
T84	1	~1.0	~1.0
	2	~0.8	~0.8
	3	~0.8	~0.9
	4	~1.0	~0.8
	5	~0.3	~1.9
	6	~1.1	~0.6
	7	~0.5	~2.1
	8	~0.4	~2.1

	1	2	3	4	5	6	7	8
IFN- γ	-	-	-	-	+	+	+	+
AG-490	-	+	-	-	-	+	-	-
SB202190	-	-	+	-	-	-	+	-
U0126	-	-	-	+	-	-	-	+

Figure 5

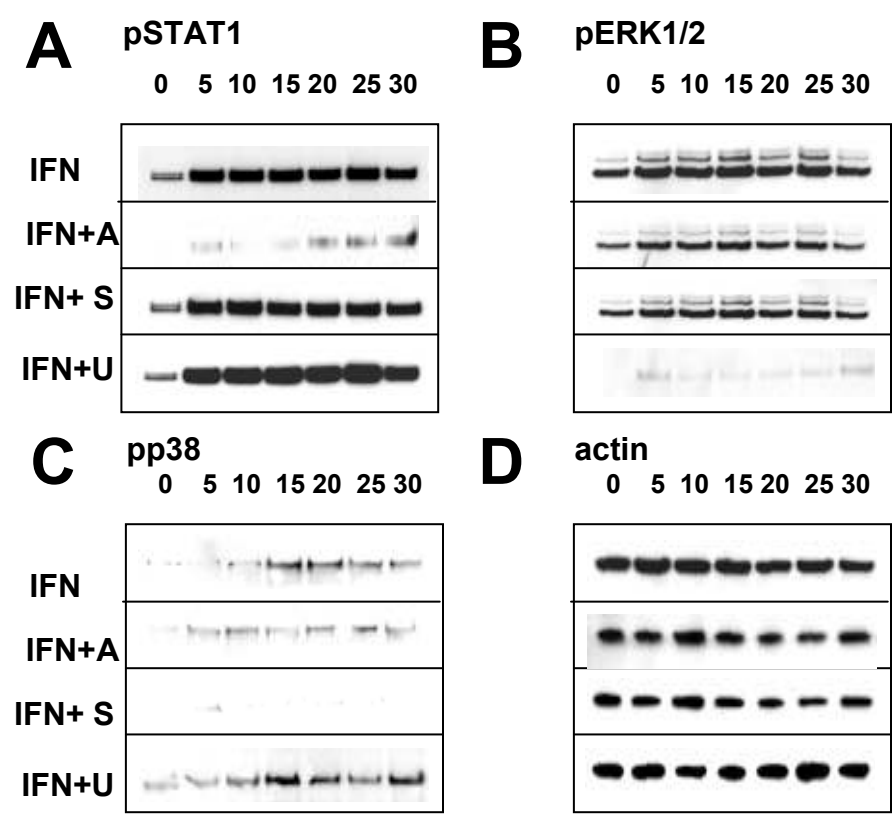


Figure 6

